Physical Modelling of the Interactions between Thermal Systems in Supermarkets

Von der Fakultät für Maschinenbau
der Technischen Universität Carolo-Wilhelmina zu Braunschweig

zur Erlangung der Würde

eines Doktor-Ingenieurs (Dr.-Ing.)

genehmigte Dissertation

von: Nicolas Fidorra
aus: Dortmund

eingereicht am: 20.07.2020
mündliche Prüfung am: 10.03.2021

Gutachter: Prof. Dr.-Ing. Jürgen Köhler
Prof. Dr.-Ing. Armin Hafner

2021

Acknowledgements

Gnothi seauton - Know thyself

Temple of Apollo at Delphi

Working on a dissertation is very special process.

Curiosity, the urge to understand, as well as the satisfaction of solving problems and possibly a glimpse of what holds the world together at its core are sources of motivation for going through this process. Admittedly, it is not unusual that frustration and exhaustion, temporarily abandoning one's social life as well as fundamental doubts are also part of this process.

Along the work on my dissertation, I had to overcome several obstacles: some inner obstacles and some other ones linked to the boundary conditions of my work. And while research itself can never end, a dissertation, however, has to be finished at some point. Finishing it ultimately depends, among other factors, on contenting oneself with writing something that cannot be completed. Thus, I believe that working on and finishing a dissertation requires what is written at the temple of Delphi: *You have to know thyself.*

In the course of my research I worked at the Institut für Thermodynamik at the TU Braunschweig. Two years I spent at Sintef Energy Research in Trondheim, Norway, which was made possible by the funding from the Research Council of Norway via the CREATIV project. Secondly, my work was funded by the European Union via the Horizon 2020 programme and the SuperSmart project, which I both gratefully acknowledge.

Like thermal systems, a doctoral candidate is not autonomous, but he interacts with others who constitute his *surroundings* and consequently are indispensable. I had the chance to collaborate with researchers not only from Braunschweig and Trondheim, but from all over Europe, to present my ideas and results at many conferences and to discuss them with experts from all over the world. During that time I could establish the contacts and collaborations that were necessary for my research and that eventually led to new projects and funding for further supermarket research at TU Braunschweig. Therefore, I have to mention the people who have *surrounded* and interacted with me and who have been an integral component in the process of research and writing the dissertation.

First of all, I have to thank my doctoral supervisor Prof. Dr.-Ing. Jürgen Köhler. He granted me immense freedom and confidence during my research and I am grateful for his support, scientific discussions and encouragement during the final steps of writing. Prof. Dr.-Ing. Armin Hafner introduced me to the topics of refrigeration and energy efficiency in supermarkets. I would like to thank him for the collaboration, his support in many joint papers and conferences, and for agreeing to be the second supervisor of my thesis. I thank Jun.-Prof. Dr. Julia Großeheilmann for taking over the roles and responsibilities of chair of the examination board.

I also have to thank Dr.-Ing. Wilhelm Tegethoff for the support during all stages of my research. His disposition at any time for scientific and personal conversations as well as critical reflections on my research were very important for my work. I also would like to thank Dr. Silvia Minetto. Working together helped me to learn how to transfer my ideas into papers and presentations and gave me essential knowledge and insights into supermarket refrigeration and display cabinets.

I would like to express deep gratitude towards three other people: The two energy managers of the test supermarket who provided me with measurement data and technical information of that supermarket and Thomas who provided me access to his laboratory and helped me carry out the experiments with display cabinets. Without their expertise and support, this thesis would not have been possible.

The Institut für Thermodynamik and TLK-Thermo GmbH work closely together which is the merit of Dr.-Ing. Nicholas Lemke and Dr.-Ing. Wilhelm Tegethoff. Besides the good working atmosphere, the readiness to help each other is a distinguished characteristic of this collaboration, wherefore I would like to thank all people from both institutions. Among them I would like to especially thank my office-room-mates Maren, Andreas and Niklas for the good atmosphere, for working and laughing *with* me – and taking care of the plants ;-). Furthermore, I would like to thank Sven for the introduction into the world of Modelica and TIL, Sebastian for the support with design and presentations, Christian for numerical help, Johannes for the assistance with Python and all other colleagues for the good working atmosphere and collaboration. Furthermore, I would like to thank the authors and co-authors of the publications that I wrote and contributed to as well as the project partners from SuperSmart and CREATIV. I also thank the students who wrote their theses under my supervision – many of them provided me with valuable input for my dissertation. Additionally, I thank Markus and Michael for proofreading the final document and Ulla Knight-Jones for improving grammar and spelling.

Besides the aforementioned people, there were also some more persons, who went through a part of the process with me and to whom I would like to say: *Gracias, Takk and Danke.*

Last, but definitely not least, I would like to thank my friends, Marusha and my family for the assistance and encouragement and the support during all stages of my education, which led me to this point and enabled me to finish my dissertation.

Considering the work on my dissertation and that the people accompanying me, *surrounding* me and interacting with me were an essential part of the process, I believe it is not only important to know thyself, but also to *know thy surroundings.*

Finally, I am glad that the work on my dissertation has come to an end and that the following assertion still holds true:

In this house, we obey the laws of thermodynamics. (Homer J. Simpson)

Braunschweig, Summer 2021 *Nicolas Fidorra*

Abstract

This thesis contributes to modelling and quantification of interactions between thermal systems in supermarkets. *The main goal of this thesis is to describe the interactions between thermal systems in supermarkets by means of physical models and to quantify their energetic impact.* To achieve this overall goal, three subgoals are defined.

The first subgoal is the breakdown of supermarkets into control volumes and the definition of physical interactions between them. In this work, the usage of *physical modelling* implies two aspects: Firstly, using first principle models and secondly using physical connections between objects. This allows to model the interactions between thermal systems in a supermarket based on transport processes of mass, energy an enthalpy. Interfaces and model equations describing the sales room air, the refrigeration system and display cabinets are presented.

The second subgoal refers to the analysis of the air exchange between refrigerated display cabinets and the sales area, which is one of the most important interactions in a supermarket. The focus lays on the quantification of the air exchange and the determination of the influence of door openings on this air exchange. In laboratory tests, an adapted tracer gas method using CO_2 is used to determine the air change rates between the display cabinets and the sales room for three typical supermarket cabinets. The specific air infiltration rates per closed and open door are estimated and used as parameters in the newly developed display cabinet model. Additionally, a second way of quantifying the impact of door openings on the air infiltration uses the so-called *thermal entrainment factor* (TEF) and is based on temperature measurements. The applications of the developed models are exemplified. Firstly, the energy consumption of the display cabinets and the refrigeration system can be predicted based on ambient temperature, temperature and humidity of the sales room as well as the number of customers. The prediction of the energy consumption of a period of 28 days deviates only 3.3 % from measurement data. Here, several parameters need to be estimated manually or via calibrations. If further parameter of display cabinets and refrigeration systems would be available in a database, the simulation methods and models could be used for planning and dimensioning of supermarkets.

The analysis of the effects of incoming and outgoing customers on fresh air change rates is the third subgoal of this thesis. This air exchange is highly relevant because it affects the thermal loads of the heating and air conditioning system as well as the need for ventilation. In order to estimate the air change rates, a model of the CO_2 concentration in the sales room air is developed, which uses the air change rates of the closed and opened entrance door as parameters. Compared to previous models of CO_2 concentration in supermarkets, several new effects are considered, for instance: the effect of joint door crossings on the total share of door opening time, or the shopping duration as a function of the number of purchased items. Data from a test supermarket is used to calibrate and validate the model. The prediction of the CO_2 concentration works very well: the mean absolute error of 25 ppm is below the accuracy of the measurement data. Air change rates of the building below $0.1\,\mathrm{h}^{-1}$ for closed doors and $0.7\,\mathrm{h}^{-1}$ to $1.9\,\mathrm{h}^{-1}$ for open doors are found.

Another application of the developed models is also exemplified: the entire supermarket is simulated with the objective to predict the humidity of the sales room air. The humidity ratio in the test supermarket for a period of 14 day could be predicted with a mean absolute error of $0.3\,\mathrm{g\,kg}^{-1}$, which again is below the accuracy of the measurement data. Finally, several of the interactions between thermal systems in a supermarket are quantified exemplarily. The energetic impact of the shopping of one customer is analysed for three scenarios.

Kurzfassung

Das Hauptziel dieser Arbeit ist die Beschreibung der Wechselwirkungen zwischen thermischen Systemen in Supermärkten sowie die Quantifizierung ihres energetischen Einflusses. Hierzu werden drei Teilziele definiert. Das erste Teilziel besteht in der Unterteilung eines Supermarktes in Bilanzräume und der Definition von Schnittstellen zur Beschreibung der Wechselwirkungen. Die typischerweise in einem Supermarkt vorhandenen Systeme Kühlmöbel, Kälteanlage sowie Verkaufsraum werden in dieser Arbeit betrachtet. Für sie werden Massen- und Energiebilanzen definiert und die Wechselwirkungen zwischen ihnen über Transportprozesse von Stoffen und Energie abgebildet. Die Modellierung eines mit Türen ausgestatteten Kühlmöbels, das insbesondere den Luftaustausch auch bei Türöffnungen berücksichtigt, stellt hierbei eine Neuigkeit dar. Das zweite Teilziel bezieht sich auf die Analyse des Luftaustausches zwischen den Kühlmöbeln und dem Verkaufsraum. Dieser ist besonders wichtig, da er einerseits zum Wärme- und Feuchtigkeitseintrag in das Kühlmöbel führt, was den Kühlbedarf erhöht. Andererseits hat dieser Luftaustausch eine Abkühlung sowie Entfeuchtung der Verkaufsraumluft zur Folge. Dies ist wichtig für die Dimensionierung und den Betrieb der Heizung und Klimatisierung. Der Schwerpunkt der Untersuchung liegt auf der Quantifizierung dieses Luftaustausches sowie der Bestimmung des Türöffnungseinflusses. In Laborversuchen wird eine adaptierte Tracergas Methode mit dem Gas CO_2 verwendet, um den Luftaustausch typischer Kühlmöbel mit Türen zu untersuchen. Die spezifischen Luftinfiltrationsraten pro Kühlmöbeltür werden als Parameter für das neu entwickelte Modell verwendet. Weiterhin wird eine zweite Methode zur Bestimmung des Türöffnungseinflusses vorgestellt, die auf dem als dimensionslose Infiltrationsrate interpretierbaren *thermal entrainment factor* (TEF) basiert. Dieser, für offene Kühlmöbel etablierte Kennwert, kann basierend auf Temperaturmessungen angenähert werden, und wird hier für geschlossene Möbel hergeleitet und für einen spezifischen Kühlmöbeltyp mit Messdaten aus einem realen Supermarkt bestimmt. Die entwickelten Simulationsmodelle und gemessenen Infiltrationsraten in Kühlmöbeln werden genutzt, um den Strombedarf der Kühlmöbel und der R-744 Verbundkälteanlage eines realen Supermarktes vorauszuberechnen. Hierbei sind Umgebungstemperatur, Temperatur und Luftfeuchtigkeit im Verkaufsraum, sowie der Kundenfrequenz die zeitlich veränderlichen Eingangsgrößen des Modells. Die Abweichung des für einen Zeitraum von 28 Tagen vorausberechneten Energiebedarfs beträgt 3.3 %. Die Untersuchung des Einflusses von herein- und herausgehenden Kunden auf die Luftwechselraten des Verkaufsraumes stellt das dritte Teilziel dieser Arbeit dar. Hierzu wird ein Modell zur Bestimmung der CO_2 Konzentration in der Verkaufsraumluft entwickelt, welches die Luftwechselraten mit geöffneter bzw. geschlossener Eingangstür als Parameter nutzt. Im Vergleich zu vorherigen Modellen werden einige Effekte erstmalig berücksichtigt. Hierzu gehören gemeinsame Türdurchgänge mehrerer Kunden sowie die Abhängigkeit der Einkaufsdauer von der Einkaufsmenge. Daten eines realen Supermarktes werden zur Kalibrierung und Validierung des Modells verwendet. Der CO_2 Gehalte kann mit einer Abweichung von 26 ppm und somit innerhalb der Messungenauigkeit vorhergesagt werden. Eine weitere Anwendung der entwickelten Simulationstechnik wird vorgestellt: Der gesamte Supermarkt wird simuliert mit dem Ziel die Wasserbeladung im Verkaufsraum vorherzusagen. Dies gelingt mit einer sehr geringen Abweichung ($0.3\,\mathrm{g\,kg^{-1}}$). Da die Luftfeuchtigkeit durch alle thermischen Systeme im Supermarkt beeinflusst wird, ist diese gute Vorhersage ein starkes Indiz dafür, dass die Wechselwirkungen realistisch modelliert und quantifiziert wurden. Abschließend wird der energetische Einfluss eines einzelnen Kunden und die von ihm verursachten Wechselwirkungen für drei Szenarien (Winter, Frühling, Sommer) bewertet.

Contents

1. Introduction

Food retail stores are highly relevant in terms of economy, energy consumption and climate impact. The total electrical energy consumption of food retail stores in Germany was approximately 16 TW h in 2013 (Skačanová and Gkizelis 2018). This is equivalent to around 3 % of the total electricity consumption of Germany. A share of 3 % to 4 % is a typical value for European countries. Since a huge share of electricity is still produced based on fossil resources, electricity consumption goes along with greenhouse gas emissions. Despite efforts to reduce the usage of fluorinated refrigerants (such as the F-gas Regulation, European Union (2014)), refrigerants with a high global warming potential are still used.

The term *food retail store* is a general term, covering various kinds of stores with different characteristics. *Convenience stores, supermarkets or hypermarkets* are commonly accepted categories that differ in terms of size and product assortment (Purper 2005, Karampour et al. 2016, Skačanová and Gkizelis 2018). For the sake of simplicity, in this work, the term *supermarket* is used as the general term for all types of food retail stores and specified where necessary. Despite the differences in terms of size and product assortment, there are several characteristics and requirements that all types of supermarkets have in common. A first characteristic is the selling of chilled and frozen food. This requires technical installations to maintain the food products at the desired temperature level: display cabinets and a refrigeration system. A second characteristic is the necessity to maintain the sales floor area at a comfortable thermal level (d'Ambrosio Alfano et al. 2019). This includes the temperature, humidity and CO_2 concentration, which consequently requires heating, ventilation and, depending on the location, an air conditioning system. All these systems consume electrical energy. Further (non-technical) requirements are the necessity of attractive product display to stimulate the purchase.

The thermal systems of a supermarket cannot be looked at independently, since there are many interactions between them. Firstly, the cooling load of the display cabinets depends on the conditions of the sales area. There is heat transfer from the sales area to the display cabinet and air exchange between them. Secondly, the heating and cooling loads to maintain the sales area at the desired conditions depend on the ambient conditions. Low ambient temperatures require more heating, and high ambient temperature more cooling. Thirdly, the electricity consumption of the refrigeration system depends on its efficiency, which tends to be lower at high ambient temperatures. Fourthly, the ventilation system depends on the number of customers, since it is often controlled by the CO_2 concentration in the sales area. These interactions have an impact on the energy consumption of the thermal systems.

1.1. Trends and developments of supermarket concepts

There are many developments in the area of thermal supermarket systems. **Usage of natural refrigerants** is a trend. As awareness of climate impact and the relevance of energy efficiency is rising, natural refrigerants are becoming the new standard (Skacanova 2017). Carbon dioxide (CO_2, R-744) is becoming the standard for centralised supermarket refrigeration systems. The number of transcritical R-744 systems in Europe increased considerably from 140 in 2008 to more than 23 000 in October 2019 (Chasserot 2020). Despite being flammable, propane (R290) and other hydrocarbon refrigerants are also getting more attraction (Skačanová et al. 2018). There are estimated to be more than 3.2 million hydrocarbon display cabinets in the world and more than 2500 so-called *water loop system* with hydrocarbons (Chasserot 2020).

Another trend is the **usage of glass doors or lids on cabinets**. In Germany, 99.5 % of low-temperature cabinets and 50.8 % of medium-temperature cabinets have doors (Chini 2019). The specific numbers depend on the kind of store and the year of construction or renovation. A door, especially when retrofitted, has a significant impact on the air exchange between the display cabinet and the sales room air. This air exchange affects both the cooling load of the refrigeration system and the cooling and heating demand of the sales room.

The integration of the different systems can be considered another trend. The main purpose of refrigeration systems in a supermarket is to provide cooling for low and medium-temperature display cabinets and cold rooms. Heat recovery for space heating is already commonly used in R-744 refrigeration systems for supermarkets (Karampour and Sawalha 2014). Current research about heat recovery focuses more and more the on the optimisation of costs and efficiency of heat recovery (Fidorra et al. 2015b, Fidorra 2015, Nöding et al. 2016, Nöding 2019). Recent investigations aim at the integration of refrigeration and air conditioning systems (Gullo et al. 2017). The integration of different functions such as refrigeration, heating and air conditioning leads to further interactions. Another way of integrating systems is the coupling of R-744 booster refrigeration system with sorption systems: a part of the waste heat from the vapour compression refrigeration system is used to drive a sorption refrigeration system (Graf et al. 2015, Gibelhaus et al. 2016b,a, 2017, Gibelhaus et al. 2019). The cooling provided by these sorption systems can be used to enhance the efficiency of the vapour compression systems by cooling the refrigerant below ambient temperature. In more general terms, integration can be found at the level of the entire supermarket. Rettich et al. (2013) evaluated and categorised different overall thermal concepts for supermarkets and discount stores. Two examples, which successfully integrated R-744 refrigeration systems with other thermal subsystems are the Aldi Süd in Rastatt, Germany (Réhault 2013) and the REMA 1000 in Trondheim, Norway (Titze 2017). Both projects successfully demonstrated that energy savings could be achieved by integrating various thermal subsystems.

The standardisation of supermarket equipment has already begun but will become more relevant in the future. The *SuperSmart-Rack* project, for instance aims at developing standardised R-744 refrigeration systems for supermarkets (Pardiñas 2019).The standardisation applies not only to equipment but also to entire *supermarket concepts*. So-called *water loop* systems consist of self-contained display cabinets, which comprise an integrated refrigeration cycle that is cooled by a water loop (Bagarella et al. 2014, Fidorra et al. 2017a,b, Fidorra 2018, Kistner et al. 2019). These systems have a lower complexity, are easier to maintain and to install and more flexible than central direct expansion refrigeration systems (Fidorra 2019a). The challenge of developing standardised concepts lay in the correct planning, dimensioning of components, and the adjustment to other thermal systems. This has to take into account the multiple interactions between these thermal systems.

The integration of supermarkets into smart grids is another trend. Normally, supermarkets are consumers and receive electrical energy from the grid. There are several options for extending this connection to the grid. One option is the integration into thermal grids. Waste heat from the supermarket could be passed to a district heating grid (Zühlsdorf et al. 2018), or the integration could encompass both district heating and district cooling (Funder-Kristensen et al. 2017). The integration, however, is not limited to the thermal grids. Supermarkets can also be integrated into electrical grids. One option is short-term reduction of power consumption by postponing the electrical defrosting of evaporators (Pedersen et al. 2015). The general potential of demand side response of supermarket refrigeration systems is evaluated in (Månsson and Ostermeyer 2019). There are actually pilot projects investigating the smart grid integration (Müller 2019, Projektträger Jülich 2020). Supermarkets could play a part in the

production of renewable energies. Many supermarkets have large roof areas, which are suitable for photovoltaic installations. This approach is already used by supermarkets in Switzerland and Germany (Réhault 2013, Perrino 2018). An important component in the demand side response of supermarket refrigeration systems are cold thermal energy storages (CTES). An overview of the ways of integrating CTES into R-744 supermarket systems is described by Fidorra et al. (2015a, 2016). Ice storages, for instance, are a way of using electricity produced by photovoltaic systems (KI Kälte Luft Klimatechnik 2017, Wiedenmann and Schönenberger 2018). In order to analyse the integration and operation strategy, new methods and tools are necessary, which for instance are investigated in the project VEOTOP (Fidorra and Schulte 2018).

1.1.1. Relevant tasks

Thermal systems in supermarkets are becoming more complex and more integrated. To achieve high energy efficiency, all systems have to be adapted to each other. To achieve proper operation and the desired results, the whole system has to be understood. This understanding implies the quantification of effects and interactions taking place in and between thermal systems in a supermarket. In this context, two tasks are becoming more and more relevant.

Prediction of energy consumption and interactions For new supermarket concepts, the planning and dimensioning of thermal systems and their adaption to each other, the prediction of their operation and energy consumption is crucial. This includes specifically the interactions between the systems: the estimation of the cooling demand of display cabinets in a supermarket is relevant for the dimensioning of the refrigeration system. Moreover, the cooling and dehumidification effect of the display cabinets on the sales room air is relevant for the dimensioning of the air conditioning system. The prediction of CO_2 concentration in the sales room air is relevant for the dimensioning of the ventilation system. In integrated supermarket systems, the air conditioning may be integrated in the refrigeration systems. Thus, the prediction of the energy consumption and the interactions between thermal systems are crucial for the planning and proper dimensioning of new supermarket concepts.

Benchmarking Once a new supermarket concept is built, it is important to benchmark and compare it with other systems. This can be relevant for fault detection in operational supermarkets. However, before the concepts can be benchmarked, the systems and its interactions first have to be understood.

The physical modelling of thermal systems and their interactions is an important tool for both tasks and consequently contributes to more efficient supermarket systems.

1.2. State of the art

This section describes the state of the art of the analysis and modelling of thermal systems in a supermarket.

1.2.1. Interactions between thermal systems in a supermarket

Supermarkets are complex systems that consist of many subsystems. The most relevant interactions take place between the following systems: 1. display cabinet 2. sales room 3. refrigeration system 4. the environment. The thermal systems, their behaviour and, from a qualitative perspective, their interactions are well known and widely described in the literature (Arias 2005, Karampour et al. 2016, Evans and Foster 2016, Månsson 2016, IEA Heat Pump Centre 2017). A quantification of these interactions has been carried out in only a few publications

and for specific cases, as described later in this section. To the author's knowledge, no systematic assessment and quantification has been published, which is why this thesis aims to help fill this gap.

Inside the display cabinets, the foodstuff is stored at low temperature levels to keep it fresh. Because of the low temperature inside the display cabinets, heat is transferred from the sales room to the cabinets. Nowadays, display cabinets are usually equipped with doors. Cabinet doors often have gaps and air is exchanged between the cabinets and the sales room. When the doors are opened, the air exchange is intensified drastically. This leads to a higher heat infiltration into the cabinet and consequently a higher cooling load. The air infiltrating into the cabinet carries moisture along with it, which condensates at the heat exchanger and often leads to frost formation. Frost formation decreases the heat transfer and leads to a lower efficiency of the refrigeration system (Evans and Foster 2016). A refrigeration system is needed to keep display cabinets at the desired, low temperature level. Central refrigeration systems are located in a separate machine room and connected via tubes with the cabinets that are located in the sales room. These so-called remote display cabinets act as a heat sink for the sales room air, since the waste heat from the central refrigeration system is released into the environment. So-called self-contained display cabinets have a small incorporated refrigeration system. They usually release the waste heat into the surrounding air. Since the dissipated electrical power of the compressor is also released into the surrounding air, these cabinets act as heat sources for the sales room air (Rhiemeier et al. 2008).

The interactions between the thermal systems in a supermarket often consist of air exchange. This air exchange is enhanced by customers and consequently affects the interactions. Customers are a fundamental part of supermarkets and have a multitude of effects on the thermal systems (Fidorra 2019b). While they stay in the sales room, they produce heat, moisture and CO_2, which affects the sales room air. The amount of heat, moisture and CO_2 produced depends on the time they spend in the supermarket. Furthermore, customers intensify the air exchange between the cabinets and sales room when they open the cabinet doors, which leads to higher cooling demands. Incoming and outgoing customers intensify the air exchange between the sales room and the environment. This usually leads to a reduction of CO_2 concentration. Depending on the outdoor temperature and humidity, the intensified air exchange may lead to a higher or lower heating or cooling demand for the building. To the author's knowledge, a combined analysis of the influence of customers on the cooling load of the display cabinet, the cooling or heating demand of the sales room, and the CO_2 concentration in the sales room air has not been carried out before, and therefore the results of this thesis (Chapter 7) contribute new knowledge to science.

The general interactions between the subsystems in a supermarket, which were briefly described above, are well known and have been often described in the literature. Arias (2005) describes the subsystems of a supermarket and their general interactions using *conceptual models*. Many of the physical effects such as "air and moisture exchange", "air leakage", or "infiltration" that lead to the "interconnections" and "interrelatedness" of the subsystems are mentioned. Månsson also uses conceptual models to describe the energy flows in a supermarket (Månsson 2016).

Besides conceptual models, there are also simulation tools and models for entire supermarkets. Overviews of current simulation tools for supermarkets can be found in IEA Heat Pump Centre (2011) and Fidorra et al. (2013) and Fidorra (2016a). Here, only the main features related to the modelling of interactions are briefly described. CyberMart (Arias 2005) is a tool specifically developed for the simulation of supermarkets. It considers the building, refrigeration system and HVAC system. The cooling load of the display cabinets is calculated based

on the humidity and temperature in the sales room air. EnergyPlus is a building simulation program that has several modules for supermarket simulations (Stovall and Baxter 2010, U.S. Department of Energy 2018). The cooling load calculation takes into account the sensible and latent heat. The retroactive effect of display cabinets on the sales room is considered via an energy balance for latent heat. EnergyPlus is used in various studies for entire supermarkets (Cecchinato et al. 2010a, Mylona et al. 2018). TRNSYS is another building simulation programme that has been used for supermarket simulations (TRNSYS 2020). Ge and Tassou (2011a) and Ge and Tassou (2011b) developed the so-called *SuperSim* tool based on TRNSYS and analysed a specific supermarket. TRNSYS has also been used for the planning of a new supermarket concept by ALDI Süd (Réhault 2013). Besides building simulation tools and the specific supermarket simulation tool CyberMart, the report about computational tools (Fidorra 2016a) from the SuperSmart project (Fidorra 2016b, Minetto et al. 2017, SuperSmart Project 2019) defines another category of "modelling and simulation platforms". One tool in this category is Modelica, an equation-based object-oriented modelling language. Titze (2017) used Modelica to model, simulate and optimise a REMA 1000 supermarket in Norway. Some of the tools mentioned account for certain interactions and retroactive effects between the thermal systems. However, to the author's knowledge, none of these tools considers the supermarket as a whole while modelling all of the interactions in a physical way. Although the interactions are qualitatively understood, they are seldom investigated. Past research has often focused on individual components or systems. There are, for instance, many studies of two- stage R-744 refrigeration systems. Often, new topologies including an internal heat exchanger and auxiliary compressors or ejectors are used to improve efficiency (Gullo et al. 2018b, Bellos and Tzivanidis 2019). Display cabinets have been investigated with the aim to improve product quality of the stored foodstuff and reduce the cooling demand. The air infiltration into open display cabinets and the dependency of the cooling load on the temperature and humidity of the sales room air have been widely investigated (see next Section 1.2.2). These studies, however, only describe the effect that the conditions in the sales room have on the display cabinet. There are also retroactive effects of the display cabinet on the sales room, some of which have been studied.

The *cold feet* effect and *cold aisle* effect describe spatial temperature gradients within the sales room and originate in the air exchange between open display cabinets and the sales room air (Orphelin et al. 1999, Ndoye et al. 2011). In the area of the sales room where many display cabinets are located, the air temperature can be lower than in other zones of the sales room. This is because of heat transfer to the cabinets and air spillage. When open display cabinets are located face to face, radiative heat transfer into the cabinets is also affected. In system simulations, this is sometimes accounted for (Cecchinato et al. 2010a). The cold feet effect describes vertical temperature gradients in the area where the display cabinets are located. The temperature difference between the feet and the head ranges between 6 °C and 13 °C (Ndoye et al. 2011). The cold aisle effect describes horizontal temperature gradients in the sales area. Specifically it refers to the lower temperature in the area where display cabinets are located, compared to other areas without display cabinets.

Other retroactive effects, such as the dehumidification of the sales room air because of the air exchange with display cabinets, are also well known (Howell et al. 1997, 1999). The building simulation program EnergyPlus (U.S. Department of Energy 2018) considers this retroactive effect of display cabinets on the sales room via an energy balance for latent heat. This approach has also been described by Howell et al. (1997). For a complete and consistent analysis and the modelling of interactions in a supermarket, the modelling of balance equations for energy and substances such as water and CO_2 is required (Howell et al. 1997, IEA Heat

Pump Centre 2011). In this thesis, this is called physical modelling. In addition to balance equations for each subsystem, the interactions between them also have to be described as transport processes for mass and energy.

Although there are several tools designed and used for the simulation of entire supermarkets, there are very few that describe the interactions based on the transport of heat and substances between the subsystems. Arias (2005) describes all the relevant interactions in the conceptual models and presents the balance equations for CO_2 and water (Equations 5.37, 5.38). However, the dehumidification effect of display cabinets is not expressed in terms of variable mass flow rates of air, but considered in one joint term together with water generation from people and equipment. The production of CO_2 by people is considered via a parameter. Marciniak (2016) states the energy and moisture balance for sales room air. The interactions between sales room air and the environment as well as sales room air and display cabinets are expressed via mass flow rates of air. This publication actually also investigates the dehumidification effects of display cabinets on the sales room air. The balance equations of this work are based on Dong et al. (2013), which gives the mass balance for water vapour of the sales room. The air flow between display cabinets and sales room area is assumed to be constant. Arias (2005) and Marciniak (2016) describe the interaction between the display cabinets and the sales room air based on the transport of heat and substance. The assumption of a constant mass flow rate is a simplification, since door openings of display cabinet doors by customers significantly increase the air exchange. This thesis analyses the effect of door openings on the air exchange between the display cabinets and the sales room air (Chapter 3) and consider these effects for the prediction of the humidity in the sales room air (Chapter 6).

Challenges

An overall high efficiency of supermarkets can only be reached if the supermarket as a whole is taken into consideration (IEA Heat Pump Centre 2011). This requires taking into account the interactions between the subsystems in a quantitative way. Many effects in supermarkets have been quantified widely, such as the dependency of the cooling load of an open display cabinet on the temperature and humidity of the sales room, which arises from the air exchange between the cabinet and the sales room. The retroactive effect, the cooling and dehumidification of the sales room air, is rarely quantified, but highly relevant for the design and operation of heating, cooling and ventilation systems. In order to consider this, physical modelling of the interactions based on balance equations and transport processes of heat and substance are necessary. Some simplified modelling of isolated effects has been done, but there is a lack of physical modelling of the interactions between thermal systems on the scale of an entire supermarket.

1.2.2. Display cabinets

Refrigerated display cabinets are a crucial element in a supermarket. They store and present chilled and frozen food. The different kinds of display cabinets can be distinguished in terms of their specific temperature range: medium temperature (MT) (0 °C to 6 °C) for chilled food, and low temperature (LT) (−20 °C to −25 °C) for frozen food. To maintain the cabinets at the desired temperature level, a refrigeration system is required. Further distinctions can be made regarding the design (vertical vs. horizontal cabinets), the existence of doors/lids (open vs. closed cabinet) and the type of refrigeration system (self-contained vs. multiplex cabinets). Self-contained display cabinets have an integrated refrigeration system inside the cabinet and only need an electricity supply. By contrast, multiplex cabinets only have a heat exchanger, which is connected to a centralised refrigeration system, typically located in a machinery room.

There are two crucial aspects to be considered regarding display cabinets. Firstly, food safety, which is linked to variations in temperature. Secondly, energy consumption, which is linked to the cooling load. In the following, the state of the art regarding relevant aspects of display cabinets is presented.

Temporal and spatial distribution of temperature

Besides an appealing presentation of the goods, refrigerated display cabinets have to maintain the food at the desired temperature level. However, the temperature fluctuates. It varies depending on the location inside the cabinet, so goods closer to the cold air supply usually have a lower temperature than those at the front. There are also temporal fluctuations. The evaporator is often on/off controlled based on the temperature inside the cabinet. Additionally, the temperature varies during the defrost cycle. In order to comply with the statutory temperature limits, the temperature distributions inside the cabinets and the temporal fluctuation are investigated. In their study on the spatial temperature distribution in open and closed display cabinets, Patryarcha and Dreisbach (2013) looked at both normal operation and faults, such as failure of a fan, frosting of the evaporator, or a blocked return air grill. They proposed a new control strategy that uses a temperature range instead of a representative foodstuff temperature for the controller. Evans et al. (2007) investigate in which location inside different types of display cabinets the highest product temperatures occur. They found that the highest and lowest temperatures can be found in similar locations. Chaomuang et al. (2019a) investigated temporal and spatial temperature variation in a vertical, closed MT cabinet. They compared operation with and without doors and found that doors are relevant.

Analysing the temporal and spatial distribution of temperature inside a refrigerated display cabinet is important with regard to its design and construction as well as food safety. As for the interactions between systems at the level of an entire supermarket, they can be initially neglected, since, on average, the temperature will fluctuate around its setpoint value. However, these aspects are important to keep in mind for the extension of simulation models to include topics such as food safety, fault detection or the integration of cold thermal storage into a display cabinet.

Cooling load of display cabinets

The energy required to maintain a display cabinet at the desired temperature level is crucial. It depends on the efficiency of the refrigeration system and the cooling load. Efficiency is affected by several factors, such as the type of refrigeration system and the temperature of the heat sink. The cooling load is the heat flow which has to be withdrawn from the interior of the display cabinet in order to maintain its desired temperature. Several effects have an impact on the cooling load. Due to the temperature difference between the sales area and the display cabinet, a heat flow occurs through the cabinet walls. Essentially, this heat flow comprises of convection on the outside of the cabinet envelope and conduction via the envelope. Secondly, internal gains as the heat is dissipated by the fans or the lighting increase the cooling load. Thirdly, the air infiltration from the sales area increases the cooling load. Fourthly, the restocking of foodstuff can lead to an increased cooling load, if the temperature of the goods is higher than the cabinet temperature. Fifthly, the defrost operation can increase the cooling load (Axell and Fahlén 2018). Sixthly, heat transfer via radiation takes places between all surfaces of the cabinet and its surroundings. However, it is usually only relevant for cabinets without doors or lids.

The cooling load and its effects have been widely investigated and quantified. The cooling load is often quantified as the cooling load per *lateral metre* and expressed using the unit $\mathrm{W\,m^{-1}}$. It depends largely on the temperature level (medium/low temperature) and on the

construction type (vertical, horizontal etc.). IEA Heat Pump Centre (2017) reports values of 1470 W m^{-1} for open vertical MT cabinets (0 °C to 2 °C), 725 W m^{-1} for closed vertical MT cabinets of the same temperature and 650 W m^{-1} for closed vertical MT cabinets at 2 °C to 4 °C. Closed LT islands are reported to have a cooling load of 420 W m^{-1} and closed MT islands of 315 W m^{-1}. These are typical values for the total cooling load. Further information can be found in (Cortella and Polonara 2000, Kosar and Dumitrescu 2005). Another topic related to the cooling load is the integration of cold thermal energy storage (CTES) integrated into display cabinets (Manescu et al. 2017, Sevault et al. 2018). They can be used to shift the cooling demand in time and consequently contribute to a demand side management, an increase in overall efficiency, the smaller dimensioning of components (Fidorra et al. 2016), or higher temperature stability inside the cabinet (Fricke et al. 2016).

Contribution of different effects on the cooling load

Depending on the type of cabinet, the share of different effects can differ. In open vertical MT cabinets, air infiltration is responsible for 60 % to 80 % of the cooling load (Faramarzi et al. 2000, Arias 2005, Gaspar et al. 2011, Evans 2014). If this kind of cabinet is equipped with doors, this percentage is reduced to 44 % (Evans 2014). In low-temperature islands the share of the cooling load caused by infiltration is even lower at around 24 % (Faramarzi et al. 2000, Arias 2005). These values do not further differentiate the cooling load caused by infiltration. Heat transfer via radiation is responsible for 6 % to 12 % of the cooling load of open vertical display cabinets (Gaspar et al. 2011). Nowadays, display cabinets usually have doors or lids and, consequently the heat infiltration via radiation is drastically reduced. The effect of air infiltration on the cooling load can be distinguished into sensible and latent heat (Kosar and Dumitrescu 2005). The air in the sales area has a certain humidity. The temperature of the heat exchanger inside the display cabinet is usually lower than the dew point of the air in the sales area. Looking at the heat exchanger inside the cabinet, the cooling load can be divided into several parts: 1. cooling the air, 2. condensation of water, 3. cooling of condensate, 4. freezing of condensate, 5. cooling of ice (Heidinger et al. 2013). The latter effects mainly occur in low-temperature cabinets. However, only the first part helps to cool the cabinet. Thus, the effects 2-5, which are related to the condensate, are attributed to the latent cooling load. In open vertical MT cabinets, this latent cooling load is responsible for approximately 35 % to 40 % of the total cooling load. Air infiltration into display cabinets is highly relevant, especially for open display cabinets. Open display cabinets have an air curtain that acts as a barrier to reduce air infiltration. This air curtain is analysed in various studies, many of them using computational fluid dynamics (CFD) (Gaspar et al. 2008, 2012, Sun et al. 2017, Axell and Fahlén 2018). Closely connected to the air curtain of open display cabinets is the so-called *thermal entrainment factor* (TEF), which is defined as the ratio of air infiltration mass flow to total mass flow of the air curtain. From the energy balance of the air curtain, a definition of the TEF can be derived that allows its calculation based on temperature data. Since it includes the total mass flow rate of the air curtain it cannot be transferred to different types of display cabinets, which may have different air curtains. However, typical TEF values of open type medium temperature vertical display cabinets are 0.1 to 0.5 (Gaspar et al. 2007, Yu et al. 2009). The quantification of the cooling load and the contribution of different physical effects are important for the modelling of display cabinets and their interactions with the sales room air, which is one objective of this thesis. For the modelling of interactions, the retroactive effects that display cabinets have on the sales room air need to be considered, for instance dehumidification. The phenomena described earlier do not include these retroactive effects, but focus on how the conditions in the sales room affect the cooling load of the display

cabinet. However, they can be used as a benchmark and plausibility check for the modelling of interactions developed in this thesis. If the results of these models are in line with previous research, this is a good indication that they also describe the interactions well (4.3).

Part load operation

As seen in the previous section, the cooling load depends on the temperature and humidity of the sales room air. The actual temperature and humidity in the sales room of a supermarket are usually lower than the design point of the cabinets (Vallée 2015), which is why part load operation plays an important role. The specific dependence of the cooling load on the temperature and humidity in the sales area has been investigated by several people. Faramarzi et al. (2000) show that the cooling load of an open vertical display cabinet is reduced by 20 % if the relative humidity is reduced from 55 % to 35 %. Kosar and Dumitrescu (2005) provide an overview of the humidity effects in supermarket display cabinets. Typically, correlations are given that indicate how the cooling load changes with temperature and humidity compared to a reference point. Howell (1993) defined indicators that describe the contribution of individual components to the cooling load at part load conditions. These correlations are often used for the simulation an entire supermarket (Arias 2005, Cecchinato et al. 2010a). Open refrigerated display cabinets often have so-called *night covers* or *night blinds*. These are closed during night time in order to reduce the air exchange between the cabinet and the sales room, significantly reducing the air exchange. This effect is often reflected in a reduced cooling load during nighttime. The assumed reduction with night covers is between 30 % (Franceschi et al. 2011) and 45 % (Cecchinato et al. 2010a). Thus, the cooling load depends both on the conditions in the sales room (temperature and humidity) and the presence of customers. The presence of customers will be described in the next section.

Influence of door openings and customers

Taking out goods from the display cabinet is an integral part of its operation, which, however, has undesired side-effects. There is a difference between open and closed display cabinets. In open display cabinets, the air curtain is affected by customers taking out food or walking in front of the cabinet. Heidinger et al. (2015) analysed the influence of consumers' movement in front of an open vertical refrigerated display cabinet using an automatically moving dummy. They investigated the variation in condensate and temperature at different locations inside the cabinet. To take out food from a closed display cabinet, the doors have to be opened. The door opening has several direct and indirect consequences. The immediate effect of a door opening is a higher air exchange between the display cabinet and the sales room. This increased air exchange leads to temperature fluctuations inside the cabinet. Additionally, it leads to higher moisture infiltration and thus a higher condensate mass flow as well as a higher cooling load. Because of the higher cooling load, electrical energy consumption also rises. The frequency of door openings and the duration of single door openings has been investigated by several authors (Fricke and Becker 2009, Lindberg et al. 2010a,b, Fricke and Becker 2010, Månsson et al. 2019). Lindberg et al. (2010a) found that door opening frequency depends on the time of the day. They also found that there is a huge variation in door openings duration. However, approximately 90 % of door opening durations were below 12 s. Fricke and Becker (2010) also investigated the effect of door openings and specifically the duration. Månsson et al. (2019) equipped the cabinet doors with an accelerometer to investigate, besides the door opening time, also the frequency and speed of the opening and closing process. The door openings affect the air exchange. Higher air exchanges lead to higher return air temperatures (Orlandi et al. 2013) affecting the temperature of goods stored in the cabinet (Lindberg et al. 2010a,b). The specific enthalpy of the return air depends on the air exchange that is affected by the door

opening. Franceschi et al. (2011) considered this by using a higher thermal entrainment factor (TEF) value for an open display cabinet during opening hours. Ultimately, door openings lead to a higher cooling load and increased electrical energy consumption of the refrigeration system (Fricke and Becker 2010, Lindberg et al. 2010a).

Frost and defrosting of heat exchanger

The condensation of water often takes place at the heat exchanger of the display cabinet. At a certain temperature the water freezes. This leads to a degradation of heat transfer. Defrosting systems are used to melt the ice and ensure a proper operation of the heat exchanger. Fricke and Sharma (2011) give an overview of different demand defrost strategies.

Calculation models

There are several approaches and models for the computation and simulation of display cabinets. Computational fluid dynamics (CFD) are widely used to compute open refrigerated display cabinets. Specifically, the airflow patterns of different types of air curtains and the contribution of the infiltrated air to the cooling load are investigated (Cortella 2002, Al-Sahhaf 2011, Sun et al. 2017). In contrast to the analysis of open display cabinets, there are only few CFD-based analyses for closed display cabinets (Orlandi et al. 2013). Visconti et al. (2014) analyse the interaction between low-temperature cabinets and the sales area using CFD. They focus on the energy balance and do not include humidity. There are also some calculations which are aimed at the description of the air curtain. Yu et al. (2009) aim at describing the thermal entrainment factor of the air curtain using correlation models. Ben-abdallah et al. (2018) present a Modelica-based model that describes the spatial and temporal distribution of temperature in an open display cabinet. Chaomuang (2019) describes a model and experimental investigations that focuses on the spatial and temporal distribution of temperature inside a vertical MT cabinet with doors.

Estimation of infiltration rates

The air infiltration from the sales room into the display cabinets is responsible for a large share of the cooling load. In his study of open display cabinets, Al-Sahhaf (2011) distinguishes different measurement techniques for infiltration rate estimation. Among them: 1. collection of condensate 2. "enthalpy measurement": using the thermal entrainment factor 3. tracer gas techniques 4. CFD simulation of tracer gas 5. psychometric method. The tracer gas measurement method has been applied in several studies. Both Vale Pereira et al. (2016) and Afonso and Castro (2008) used sulphur hexafluoride (SF_6) to investigate the air exchange of a household refrigerator. Amin et al. (2009) used CO_2 as a tracer gas to investigate infiltration into open vertical refrigerated display cabinets. They used the "constant concentration method" to estimate the "non-dimensional infiltration rate" (NIR), which is defined as the ratio of infiltration to the total mass flow rate. The NIR is the same as the thermal entrainment factor, but based on the concentration of the tracer gas. Bender (1997) used CO_2 as a tracer gas to estimate air change rates for vehicle cabinets.

Challenges

Display cabinets are very important. They form the connection between the sales room and the refrigeration system. The air infiltration plays a key role for the interaction between the two systems. Nowadays, closed display cabinets are the state of the art. In general, there is a lack of research into closed display cabinets compared to open display cabinets. There is a lack of information about specific values for the air exchange between display cabinets and about the effect of door opening frequency on the air exchange. It is evident and well-documented

that door openings lead to a higher cooling load. However, only the door opening itself and the consequences of the higher air exchange have been investigated. To the author's knowledge, the air exchange that is caused by door openings has not been investigated.

1.2.3. Air exchange between the sales room and the environment

The air exchange between the inside of a building and the ambient air is very important for supermarkets. On the one hand, it increases the heating and cooling demand. On the other hand, it can reduce pollutants in the sales room (Zaatari et al. 2014). The air exchange is often expressed as the *air change rate* ACR (Laussmann and Helm 2011). The air change rate is defined as the ratio between the volume flow of infiltration $\dot{V}$ and the indoor air volume V :

$$\mathrm{ACR} = \frac{\dot{V}}{V} \tag{1.1}$$

It describes how many times the air inside the building is exchanged within a certain time interval. The uncontrolled ventilation of infiltration is often distinguished from mechanical ventilation. The latter type is used on purpose to reduce pollutants. Different factors affect the air exchange, such as location, orientation, building code, wind, and opening areas such as windows or doors (Sawaf et al. 2011). The relevance of each factor depends mainly on the building type. Commercial buildings such as offices or retail stores have a higher occupancy than residential buildings. Consequently, the effect of door openings is more significant. Among commercial buildings, supermarkets are a special case. They usually consist of one large open space, while office buildings usually have many smaller rooms. Additionally, the duration of stay is lower in a supermarket than in an office building and thus the footfall, which will later be defined as customer change rate, is higher. More people enter and leave a supermarket building than an office building. Additionally, people entering and leaving supermarkets use shopping carts. Therefore, the entrance doors in a supermarket are usually larger than in office buildings. The higher people flow through the doors and the typically larger door opening make the entrance one of the predominant factors for air exchange in a supermarket building.

The entrance area is very important for free-standing supermarket buildings. There are different types of entrance door, such as swinging doors, sliding doors or revolving doors. Different measures such as air curtains or vestibules can reduce the air exchange through the doors (Cho et al. 2010, Sawaf et al. 2012, Ye et al. 2017). Although these measures reduce the air infiltration, the number of customers remains an important factor influencing the air exchange: the more people crossing the door, the higher the air infiltration. Yuill et al. (2000) studied air leakage through automatic doors. They describe relevant effects of people crossing automatic doors. These effects, such as the simultaneous crossing of several people, are described as a function of people per hour. Field observations were carried out taking into account the base open time of the door and regression analyses made for these observations. One main result is that the open time fraction of the door and a so-called *air flow coefficient* describing the air exchange can be approximated well by an exponential saturation curve. Kohri (2001) analyses the effect of the opening area of entrance doors on the air flow into an office building. A simulation method is described that takes into account specifically an automatic sliding door and the door opening mechanism. The result consists in the opening time ratio of the door as a function of the number of people crossing through the door. These values are compared with measured data.

There are different methods for an estimation of the air change rates for buildings, such as those described by Younes et al. (2012). Besides theoretical and model-based methods, empir-

ical techniques to estimate the air change rate of existing buildings also exist. The so-called *blow door* method aims at assessing air tightness. It represents a relation between air flow and the pressure difference. For the measurement, a fan is attached to a door or window and used to set a specific pressure difference between the indoor and ambient air and consequently measure the air flow (Sherman and Chan 2004). Other widely used methods are the so-called tracer gas measurements. The concentration measurements of a tracer gas in a mixture of gases is combined with a mass balance, with the aim of estimating the exchange rates of the mixture of gases. Laussmann and Helm (2011) give an overview of tracer gas methods, such as the *concentration decay* method, the *constant injection* method or the *constant concentration* method. Sulphur hexafluoride (SF_6) or carbon dioxide (CO_2) are often used as tracer gases. The tracer gas methods for the estimation of the air exchange in buildings can be distinguished regarding the source of tracer gas. Some methods require dedicated sources of tracer gas, while other methods use the CO_2 produced by the occupants of the building to estimate the air flow rates. Wenig et al. (2017), and Roulet and Foradini (2002) use modified concentration decay methods to estimate the air change rates. They analyse the decay of concentrations after the occupants have left the building and thus no longer serve as a source of CO_2. In addition to the estimation of air change rates, measurement data of CO_2 concentration is also used to estimate the number of occupants (Lu et al. 2011, Titze 2017). Besides the possible usage as a tracer gas, CO_2 in a supermarket is also important for other reasons. It is often used as an indicator for the control of the ventilation system, because it is treated as an indicator of air quality (Umweltbundesamt 2008, Zaatari et al. 2014). There are limits for the concentration of CO_2 in the air; when it becomes too high, the ventilation system is activated. The ventilation system accounts for up to 10 % of a supermarket's energy consumption (Kolokotroni et al. 2014). The factors influencing the CO_2 concentration in the sales room of supermarkets are well known: customers and employees breathe and produce CO_2. The amount depends on the number of customers and their duration of stay. Fruit respiration is another factor that increases the concentration (Poppi 2010, Titze 2017). Air infiltration from the environment, on the other hand, reduces concentration. This can be air infiltration or mechanical ventilation. The natural air infiltration through the doors is affected mostly by customers entering and leaving. The shopping behaviour of customers over the course of a week are repetitive and repetitive patterns of CO_2 concentration can therefore be identified (Poppi 2010, Fidorra 2019b). The overall balance equations for CO_2 considering these effects have been described by Arias (2005), Poppi (2010), and Titze (2017). Marciniak (2016) calculates the air balance of a supermarket sales room. This includes the heating, ventilation and air conditioning (HVAC) system and infiltration via the entrance door. The air exchange through the entrance door with vestibule is approximated with a linear dependency on the number of customers. A CO_2 balance is not included.

Challenges

Air infiltration into buildings and its general effects on the CO_2 concentration in a supermarket building are well understood. The door crossing patterns of entering and leaving occupants, as described by Yuill et al. (2000) and Kohri (2001), show a highly non-linear relation between the flow of occupants and the door opening time. However, to the author's knowledge, relevant effects, such as door crossing patterns as described by Yuill et al. (2000) and Kohri (2001) have not been accounted for in the modelling of supermarket buildings and the estimation of CO_2 concentration.

1.3. Objectives of this thesis

Based on the challenges described in the previous section, the main objective of the thesis is: **Describing the interactions between the thermal systems in supermarkets by means of physical models and quantifying their energetic impact.** The following sub goals are defined:

1. Breakdown of supermarkets into control volumes and definition of *physical interactions* between them. Definition of interfaces that enable modelling of the interactions based on physical phenomena such as heat and mass exchange.
2. Analysis of the air exchange between refrigerated display cabinets and the sales area, in order to model and quantify the relevant interactions between the display cabinets, sales area and refrigeration system.
3. Analysis and description of effects of customers entering and leaving on fresh air change rates

Outlook on the analysis

This thesis develops models and methods for the description and quantification of the interactions between the thermal systems in a supermarket, which are independent of a specific supermarket and can be applied to different topologies of supermarkets. However, one specific *test supermarket* is used throughout this thesis for the exemplification of modelling and simulation methods, for the assessment of the plausibility and accuracy of simulations results, and for the quantification of the interactions. This test supermarket was chosen because, as a modern store, it allows the analysis of the most important energetic interactions.

Chapter 2 deals with **simulation methods and models** that allow the simulation of entire supermarkets with all relevant interactions. It specifies the approach of physical modelling of the interactions. Section 2.3 describes specifically the division of a supermarket into control volumes and the usage of *physical connections* to describe energy and mass flows between these volumes. Physical models of typical supermarket systems such as sales room air, refrigeration system and closed display cabinets are presented.

A specific feature of physical modelling is that the retroactive effects of an interaction between two thermal systems can be described. Figure 1.1 shows a simplified scheme of the supermarket and different control volumes. Each chapter of this thesis will focus on a different control volume and a different interaction will be looked at primarily.

The **air exchange between display cabinets and sales room**, Chapter 3, is one of the most important interactions in a supermarket. For the analysis of this interaction, *individual cabinets* (figure 1.1) are looked at. Firstly, experiments in a laboratory are carried out using CO_2 as the tracer gas. The air infiltration rates into vertical medium-temperature (MT) cabinets, horizontal low-temperature (LT) cabinets and vertical low-temperature cabinets are estimated both for open and closed doors. These results are the main variables describing the interaction between the cabinets and the sales room air. Secondly, the dimensionless air infiltration rate called *thermal entrainment factor (TEF)* for a specific type of display cabinet is estimated based on temperature data from the test supermarket.

The results of the analysis of the air exchange between display cabinets and the sales room are used to parametrise a model of the *refrigeration system and the display cabinets* (Figure 1.1) in the test supermarket. The objective is **to predict the energy consumption of the refrigeration system and display cabinets** (Chapter 4). Especially the electrical power of the compressors and the display cabinets as a function of the ambient temperature, sales room temperature and humidity as well as the customer flow shall be predicted. A good agreement

between measurement data and simulation results is achieved and a thorough plausibility check is carried out.

The second main interaction in a supermarket that is analysed in this thesis is the **air exchange between the sales room and the environment**, Chapter 5. The aim of the analysis is to estimate the air change rates for open and closed doors in an operational supermarket. A model is developed that predicts the CO_2 concentration in the sales room air as a function of sales data, namely the number of receipts and the average number of items per receipt. The control volume looked at in this chapter are *sales room air, ventilation system and occupants* (Figure 1.1).

The **prediction of humidity in the sales room air** is affected by all subsystems of a supermarket, which is why the entire supermarket (Figure 1.1) has to be considered as the control volume. The objective of this chapter 6 is to predict the humidity in the sales room air. Humidity sources inside the sales room, such as plants or bakery ovens, are also relevant; they are therefore analysed and quantified in this chapter.

The final chapter 7 exemplifies several aspects of the planning and benchmarking of a supermarket by using physical models. In particular, it assesses the impact of customers on the cooling load and energy consumption in a supermarket.

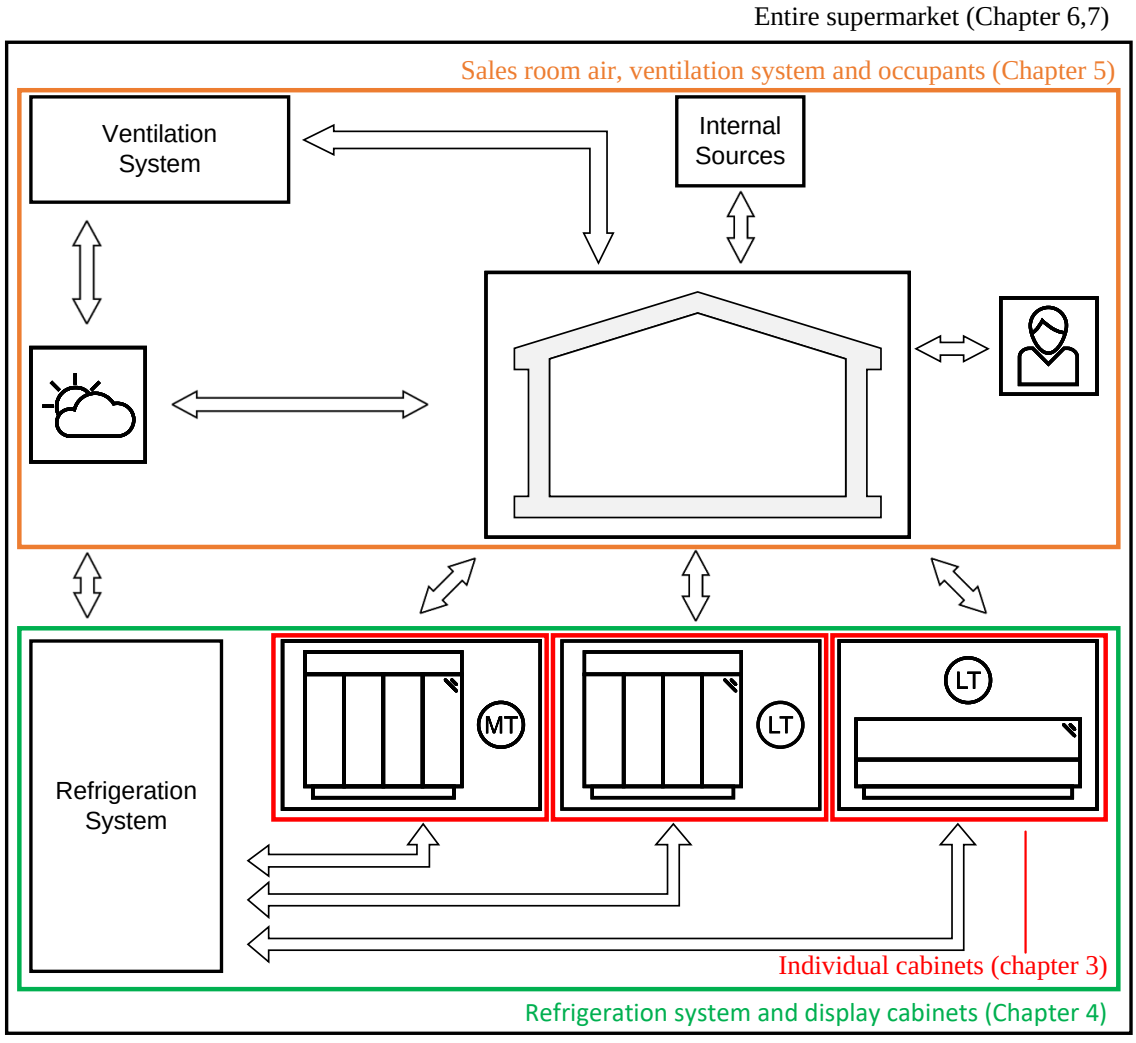

Figure 1.1.: Supermarket subsystems, interactions and analysed control volumes

2. Simulation methods and models

This chapter presents simulation methods and models that allow the modelling of entire supermarkets and prediction of the overall energy consumption. Some of them have been described in previous publications (Fidorra et al. 2014b, Jäschke 2015, Fidorra and Köhler 2016, Martin 2017). The chapter also describes the approach of physical modelling of interactions between subsystems in supermarkets. The term *physical modelling* is somewhat ambiguous and can be used to describe two aspects. Firstly, it can refer to the usage of commonly accepted physical laws for the description of the model behaviour, such as balance equations for energy, mass or momentum. This is often also referred to as *first principle models*. Secondly, it can refer to the physical connection between objects. In the model of a refrigeration cycle, for instance, the outlet of an evaporator can be connected to the inlet of a compressor via a tube. In a graphical representation, this physical connection between the evaporator and the compressor can be drawn as one line. This depiction implies that the conservation laws apply to the transport processes represented by this connection. In the context of the thermal systems in a supermarket, typical connections between objects are the transport of mass and heat. This thesis considers both aspects of physical modelling - model equations based on physical laws and *physical connections* - and, where necessary, specifies which aspect is referred to.

The first section describes how the interactions in a supermarket are considered based on the principles of physical modelling. The second section defines a substance model of air as a mixture of dry air, moisture and CO_2 as it is used here. In the third section, the implementation of simulation models is exemplified by means of the test supermarket. The last section describes the simulation models that are built based on the principles of object orientation and physical modelling according to the usage of balance equations for energy and mass. They can therefore be used for the description of different supermarkets and adapted for further analysis, in addition to the prediction of energy consumption.

The simulation methods and models described here are innovative in several ways. Previous research dealing with the entire supermarket (Cecchinato et al. 2010a, Ge and Tassou 2011a,b, Réhault 2013, Titze 2017) focused on the energetic analysis of a specific supermarket. While this dissertation also gives an energetic analysis (Chapter 7) of the specific test supermarket used throughout, it also has a strong focus on modelling approaches and methods. This supports transferability, so they can be applied to many different types of supermarkets and adapted to different research purposes that go beyond the prediction of energy consumption.

Tools like CyberMart (Arias 2005) or Energy Plus (Stovall and Baxter 2010) are designed for building models of different supermarkets and they include component libraries. However, relevant interactions between supermarket objects, such as the variable air exchange between a display cabinet and the sales room (Chapter 3), are not modelled via *physical connections*. The models described in this thesis depict the interactions between objects in a supermarket as *physical connections* and demonstrate the energetic relevance of these interactions (chapter 7). This physical modelling and the quantification of interactions between the thermal systems in supermarkets is a new contribution to science.

2.1. Modelling of interactions in supermarkets

Supermarkets are complex thermal systems, composed of various subsystems that interact with each other 1.2.1. These interactions often result in effects that can be observed and measured.

A widely investigated effect is the dependence of the cooling load of display cabinets on the temperature and humidity of the sales room air (1.2.2). Thus, the sales room air has an impact on the display cabinet. It is a result of the heat transfer from the sales room into the cabinet and the air exchange between the display cabinet and the sales room. However, there are also retroactive effects of the display cabinet on the sales room air. The sales room air is cooled and dehumidified by the heat transfer from the sales room into the cabinet and the air exchange, because absolute humidity in the cabinet is usually lower than in the sales room. The modelling of an interaction has to consider both the effect and the retroactive effect. This can be achieved by modelling *physical connections*.

There are many relevant aspects of modelling thermal systems such object orientation, information flow and causality, calculation of thermophysical properties, or numerical aspects (Cellier 1991, Tegethoff 1999, Cellier and Kofman 2006, Schulze 2013). This thesis uses the physical modelling approach from Modelica and the TIL library (Richter 2008, Schulze 2013). Modelica is an object-oriented and equation-based modelling language, which is, for instance, implemented in the software tool Dymola. An important feature of Modelica are the connector classes that combine several variables, which are necessary to describe the transport processes between objects (Franke et al. 2009). In this thesis, the connector classes 1. *HeatPort* 2. *GasPort* 3. *LiquidPort* 4. *VLEFluidPort* from the TIL library are used (Schulze 2013). The *heat port* connector is used to describe the transport of a heat flow between control volumes. Two values are needed to be exchanged, temperature T and heat flow $\dot{Q}$. Here, the temperature is the *potential variable*, while the heat flow describes the *flow variable*. For the description of the transport of a substance, there are also flow and potential variables, namely, the potential variable pressure p and the mass flow $\dot{m}$. Furthermore, the concentration vector $\vec{\xi}$ and the mass-specific enthalpy h are the so-called *advective* variables, which specify the substance that is being transported. The models in this thesis use the connector classes that are implemented using Modelica, Dymola and the TIL and TILMedia libraries. Further information can be found in (Richter 2008, Franke et al. 2009, Schulze 2013).

The implementation of models and interactions is, however, not limited to Modelica. The models are presented as general equations for balances and transport processes and can be implemented in any suitable modelling and simulation tool. The *Functional Mockup Interface (FMI)* standard allows the exchange and coupling of models from different simulation environments (Blockwitz et al. 2012). Some considerations developed in this thesis have contributed to the application of *physical connections* using the FMI standard (Tegethoff et al. 2016b,a, Jäschke et al. 2016).

Control volumes and transport processes between them

In this thesis, the subsystems of supermarkets are treated as *control volumes*. A control volume is characterised by several requirements: 1. System boundaries of the control volumes need to be defined. 2. Balance equations need to be fulfilled. 3. The type of interactions with other control volumes needs to be defined.

The choice and definition of control volumes depends on the objective of the analysis. For the analysis of the air exchange between display cabinets and the sales room air 3, individual display cabinets are treated as one control volume. For the analysis of overall energy consumption in the entire supermarket, the control volume is extended and multiple display cabinets of the same type are treated as one control volume. This control volume is called *equivalent display cabinet*, because its interactions are equivalent to those of the multiple, individual cabinets it comprises (see A.1). Depending on the objective of the simulation, dynamic balance equations may be necessary, such as for the description of humidity and CO_2 concentration

in the sales room air (5.4, 6). In other cases, as for instance superheat control of evaporators, dynamic effects can be neglected when only the overall energy consumption of the entire supermarket is of interest (2.4.3).

Interactions between the control volumes are modelled by the transport of heat and substance between them. Two main approaches can be distinguished: 1. calculating the flow variable, such as heat flow or mass flow, as a function of potential variables 2. defining the flow without considering the potential variables. One example of the approach using potential variables is exemplified using the modelling of heat transfer into a display cabinet (see Section 2.4.4). The different mechanisms such heat conduction or convection, are expressed by one overall thermal transmittance. The heat transfer from the sales room air via the cabinet envelope into the cabinet depends on the temperature difference (Equation 2.61):

$$\dot{Q}_{\mathrm{wall}} = (T_{\mathrm{sa}} - T_{\mathrm{cs}}) \cdot k \cdot A \tag{2.1}$$

Here, the flow variable $\dot{Q}_{\mathrm{wall}}$ is calculated based on the difference between the potential variables T_{sa} and T_{cs} using the overall surface of the cabinet A and the thermal transmittance k. This approach of modelling the transport process based on potential variables can be applied because the underlying physics are known and understood.

Another way is modelling without using the potential variable. This approach can be expedient if there is no strong dependency between the flow variable and the potential difference, or if models or required data are not available.

The latter is the case in this thesis: although the air exchange between display cabinets and the sales room has been extensively investigated for cabinets without doors (Yu et al. 2009, Gaspar et al. 2007) there are very few studies of cabinets with doors. This thesis contributes to this field by estimating the air change rates, i.e. is the flow variable, using tracer gas measurements (see Chapter 3). Although it would be possible to develop models describing the air exchange through the gaps between display cabinet doors as a function of geometry and density or pressure difference, no such models are currently available. For the modelling of the air exchange between closed cabinets and the sales room, this thesis uses a simplified approach of calculating the flow variable without considering the potential variable.

2.2. Substance models

The physical modelling of interactions in supermarkets is based on the transport of heat and substances. These substance are air, liquids and refrigerants. The thermophysical properties of these substances are calculated mainly using the TILMedia library (Schulze 2013).

In the context of supermarket modelling, both water vapour and CO_2 are relevant components of air. Water vapour is relevant because it often condenses on the surface of heat exchangers in display cabinets. This increases the cooling load and can lead to frost formation and thus a defrost demand. CO_2 is relevant, because its concentration in the air is a control variable for the ventilation system. Additionally, it is used as tracer gas in this thesis to estimate air change rates between the sales room and the environment (Chapter 5). This section presents the substance model of air used in this thesis, describing specifically the relevant metrics of concentrations and conversions, and is based on Baehr and Kabelac (2012)

Air is a mixture of several gases, such as nitrogen, oxygen, carbon dioxide and water vapour (Tschegg et al. 1984). In this thesis, air is assumed to be a mixture of the ideal gases *dry air*, *gaseous water* and CO_2. This mixture of air has the index *air*. The mass balance can consequently be calculated as:

$$m_{\mathrm{air}} = m_{\mathrm{dryair}} + m_{\mathrm{water}} + m_{\mathrm{CO_2}} \tag{2.2}$$

The mass fractions for each component are consequently defined as:

$$\xi_{\text{dryair}} = \frac{m_{\text{dryair}}}{m_{\text{air}}} \tag{2.3}$$

$$\xi_{\text{water}} = \frac{m_{\text{water}}}{m_{\text{air}}} \tag{2.4}$$

$$\xi_{\text{CO}_2} = \frac{m_{\text{CO}_2}}{m_{\text{air}}} \tag{2.5}$$

The concentration vector $\vec{\xi}$ describes the concentration of the air mixture:

$$\vec{\xi} = \begin{pmatrix} \xi_{\text{dryair}} \\ \xi_{\text{water}} \\ \xi_{\text{CO}_2} \end{pmatrix} \tag{2.6}$$

The concentration of CO_2 is usually expressed as a mole fraction:

$$c_{\text{CO}_2} = \frac{n_{\text{CO}_2}}{n_{\text{air}}} \tag{2.7}$$

The amount of substance n can be converted into the mass m via the molar mass M:

$$m_{\text{CO}_2} = c_{\text{CO}_2} \cdot m_{\text{air}} \cdot \frac{M_{\text{CO}_2}}{M_{\text{air}}} \tag{2.8}$$

The mass fraction of CO_2 can consequently be calculated as:

$$\xi_{\text{CO}_2} = \frac{m_{\text{CO}_2}}{m_{\text{air}}} = c_{\text{CO}_2} \cdot \frac{M_{\text{CO}_2}}{M_{\text{air}}} \tag{2.9}$$

For the description of moist air, the so-called humidity ratio x is often used that is defined as the ratio of water to dry gas:

$$x = \frac{m_{\text{water}}}{m_{\text{dryair}}} \tag{2.10}$$

The concentration of CO_2 in the air considered in this work is typically below $n_{\text{CO}_2} < 2500\,\text{ppm}$ and consequently the mass fraction of CO_2 is small: $\xi_{\text{CO}_2} < 0.5\,\%$. Here, the humidity ratio of the mixture of air is approximated by considering the gaseous CO_2 as part of the dry gas:

$$x = \frac{m_{\text{water}}}{m_{\text{dryair}}} \approx \frac{m_{\text{water}}}{m_{\text{dryair}} + m_{\text{CO}_2}} \tag{2.11}$$

This thesis uses the following nomenclature. The subscript *air* refers to air as a mixture of dry air, water vapour and CO_2. If the mass or mass flow of one of these components is meant, it is indicated by the corresponding subscript. The specific enthalpy h is used as the mass-specific enthalpy of the entire air.

2.3. Modelling entire supermarkets

In the previous section, general considerations regarding physical modelling were presented. The test supermarket used in this thesis A.1 is shown in Figure 1.1 using an abstract representation of interactions.

This section describes the physical interactions in a supermarket. The objective of the analysis shall be the estimation of overall energy consumption of the refrigeration system and

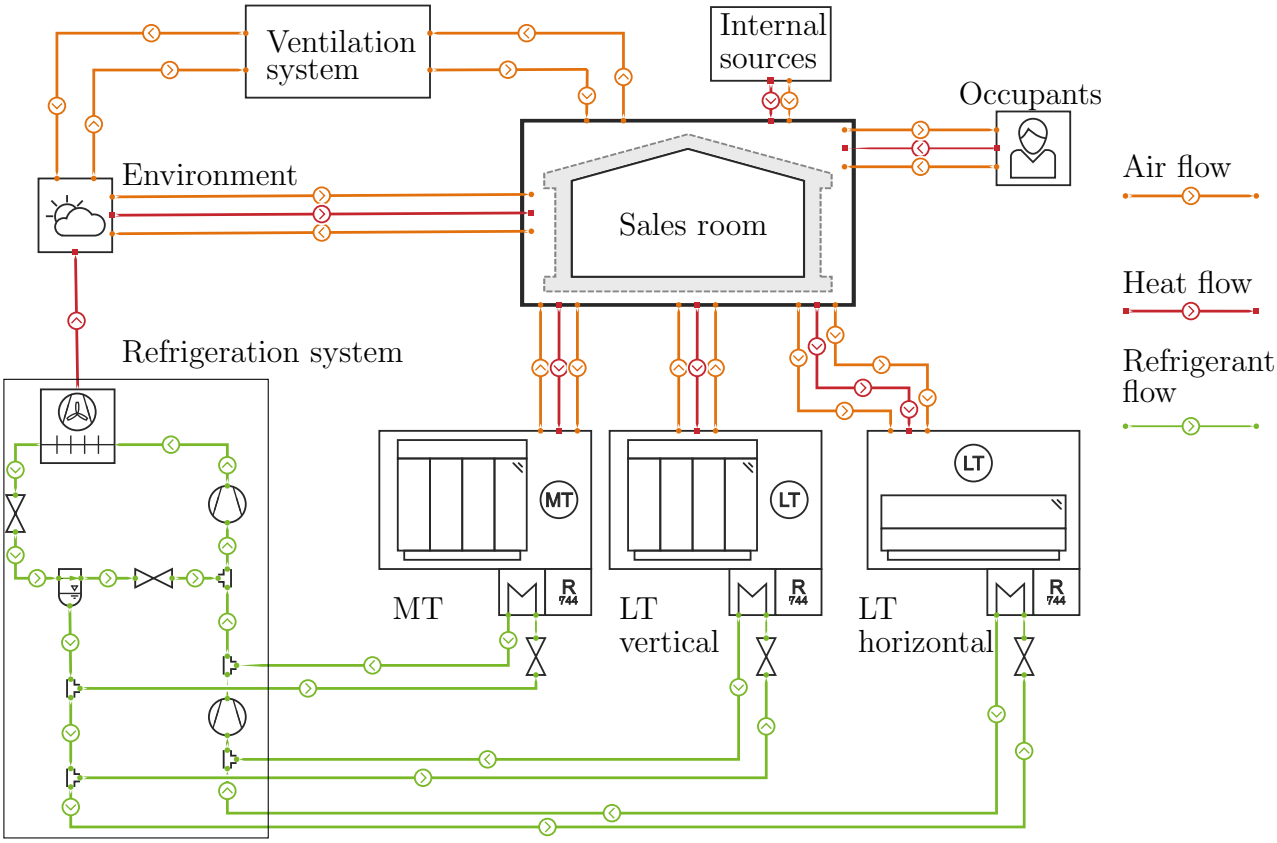

Figure 2.1.: Entire supermarket and *physical connections* (Chapter 2.1) between subsystems. The air exchange between display cabinets and the sales room air is analysed in Chapter 3. The air exchange between the sales room and the ambient air is analysed Chapter 5. The humidity sources are quantified in in Chapter 6.

the display cabinets. Figure 2.1 shows the test supermarket comprising of different control volumes. The interactions are represented as *physical connections*, i.e. each line drawn between two control volumes represents one of the heat or mass flows described above. It is important to note that both the graphical representation and the physical modelling of these connections is tool-independent. Modelica is used in this thesis but the models and approaches that are presented can also be implemented using other tools.

The interactions between display cabinets and the sales room air are described by two mass flows of air, one inflowing and one outflowing, and one heat flow. The air is a mixture of gases (see previous section) that includes humidity. The air exchange between display cabinet and sales room is expressed by two air flows that combine all air flows that enter and leave the cabinet. All heat flows entering the display cabinet via different parts of the casing are summarised in one heat flow. The interaction between the display cabinets and the central refrigeration system is represented by two mass flows of refrigerant: one liquid refrigerant entering the cabinet, and one of gaseous refrigerant flowing back into the refrigeration system.

The customers staying in the sales room act as a source of heat, moisture and CO_2. The heat transfer to the sales room air is represented by one heat flow. Inhaling and exhaling are represented by two mass flows of air. Again, the air is a mixture of dry air, moisture and CO_2.

The air exchange between the sales room air and the environment via the entrance is represented by two air flows, one represents the inflowing air and the other the outflowing air. The interaction between the building and the environment cannot be generalised, since it is

largely specific to the kind of building, its location, the building code and other aspects.

For the control volume of the display cabinets, the approach of *equivalent cabinets* mentioned earlier is used. This means that display cabinets of a similar type are combined into one model. The display cabinets in this supermarket (see detailed description in Section A.1) are represented by three *equivalent cabinets* that are connected to the central refrigeration system (Figure 2.1):

1. medium-temperature cabinets *MT*
2. vertical low-temperature cabinets *LT,vertical*
3. horizontal low-temperature cabinets *LT,horizontal*

Advantages of physical modelling

The breakdown of a supermarket into control volumes as described earlier and the modelling of interactions via *physical connections* have several advantages. Firstly, modelling and simulation are independent of a specific software, tool or language. Modelica, which is used in this thesis, is just one example. Previous publications have shown how a supermarket can be aggregated using several *Functional Mockup Units (FMU)* (Tegethoff et al. 2016a, Jäschke et al. 2016). Secondly, the object-oriented approach allows the definition of an arbitrary system layout of a supermarket. This aspect is a basic feature of the Modelica language and its libraries. However, applying this approach to the modelling of supermarkets is not very common. Thirdly, the structure of the model based on control volumes and physical relations simplifies the modelling process. The connecting lines between the control volumes represent *physical connections* and are, consequently, easier to understand. Figure 2.2a shows a very simple supermarket comprising of only four control volumes: one cabinet, a refrigeration system, a building and the ambient air. In Figure 2.2a, each connecting line between control volumes represents a heat or mass flow. The same system of four control volumes but with signal-oriented connections is shown in Figure 2.2b. The underlying physical interactions between the control volumes are barely recognisable. Given a modelling environment that implements the usage of physical relations (such as Modelica/TIL), building and understanding a complex system model is much easier than using a software that is signal-oriented.

Summary physical modelling

In the following, models for each control volume will be presented, which are suitable for the simulation of a supermarket. For each of the control volumes, balance equations and transport processes describing the heat and mass transfer between them are defined. The models are chosen with the objective of predicting the energy consumption of the refrigeration system and display cabinets as well as the humidity and CO_2 concentration in the sales room. This is an object oriented approach for simulation of the supermarket. Thus, different models and equations can be implemented, depending on the objective of the simulation.

2.4. Simulation models

The simulation models described here are based on object oriented principles. That means: 1. The models can be used to build different topologies of supermarkets. 2. The models can be replaced by other models that consider more details. For instance, it would be possible to build dynamic models with controllers and use them in combination with the other models.

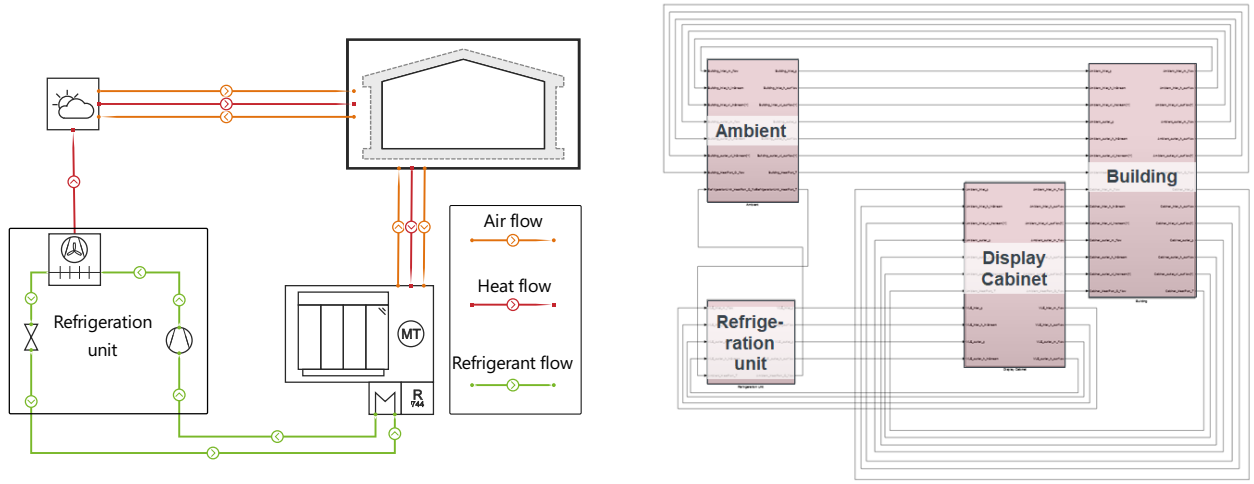

(a) Representation using *physical connections*. Each connecting line between control volumes represents a heat, mass or enthalpy flow.

(b) Representation using signal oriented connections. Each connecting line represents the signal flow of a single variable from one control volume to another.

Figure 2.2.: Representations of a simple supermarket system based on the physical modelling and signal-oriented modelling of interactions respectively (Tegethoff et al. 2016b).

2.4.1. Occupants

Both customers and employees in the sales room are modelled using the occupant model. The control volumes comprise bodies and clothes. Occupants, also referred to as *people staying the in sales room*, breathe and release heat into the sales area. Additionally, they release moisture because of sweating. These aspects can be modelled using three physical interactions: 1. mass flow of air representing inhaling 2. mass flow of air representing exhaling 3. heat flow $\dot{Q}_{\text{people}}$. The mass flow rates of inhaling and exhaling are assumed to be equal and are referred to as $\dot{m}_{\text{breathing,per,person}}$. On rainy days customer may also enter the supermarket with wet clothes which can also lead to a release of moisture into the sales room air. However, this aspect is not modelled here. It is assumed that all people staying in the supermarket are equal in terms of breath mass flow and produced heat. The corresponding flows are defined as specific values for each person. To estimate the total heat and mass flows, the specific values are multiplied with the number of people staying inside the sales area at each point in time. This number is called n_{people} and its estimation will be described later when establishing the balance equation for the number of occupants for the sales room (see 5.1). The overall mass flow rate of breathing is:

$$\dot{m}_{\text{breathing,people}} = n_{\text{people}} \cdot \dot{m}_{\text{breathing,per,person}} \tag{2.12}$$

The heat flow released by occupants is:

$$\dot{Q}_{\text{people}} = n_{\text{people}} \cdot \dot{Q}_{\text{per,person}} \tag{2.13}$$

The parameters of the people model are shown in Table 2.1 and are based on Voigt (2018).

2.4.2. Sales room air

The sales room is the place where display cabinets are located and where customers shop. Additionally, it exchanges air with the environment. These interactions take place via the air of the sales room, which is why the *sales room air* is a separate control volume that consist

Parameter	Value	Description
$\dot{m}_{\text{breathing,per,person}}$	$0.7\,\text{kg}\,\text{h}^{-1}$	Mass flow rate of breathing
$\dot{Q}_{\text{per,person}}$	$50\,\text{W}$	Heat flow produced
$T_{\text{breathing}}$	$30\,^{\circ}\text{C}$	Temperature of breathed air
$x_{\text{breathing}}$	$22\,\text{g}\,\text{kg}^{-1}$	Humidity ratio of breathed air
$c_{\text{CO}_2\text{,breathing}}$	$40\,000\,\text{ppm}$	CO_2 concentration of breathed air

Table 2.1.: Parameters of the people model

of the entire air inside the sales room. The boundaries of this control volume are all the surfaces that the air in the sales room comes into contact with. The sales room air interacts with people, display cabinets, the ventilation system, internal sources and the environment via heat and air flows. Air flows are exchanged with people, display cabinets, the environment, and the ventilations system. Each exchange of air flows is modelled as one ingoing and one outgoing air flow. Heat flows leave the control volume towards the display cabinets; they enter the control volume from customers and other heat sources in the sales room. Depending on the ambient conditions and the building envelope, additional heat transfer from or to the building envelope may occur.

The sales room air control volume includes only balance equations. The transport processes of interactions with other control volumes are defined by these other control volumes. The people model, for instance, defines the mass flow rate of breathing.

Balance equations sales room air

As previously defined, the air is a mixture of several gases with $\vec{\xi}$ being the vector describing the concentration of the components the gas mixture is composed of. Here, a dynamic mass balance is needed, because the dynamic behaviour of CO_2 and humidity concentrations are of interest for the analysis in this work. The mass balance considers the mass flows of each control volume interacting with the sales room air (Figure 2.1). The general mass balance of the sales room air is:

$$\begin{aligned} m_{\text{air,sa}} \cdot \frac{\mathrm{d}\vec{\xi}_{\text{sa}}}{\mathrm{dt}} = {} & (\dot{m}_{\text{air,inf}} + \dot{m}_{\text{air,vent}}) \cdot (\vec{\xi}_{\text{amb}} - \vec{\xi}_{\text{sa}}) \\ & + \dot{m}_{\text{air,MT,cab}} \cdot (\vec{\xi}_{\text{MT,cab}} - \vec{\xi}_{\text{sa}}) \\ & + \dot{m}_{\text{air,LT,cab,horiz}} \cdot (\vec{\xi}_{\text{LT,cab,horiz}} - \vec{\xi}_{\text{sa}}) \\ & + \dot{m}_{\text{air,LT,cab,vert}} \cdot (\vec{\xi}_{\text{LT,cab,vert}} - \vec{\xi}_{\text{sa}}) \\ & + \dot{m}_{\text{air,ac}} \cdot (\vec{\xi}_{\text{ac}} - \vec{\xi}_{\text{sa}}) \\ & + \dot{m}_{\text{air,breathing,people}} \cdot (\vec{\xi}_{\text{breathing}} - \vec{\xi}_{\text{sa}}) \\ & + \dot{m}_{\text{water,source}} \\ & + \dot{m}_{\text{CO}_2\text{,source}} \end{aligned} \tag{2.14}$$

Since the air is assumed to be a mixture of ideal gases, this mass balance could also be expressed by three separate mass balances for dry air, CO_2 and water. As the concentrations for all components are known, separate mass balances for CO_2 5.4 and water 6 will be used in later chapters.

2.4.3. Refrigeration system

This section describes a model for the simulation of refrigeration systems. The refrigeration system is composed of several control volumes, which often comprise several components including sensors and controllers.

R-744 booster system layout

Refrigeration systems using carbon dioxide (CO_2, R-744) as a refrigerant are the state of the art in supermarket refrigeration. In 2019, more than 23 000 stationary R-744 refrigeration systems were in use in Europe. Around 18 % of supermarkets were equipped with transcritical R-744 refrigeration systems (Chasserot 2020).

Figure 2.3 shows a so-called *R-744-booster* layout with a flash-gas bypass, such as is often used in supermarkets. This system consists of two compressors for low pressure (LP) and high pressure (HP) and two evaporators for low temperature (LT) and medium temperature (MT).

Heat is released into the ambient air in an air-cooled heat exchanger. Depending on the ambient temperature, *subcritical* or *transcritical* operation are distinguished. At low ambient temperatures, the refrigerant coming from the HP compressor condenses in the heat exchanger (subcritical operation). At high ambient temperatures, the refrigerant leaving the HP compressor is in a transcritical state (1). Heat is released into the ambient air through gas cooling, and the heat exchanger (for heat release) is therefore called *gas cooler*. The refrigerant leaving the gas cooler (2) is throttled down to an intermediate pressure level in the *high pressure valve*. After it leaves the high pressure valves (3), it enters the *separator* in the two-phase area. Here it is separated into gaseous (3") and liquid (3') phases. The gaseous phase, called *flash gas*, is throttled to the MT evaporation pressure level in the so-called *flash gas bypass (FGB) valve*. This bypass gives the layout its name, booster FGB. The liquid phase (3') is supplied to the expansion valves and evaporators, which are usually located inside the display cabinets in the sales room. Compressors, valves and separator are located in the machinery room and the gas cooler outside the building. This layout is called a central refrigeration system and the cabinets are *remote display cabinets* with direct evaporation. In the display cabinets, the liquid refrigerant is throttled to the corresponding evaporation pressure. It enters the evaporators as a two-phase fluid (4a, 4b). The expansion valves are controlled by superheat controllers. Consequently, the refrigerant at the evaporator outlet is in the state of superheated gas (5,7). The gaseous refrigerant from the LT evaporator (5) flows back to the LP compressor in the machinery room. The same applies to the gaseous refrigerant from the MT evaporator (7). In the suction manifold of the HP compressor, the superheated gas from the MT evaporator (7), the refrigerant leaving the LP compressor (6), and the refrigerant leaving the flash gas bypass valve (8) are mixed.

The vapour quality at the separator inlet (3) depends largely on the ambient temperature. The higher the ambient temperature, the higher the vapour quality at the separator inlet and the higher the mass flow of the flash gas. Figure 2.3 (right) shows transcritical and subcritical operation of the refrigeration system. The higher mass flow rate of flash gas affects the suction gas temperature of the HP compressor, which will be analysed later (Figure 4.3).

This is the basic layout of a R-744 booster system; there are several modifications and improvements, such as an internal heat exchanger, parallel compression, flooded evaporators, or use of one or multiple ejectors (Gullo et al. 2018a). This basic system is used to exemplify the modelling approach.

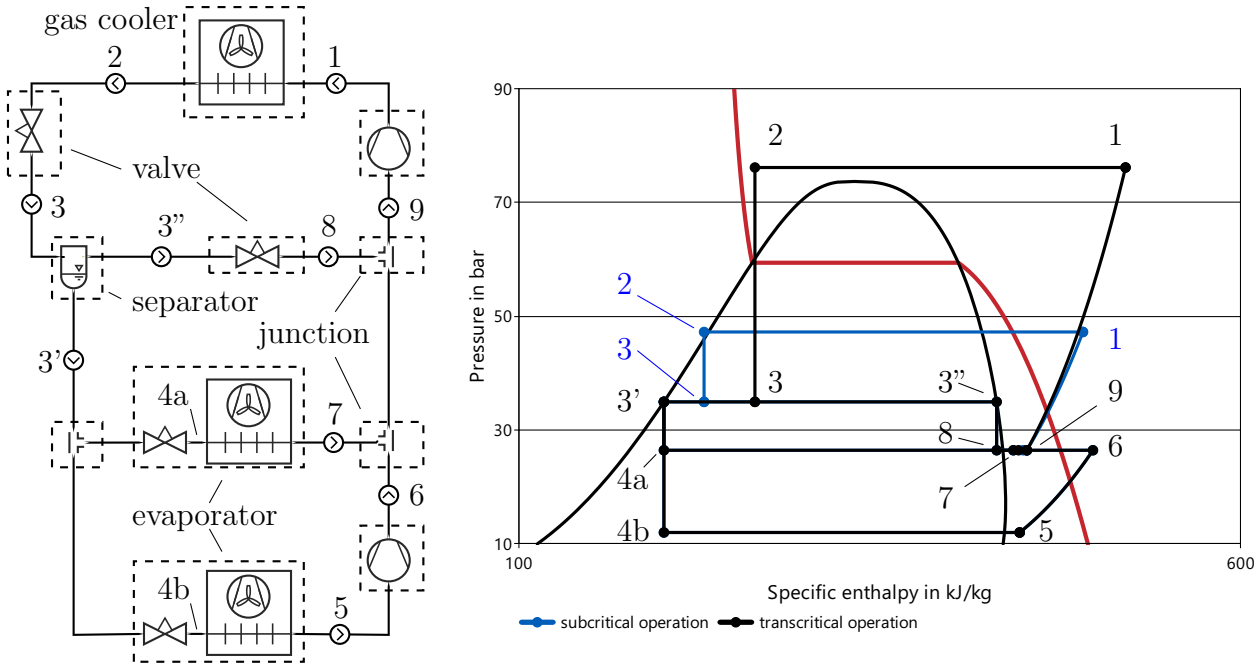

Figure 2.3.: Process flow diagram (left) and ph diagram of a R-744 Booster refrigeration cycle. Additionally, the control volumes for modelling are shown.

Considerations for modelling

The objective of the model is to calculate the electrical compressor power as a function of the cooling load and the ambient temperature. The cooling load is defined as the heat flow absorbed by the refrigerant in the evaporators (Equation 2.20). Faults in single cabinets can have retroactive effects on the refrigeration system. For instance, a fouled evaporator may required the evaporation temperature of the entire refrigeration system to be reduced. This kind of retroactive effect is not considered here.

Following the basic rule for modelling -*as simple as possible, but as complex as necessary*- helps to simplify matters and focus on the relevant aspects. This consideration depends both on the above-mentioned objective of the modelling, and on the available data for verification and validation. Different kinds of models with different degrees of complexity are used in literature for the modelling and simulation of R-744 booster systems. Steady-state models are widely used for the analysis of such systems (for instance, Karampour and Sawalha (2015) and Bellos and Tzivanidis (2019)). Dynamic models that include the sensors and controllers as well as pressure drop and heat transfer models using Modelica and the TIL library have been used by Hafner et al. (2014) and Titze (2017). The measurement data for the test supermarket used in this thesis comprise only a limited number of pressure and temperature sensors with a temporal resolution of 1 h. Neither dynamic effects of single controllers nor the effects of pressure drops on refrigeration or different heat transfer coefficients could be verified using these data. Modelling these effects would be quite a complex undertaking, and whether considering them would contribute to higher accuracy cannot be determined a priori. Therefore, steady-state models are used as an initial approach, and both pressure drops and transport processes in heat exchanger are neglected. Thanks to, the object-oriented approach and physical modelling of interactions, however, it will be easy to use more complex models in the future.

The model equations, which are described in the following section, consist of energy and mass balances and are widely used (Richter 2008, Fidorra et al. 2014b). The model described here

uses the object-oriented modelling language Modelica and implements the energy and mass balance equations. Fluid property data of the refrigerant are calculated using the TILMedia library (Schulze 2013).

Figure 2.3, left shows the process flow diagram and the main components of the R-744 booster refrigeration system. The system is divided into several control volumes such as compressors, evaporators, separator, valve, gas cooler and junction. The model is built following an object-oriented approach, which allows replacing single components of the refrigeration system with more complex models. The model equations are described for each of these components.

Evaporator

The evaporator model includes the evaporator itself, the expansion valves and the superheat controller. A main assumption is that the superheat controller works perfectly and is able to reach the superheat setpoint $\Delta T_{\mathrm{sh,evap,setpoint}}$. The specific enthalpy at the evaporator outlet can consequently be calculated as:

$$h_{\mathrm{out}} = f(p_{\mathrm{out}}, \Delta T_{\mathrm{sh,evap,setpoint}}) \tag{2.15}$$

The steady-state mass balance of the refrigerant is:

$$0 = \dot{m}_{\mathrm{in}} - \dot{m}_{\mathrm{out}} \tag{2.16}$$

The energy balance is:

$$0 = \dot{m}_{\mathrm{in}} \cdot (h_{\mathrm{in}} - h_{\mathrm{out}}) + \dot{Q} \tag{2.17}$$

Suction line

The suction line represents the tubes that transport gaseous refrigerant from the display cabinets to the machinery room. Often, a heat flow is transferred from the surrounding area into the refrigerant inside the tubes, which leads to a *suction line superheat* $\Delta T_{\mathrm{sh,suct,line}}$. It is often described by the temperature difference between inlet and outlet:

$$\Delta T_{\mathrm{sh,suct,line}} = T_{\mathrm{out}} - T_{\mathrm{in}} \tag{2.18}$$

The mass balance is:

$$0 = \dot{m}_{\mathrm{in}} - \dot{m}_{\mathrm{out}} \tag{2.19}$$

The energy balance is:

$$0 = \dot{m}_{\mathrm{in}} \cdot (h_{\mathrm{in}} - h_{\mathrm{out}}) + \dot{Q} \tag{2.20}$$

Pressure losses are generally neglected in the models.

Compressor

The model includes the compressor, a sensor and the suction pressure controller. The compressor is assumed to be adiabatic. This compressor component and its incorporated controller defines the pressure at the inlet, which is the suction pressure. Since the pressure losses are neglected, the suction pressure equals the evaporation pressure p_{evap} that is a parameter of this component. The model is adiabatic and heat losses are therefore not considered. The conditions of the compressor outlet are calculated based on the compressor efficiency. The compressor's effective efficiency equals the isentropic efficiency and as a function of the pressure ratio:

$$\eta_{\mathrm{effis}} = \eta_{\mathrm{is}} = f(\pi) \tag{2.21}$$

The pressure ratio is defined as:

$$\pi = \frac{p_{\text{out}}}{p_{\text{in}}} \tag{2.22}$$

The specific enthalpy at the compressor outlet can be calculated using:

$$h_{\text{out}} = \frac{h_{\text{out,is}} - h_{\text{in}}}{\eta_{\text{is}}} + h_{\text{in}} \tag{2.23}$$

The mass balance is:

$$0 = \dot{m}_{\text{in}} - \dot{m}_{\text{out}} \tag{2.24}$$

The energy balance is:

$$0 = \dot{m}_{\text{in}} \cdot (h_{\text{in}} - h_{\text{out}}) + P_{\text{el}} \tag{2.25}$$

Valve

This component describes a valve that controls the pressure at the inlet, which is an input for this model.

$$p_{\text{in}} = p_{\text{setpoint}} \tag{2.26}$$

This model can be used both for the flash gas valve and the high pressure valve. Isenthalpic throttling is assumed:

$$h_{\text{in}} = h_{\text{out}} \tag{2.27}$$

The mass balance is:

$$0 = \dot{m}_{\text{in}} - \dot{m}_{\text{out}} \tag{2.28}$$

The energy balance is:

$$0 = \dot{m}_{\text{in}} \cdot (h_{\text{in}} - h_{\text{out}}) \tag{2.29}$$

Junction

The junction model is used for splitting or joining three mass flows, which may enter or leave at the connectors named A,B,C. The mass balance is:

$$0 = \dot{m}_{\text{A}} + \dot{m}_{\text{B}} + \dot{m}_{\text{C}} \tag{2.30}$$

The energy balance is:

$$\dot{m}_{\text{A}} \cdot h_{\text{A}} + \dot{m}_{\text{B}} \cdot h_{\text{B}} + \dot{m}_{\text{C}} \cdot h_{\text{C}} = 0 \tag{2.31}$$

Gas cooler

The gas cooler model describes the heat release into the ambient air. The control volume includes the heat exchanger, a fan and a controller. In subcritical operation mode, the gas cooler works as a condenser. The temperature difference between the refrigerant outlet and the ambient air is controlled by the controller and the fan. A refrigerant flow enters and leaves the gas cooler and a heat flow is released into the environment. The refrigerant mass balance is:

$$0 = \dot{m}_{\text{in}} - \dot{m}_{\text{out}} \tag{2.32}$$

The energy balance is:

$$0 = \dot{m}_{\text{in}} \cdot (h_{\text{in}} - h_{\text{out}}) - \dot{Q} \tag{2.33}$$

The specific enthalpy at the outlet of this component is a function of pressure and temperature:

$$h_{\text{out}} = f(T, p) \tag{2.34}$$

The temperature difference between the gas cooler outlet and the ambient air $\Delta T_{\mathrm{gc,amb}}$ is a function of the operation mode and consequently of the ambient temperature:

$$\Delta T_{\mathrm{gc,amb}} = f(T_{\mathrm{amb}}) \tag{2.35}$$

During subcritical operation, there is usually a fixed subcooling and minimum outlet temperature. For transcritical operation, a fixed temperature difference between the ambient air and the gas cooler outlet is normally set. For low ambient temperatures the refrigerant outlet temperature is maintained on a fixed value. Instead of defining the temperature difference, alternatively the gas cooler outlet temperature $T_{\mathrm{gc,out}}$ could be defined.

High pressure control

In subcritical operation, temperature and pressure are not independent, but coupled via the vapour pressure curve. High pressure control for subcritical operation is consequently based on this curve. A specific characteristic of the refrigerant R-744 is the low temperature at the critical point (30.98 °C). For ambient temperatures above this critical temperature, the heat release takes place as gas cooling. In transcritical operation, pressure and temperature are independent and therefore have to be controlled independently. There are advanced control strategies for high pressure control, such as developed by Nöding (2019), but usually the setpoint for high pressure is calculated as a function of the ambient temperature (Liao et al. 2000, Cecchinato et al. 2010b).

$$p_{\mathrm{gc,setpoint}} = f(T_{\mathrm{amb}}) \tag{2.36}$$

The specific function is adapted for each refrigeration system. The function for the test supermarket used in this thesis is described in Section 4.2.1.

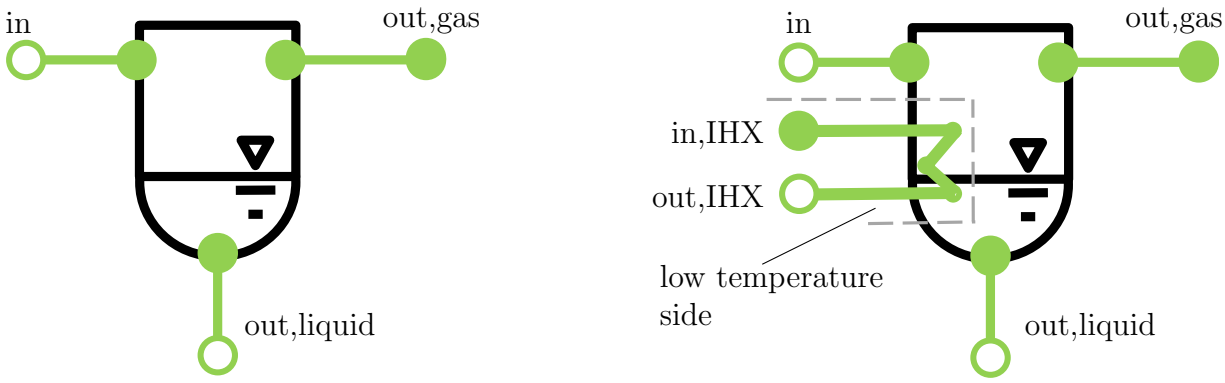

Figure 2.4.: Models of separator. Inflowing two-phase refrigerant is separated into its liquid and gaseous parts. Left: basic separator layout. Right: separator with internal heat exchanger

Separator

The refrigerant leaving the high-pressure valve is usually in the two-phase area. To enhance the efficiency of the refrigeration cycle, separators are used to separate the flow into a liquid and gas flow (Figure 2.4). The inlet flow is assumed to be always in the two-phase area and the separator is assumed to work perfectly. Thus, the state of the gas flow leaving the separator is on the dew line:

$$h_{\mathrm{out,gas}} = h_{\mathrm{gas}} \tag{2.37}$$

Parameter	Unit	Description
$p_{\text{evap,LT}}$	bar	LT evaporation pressure
$p_{\text{evap,MT}}$	bar	MT evaporation pressure
$p_{\text{in,FGB,valve}}$	bar	pressure flash gas bypass valve
$\Delta T_{\text{sh,suct,line}}$	K	MT suction line superheat
$p_{\text{HP}} = f(T_{\text{amb}})$	bar	High pressure function
$T_{\text{gc,out}} = f(T_{\text{amb}})$	K	Gas cooler outlet temperature
$\eta_{\text{eff,is,LP}} = f(\pi)$	-	Effective isentropic efficiency LP
$\eta_{\text{eff,is,HP}} = f(\pi)$	-	Effective isentropic efficiency LP

Table 2.2.: Parameters of the R-744 booster refrigeration system

The liquid outlet is saturated liquid:

$$h_{\text{out,liquid}} = h_{\text{liquid}} \tag{2.38}$$

The mass balance is:

$$0 = \dot{m}_{\text{in}} - \dot{m}_{\text{out,gas}} - \dot{m}_{\text{out,liquid}} \tag{2.39}$$

The energy balance is:

$$0 = \dot{m}_{\text{in}} \cdot h_{\text{in}} - \dot{m}_{\text{out,gas}} \cdot h_{\text{out,gas}} - \dot{m}_{\text{out,liquid}} \cdot h_{\text{out,liquid}} \tag{2.40}$$

Pressure losses are neglected

$$p_{\text{in}} = p_{\text{out,gas}} = p_{\text{out,liquid}} \tag{2.41}$$

and the temperature of the refrigerant depends on the pressure:

$$T_{\text{sep}} = f(p_{\text{sep}}) \tag{2.42}$$

Separator with internal heat exchanger

Many separators have an internal heat exchanger (IHX), which consists of an additional tube inside the separator vessel. The refrigerant inside the IHX tubes has a lower temperature than the refrigerant in the vessel. The purpose of the internal heat exchanger is to condense part of the gaseous refrigerant inside the vessel, reduce the mass flow rate of gas and increase the mass flow rate of liquid refrigerant, which is then fed to the evaporators. The previous separator model is extended to model the internal heat exchanger (Figure 2.4).

A perfect heat transfer is assumed between the refrigerants in the vessel and in the IHX tube: The refrigerant at the IHX outlet reaches the temperature of the refrigerant inside the vessel:

$$T_{\text{out,IHX}} = T_{\text{sep}} \tag{2.43}$$

The mass balance of the high-temperature side is:

$$0 = \dot{m}_{\text{in}} - \dot{m}_{\text{out,gas}} - \dot{m}_{\text{out,liquid}} \tag{2.44}$$

The mass balance of the IHX tube is:

$$\dot{m}_{\text{in,IHX}} - \dot{m}_{\text{out,IHX}} = 0 \tag{2.45}$$

The energy balance is:

$$\begin{aligned} 0 = {} & \dot{m}_{\text{in}} \cdot h_{\text{in}} - \dot{m}_{\text{out,gas}} \cdot h_{\text{out,gas}} - \dot{m}_{\text{out,liquid}} \cdot h_{\text{out,liquid}} \\ & + \dot{m}_{\text{in,IHX}} \cdot (h_{\text{in,IHX}} - h_{\text{out,IHX}}) \end{aligned} \tag{2.46}$$

Summary refrigeration system model

The model described above permits calculation of the compressor power based on the cooling loads in the evaporators and the ambient temperatures. Table 2.2 shows the parameters for a standard R-744 booster system with flash gas bypass as illustrated in Figure 2.3. Some of the parameters describe setpoints of the controllers. For the modelling of an existing refrigeration system, these setpoint parameters can be obtained directly from the monitoring system. Other parameters describe the component behaviour, such as the compressor efficiencies. These parameters can be adapted to catalogue data provided by manufacturers. Chapter 4 describes the validation of a R-744 Booster system. It should be noted that the modelling of the refrigeration system is based on object-oriented principles and *physical connections*. Thus, single models can be replaced with different models that include more effects. Additionally, different refrigeration system topologies, including parallel compression, ejectors etc., can be simulated.

2.4.4. Display cabinets

This section describes a simulation model of a display cabinet. The objective of the model is to calculate the cooling load and condensate mass flow as a function of the temperature and humidity of the sales room air, and the door opening frequency. At the same time, it is intended to account for the retroactive effects of the cabinet on the sales room air, such as dehumidification. The overall aim of the analysis in this thesis is the quantification of interactions between subsystems at the level of an entire supermarket (Section 1.3). Specific details, such as the spatial temperature distribution or air flow patterns inside the cabinet, are not of interest at the moment. The structure of the model is exemplified using a vertical closed display cabinet, but it can also be adapted to cabinets without doors or horizontal cabinets. The model can be used to describe both an individual cabinet and multiple cabinets that are jointly treated as one *equivalent cabinet* (see Section A.1).

The structure of the model described in this section is based on the work by Franceschi et al. (2011) and Ronzoni et al. (2018). A first version of a refrigerated display cabinet model using *physical interactions* was described in Fidorra and Köhler (2016). However, the model used here implies several novelties. Franceschi et al. (2011) describe an open display cabinet using predefined TRNSYS models. The air infiltration is modelled based on fixed parameter values for a dimensionless air infiltration rate, namely the thermal entrainment factor. In this work, the air infiltration is modelled via *physical connections* using parameter values of the actual mass flow rate. This allows specifically state balance equations for dry air and humidity. Ronzoni et al. (2018) describe a self-contained cabinet with doors and an evaporator mounted in the upper part of the cabinet. Although they state energy and mass balances also for water, the analysis focuses on the energy performance of the cabinet and its integrated refrigeration system. They do not specifically analyse retroactive effects on the sales room, such as sensible cooling and the dehumidification of the sales room air. The specific layout of the cabinet with the evaporator mounted in the upper part of the cabinet results in air flows that differ from those of typical remote cabinets with the evaporator located at the bottom of the cabinet.

Chaomuang et al. (2019c) analyse vertical display cabinets with doors and an evaporator mounted in the bottom part (see also Chaomuang (2019) and Chaomuang et al. (2020)). The air mass flow rates of the fan and through the gaps of the door are considered in the balance equations and quantified. However, their focus are on the dynamic air and foodstuff temperatures on different shelves. The retroactive effects on the sales room are not specifically analysed. Door openings are not specifically considered in this model.

The model described in this section consequently contributes some novel aspects to science. It describes all balance equations for water and dry air in such a way that the retroactive effects of cabinets on the sales room air can be analysed and quantified. Additionally, the model describes the influence of door openings on the air infiltration and consequently on the cooling load. The modelling approach, which is based on physical interactions and balance equations, can be easily adapted to include further effects, such as dynamic and spatial temperature distribution.

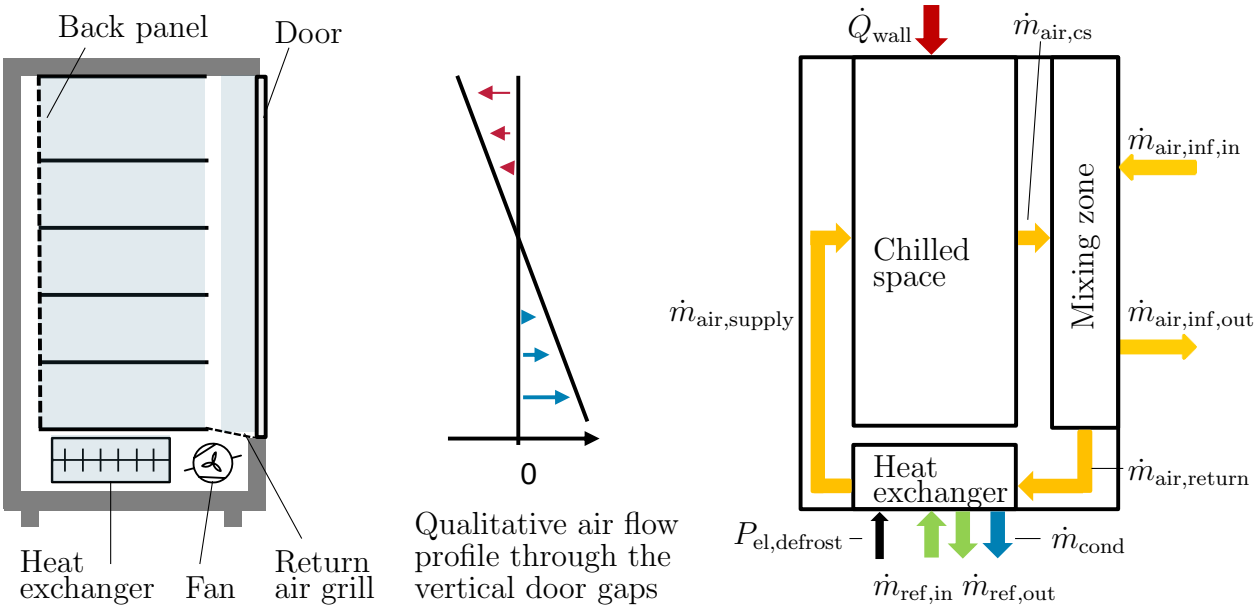

Figure 2.5.: Scheme of a closed vertical display cabinet with doors, the air profile and the control volumes considered for modelling. Air infiltration tends to take place in the upper part of the cabinet and air spillage to the sales room in the lower part.

Overview model

The display cabinet model is based on both aspects of physical modelling: balance equations based on physical laws and *physical connections* (Chapter 2). The model is based on several simplifying assumptions but still satisfies all balance equations. In order to form these balance equations, the display cabinet is divided into three control volumes (Figure 2.5): 1. Chilled space 2. Mixing zone 3. Heat exchanger. Heat and moist air are exchanged between them and the sales area.

The first control volume, called *chilled space*, includes the shelves, back panel, isolated envelope and goods stored in the cabinet. The boundaries of the *chilled space* are crossed by air and heat flows: the *supply air* $\dot{m}_{air,supply}$, coming from the heat exchanger enters the control volume; air leaves the control volume towards the mixing zone ($\dot{m}_{air,cs}$); a heat flow $\dot{Q}_{wall}$ enters the chilled space via the walls, coming from the sales area.

The *mixing zone* is a volume of air that is located between the door and the chilled space. It corresponds to the control volume of an air curtain in open display cabinets. It is called mixing zone, because the air infiltrating from the surroundings $\dot{m}_{air,inf,in}$ mixes with the airflow $\dot{m}_{air,cs}$ coming from the chilled space . There are four air flows entering and leaving the mixing zone. The air flow $\dot{m}_{air,cs}$ from the chilled space enters the mixing zone and leaves it via the *return air grill* (RAG) towards the heat exchanger ($\dot{m}_{air,return}$). Additionally, an air flow from the surroundings $\dot{m}_{air,inf,in}$ enters the mixing zone and leaves the mixing zone again towards

the surroundings $\dot{m}_{\mathrm{air,inf,out}}$. Assumptions regarding the processes inside the mixing zone will be described in the next section.

The third control volume is the *heat exchanger*. It includes both the solid material as well as the fluid inside. Several mass flows cross the boundaries of this control volume. Return air enters the heat exchanger and supply air leaves the heat exchanger. Liquid refrigerant enters the heat exchanger and gaseous refrigerant leaves the heat exchanger. If condensation of water takes places in the air path, an additional mass flow of condensate leaves the heat exchanger control volume.

The air exchange between the cabinet and the sales room is modelled by one incoming $\dot{m}_{\mathrm{air,inf,in}}$ and one outgoing mass flow $\dot{m}_{\mathrm{air,inf,out}}$. The convective and radiative heat flow from the sales room into the cabinet is described by one heat flow ($\dot{Q}_{\mathrm{wall}}$). The model structure is exemplified by a remote vertical display cabinet. The evaporator (Section 2.4.3) is included in this model. The interaction with the refrigeration system is modelled via two mass flows of refrigerant: incoming liquid refrigerant $\dot{m}_{\mathrm{ref,in}}$ and outgoing gaseous refrigerant $\dot{m}_{\mathrm{ref,out}}$. Finally, a mass-flow of condensate leaves the control volume $\dot{m}_{\mathrm{cond}}$.

Assumptions

The model is based on several assumptions. The temperature in the chilled space always equals the setpoint $T_{\mathrm{cs}} = T_{\mathrm{setpoint}}$. The temperature in real cabinets fluctuates because of goods are taken out and because of the dynamic effects of the control system (Chaomuang et al. 2019b). However, in the long term, the average temperature equals the setpoint temperature. The goods are not modelled and consequently the mass of air in the chilled space is assumed to be constant. There are no humidity sources in the display cabinet. The humidity ratio x of the supply air is saturated, unless the humidity in the sales room is below this value:

$$x_{\mathrm{air,supply}} = min(x_{\mathrm{sat}}(T_{\mathrm{air,supply}}), x_{\mathrm{sa}}) \tag{2.47}$$

A comparison with data from the literature (for instance Gaspar et al. (2011)) indicates that these assumptions are justified.

The assumption about the thermophysical condition of air spilled back from the cabinet into the sales room ($\dot{m}_{\mathrm{air,inf,out}}$) differs from those made in other publications. The temperature and humidity of this air flow is important, because it has a huge impact on the retroactive effects of the cabinet on the sales room air. Considering these effects is crucial for the physical modelling of the interactions at the level of the entire supermarket. The lower the temperature and humidity of this air flow, the higher the cooling and dehumidification effect on the sales room air.

For open display cabinets, it is typically assumed that the condition of the air spilled back into the sales area is the same as that of the supply air coming from the discharge air grill (Franceschi et al. 2011). For a closed cabinet with the evaporator mounted in the upper part of the cabinet, the condition of the air flowing from the cabinet into the sales room is the same as that of the air in the chilled space (Ronzoni et al. 2018). Here, a vertical display cabinet with doors and an evaporator located in the bottom of the cabinet is modelled. Research with this kind of cabinet shows the complex pattern of the air flows inside a closed cabinet (Chaomuang 2019), and that the presence of an air curtain affects these patterns. However, the overall tendency is for air infiltration from the sales room into the cabinet to occur in the upper part of the cabinet, while air spillage from the cabinet into the sales room occurs in the lower part of the cabinet (Orlandi et al. 2013). Smoke visualisation carried out complementary to the tracer gas experiments (Section 3.1) supports this observation; the qualitative air flow profile is shown in Figure 2.5. The air flows into and out of the cabinet are modelled using two

air flows: one incoming $\dot{m}_{\mathrm{air,inf,in}}$ and one outgoing $\dot{m}_{\mathrm{air,inf,out}}$. The outgoing air flow represents the air spilled back into the sales room. In this work, it is assumed that the condition of the air spilled into the sales room $\dot{m}_{\mathrm{air,inf,out}}$ is the same as that of return air flowing back towards the heat exchanger inlet $\dot{m}_{\mathrm{air,return}}$.

The electrical power of fans and lighting P_{int} is assumed to be dissipated entirely and added to the energy balance of the chilled space (Equation 2.51).

$$\dot{Q}_{\mathrm{int}} = P_{\mathrm{el,int}} \tag{2.48}$$

Since electric light inside the cabinets is usually switched off at night, the internal electric power is distinguished into $P_{\mathrm{el,int,night}}$ and $P_{\mathrm{el,int,day}}$. The total electrical power consumption of a cabinet consists of the power of fans and lighting and -if applicable- the electrical defrost power, which is described in the following paragraph:

$$P_{\mathrm{el,cab}} = P_{\mathrm{el,int}} + P_{\mathrm{el,defrost}} \tag{2.49}$$

Many effects occurring in the evaporator have an influence on the specific cabinet. Frosted evaporators can increase air pressure losses and reduce air volume flows and the overall heat transfer coefficient (Getu and Bansal 2007, Heidinger et al. 2013) A regular defrost operation can reduce these undesired effects and reduce their energetic impacts (Fricke and Sharma 2011). There are two main defrost strategies, which are typically used and both implemented here: air recirculation and electrical defrosting. Defrosting using air recirculation is only possible in medium-temperature cabinets with an air temperature above 0 °C. During defrost, the evaporator operation stops and frost is melted by recirculating the cabinet air across the heat exchanger. This way, no additional heat enters the cabinet. During electrical defrosting, the evaporator operation stops and frost is melted using an electric heater. During this operation, a large share of the heat is lost to the cabinet, increasing its temperature. This additional heat has to be removed from the cabinet after the defrost operation. In this model, electrical defrosting is considered as an additional heat source for the cabinet.

Balance equations

This section presents the balance equations for the three control volumes (2.5). The enthalpies are mass-specific for the entire mass of air (Section 2.2). If not specified otherwise, the mass flow rates refer to the entire air (subscript *air*). If only dry air or water vapour is referred to, this is indicated by the corresponding subscripts (*dryair*, *water*). Values that are not specifically named in the following equations can be calculated based on the concentration or enthalpy, for instance $T_{\mathrm{supply}} = f(h_{\mathrm{supply}}, \xi_{\mathrm{supply}})$. Together, the equations presented in the following sections form one system of equations that describes the behaviour of the display cabinet model.

Chilled space

The mass balance is:

$$0 = \dot{m}_{\mathrm{air,supply}} - \dot{m}_{\mathrm{air,cs}} \tag{2.50}$$

The energy balance is:

$$\begin{aligned} 0 = {} & \dot{Q}_{\mathrm{wall}} \\ & + \dot{Q}_{\mathrm{int}} \\ & + \dot{m}_{\mathrm{air,supply}} \cdot (h_{\mathrm{air,supply}} - h_{\mathrm{air,cs}}) \end{aligned} \tag{2.51}$$

Mixing zone

There are four mass flows crossing the boundaries of the mixing zone: air from the chilled space $\dot{m}_{\text{air,cs}}$ and the sales room $\dot{m}_{\text{air,inf,in}}$ enter the control volume, and the return air $\dot{m}_{\text{air,return}}$ and air spilled back to the sales room $\dot{m}_{\text{air,inf,out}}$ leave the control volume (Figure 2.5). The humidities of the air flows are usually different and the mass balances for water and dry air are therefore stated separately: Mass balance dry air:

$$\begin{aligned} 0 = &\dot{m}_{\text{dryair,cs}} \\ &+ \dot{m}_{\text{dryair,inf,in}} \\ &- \dot{m}_{\text{dryair,return}} \\ &- \dot{m}_{\text{dryair,inf,out}} \end{aligned} \tag{2.52}$$

Mass balance water:

$$\begin{aligned} 0 = &\dot{m}_{\text{water,cs}} \\ &+ \dot{m}_{\text{water,inf,in}} \\ &- \dot{m}_{\text{water,return}} \\ &- \dot{m}_{\text{water,inf,out}} \end{aligned} \tag{2.53}$$

Energy balance:

$$\begin{aligned} 0 = &\dot{m}_{\text{air,cs}} \cdot h_{\text{air,cs}} \\ &+ \dot{m}_{\text{air,inf,in}} \cdot h_{\text{air,inf,in}} \\ &- \dot{m}_{\text{air,return}} \cdot h_{\text{air,return}} \\ &- \dot{m}_{\text{air,inf,out}} \cdot h_{\text{air,inf,out}} \end{aligned} \tag{2.54}$$

Heat exchanger

Condensation may take place in the heat exchanger and consequently the mass balances both for water and dry air have to be considered. If the dew point of the return air is below the supply air temperature, no condensation takes place and the condensate mass flow is zero (see Equation 2.47). Mass balance of dry air:

$$\begin{aligned} 0 = &\dot{m}_{\text{dryair,return}} \\ &- \dot{m}_{\text{dryair,supply}} \end{aligned} \tag{2.55}$$

Mass balance of water:

$$\begin{aligned} 0 = &\dot{m}_{\text{water,return}} \\ &- \dot{m}_{\text{water,supply}} \\ &- \dot{m}_{\text{cond}} \end{aligned} \tag{2.56}$$

Mass balance of refrigerant:

$$0 = \dot{m}_{\text{ref,in}} - \dot{m}_{\text{ref,out}} \tag{2.57}$$

The following energy balance is valid for MT cabinets with air recirculation defrost:

$$\begin{aligned} 0 = &\dot{m}_{\text{air,return}} \cdot h_{\text{air,return}} \\ &- \dot{m}_{\text{air,supply}} \cdot h_{\text{air,supply}} \\ &- \dot{m}_{\text{cond}} \cdot \Delta h_{\text{water,evap}} \\ &+ \dot{m}_{\text{ref,in}} \cdot (h_{\text{ref,in}} - h_{\text{ref,out}}) \end{aligned} \tag{2.58}$$

Frosting and defrosting do not need to be considered in this energy balance. During the formation of frost, the additional heat of solidification has to be removed from the heat exchanger and consequently the cooling load is increased. However, during defrosting the refrigerant mass flow is zero and the frost/ice is melted by the recirculating air from the cabinet. Thus, the frost cools down the air reducing the cooling load. As long as the specific dynamic effects during defrosting are not of interest, this simplified steady-state energy balance can be applied. However, the condensation of water vapour is very relevant, because of the high specific enthalpy of evaporation $\Delta h_{\mathrm{water,evap}} = 2500\,\mathrm{kJ\,kg^{-1}}$ (Weigand et al. 2010).

Frost formation is more relevant in low-temperature than in medium-temperature cabinets. The condensate solidifies and is cooled down, both of which requires the withdrawal of additional heat by the refrigerant. For the solidification, which starts at $T_{\mathrm{solidif}} = 0\,^{\circ}\mathrm{C}$, the specific enthalpy of fusion $\Delta h_{\mathrm{water,solidif}} = 334\,\mathrm{kJ\,kg^{-1}}$, and for the cooling of the ice $c_{\mathrm{ice}} = 2.1\,\mathrm{kJ\,kg^{-1}\,K^{-1}}$, are relevant parameters (Weigand et al. 2010). During defrosting, which is activated based on a schedule, the ice is melted using electrical heaters that are supplied with the power $P_{\mathrm{el,defrost}}$. Only part of the supplied heat melts the ice, while the remaining part heats up the cabinet. Energy balance for low-temperature (LT) cabinets with electrical defrosting:

$$\begin{aligned} 0 = {} & \dot{m}_{\mathrm{air,return}} \cdot h_{\mathrm{air,return}} \\ & - \dot{m}_{\mathrm{air,supply}} \cdot h_{\mathrm{air,supply}} \\ & - \dot{m}_{\mathrm{cond}} \cdot (\Delta h_{\mathrm{water,evap}} + \Delta h_{\mathrm{water,solidif}} + c_{\mathrm{ice}} \cdot (T_{\mathrm{solidif}} - T_{\mathrm{air,supply}})) \\ & + \dot{m}_{\mathrm{ref,in}} \cdot (h_{\mathrm{ref,in}} - h_{\mathrm{ref,out}}) \\ & + P_{\mathrm{el,defrost}} \end{aligned} \tag{2.59}$$

The relevant effects contributing to the cooling load (sensible cooling of air, condensation of water, solidification of water and cooling of ice) are well known (Heidinger et al. 2013). The objective of this display cabinet model is to assess the interactions in the entire supermarket and their energetic impact. Therefore, this heat exchanger model does not model the heat transfer between the air and the refrigerants. Assuming that a regular and correct defrost operation takes place and that the heat exchanger is properly designed, the specific transport processes inside the heat exchanger can be neglected. This assumption implies that the refrigerant temperature is always lower than the air temperature. These assumptions are justified, since neither the spatial nor the temporal distribution of temperature in single cabinets nor fault detection are of interest here. When referring to the cooling load of a display cabinet $\dot{Q}_{\mathrm{cab}}$, the heat flow absorbed by the refrigerant in the evaporator is meant:

$$\dot{Q}_{\mathrm{cab}} = \dot{m}_{\mathrm{ref,in}} \cdot (h_{\mathrm{ref,in}} - h_{\mathrm{ref,out}}) \tag{2.60}$$

Transport processes across system boundaries of display cabinet

So far, the balance equations for the mass and heat have been described. The interactions of the cabinet are described via *physical connections*, i.e. transport processes of heat and mass across system boundaries. As previously described (Chapter 2), there are different ways of modelling these transport processes. The heat flow transferred from the sales room into the cabinet via radiation and convective heat transfer is treated as one heat flow that enters the cabinet through the walls. This heat flow is determined using a transport relation for heat transfer:

$$\dot{Q}_{\mathrm{wall}} = (T_{\mathrm{sa}} - T_{\mathrm{cs}}) \cdot k \cdot A \tag{2.61}$$

The temperature of the sales room T_{sa} and the temperature inside the cabinet T_{cs} are the potential variables in this interaction. The overall surface of the cabinet is referred to as A.

The thermal transmittance k is assumed to account for all heat transfer mechanisms between the sales room and the chilled space in the display cabinet. The air exchange between the cabinet and the sales room depends on the buoyancy and geometric factors of the gaps between the cabinet doors. The dynamic effects that occur during door opening are even more complex (Orlandi et al. 2013). Therefore, in a first step, the air flow rates are set to fixed values. However, two approaches are described, to take into account door opening frequency, which considerably affects the air infiltration rate.

Infiltration as a function of door opening frequency

Here, a model is described that calculates the overall air infiltration rate. A typical display cabinet has several doors, with the total number of doors n_{door}. Infiltration rates will clearly differ depending on whether a door is open or closed.

In the following, *specific infiltration rates per door* are used: the infiltration rate through the gaps of one closed door is called $\underline{\dot{m}}_{\text{door,closed}}$, the infiltration rate through one open door is called $\underline{\dot{m}}_{\text{door,open}}$. The total infiltration rate of a cabinet can consequently be calculated as:

$$\dot{m}_{\text{inf}} = n_{\text{door,open}} \cdot \underline{\dot{m}}_{\text{door,open}} + n_{\text{door,closed}} \cdot \underline{\dot{m}}_{\text{door,closed}} \tag{2.62}$$

With $n_{\text{door,open}}$ being the number of cabinet doors that are currently open and $n_{\text{door,closed}}$ the number of doors that are currently closed. The number of cabinet doors that are closed can be calculated using the total number of doors:

$$n_{\text{door,closed}} = n_{\text{door}} - n_{\text{door,open}} \tag{2.63}$$

The previous equation 2.62 can be rewritten as:

$$\dot{m}_{\text{inf}} = n_{\text{door,open}} \cdot (\underline{\dot{m}}_{\text{door,open}} - \underline{\dot{m}}_{\text{door,closed}}) + n_{\text{doors}} \cdot \underline{\dot{m}}_{\text{door,closed}} \tag{2.64}$$

This equation is valid for one single moment with a specific number of open and closed doors. In an operational supermarket, cabinet doors are opened and closed all the time and consequently, the number of open and closed doors is changing continuously. The door opening frequency f_{door} can be calculated based on the customer flow $\dot{n}_{\text{customer}}$, which will be presented in Section 5.1, and the number of cabinet doors one customer opens during a visit to the supermarket $n_{\text{door,per,customer}}$

$$f_{\text{door}} = \dot{n}_{\text{customer}} \cdot n_{\text{door,per,customer}} \tag{2.65}$$

The duration of a door opening is not constant. It is specific to each customer and also depends on other factors. It has been investigated by several authors (Fricke and Becker 2009, 2010, Lindberg et al. 2010a,b, Månsson et al. 2019). Here the average duration of one door opening $d_{\text{door,cabinet}}$ is assumed to be constant. The previous equation for the average air infiltration rate can consequently be rewritten as:

$$\dot{m}_{\text{inf}} = f_{\text{door}} \cdot d_{\text{door,cabinet}} \cdot (\underline{\dot{m}}_{\text{door,open}} - \underline{\dot{m}}_{\text{door,closed}}) + n_{\text{door}} \cdot \underline{\dot{m}}_{\text{door,closed}} \tag{2.66}$$

This allows calculation of the total air infiltration into a display cabinet. The required parameters are the specific infiltration rate for each open and closed door as well as the average door opening time. The door opening frequency is an input value and can be calculated based on the customer flow.

Parameter	Unit	Description
n_{door}	-	Number of doors
defrost type		
T_{setpoint}	°C	Temperature setpoint
$t_{\text{defrost,start}}$	time of day	Start defrost
$t_{\text{defrost,end}}$	time of day	End defrost
$P_{\text{el,defrost}}$	kW	Electrical power defrost
$P_{\text{el,int,night}}$	kW	Electrical power nighttime
$P_{\text{el,int,day}}$	kW	Electrical power daytime
$\Delta T_{\text{sh,evap,setpoint}}$	K	Evaporator superheat setpoint
$\dot{m}_{\text{air,fan}}$	$\mathrm{kg\,s^{-1}}$	Fan mass flow rate
$d_{\text{door,cabinet}}$	s	Average duration of door opening
$\underline{\dot{m}}_{\text{door,closed}}$	$\mathrm{g\,s^{-1}}$	Specific infiltration rate, door closed
$\underline{\dot{m}}_{\text{door,open}}$	$\mathrm{g\,s^{-1}}$	Specific infiltration rate, door open
k	$\mathrm{W\,m^{-2}\,K^{-1}}$	Average thermal transmittance
A	$\mathrm{m^2}$	Total surface area of the display cabinet
$n_{\text{door,per,customer}}$	$\mathrm{customer^{-1}}$	Number of door openings per customer

Table 2.3.: Parameters of the display cabinet model

Modelling of infiltration using the thermal entrainment factor

In this section, the definition of the thermal entrainment factor (TEF) is adapted to closed display cabinets. This allows analysis of the air exchange between closed display cabinets and the sales room in operational supermarkets.

The so-called thermal entrainment factor (TEF) is a well-established indicator for open display cabinets, describing infiltration across the air curtain (Section 1.2.2). It is defined as the ratio between the infiltration air flow and the air flow of the fan.

$$\mathrm{TEF} = \frac{\dot{m}_{\text{air,inf,in}}}{\dot{m}_{\text{fan}}} \tag{2.67}$$

While the air flow of the fan is often known, based on a technical data sheet, the air infiltration through the curtain is difficult to measure. But, there are ways to estimate the thermal entrainment factors. For open type cabinets, correlation models are available that describe the effectiveness of the air curtain based on known parameters of the air curtain such as temperature, velocity or geometry (Yu et al. 2009). Based on the energy balance of the air curtain, a formula can also be derived that describes the TEF as a function of the temperatures of the air at the discharge and return air grills and the ambient air (see next section). This allows estimation of the TEF from measurements in experiments (Gaspar et al. 2007). The main benefit of the TEF is thus that the effect of door openings on the infiltration rate can be assessed solely based on temperature measurement data. In a later chapter, this will be demonstrated using a large amount of measurement data and statistical methods (Section 3.2). Knowing the TEF and the mass flow rate of the fan, the infiltration rate can be estimated as:

$$\dot{m}_{\text{air,inf,in}} = \dot{m}_{\text{fan}} \cdot \mathrm{TEF} \tag{2.68}$$

The air infiltration could be consequently be modelled using the TEF as parameter. Franceschi et al. (2011) simulate open display cabinets using fixed parameters for the TEF during daytime and nighttime operation.

One main shortcoming of the TEF is dependency on the fan mass flow rate. The mass flow rate can vary if the evaporator is covered with frost, and a comparison between different types of display cabinets is difficult, since they may have different fan mass flow rates. However, the TEF can be used to compare the operation of display cabinets of the same type. The next section (3.2) describes, how the thermal entrainment factor for closed display cabinets can be estimated based on monitoring data from an operational supermarket. This allows an assessment of the air exchange between a display cabinet and the sales room air based on monitoring data.

Definition of TEF for closed display cabinets

In the following paragraph, the definition of the thermal entrainment factor is derived for closed display cabinets. To best of the author's knowledge, this is new. For open display cabinets, the air curtain is used as the control volume to derive the definition of the thermal entrainment factor. In this thesis, the mixing zone is used as the control volume for closed display cabinets. The steady-state energy balance of a closed display cabinet forms the basis (Equation 2.54).

Assuming that $\dot{m}_{\mathrm{air,return}} = \dot{m}_{\mathrm{air,cs}}$ and $\dot{m}_{\mathrm{air,inf,in}} = \dot{m}_{\mathrm{air,inf,out}}$ and $\dot{m}_{\mathrm{air,return}} = \dot{m}_{\mathrm{fan}}$ we obtain:

$$\begin{aligned} 0 = {} & \dot{m}_{\mathrm{air,return}} \cdot h_{\mathrm{air,cs}} \\ & + \dot{m}_{\mathrm{air,inf,in}} \cdot h_{\mathrm{air,inf,in}} \\ & - \dot{m}_{\mathrm{air,return}} \cdot h_{\mathrm{air,return}} \\ & - \dot{m}_{\mathrm{air,inf,in}} \cdot h_{\mathrm{air,inf,out}} \end{aligned} \tag{2.69}$$

Transforming the equation gives:

$$\dot{m}_{\mathrm{air,return}} \cdot (h_{\mathrm{air,cs}} - h_{\mathrm{air,return}}) = \dot{m}_{\mathrm{air,inf,in}} \cdot (h_{\mathrm{air,inf,out}} - h_{\mathrm{air,inf,in}}) \tag{2.70}$$

This gives:

$$\mathrm{TEF} = \frac{\dot{m}_{\mathrm{air,inf,in}}}{\dot{m}_{\mathrm{air,return}}} = \frac{(h_{\mathrm{air,cs}} - h_{\mathrm{air,return}})}{(h_{\mathrm{air,inf,out}} - h_{\mathrm{air,inf,in}})} \tag{2.71}$$

The air in the mixing zone is assumed to be perfectly mixed. Thus, $h_{\mathrm{return,air}} = h_{\mathrm{air,inf,out}}$. This gives:

$$\mathrm{TEF} = \frac{\dot{m}_{\mathrm{air,inf,in}}}{\dot{m}_{\mathrm{air,return}}} = \frac{(h_{\mathrm{air,cs}} - h_{\mathrm{air,return}})}{(h_{\mathrm{air,return}} - h_{\mathrm{air,inf,in}})} \tag{2.72}$$

For low humidities, the heat capacity of air can be assumed to be constant. The specific enthalpy can then be assumed to only depend on the temperature. The formula can then be rewritten with temperatures instead of enthalpies as: (Gaspar et al. 2011)

$$\mathrm{TEF} = \frac{\dot{m}_{\mathrm{air,inf,in}}}{\dot{m}_{\mathrm{air,return}}} = \frac{(h_{\mathrm{air,cs}} - h_{\mathrm{air,return}})}{(h_{\mathrm{air,return}} - h_{\mathrm{air,inf,in}})} = \frac{(T_{\mathrm{air,cs}} - T_{\mathrm{air,return}})}{(T_{\mathrm{air,return}} - T_{\mathrm{air,inf,in}})} \tag{2.73}$$

This definition of TEF is very similar to other definitions for open cabinets (Gaspar et al. 2007, Yu et al. 2009). However, one main assumption is different: the air is mixed in the mixing zone and the condition of the air spilled into the sales room is the same as that inside the mixing zone. For open cabinets and air curtains, the assumption is that the condition of the air spilled into the sales room is the same as that in the discharge air grill.

Outlook cabinet model

In this section, the simulation model of a display cabinet has been described. This model allows the estimation of the cooling load as a function of the temperature and humidity of the sales room air, and as the door opening frequency. With this model, the retroactive effects of the cabinets on the sales room air can also be described. The model structure is exemplified using a remote vertical closed display cabinet, but the modelling approach can be adapted to other types of cabinets (horizontal, self-contained). Table 2.3 gives an overview of the parameter of the display cabinet model. Some of the parameters, such as the number of doors, the surface area, the defrost type or the internal electrical power consumption, can be taken from a technical data sheet. Other parameters, such as thermal transmittance or air infiltration can be measured in experiments (see Chapter 3) or calibrated using measurement data (see Chapter 4.3). The object-oriented approach used here makes it easy to adapt this model for dynamic models that allow the description of foodstuff and spatial temperature distribution.

3. Analysis of air exchange between refrigerated display cabinets and the sales room

The air exchange between the display cabinets and the sales room is one of the most important interactions in a supermarket. This chapter investigates this air exchange. The objectives are to, firstly, quantify the air exchange between different types of closed display cabinets and the sales room, and, secondly, investigate the impact of door openings on the air exchange. Two approaches are used to investigate these two aspects, namely experiments with tracer gas in a laboratory and the analysis of monitoring data from an operational supermarket. The object of the analyses described here are the *individual cabinets* (figure 1.1).

The air exchange between the display cabinets and the sales room depends on the door openings. More and longer door openings lead to a higher air exchange, which consequently affects the temperature in the cabinet and the cooling load. Previous research focuses on the door opening itself or on the consequences of the air exchange, namely temperature fluctuations and cooling load (Fricke and Becker 2009, Lindberg et al. 2010a,b, Månsson et al. 2019). However, to the author's knowledge, there is no specific research investigating how the mass flow rate of air exchange in closed display cabinets is affected by door openings.

3.1. Experimental investigation of air infiltration rate of display cabinets with doors

The air exchange between refrigerated display cabinets and the sales room is one of the main interactions between the thermal systems in a supermarket. For this dissertation, experiments were carried out with different types of closed display cabinets in order to quantify this interaction. In the experiments, carbon dioxide (CO_2) has been used as a tracer gas for the estimation of typical mass flow rates of the air exchange between the cabinet and the sales area. The experiments and the results imply several novelties that are explained by comparing them with previous research.

Several authors have investigated air infiltration rates using tracer gas. Afonso and Castro (2008) and Vale Pereira et al. (2016) studied the air infiltration of a household refrigerator/freezer. Both used sulphur hexafluoride (SF_6) as a tracer gas. Amin et al. (2009) studied an open refrigerated display cabinet using CO_2 as the tracer gas and steady state methods. Their experiments resulted in non-dimensional infiltration rates.

To the best of the author's knowledge, no tracer gas experiments with closed refrigerated display cabinets have been carried out to date. Thus, the experiments described in this section and the quantification of the air change rates are a new contribution to science.

Experiments with three kind of display cabinets were carried out. This section explains, firstly, the method of tracer gas that was used. It then presents the experiments for a vertical medium temperature, a horizontal low temperature and a vertical low temperature cabinet. The experiments described here estimate the parameters for specific, single cabinets.

3.1.1. Adapted tracer gas method

The usage of a tracer gas to estimate air change rates is a well-established method. Different methods can be distinguished, such as the *concentration decay* method, the *constant injection* method or the *constant concentration* method (Laussmann and Helm 2011). In the experiments described in this section, a modified concentration decay method was used.

The experiments were carried out in a laboratory that has a floor area of 54 m^2 and a height of 2.8 m. In the following, the laboratory is referred to as the *sales area*. It is equipped with two closed vertical medium temperature (MT) cabinets, a vertical low temperature (LT) cabinet and a horizontal low temperature cabinet (*island*).

The small size of the laboratory allowed a specific experiment procedure. At the beginning of each experiment, the room was ventilated until the CO_2 concentration both in the cabinets and the sales area was at an ambient level of approximately 410 ppm. Then, a plastic bag filled with approximately 100 L of gaseous CO_2 was opened, which rapidly increased the concentration in the sales area. Several fans were placed inside the sales area and ensured an evenly mixed air. The CO_2 concentration in the sales area and the display cabinets was measured using Rotronic CP11 measurement devices with a measurement frequency of 0.5 Hz. The accuracy was +/-30 ppm or +/-5 %. When the concentration in the cabinet reached the level of the sales area, the ventilation system was activated again and when the CO_2 concentration in the sales area was at the level of the ambient air a new experiment was started. In the course of the experiments, the method was adapted to the specific requirements of vertical low temperature cabinets (Section 3.1.4). In total, twenty different tests, including those with door openings, were carried out for the three display cabinets.

Parameter estimation

A mathematical model allows the calculation of the air infiltration rates based on the measured concentration curves. This model is described in the following.

There are no sources or sinks of CO_2 inside the refrigerated cabinet. Consequently, the concentration in the cabinet changes solely because of the air infiltration from the sales area. For the following considerations, the entire air inside the display cabinet is treated as the control volume. Assuming that the air in the sales area and in the cabinet is perfectly mixed at all times, the dynamic mass balance for the gaseous CO_2 can be written as follows:

$$\frac{\mathrm{d}}{\mathrm{dt}} m_{\mathrm{CO_2}} = \dot{m}_{\mathrm{CO_2,inf,in}} - \dot{m}_{\mathrm{CO_2,inf,out}} \tag{3.1}$$

The amount of CO_2 inside the cabinet changes because of the air flows exchanged with the sales area. The mass flow of air from the sales area into the cabinet is called $\dot{m}_{\mathrm{air,inf,in}}$ and the mass flow of air from the cabinet into the sales area is called $\dot{m}_{\mathrm{air,inf,out}}$. The mass of the gaseous CO_2 is expressed as a function of the mass of the air $m_{\mathrm{air,cab}}$ and the CO_2 concentration c_{cab}. The corresponding equations have been described in Section 2.2.

It is assumed that the mass flow of water condensing in the evaporator is much smaller than the mass flow rate of air infiltration. Furthermore, it is assumed that the mass variation of air caused by temperature variations inside the cabinet is much smaller than the air infiltration rate. Based on these assumptions, the absolute values of the mass flow of air entering and leaving the cabinet can be considered equal:

$$\dot{m}_{\mathrm{air,inf,in}} = \dot{m}_{\mathrm{air,inf,out}} \tag{3.2}$$

The balance equation for the CO_2 in the cabinet becomes:

$$m_{\mathrm{air,cab}} \cdot \frac{\mathrm{d}c_{\mathrm{cab}}}{\mathrm{dt}} = \dot{m}_{\mathrm{air,inf,in}} \cdot (c_{\mathrm{sa}} - c_{\mathrm{cab}}) \tag{3.3}$$

This can be rewritten

$$\frac{\mathrm{dc_{cab}}}{\mathrm{dt}} = \frac{\dot{m}_{\mathrm{air,inf,in}}}{m_{\mathrm{air,cab}}} \cdot (c_{\mathrm{sa}} - c_{\mathrm{cab}}) \tag{3.4}$$

This equation is an ordinary differential equation. The time constant of the system can consequently be calculated:

$$\tau = \frac{m_{\mathrm{air,cab}}}{\dot{m}_{\mathrm{air,inf,in}}} \tag{3.5}$$

This model has two parameters and two time-dependent variables. The mass of air in the cabinet $m_{\mathrm{air,cab}}$ is the first parameter. It can be calculated with the volume of the cabinet and its air density. As the temperature inside the cabinet is constant, the mass of air is also considered constant.

The temporal progressions of the CO_2 concentrations in the cabinet and the sales area were measured during the experiments. The air infiltration rate is a parameter which is unknown.

There is only one unknown value in an ordinary differential equation. Consequently, it can be estimated. To do so, a dynamic parameter estimation problem must be solved, which is described in the following section.

Dynamic parameter estimation

The aim is to estimate the value of the infiltration mass flow, $\dot{m}_{\mathrm{air,inf,in}}$. The model describes the course of the CO_2 concentration in the cabinet by providing the concentration in the sales area as an input. The simulated concentration $c_{\mathrm{cab,sim}}$ should correspond as closely as possible to the course of the concentration of the measurement $c_{\mathrm{cab,meas}}$. For this purpose, the sum of squared errors *sqe* is defined as:

$$sqe = \int_{\mathrm{t_0}}^{t_1} (c_{\mathrm{cab,meas}} - c_{\mathrm{cab,sim}})^2 \mathrm{dt} \tag{3.6}$$

Equation 3.4 is implemented using Python and an explicit Euler algorithm. The SciPy library (*SciPy* 2019) was used to minimise the sum of squared errors *sqe* 3.6 by variation of the infiltration mass flow.

The Mean Absolute Percentage Error (*Mean Absolute Average Error: MAPE*, Quaas (2019)) was selected as the evaluation variable for the quality of the parameter fitting. This indicator was already used by Titze (2017) to assess the agreement between measured and simulated variables. Here, the MAPE between the estimated and measured concentration in the cabinet is defined as:

$$\mathrm{MAPE} = \frac{\int_{\mathrm{t_0}}^{t_1} \frac{(c_{\mathrm{cab,meas}} - c_{\mathrm{cab,sim}})}{c_{\mathrm{cab,meas}}} \mathrm{dt}}{t_1 - t_0} \tag{3.7}$$

Summary

The method described here differs from the usual concentration decay method. The concentration in the surrounding space was increased and the response of the concentration inside the cabinet was measured. A difference compared to the normal concentration decay method is that the concentration in the sales area was not constant and the differential equation was solved numerically.

3.1.2. Vertical medium temperature cabinet

Initially, tests were carried out on the medium temperature cabinets. These were two adjacent 3.75 m wide cabinets, each with six doors. A total of twelve tests were carried out, eight with the doors closed and four with brief openings of one or more doors to simulate the withdrawal

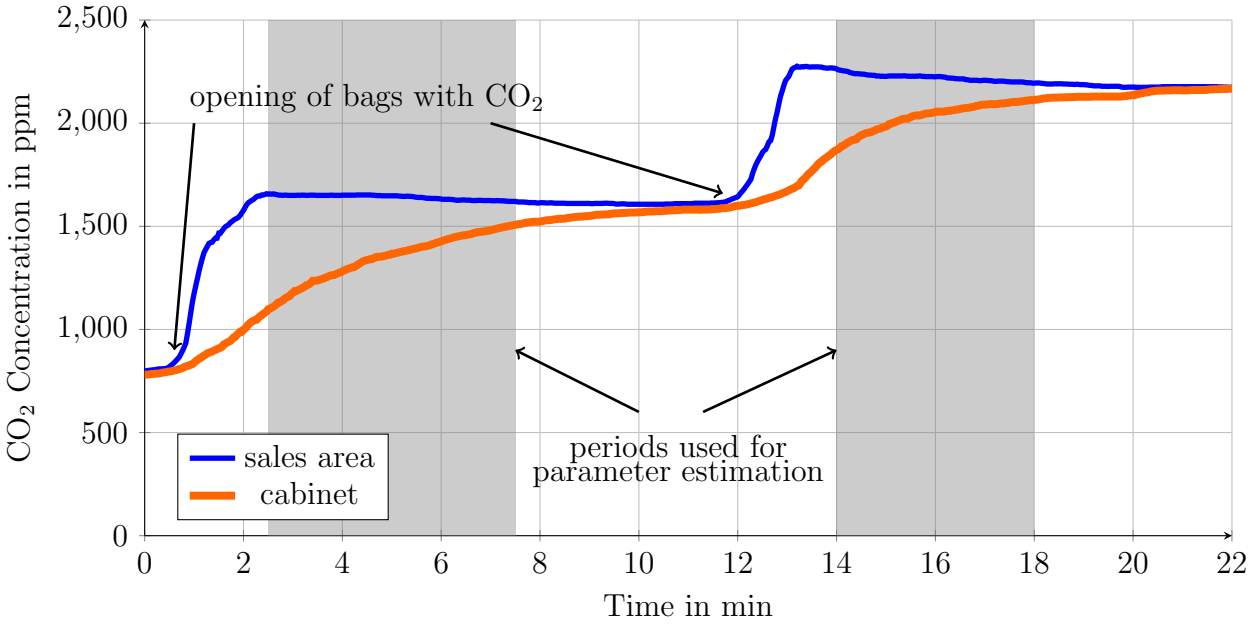

Figure 3.1.: CO_2 concentration in the sales room and in a MT display cabinet as a function of time

of goods. Several of these tests involved two CO_2 sensors, which were located at different positions inside the cabinets. A total of nineteen data sets are available for infiltration rate determination. In the following, an exemplary test run is described.

Experiment description

At the beginning of each test, the sales area and the refrigerated cabinets were ventilated to ensure an equal concentration both in the cabinet and the sales area. In some experiments, the initial concentration was above ambient level because ventilation becomes less efficient and takes more time when the indoor concentration is close to ambient level. Afterwards, a plastic bag filled with gaseous CO_2 was opened and the gas released to the sales area. This led to a sudden increase of the CO_2 concentration by approximately 800 ppm. The temporal behaviour of the concentration inside the cabinet is that of a first order time delay element.

Figure 3.1 shows an example of the CO_2 concentration during a test. The concentration in the sales area and inside the cabinets is shown over the course of time. After opening a bag with CO_2, the concentration in the sales area quickly increases. The concentration inside the cabinet follows the concentration in the sales area with a time delay. After approximately 11 min, the two concentration levels have converged and a second bag with CO_2 is opened. Again, the concentration in the sales area increases rapidly, while the concentration in the cabinet follows with a first order time delay. The concentration levels converge after 8 min.

The difference between the two concentration curves of the cabinet and the sales area (Figure 3.1) will be used to estimate the air infiltration rate between the cabinet and the sales area. The method has some requirements, which have to be considered. For the derivation of the balance equation, a homogeneous concentration of CO_2 in the sales area and inside the cabinet are assumed. Although there are several fans located in the sales area, it takes some time until the CO_2 is evenly distributed in the sales area. A nearly constant concentration in the sales area has been used as an indicator for homogeneously mixed air.

A second requirement for the method is a change in concentration inside the cabinet. This requires a minimal difference in concentration between the cabinet and the sales area. Thus,

No	d_{exp} in s	T_{sa} in °C	T_{cab} in °C	Position	$d_{door,open}$ in s	$\dot{m}_{inf,in}$ in g s^{-1}	MAPE in %
Experiments with closed doors							
1	420	19.9	9.1	Right	Closed	28.2	0.3
2	360	20.2	7.5	Right	Closed	35.7	1.4
3	165	20.7	8.5	Right	Closed	33.4	0.2
3	165	20.7	9.8	Left	Closed	38.2	0.3
4	240	20.9	9.8	Right	Closed	25.8	0.6
4	240	20.9	9.8	Left	Closed	38.3	0.6
5	300	20.2	8.4	Right	Closed	30.6	0.8
6	330	14.8	5.7	Right	Closed	30.1	1.0
7	330	14.9	5.7	Right	Closed	30.6	0.4
7	330	14.9	6.3	Centre	Closed	30.8	1.7
8	330	22.6	4.7	Right	Closed	36.5	0.8
8	330	22.6	10.1	Centre*	Closed	33.9	0.4
Experiments with one door briefly opened							
9	330	14.8	5.9	Centre	10.5	38.4	1.8
10	240	20.3	8.7	Right	7.1	43.9	0.5
			8.5	Centre		47.9	1.8
11	220	20.9	8.9	Right	7.6	50.7	0.5
	220	20.9	8.7	Centre		59.4	1.1
12	300	23.1	5.1	Right	10.0	41.9	0.4
	300	23.1	10.6	Centre*	13.7	41.0	0.4

Table 3.1.: Boundary conditions of the experiments and estimated air infiltration rates into the vertical MT cabinet; (lines marked with "*": sensor located in left cabinet)

the last moments before the two concentrations are the same cannot be used. The periods that fulfil these requirements are marked in Figure 3.1.

Using only periods fulfilling these two conditions has a positive side effect. The CO_2 sensors had a time constant of about 20 s. Using only the periods that fulfil these requirements for the parameter estimation, the effect of the sensor time constant is negligible.

Results and discussion

A total of twelve experiments were carried out using both MT cabinets. The doors of the cabinets were opened during part of the experiments. The position of the sensor inside the cabinet was varied between the experiments. The possible locations were: left, right or centre position on the top shelves of the cabinets (Table 3.1). Some of the experiments included the usage of two sensors in different locations inside the cabinets. In total, nineteen time series from twelve experiments could be used to estimate infiltration rates using the method described.

The boundary conditions of the experiments and the estimated air infiltration rates are shown in Table 3.1 and Figure 3.2. For each parameter estimation, the duration of the time series, the temperature in the sales area and cabinet, the location of the sensor and the door status are given. The parameter estimation implies the calculation of the concentration curve inside the cabinet. The mean absolute percentage error (MAPE) between the calculated and measured concentration curve in the cabinet (Equation 3.7) is always lower than 1.9 %,

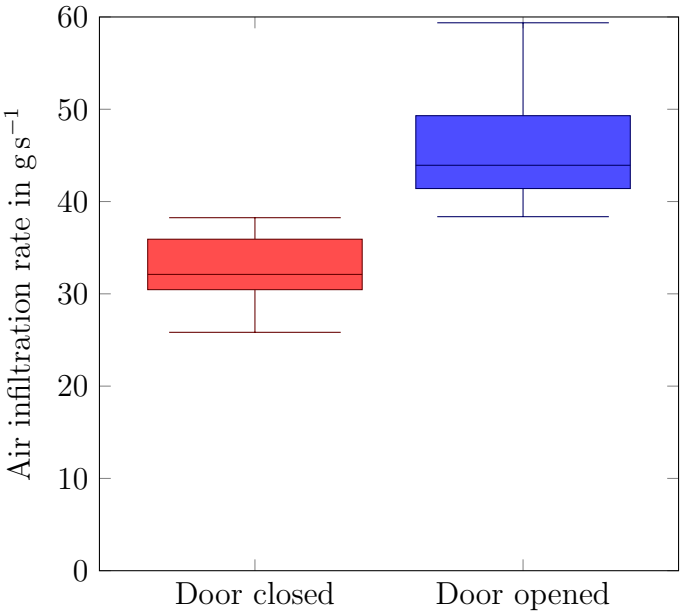

Figure 3.2.: Boxplot of estimated air infiltration rates into a vertical medium temperature cabinet in g s^{-1} depending on the opening status of the cabinet doors. The experiments lasted between 165 s to 420 s and the door openings lasted 7 s to 14 s

which means that the simulated dynamic concentration inside the cabinet is in very good agreement with the measured concentration. The mathematical model (Equation 3.4) seems to be suitable for describing the air exchange between the cabinet and the sales area.

The opening of the doors has a huge impact on the infiltration rate. Therefore, the results for closed and opened doors have to be looked at separately. The infiltration rate of a cabinet is generally lower with closed doors than with open doors (Figure 3.2), which is plausible. The estimated infiltration rates from experiments with closed doors show certain fluctuations. Several effects could be the cause: the temperature difference between the cabinet and the sales area; a specific sensor position inside the cabinet; or other, non-systematic influences. Further experiments with systematic variations of these factors would be necessary to assess their impact.

The door opening is a factor with a high impact on the infiltration rate. During the experiments, the doors were opened briefly, for approximately 7 s to 14 s. Figure 3.2 shows clearly that the infiltration rates were higher than in those experiments with closed doors.

A detailed analysis of the influence of door openings on the air exchange is challenging. Opening one door leads to further effects, such as local concentration gradients inside the cabinet. Opening the leftmost door of a cabinet with six doors will have a different impact on the left-hand area inside cabinet than on the right-hand area. During experiment No 11 (Table 3.1) the second door from the left was briefly opened. The infiltration rate estimated with data from the sensor located in the centre was higher (59.4 g s^{-1}) than the infiltration rate based on sensor data from the right-hand side (50.7 g s^{-1}). The same effect can be seen in experiment No 10. This supports the assumed spatial concentration gradients inside the cabinets during door openings. In order to analyse the door openings more precisely, several sensors in different locations would be necessary.

Besides the specific values of infiltration rates, another result of the experiments is that the method presented for estimating the infiltration rate into the cabinet is shown to be working well. The dynamic course of concentration inside the cabinet could be very well described by

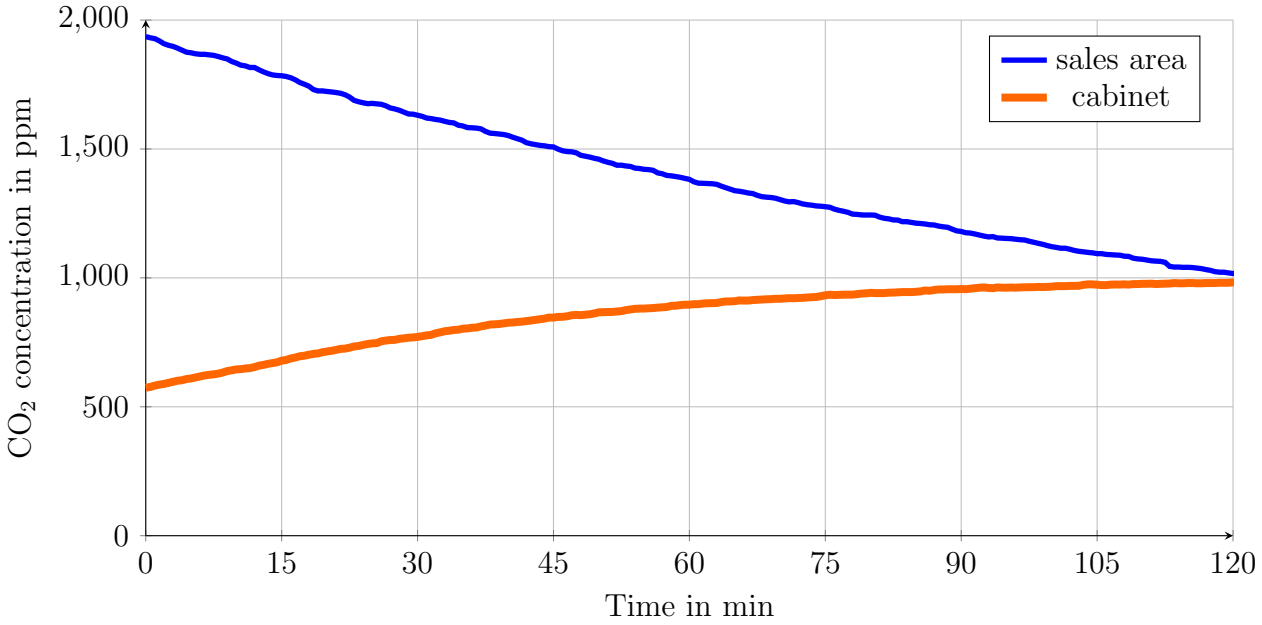

Figure 3.3.: CO_2 concentration in ppm of the sales area and inside the horizontal LT cabinet during experiment 1 as a function of time in min. For the analysis, the experiment has been divided into 7 intervals of 15 min length.

the mathematical model. A typical infiltration rate for closed vertical MT cabinets with six doors could be estimated to be around $32.6\,\mathrm{g\,s^{-1}}$.

A more intuitive indicator for describing the air exchange are its time constant τ (Equation 3.5) or the air change rate ACR. It is the reciprocal value of the time constant:

$$\mathrm{ACR} = \frac{1}{\tau} = \frac{\dot{m}_{\mathrm{air,inf,in}}}{\dot{m}_{\mathrm{air,cab}}} \tag{3.8}$$

Using the time constant or air change rate, however, has one main disadvantage: Its definition refers to the mass of air inside the cabinet. This mass depend on its inner volume that is largely affected by the restocking and withdrawal of goods stored in the cabinet. Thus, the time constant and air change rate of cabinets are not suitable to describe the air exchange of cabinets in an operational supermarket. Nevertheless, providing the time constant and air change rate can contribute to compare the different types of cabinets (MT vertical, LT horizontal, LT vertical), since there were no goods in the cabinets during the experiments. For vertical MT cabinets, the time constant τ with closed doors were around 230 s which corresponds to an air change rate ACR of approximately $15.6\,\mathrm{h^{-1}}$.

3.1.3. Horizontal low temperature cabinet

This section describes the experiments for the low temperature islands. In the laboratory supermarket there were two islands *back to back* with total dimensions 2.5 m width, 2.23 m length and 0.9 m height. The cabinets are equipped with sliding glass lids, which have to be opened to access the foodstuff.

Experiment description

Experiments with opened and closed lids were carried out for the low temperature islands. The infiltration rates of this type of cabinet are very low and its time constant is therefore

No	Interval	d_{exp} in min	T_{sa} in °C	T_{cab} in °C	$d_{lid,open}$ in s	$\dot{m}_{inf,in}$ in g s^{-1}	MAPE in %
Experiment with closed lids							
1	1	15	19.1	-12.1	closed	0.4	0.2
1	2	15	19.4	-13.3	closed	0.5	0.2
1	3	15	19.5	-13.8	closed	0.5	0.3
1	4	15	19.5	-14.0	closed	0.4	0.1
1	5	15	19.5	-13.7	closed	0.4	0.1
1	6	15	19.5	-13.9	closed	0.4	0.2
1	7	15	19.4	-14.0	closed	0.4	0.2
Experiment with opened lids							
2	1	40	23.0	-12.1	76	0.8	0.5
2*	1	40	23.0	-11.9	76	0.7	0.5
3	1	14	19.0	-10.7	840	2.4	1.6

Table 3.2.: Air infiltration rates into the horizontal low temperature cabinet. *: second sensor

very high. Initially one test was carried out at night, lasting approximately 2 h (experiment No 1).

At the beginning of the test, the cabinet and sales area were ventilated. Afterwards, concentration in the sales room was increased to about 2000 ppm. Figure 3.3 shows the course of the CO_2 concentration in the sales room and inside the horizontal cabinet during experiment No 1. The concentration in the sales room decreases during the entire experiment because of air exchange between the sales area and the ambient air. The concentration level inside the island increases slowly and converges after approximately 120 min.

As described above, certain conditions must be met to determine infiltration rates with the mathematical model. Firstly, a homogeneous distribution of the air in the sales room and inside the cabinet is required. Due to the low air change rates, a homogenous distribution of air can be assumed. Secondly, a minimal difference in concentration between the cabinet and the sales area is necessary. To this end, the last 15 min before convergence of the level of concentration were not used for parameter estimation. This ensured a minimum concentration difference of 120 ppm. The useable period of the experiment was divided into seven time intervals of 15 min length (Experiment No 1, Intervals 1 to 7, Table 3.2). The aim of this division was to check whether the difference in concentration between sales room and cabinet affects the estimated air infiltration rates.

Experiments with opened lids were also conducted. During experiment No 2, which lasted 40 min, the lids were *opened* several times. In this experiment, two sensors were measuring the concentration inside the cabinet. The total duration of lid opening was 76 s. In experiment No 3, one of the four lids was kept *open* for 14 min.

Results and discussion

Table 3.2 shows the results of the experiments with the horizontal LT cabinet and the parameter estimation. For each parameter estimation, the duration of the time series, the temperature of the sales area and the cabinet, as well as the status of the lid are given. Again, the mean absolute percentage error (MAPE) is used to assess the quality of the parameter estimation.

The mass flow rate of air infiltration into the cabinet with closed lids lies in the range 0.4 g s^{-1} to 0.5 g s^{-1}. The MAPE is smaller than 0.3 %, which means that the mathematical model (Equation 3.4) describes the measured course of concentration in the cabinet very well.

A dependency of the infiltration rate on the difference in CO_2 concentration between sales room and cabinet could not be observed. The time constant of the air exchange of the LT cabinet with closed lids is approximately $\tau = 187\,\mathrm{min}$ which corresponds to an air change rate of approximately $0.3\,\mathrm{h}^{-1}$. This cabinet has 4 lids. Thus, the specific infiltration rate per lid is $\underline{\dot{m}}_{\mathrm{door,closed}} \approx 0.1\,\mathrm{g\,s}^{-1}$.

The mass flow rate of the cabinet with one open lid is estimated to be $2.4\,\mathrm{g\,s}^{-1}$, which is approximately 5 times higher than with closed lids. The overall air infiltration rate into one cabinet is composed of the infiltration through open doors and the gaps between closed doors/lids (Equation 2.62):

$$\dot{m}_{\mathrm{inf,in}} = n_{\mathrm{door,open}} \cdot \underline{\dot{m}}_{\mathrm{door,open}} + n_{\mathrm{door,closed}} \cdot \underline{\dot{m}}_{\mathrm{door,closed}} \tag{3.9}$$

In this experiment $n_{\mathrm{door,open}} = 1$ and $n_{\mathrm{door,closed}} = 3$. The infiltration rate of a single open lid is therefore $\underline{\dot{m}}_{\mathrm{door,open}} = 2.1\,\mathrm{g\,s}^{-1}$. If one lid of this cabinet is open, the time constant of the air exchange is reduce to approximately 31 min and the air change rate is increased to almost $2.0\,\mathrm{h}^{-1}$. The mass flow rate of experiment No 2 simulated the withdrawal of goods and included a total duration of open lids of 76 s. The estimated infiltration rate is approximately $0.7\,\mathrm{g\,s}^{-1}$ to $0.8\,\mathrm{g\,s}^{-1}$.

Compared to the vertical MT cabinet, the infiltration rate of horizontal LT cabinets is 50 to 100 times smaller. These low values are plausible. Air exchange is lower for horizontal cabinets, because they are only opened on the upper side. Cold air inside the horizontal cabinets has a higher density than air in the sales area and therefore is *trapped* in the cabinet. Despite the significantly lower absolute infiltration rates the opening of the glass lid has a noticeable impact on the air exchange between cabinet and sales area again. It has to be noted that the temperature inside the cabinet was higher ($-14\,^{\circ}\mathrm{C}$ to $-10.7\,^{\circ}\mathrm{C}$) than typical in cabinets in operational supermarkets (around $-20\,^{\circ}\mathrm{C}$).

3.1.4. Vertical low temperature cabinet

In addition to horizontal low temperature cabinets, there are also vertical ones. They are equipped with doors that are typically well sealed. Here, a cabinet of 2.34 m width with three doors was tested. In some initial experiments, the CO_2 concentration in this cabinet was measured during a 7 h period with closed doors. No notable change in concentration could be observed. Therefore, it can be assumed that the infiltration rate of closed doors in vertical LT cabinets is zero. Consequently, the experiments focused on the effect of door openings.

Experiment description

An experiment was carried out in which five food withdrawal processes were simulated by door openings. Both the concentration inside the cabinet and in the sales room were measured. The duration of the door opening was measured with a stop watch. As previously done by Månsson et al. (2019), an accelerometer (Voltcraft DL-131G) was attached to the door.

Method

The method used earlier in the experiments for estimating the infiltration rate is not suitable for door openings with vertical low temperature cabinets. Door openings are usually short: mean and median values are smaller than 15 s (Månsson et al. 2019). Consequently the distribution of CO_2 inside the cabinet cannot be assumed to be homogeneous during the door opening, which is a main assumption of the mathematical model described above (Equation 3.4). For vertical MT and horizontal LT cabinets with closed doors or short door openings, this assumption could be made, because there was constant infiltration, also with the doors

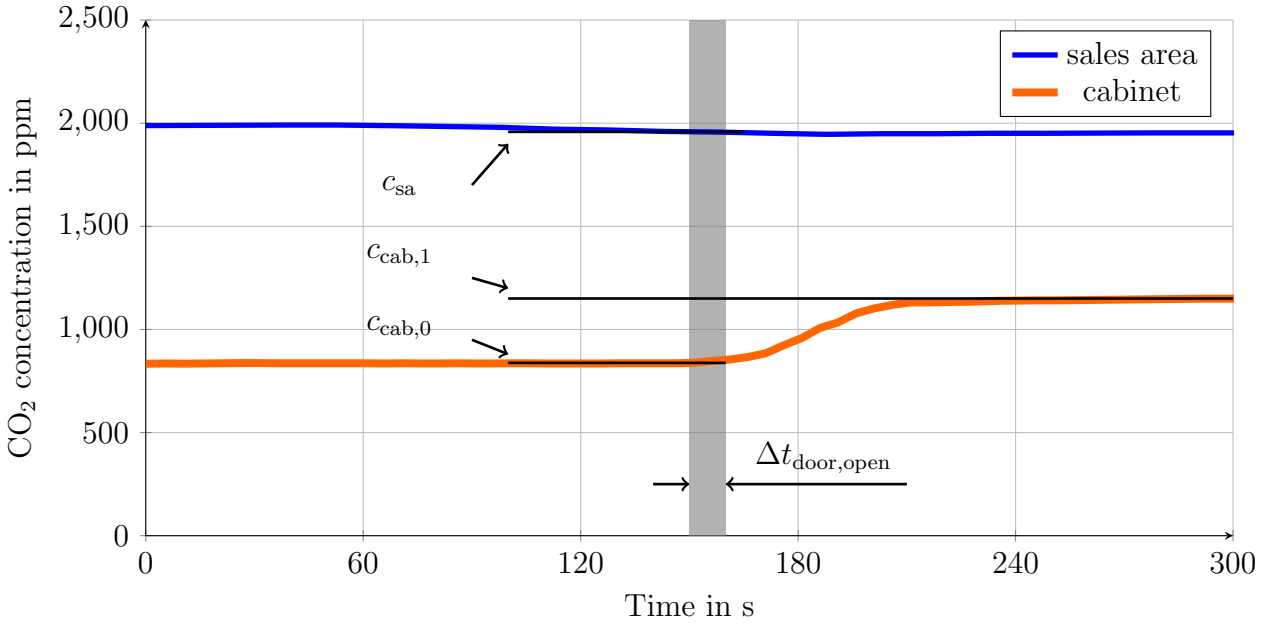

Figure 3.4.: CO_2 concentration in the sales area and the vertical LT cabinet as a function of time before, during and after a door opening

and lids being closed. The time constant of the CO_2 sensor is in the order of 20 s. The CO_2 concentration inside the cabinet varies within 10 s to 20 s (Figure 3.4). Thus, the sensor is not fast enough to measure the course of the CO_2 concentration inside the cabinet. The air infiltration rate cannot be calculated via a dynamic parameter estimation problem.

An alternative method for calculating the average infiltration rate during a door opening shall be presented here. This method, however, uses again the mass of CO_2 entering the cabinet to calculate the infiltration rate. When the doors are closed, no air exchange takes place and the concentration inside the cabinet remains constant. After the doors have been closed, the CO_2 is distributed homogeneously after a short while. The concentrations in the cabinet are referred to as $c_{cab,0}$ (before door opening) and $c_{cab,1}$ (after door opening) (Figure 3.4).

Since there is a difference in concentration between the cabinet and the sales area, an exchange of air also leads to a change in mass of the CO_2 inside the cabinet. The mass of CO_2 exchanged with the sales area during the door opening is the difference between mass inside the cabinet after and before the door opening:

$$\Delta m_{CO_2,cab} = m_{CO_2,cab,1} - m_{CO_2,cab,0} \tag{3.10}$$

Using formula 2.9, this mass of CO_2 exchanged with the sales area can be expressed based on concentrations of CO_2 and mass of air inside the cabinet $m_{air,cab}$, which has been estimated to be 6.5 kg :

$$\Delta m_{CO_2,cab} = m_{air,cab} \cdot \frac{M_{CO_2}}{M_{air}} \cdot (c_{cab,1} - c_{cab,0}) \tag{3.11}$$

The duration of door opening is referred to as $\Delta t_{door,open}$. The average mass flow rate of CO_2 between the cabinet and the sales area during the door opening can be calculated as:

$$\dot{m}_{CO_2,cab} = \frac{\Delta m_{CO_2,cab}}{\Delta t_{door,open}} \tag{3.12}$$

No	d_{exp} in s	$c_{cab,0}$ in ppm	$c_{cab,1}$ in ppm	c_{sa} in ppm	$\dot{m}_{inf,in}$ in $g\,s^{-1}$
1	10.0	838	1150	1958	181.1
2	3.8	1149	1220	1927	158.2
3	5.2	1169	1067	443	176.0
4	7.9	1067	926	443	185.7
5	10.5	926	785	464	188.9

Table 3.3.: Door opening duration, CO_2 concentrations before and after the door opening and Air infiltration rates of the experiments with a vertical LT cabinet

During a door opening, two air flows are exchanged: air from the cabinet flows into the sales area ($\dot{m}_{cab,out}$) and air from the sales area flows into the cabinet ($\dot{m}_{cab,in}$). It is assumed that their absolute values are equal

$$\dot{m}_{air} = \dot{m}_{cab,out} = \dot{m}_{cab,in} \tag{3.13}$$

The air leaving the cabinet has the concentration $c_{cab,0}$ before the door opening. Using formula 2.9, we get:

$$\dot{m}_{CO_2,cab} = \dot{m}_{air} \cdot \frac{M_{CO_2}}{M_{air}} \cdot (c_{sa} - c_{cab,0}) \tag{3.14}$$

Equating equations 3.12 and 3.14, we get:

$$\dot{m}_{CO_2,cab} = \frac{\Delta m_{CO_2}}{\Delta t_{door,open}} = \dot{m}_{air} \cdot \frac{M_{CO_2}}{M_{air}} \cdot (c_{sa} - c_{cab,0}) \tag{3.15}$$

Substituting $\Delta m_{CO_2,cab}$ with Equation 3.11:

$$\frac{m_{air,cab}}{\Delta t_{door,open}} \cdot \frac{M_{CO_2}}{M_{air}} \cdot (c_{cab,1} - c_{cab,0}) = \dot{m}_{air} \cdot \frac{M_{CO_2}}{M_{air}} \cdot (c_{sa} - c_{cab,0}) \tag{3.16}$$

This results in:

$$\dot{m}_{air} = \frac{m_{air,cab}}{\Delta t_{door,open}} \cdot \frac{c_{cab,1} - c_{cab,0}}{c_{sa} - c_{cab,0}} \tag{3.17}$$

This equation could alternatively be derived by transforming differential equation 3.3 into a difference equation.

Results and discussion

Table 3.3 shows the results of the infiltration rate estimations for the vertical LT cabinet.

The infiltration rates are comparatively high and in the order of $180\,g\,s^{-1}$. The value of test 2 deviates slightly. The reason could be the relatively short door opening time. The door opening always consists of various steps (Månsson et al. 2019): 1. door moving until it is open 2. door being open 3. door moving until it is closed. With very short overall door opening times, the dynamic effects while the door is moving could play a role. Additionally, a short overall duration of the door opening leads to less accurate time measurements. The accelerometer data were only used to check the total duration of the door opening. Since the closed doors were found to seal the cabinet very well, the air change rate of the closed doors can be assumed to be zero. Assuming that the specific an air infiltration per door is $180\,g\,s^{-1}$, the time constant of vertical LT cabinet with three doors is approximately 36 s, which correspond to approximately an air change rate of $100\,h^{-1}$.

Parameter	Vertical MT cabinet	Horizontal LT cabinet	Vertical LT cabinet
$\underline{\dot{m}}_{\text{door,closed}}$	$5\,\text{g}\,\text{s}^{-1}$	$0.1\,\text{g}\,\text{s}^{-1}$	$\approx 0\,\text{g}\,\text{s}^{-1}$
$\underline{\dot{m}}_{\text{door,open}}$	$>> 5\,\text{g}\,\text{s}^{-1}$	$2.1\,\text{g}\,\text{s}^{-1}$	$160\,\text{g}\,\text{s}^{-1}$ to $190\,\text{g}\,\text{s}^{-1}$

Table 3.4.: Summary of specific air infiltration rates of cabinets per door

Overall, it should also be noted that the temperature in the freezer cabinet was only $-5\,°\text{C}$ and that no goods were inside. In operational supermarkets, the temperature in low temperature cabinets is around $-20\,°\text{C}$. Compared to the experiments described here, that temperature is significantly lower and consequently the difference in air-density between the cabinet and the sales room is much higher. Therefore, it is very likely that the infiltration rate in real vertical low temperature cabinets would be higher.

3.1.5. Summary infiltration experiments

This subchapter described tracer gas measurements for typical closed refrigerated display cabinets with doors. The aim was to determine typical infiltration rates of ambient air into the cabinet for both closed and open doors/lids.

The basic method of determining the infiltration rate by solving a dynamic parameter estimation problem has proven to be very successful for vertical medium temperature and horizontal low temperature cabinets. A modified method has been applied to the vertical low temperature cabinets and also provided good results.

A summary of the specific infiltration rates for the three types of display cabinets is shown in Table 3.4. In these tables, the infiltration rates are shown as specific values per door. Cabinets in supermarkets have different sizes and using specific values per door eases the usage for different cabinet sizes. When their closed doors/lids are closed, vertical medium temperature cabinets have the highest infiltration rates. Vertical low temperature cabinets have a near zero infiltration rate because the doors are very well sealed. Opening the doors/lids has a significant impact on the infiltration rates of all cabinets.

There are many different manufacturers of display cabinets each with different designs and door geometry. Consequently, the results of the tested cabinets only give an indication of the order of magnitude of infiltration rates into different types of refrigerated display cabinets.

Comparison with the literature

To the authors's knowledge, so far, only Marciniak (2016) and Chaomuang et al. (2019c, 2020) have specifically indicated a mass flow rate of air exchanged between a refrigerated display cabinet with doors and the sales area. Chaomuang et al. (2019c, 2020) reported a mass flow rate of $5.1\,\text{g}\,\text{s}^{-1}$ through the gaps between the doors of a vertical MT cabinet with two doors and a width of 1.25 m. The specific infiltration rate per door $\underline{\dot{m}}_{\text{door,closed}}$ is $2.55\,\text{g}\,\text{s}^{-1}$. Comparing this with data obtained here (around $5\,\text{g}\,\text{s}^{-1}$), this is a similar order of magnitude, despite the factor of 2 between them. It has to be noted that the MT cabinet used for the measurements described here had broad gaps between the doors, which may be the reason for the higher specific infiltration rates.

Marciniak (2016) reports specific values per lateral metre of display cabinet width. The reported values are $3.9\,\text{g}\,\text{m}^{-1}\,\text{s}^{-1}$for vertical MT cabinets with doors, $2.48\,\text{g}\,\text{m}^{-1}\,\text{s}^{-1}$ for vertical LT cabinets and $0.83\,\text{g}\,\text{m}^{-1}\,\text{s}^{-1}$ for horizontal LT cabinets. The specific infiltration rates per closed door $\underline{\dot{m}}_{\text{door,closed}}$ would then be $2.4\,\text{g}\,\text{s}^{-1}$ for vertical MT cabinets. The values are in a similar order of magnitude. It has to be considered that these literature values were

estimated based on other literature data (Faramarzi et al. 2002, Kosar and Dumitrescu 2005) and additional assumptions.

Al-Sahhaf (2011) found a value of $93\,\mathrm{g\,s^{-1}}$ as infiltration rate for an open cabinet with a width of 1.2 m. This open cabinet has no doors, but a similar width as the cabinet investigated by Chaomuang et al. (2020) (1.25 m). The infiltration rate into the open cabinet is significantly higher than into the closed cabinet, which is plausible.

3.2. Data-based estimation of the dimensionless air infiltration rate into a specific type of cabinet in an operational supermarket

The thermal entrainment factor (TEF) is the ratio between air infiltration and fan mass flow rate and can be interpreted as a dimensionless infiltration rate. Because of it dependency on the fan mass flow rate, it cannot be used to compare different types of cabinets. However, it can be used to compare the infiltration into a specific cabinet under different boundary conditions. A main advantage of the TEF is that it can be estimated using solely temperature data of a cabinet and the sales room (Equation 2.73). This allows to estimate a typical TEF values of a specific type of cabinet located in an operational supermarket.

The objective of the following analysis is to estimate the TEF value of specific vertical, doored MT cabinets located in the test supermarket. It shall be assessed to what extend differences in the TEF can be identified between periods with and without customers in the store (supermarket open/closed). If there are significant differences in the TEF between open and closed supermarket, they can be used to validate the simulation models. To this end, a method is presented that allows estimating the TEF values based on monitoring data. Specifically, filter criteria will be presented that allow excluding undesired operation conditions of the cabinet. In the end, the TEF of several, individual cabinets from a time period of two years will be analysed.

3.2.1. Methods

The objective of the analysis is to estimate typical TEF values. Orlandi et al. (2013) showed that opening a cabinet door directly affects the air temperature at the return air grill. This temperature is part of the formula for approximating the TEF (Equation 2.73), so it can be expected that door openings will increase the TEF value. If there is a noticeable effect of door openings on the TEF value, this variation of TEF values can be used to validate the simulations (Section 4.3). Namely, it is expected that during opening hours of a supermarket the TEF value is higher than in periods when the supermarket is closed. This ratio between the TEF of an open supermarket and a closed supermarket can be used to validate the simulations models. However, firstly, the possible effect of door openings on the TEF value has to be assessed.

Experiments with display cabinets typically take place in laboratories where boundary conditions can be controlled. Thus, the variables that influence the investigated object can be controlled. However, such experiments are costly and time consuming. In operational supermarkets, an abundance of display cabinets are in operation and much data is collected via the monitoring system. But in the field, boundary conditions are variables that cannot be controlled. Many of those variables affecting the cabinet's performance are measured. Processing these large amounts of data, the effect of single variables on the investigated object may be uncovered. This processing of data will be described in the following section.

The aim is to estimate the effect of door openings on the thermal entrainment factor. Door openings are not typically measured via monitoring systems. However, they are correlated to the opening of a supermarket: when the store is closed, the doors of the cabinets are closed; when it is open, they are sometimes opened. Therefore, the TEF is compared for periods during which the store is open and closed.

Description of data processing

The estimation of the TEF (Equation 2.73) is based on data from eight closed vertical dairy product cabinets, which are located in the test supermarket, over a period of two years. Temperature data of different air flows, a variable indicating defrost operation, the evaporation temperature of the refrigeration system as well as relative humidity in the sales area are available as hourly average values. Each hour corresponds to one row in the data set.

The thermal entrainment factor shall be used to validate the simulation results. The objective of the simulations is to estimate energy consumption during *normal operation*. Certain effects, such as faults in single cabinets or dynamic temperature behaviour are not considered in the models. For checking the simulation models the TEF during *normal operation* has to be used.

Abnormal operation has consequently been excluded from the calculation of the TEF from measurement data. Examples of such *abnormal operation* modes are defrosting, restocking of goods or faults such as a heat exchanger that is heavily covered with a frost layer. In the following, filter criteria are presented that help to exclude these operation conditions.

Firstly, defrost operations are excluded. All data rows where the corresponding variable indicated a defrost operation, were removed from the data set.

Secondly, iced/blocked heat exchangers shall be excluded. If a heat exchanger is covered with frost or ice, the heat transfer to the air is hindered. If a cabinet is unable to maintain the desired setpoint temperature, the control system reacts by lowering the evaporation temperature. The increased temperature difference between the refrigerant and the air usually compensates for the worsened heat transfer allowing the desired temperature to be reached inside the cabinet. If the evaporation temperature is in a normal range, this is an indicator that no evaporator is severely covered with frost or ice. That is why a normal evaporation temperature is used as an indicator for heat exchangers without ice build-up. Evaporation temperatures below $-5\,°C$ are filtered to exclude this kind of operation. These filters are believed to exclude most of the abnormal operation modes.

3.2.2. Results and discussion

Eight dairy product cabinets from the test supermarket were analysed over a period of two years. The data for each cabinet has been processed according to the above filters. In total, 29 085 values were obtained in the open store category and 32 737 in the closed store category. In the closed supermarket, 52 % of the data was excluded by the filters and for the open supermarket, 60 % of the data was excluded. Figure 3.5 shows the histogram and Figure 3.6 the box plot of the TEF values for both categories. For a closed store, the mean TEF value is 0.058 (median 0.057). While the store is open the mean value of TEF is 0.074 (median 0.077). The TEF is the ratio of infiltration mass flow rate to fan mass flow rate. Assuming that the fan mass flow rate does not vary, a higher TEF means a higher air infiltration. Based on the average values, the air infiltration would be approximately 30 % higher with an open store than with a closed store. When the store is open, customers visit the market and open the cabinet doors, so it is plausible that infiltration is higher. This increase of approximately 30 % of air infiltration rate can be used to validate the simulation results (Section 4.3).

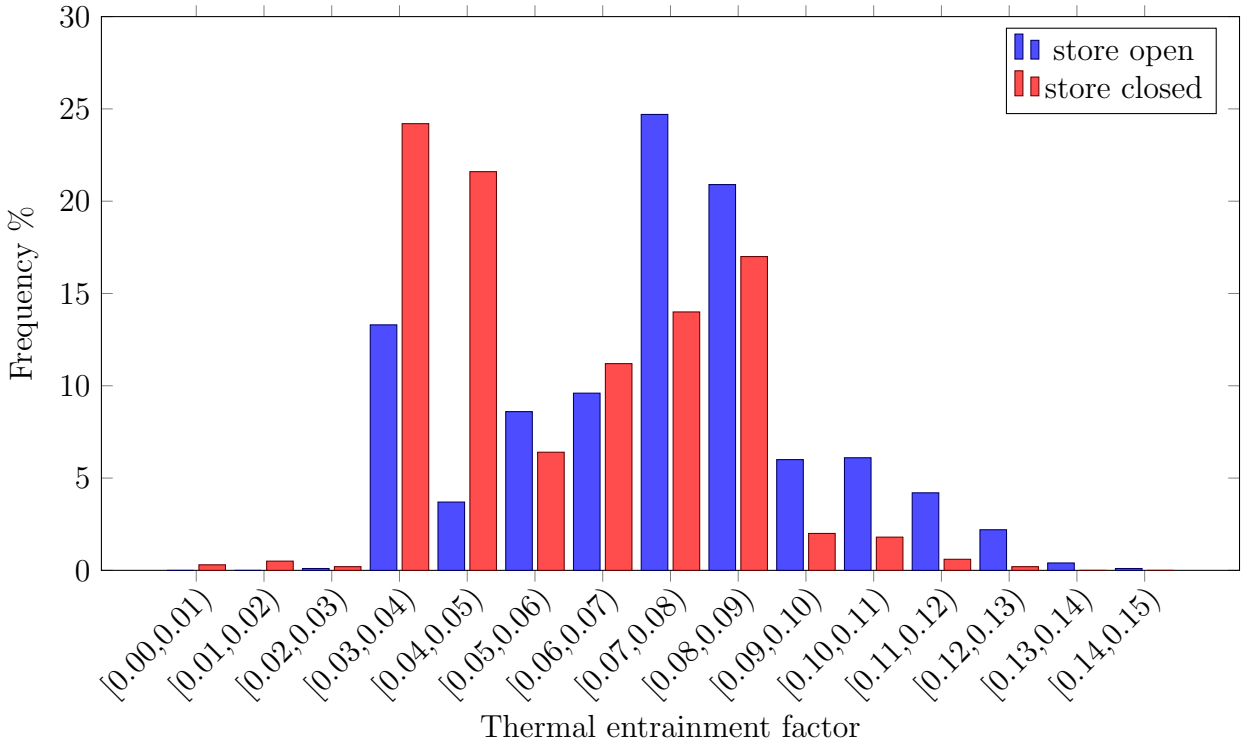

Figure 3.5.: Histogram of the dimensionless air infiltration rate TEF for 8 vertical MT cabinets of the same type located in the test supermarket. The results for open and closed store are distinguished.

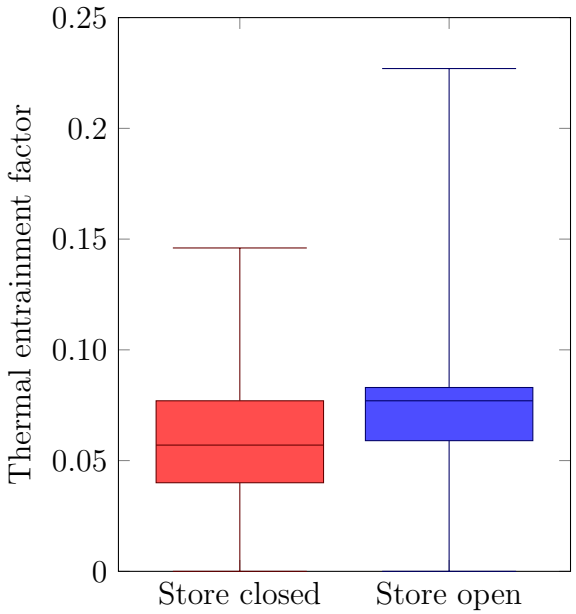

Figure 3.6.: Box plot of the dimensionless air infiltration rate TEF for open and closed store based on data from 8 vertical MT cabinets of the same type located in the test supermarket. The air infiltration during periods of an open store is approximately 30 % higher than in periods of the store being closed.

The majority of values are in the range of 0.03 to 0.09. However, there are differences in distribution depending on whether the store is open or closed. There are distinctive features of the distribution of TEF values that require further research. For instance, the frequency of TEF values between 0.06 to 0.09 is very similar for open and closed markets, except for TEF = 0.07. There are several factors that have to be discussed. The restocking of goods implies door openings and often takes place before or after the opening of the supermarket. This could be a possible explanation for the increased frequency of TEF values between 0.06 to 0.09. Although the specific data rows including defrost periods are filtered out, they may lead to higher TEF values in the subsequent time intervals. During defrosting, the evaporator is switched off, which may lead to an increased temperature in the display cabinet and affect the calculation of the TEF (Equation 2.73). These aspects remain to be investigated in further studies.

Comparison with the literature

There is little literature of laboratory experiments with closed type display cabinet. Chaomuang et al. (2019a) investigate the temperature variation and profile in a closed display cabinet in a laboratory. Using their data (Chaomuang et al. (2019a), Figure 8a) the TEF value for closed doors is 0.067, which is in line with the values calculated in this section.

Summary and outlook

This section estimated the dimensionless air infiltration rate, namely the thermal entrainment factor (TEF), for one specific type of closed vertical MT cabinets under different boundary conditions. For the estimation, a statistical analysis of data from the test supermarket was carried out. The main result is that the average air infiltration rate in the investigated type of cabinet seem to increase by approximately 30 % during opening hours compared to periods of the supermarket being closed.

This result is estimated using solely temperature data of the cabinet and the sales room air. The actual temperatures in the cabinets are not used for the calibration process of the simulations models (Chapter 4). Therefore, these results can be used as one additional way of validating the simulation results (Section 4.3).

The method described in this section can be refined using additional data. Door openings are typically not logged. However, there is ongoing research in this field (Månsson et al. 2019). Further aspects to refine this methods are: using a higher temporal resolution of temperature data, studying the location of temperature sensors etc.

4. Prediction of energy consumption of the refrigeration system and display cabinets

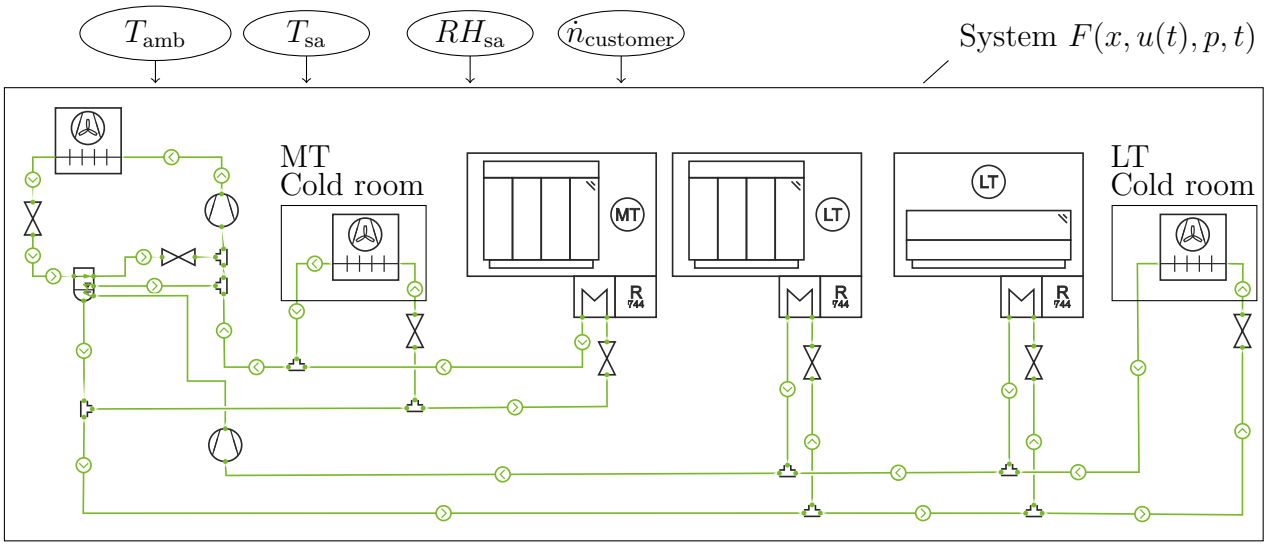

Figure 4.1.: Control volume used for prediction of electrical energy consumption: refrigeration system and display cabinets. The refrigeration system is a R-744 booster system with flash gas bypass and internal heat exchanger and three *equivalent MT, horizontal LT and vertical LT display cabinets* and two cold rooms

This chapter looks at a system consisting of R-744 refrigeration system, display cabinets and cold rooms (Figure 4.1). The objective of the model is to predict the electrical energy consumption of the central refrigeration system and the display cabinets based on the ambient temperature, temperature and humidity in the sales room as well as the customer flow. The system is built using the *physical connections* and the models described in the previous chapter (2). Many of the required parameters are available from technical data sheets, the monitoring system or the experiments (Section 4.2). However, not all parameters can be estimated this way, which is why some parameters are calibrated using measurement data. Specifically, the overall thermal transmittance of the display cabinets and the number of door openings per customer are calibrated.

This chapter describes specifically the parametrisation of the simulation models, as well as the calibration and validation of the model. It then discusses the ability to predict the energy consumption of a supermarket. The prediction of the energy consumption of the refrigeration system and display cabinets using the ambient temperature, the temperature and humidity of the sales room air and the customer flow as input values and the physical parameters imply several novelties. The dependency of cooling load on the temperature and humidity is well known for open display cabinets. However, the cooling load and consequently the energy consumption of the refrigeration system, has not yet been described for closed display cabinets considering specifically the number of customers as an input value.

4.1. System overview

The system (Figure 4.1) and measurement data used in this chapter are based on the example supermarket (Section A.1). The central refrigeration system is a R-744 booster refrigeration system with flash gas bypass (Section 2.4.3) and an internal heat exchanger. This heat exchanger is located inside the separator and is used for superheating the suction gas of the low-pressure compressor. The refrigeration system has two evaporating temperature levels for medium and low-temperature cabinets. At both temperature levels, there are display cabinets and cold rooms. Expressed in a generalised way, the system model (Figure 4.1) describes the behaviour x of the display cabinets, cold rooms and the refrigeration system as a function of time-dependent input variables $u(t)$, the time t and a set of parameters p:

$$x = F(u(t), p, t) \tag{4.1}$$

The time dependent input values $u(t)$ are:

- ambient temperature T_{amb}
- temperature of the sales area T_{sa}
- relative humidity in the sales area RH_{sa}
- rate of customers $\dot{n}_{\text{customer}}$

All temperature and humidity values are taken as hourly average values from the monitoring system. The customer rate was not available, and a generic customer flow profile was therefore used, which is based on the available data for a single week. Among all variables x, the power consumptions of compressors P_{el} (Equation 2.25) and display cabinets $P_{\text{el,cab}}$ (Equation 2.49) are of primary interest for the validation. Specifically, the following power consumptions are considered:

- high pressure compressor $P_{\text{el,comp,HP}}$
- low pressure compressor $P_{\text{el,comp,LP}}$
- all medium temperature cabinets $P_{\text{el,cab,MT}}$
- all low temperature cabinets $P_{\text{el,cab,LT}}$

Besides the comparison of these power consumptions, the suction and discharge temperature of the HP compressor will moreover be used to validate the model (Section 4.3).

4.2. Parametrisation

There are different ways of obtaining parameter values required for the simulations models:

- planning data: the refrigeration system layout, number and types of display cabinet can be found in the planning data
- monitoring system: setpoints for controllers can be taken from the monitoring system, for instance, temperature or pressure setpoints
- catalogue data: this refers to all kinds of data provided by the manufacturer, such as a catalogue, data sheets or type plates
- literature data: some typical values can be estimated based on literature data: for instance, the average door opening duration of a display cabinet
- measurements: this refers to direct measurements or experimental data used to estimate certain parameters
- calibration: measurement data are used to calibrate certain parameters

In this work, there are two specific challenges regarding parametrisation.

A first challenge results from the fact that some of the simulation models that use the approach of *physical interactions* are new and consequently some of the required parameters cannot be found in data from manufacturers or in the literature. The three new parameters are the specific air infiltration rates into the display cabinets $\underline{\dot{m}}_{\text{door,open}}$ and $\underline{\dot{m}}_{\text{door,closed}}$ as well as the number of cabinet door openings per customer $n_{\text{door,per,customer}}$. Although these parameters cannot be found in the literature, they can in fact be determined. A method to determine the specific air infiltration rates was described in the previous chapter 3.1. Combining an analysis of door openings (Månsson et al. 2019) and customer balance (see Section 5.1), it would be possible to estimate the number of door openings per customer in the future.

A second challenge is the limited possibility to carry out experiments with the cabinets in the test supermarket. Although the method to estimate specific air infiltration rates was successfully demonstrated in a laboratory, it was not possible to repeat the experiments with the specific cabinet in the test supermarket. Therefore, the values of the specific air infiltration rates for the test supermarket are based on assumptions and further parameters are calibrated.

The calibration and validation process uses two different periods of measurement data. One period to calibrate the parameters and a second period to validate them.

If the specific parameters of the display cabinet were available from previous measurements or a catalogue, it would be possible to build a simulation model that allows prediction of the energy consumption of the supermarket based on catalogue data and the previously mentioned input data. Unfortunately, these experiments could not be carried out for the cabinets located in the test supermarket. Therefore, some of the parameters in this thesis need to be calibrated, specifically the thermal transmittance of the display cabinet envelope and the number of door openings per customer. In the following, the parameters for the refrigeration system and the display cabinets are presented. The specific method of estimating the parameter values via calibration will be explained.

4.2.1. Refrigeration system

The topology of the refrigeration system, namely the R-744 booster layout (see Section 2.4.3) with an internal heat exchanger, is based on the planning data for the test supermarket. The required parameters (Table 4.1) are estimated in different ways that are described below.

The compressor efficiencies are estimated based on catalogue data from the manufacturer. The effective isentropic efficiency $\eta_{\text{effis,HP}}$ of the high pressure compressor is a function of the pressure ratio π (Equation 2.21):

$$\eta_{\text{effis,HP}} = 0.02771 \cdot \pi^3 - 0.25477 \cdot \pi^2 + 0.73423 \cdot \pi + 0.05759 \tag{4.2}$$

Since the suction and discharge pressure levels of the low pressure compressor are nearly constant, the effective isentropic efficiency is set to the fixed value $\eta_{\text{effis,LP}} = 0.62$. The pressure setpoint of the flash gas bypass (FGB) valve, which controls the pressure in the separator, is obtained from the monitoring system. The cold rooms are assumed to have a fixed cooling load $\dot{Q}_{\text{CR}}$, which is obtained from the planning data. The setpoints for the evaporation pressure p_{evap} were retrieved from the monitoring system. However, the actual evaporation pressure is usually lower than the setpoint. The specific reasons are unknown, but it is very likely that single evaporators are sometimes covered with ice and consequently require a lower evaporation temperature in order to maintain the cabinet temperature. The actual evaporation pressure during the calibration period was analysed and the evaporation pressure setpoints of the simulation model are set to the average values during the calibration period. The specific high pressure function (Equation 4.3) for the gas cooler $p_{\text{setpoint}} = f(T_{\text{amb}})$ is not explicitly

Parameter	Value	Unit	Description	Determination
$\eta_{\text{effis,HP}}$	Equation 4.2		Effective isentropic efficiency HP	Catalogue data
$\eta_{\text{effis,LP}}$	0.62	-	Effective isentropic efficiency LP	
p_{sep}	36.0	bar	Separator pressure	Monitoring system
$\dot{Q}_{\text{LT,CR}}$	1.5	kW	Cooling load LT cold room	Planning data
$\dot{Q}_{\text{MT,CR}}$	4.0	kW	Cooling load MT cold room	
$p_{\text{evap,LT}}$	14.7	bar	LT evaporation pressure	Calibration
$p_{\text{evap,MT}}$	30.3	bar	MT evaporation pressure	
$\Delta T_{\text{sh,suct,line,MT}}$	5.0	K	MT suction line superheat	Assumption
$p_{\text{gc,setpoint}}$	Equation 4.3		Setpoint gas cooler pressure	Calibration
$T_{\text{gc,out}}$	Equation 4.4		Setpoint gas cooler temperature	

Table 4.1.: Parameters of the R-744 booster refrigeration system

available in the monitoring system. However, based on the pair of T_{amb} and p_{setpoint}, the following function was approximated (see a plot in Figure A.2) :

$$p_{\text{gc,setpoint}}[bar] = \begin{cases} 48 & 8\,°\text{C} >= T_{\text{amb}} \\ 1.4110 \cdot T_{\text{amb}} + 36.706 & 8\,°\text{C} < T_{\text{amb}} <= 25\,°\text{C} \\ 1.7400 \cdot T_{\text{amb}} + 28.500 & 25\,°\text{C} < T_{\text{amb}} <= 35\,°\text{C} \\ 0.4227 \cdot T_{\text{amb}} + 74.630 & 35\,°\text{C} < T_{\text{amb}} \end{cases} \tag{4.3}$$

The same applies to the function that controls the outlet temperature of the refrigerant from the gas cooler:

$$T_{\text{gc,out}}[°\text{C}] = \begin{cases} 9 & 8\,°\text{C} >= T_{\text{amb}} \\ T_{\text{amb}} + 1\,\text{K} & 8\,°\text{C} < T_{\text{amb}} <= 25\,°\text{C} \\ T_{\text{amb}} + 2\,\text{K} & 25\,°\text{C} < T_{\text{amb}} \end{cases} \tag{4.4}$$

This approach of different functions for the high pressure setpoints depending on the ambient temperature has, for instance, been used by Gullo et al. (2017). Heat recovery is not included here.

4.2.2. Low-temperature display cabinets

Typically, there are a large number of similar display cabinets in a supermarket. If the behaviour of individual cabinets is not of specific interest, several cabinets of the same type can be combined into a so-called *equivalent cabinet* model. An equivalent cabinet is defined as a control volume that comprises several identical or similar display cabinets. The equivalent cabinet provides the same interactions between the sales area and the refrigeration system as the individual display cabinets combined.

The parameters of the low-temperature cabinets are shown in Table 4.2. The number of doors or lids n_{door} as well as the overall surface area of the cabinet envelope A are estimated based on the planning data of the supermarket. A schematic floor plan is shown in Figure A.1 and a list of display cabinet line-ups is given in Table A.1. The temperature setpoint is taken from the monitoring system. No data sheets were available for the specific display cabinets, but the total electrical power consumption $P_{\text{el,cab,LT}}$ of all low-temperature cabinets, both horizontal and vertical, was available from the monitoring system (Figure A.3). This profile allows approximating the power consumption during daytime $P_{\text{el,int,day}}$ and nighttime

Parameter	Value		Description	Determination
LT horizontal cabinet				
n_{door}	34.0	-	Number of doors	Planning data,
A	65.6	m^2	Total surface area of the cabinet	Section A.1
$P_{\text{el,defrost}}$	2.5	kW	Electrical defrost power	Monitoring system
T_{setpoint}	−20.0	°C	Temperature setpoint	
$t_{\text{defrost1,start}}$	4.00	h	Start first defrost	
$t_{\text{defrost1,end}}$	5.00	h	End first defrost	
$P_{\text{el,int,day}}$	1.4	kW	Electrical power daytime	
$P_{\text{el,int,night}}$	1.2	kW	Electrical power nighttime	
$\Delta T_{\text{sh,evap,setpoint}}$	9.0	K	Evaporator superheat setpoint	
$\dot{m}_{\text{air,fan}}$	4.0	$\text{kg}\,\text{s}^{-1}$	Fan mass flow rate	Assumption and literature
$d_{\text{door,open}}$	10.0	s	Average duration of door opening	
$\underline{\dot{m}}_{\text{door,closed}}$	0.1	$\text{g}\,\text{s}^{-1}$	Specific infiltration, door closed	Assumption and experiments
$\underline{\dot{m}}_{\text{door,open}}$	2.1	$\text{g}\,\text{s}^{-1}$	Specific infiltration, door open	
k_{LT}	0.67	$\text{W}\,\text{m}^{-2}\,\text{K}^{-1}$	Average thermal transmittance	Calibration
$n_{\text{door,per,customer,LT}}$	0.2	customer^{-1}	doors opened per customer	
LT vertical cabinet				
n_{door}	20.0	-	Number of doors	Planning data,
A	109.0	m^2	Total surface area of the cabinet	Section A.1
$P_{\text{el,defrost}}$	5.1	kW	Electrical defrost power	Monitoring system
T_{setpoint}	−20.0	°C	Temperature setpoint	
$t_{\text{defrost1,start}}$	1.00	h	Start first defrost	
$t_{\text{defrost1,end}}$	2.00	h	End first defrost	
$P_{\text{el,int,day}}$	2.9	kW	Electrical power daytime	
$P_{\text{el,int,night}}$	2.4	kW	Electrical power nighttime	
$\Delta T_{\text{sh,evap,setpoint}}$	9.0	K	Evaporator superheat setpoint	
$\dot{m}_{\text{air,fan}}$	10.0	$\text{kg}\,\text{s}^{-1}$	Fan mass flow rate	Assumption and literature
$d_{\text{door,open}}$	10.0	s	Average duration of door opening	
$\underline{\dot{m}}_{\text{door,closed}}$	0.0	$\text{g}\,\text{s}^{-1}$	Specific infiltration, door closed	Assumption and experiments
$\underline{\dot{m}}_{\text{door,open}}$	180.0	$\text{g}\,\text{s}^{-1}$	Specific infiltration, door open	
k_{LT}	0.67	$\text{W}\,\text{m}^{-2}\,\text{K}^{-1}$	Average thermal transmittance	Calibration
$n_{\text{door,per,customer,LT}}$	0.2	customer^{-1}	doors opened per customer	

Table 4.2.: Parameters of the equivalent LT cabinets

$P_{\text{el,int,night}}$, the defrost power $P_{\text{el,defrost}}$, and the start and end of the defrost periods. However, this monitoring data only shows the total sum of power consumption for horizontal and vertical LT cabinets. Using data from name plates on similar types of cabinets, the measured power consumption (Figure A.3) could be divided on the horizontal and vertical type of cabinet.

The fan mass flow rates $\dot{m}_{\text{air,fan}}$ are based on assumptions. The average door opening duration $d_{\text{door,open}} = 10\,\text{s}$ is a realistic assumption based on literature data (Månsson et al. 2019). The specific air infiltration rates $\underline{\dot{m}}_{\text{door,open}}$ and $\underline{\dot{m}}_{\text{door,closed}}$ of the LT cabinets in the test supermarket are assumed to be the same as in the experiments (Table 3.4). The cabinets used in the experiments were not from the same manufacturer, but can be reasonably expected to have very similar infiltration rates. It is an educated guess to assume that the infiltration rates are the same.

Calibration step	Fitting target	Calibration variable	Condition
1	$P_{\text{el,comp,LP}}$	k_{LT}	supermarket closed
2	$P_{\text{el,comp,LP}}$	$n_{\text{door,per,customer,LT}}$	supermarket open

Table 4.3.: Calibration steps LT cabinets

The remaining parameters, thermal transmittance k_{LT} and the number of door openings per customer $n_{\text{door,per,customer,LT}}$, are calibrated using measurement data of the electric power $P_{\text{el,comp,LP}}$ of the low pressure compressor. Both are assumed to be identical for horizontal and vertical LT cabinets, i.e. each customer is assumed to open the same number of lids of horizontal LT cabinets as doors of vertical LT cabinets. The calibration is carried out in two steps (Table 4.3). During each step, one parameter is varied in order to find a good match between the simulated and the measured values of the target variable. The calibration process is carried out in a specific order so the target variable can depend on only one unknown parameter, which is calibrated in this step.

In the first step, the thermal transmittance of the LT cabinets k_{LT} is calibrated using the power consumption of the LP compressor $P_{\text{el,comp,LP}}$ as the target variable. When the supermarket is closed, there are no customers and consequently $n_{\text{door,per,customer,LT}} = 0$. Thus, the compressor power only depends on the unknown variable of thermal transmittance, which can now be calibrated. In the second step, the number of opened LT cabinet doors per customer $n_{\text{door,per,customer,LT}}$ is calibrated, which is the only remaining unknown parameter affecting the low-pressure compressor power.

For the calibration process, the previously described system $F(u(t), p, t)$ (Equation 4.1) is simulated using the input values $u(t)$ from the calibration period (Tables A.8,A.9,A.10,A.11). The integrated square of the error *sqe* between the measured and the simulated fitting target is defined as:

$$sqe = \int_{t_0}^{t_1} (P_{\text{el,comp,LP,meas}} - P_{\text{el,comp,LP,sim}})^2 dt \tag{4.5}$$

The SciPy-library (*SciPy* 2019) is used to minimise the sum of squared errors *sqe* by variation of the calibration parameter.

4.2.3. Medium-temperature display cabinets

The parametrisation of the medium-temperature (MT) cabinets presents several challenges, since there are different types of MT cabinets in the test supermarket. A schematic floor plan is shown in Figure A.1 and a list of display cabinet line-ups is given in Table A.1. There are

predominantly vertical MT cabinets for dairy products, which have a recirculation defrost. There is also one meat cabinet with an electrical defrost, and several service counter. Since no measurement data are available, the service counters are assumed to have the same behaviour as one line-up of dairy product cabinets (*MT3 line-up*, Table A.1). The internal electrical loads of the MT cabinets $P_{\mathrm{el,cab,MT}}$ are estimated based on a typical profile of the total electrical load of all MT cabinets (Figure A.4). Again, the thermal transmittance k_{MT} of the equivalent MT cabinet and the number of door openings of the equivalent MT cabinet $n_{\mathrm{door,per,customer,MT}}$ are calibrated using measurement data. The calibration process (Table 4.4) is analogous to that for the LT cabinet (Table 4.3).

Calibration step	Fitting target	Calibration variable	Condition
1	$P_{\mathrm{el,comp,HP}}$	k_{MT}	Supermarket closed
2	$P_{\mathrm{el,comp,HP}}$	$n_{\mathrm{door,per,customer,MT}}$	Supermarket open

Table 4.4.: Calibration steps MT cabinets

Results of the calibration

The parameters calibrated in the process described earlier are shown in the corresponding tables of display cabinet parameters (4.2, 4.5). During the calibration process, the integrated squared errors were used in the optimisation algorithm.

Three indicators are used to assess how reliably the models predict the energy consumption: 1. the deviation between the simulated and the measured electrical energy consumption; 2. the mean absolute percentage error (MAPE) of power consumption (Equation 3.7); 3. the mean absolute error (MAE). The mean absolute error (MAE, Quaas (2019)) is defined as :

$$\mathrm{MAE} = \frac{\int_{t_0}^{t_1}(|y_{\mathrm{meas}} - y_{\mathrm{sim}}|)dt}{t_1 - t_0} \tag{4.6}$$

The simulated energy consumption and the consumption measured during the calibration period are shown in Table 4.6. Besides the energy consumption by the compressors of the central refrigeration system, the electrical energy consumption by the display cabinets is also shown. During the calibration, the simulated and measured energy consumption matched very well and deviated only by 0.2 %. The mean absolute percentage error (MAPE) of the compressor power is approximately 7 %. The MAPE of power consumption by the LT cabinet is higher (13.6 %). The reason for this is the schedule-based, constant defrost duration. The actual defrost operation and consequently the energy consumption of LT cabinets depends on the actual frosting status and can vary. However, during the calibration period, the model is able to predict the energy consumption of the real supermarket very well. In future research, sensitivity analyses could be carried out to assess the effect of those parameters based on assumptions on those parameters that are calibrated.

4.3. Results of the validation and prediction of energy consumption

This section presents the results of the validation. During calibration certain unknown parameters were calibrated. The entire system was then simulated again using these parameters for a separate period, the validation period.

Parameter	Value	Description	Determination
MT vertical cabinet			
n_{door}	84.0	-	Number of doors	Planning data, Section A.1
A	342.0	m^2	Total surface area of the cabinet	
$P_{\text{el,defrost}}$	0.5	kW	Electrical defrost power	Monitoring system
T_{setpoint}	6.0	°C	Temperature setpoint	
$t_{\text{defrost1,start}}$	4.00	h	Start first defrost	
$t_{\text{defrost1,end}}$	5.00	h	End first defrost	
$t_{\text{defrost2,start}}$	13.00	h	Start second defrost	
$t_{\text{defrost2,end}}$	14.00	h	End second defrost	
$P_{\text{el,int,day}}$	3.4	kW	Electrical power daytime	
$P_{\text{el,int,night}}$	1.5	kW	Electrical power nighttime	
$\Delta T_{\text{sh,evap,setpoint}}$	9.0	K	Evaporator superheat setpoint	
$\dot{m}_{\text{air,fan}}$	4.0	$\text{kg}\,\text{s}^{-1}$	Fan mass flow rate	Assumption and literature
$d_{\text{door,open}}$	10.0	s	Average duration of door opening	
$\underline{\dot{m}}_{\text{door,closed}}$	3.5	$\text{g}\,\text{s}^{-1}$	Specific infiltration, door closed	Assumption and experiments
$\underline{\dot{m}}_{\text{door,open}}$	150.0	$\text{g}\,\text{s}^{-1}$	Specific infiltration, door open	
k_{MT}	2.02	$\text{W}\,\text{m}^{-2}\,\text{K}^{-1}$	Average thermal transmittance	Calibration
$n_{\text{door,per,customer,MT}}$	3.6	customer^{-1}	doors opened per customer	

Table 4.5.: Parameters of the equivalent MT cabinets

The results show that the model describes the actual supermarket system very well (Figures A.12,A.13). Table 4.6 shows the simulated and measured energy consumption from the validation period. The energy consumption of low and high pressure compressors as well as the energy consumption of the cabinets are shown. The simulated energy consumption values differ from the measured values by 3.3 %. The higher deviation of the MAPE of the power consumption of LT cabinets is caused by the defrost which can vary in length but is modelled with a constant duration.

Figure 4.2 shows an additional representation, i.e. the daily deviation between predicted and measured total energy consumption. This includes energy consumption by LP and HP compressors as well as by LT and MT cabinets. Deviation in the calibration period was in the range −2.5 % to 3.5 %. Approximately 60 % of the time, the energy consumption was overestimated by the simulation and the rest of the time it was underestimated. In the validation period, deviation was in the range −8.4 % to 0.8 %. During the validation period, approximately 93 % of the days, energy consumption was underestimated. The main reason is that the evaporation pressure was set to fixed values. These fixed values are the mean values of evaporation pressure during the calibration period. The average measured evaporation pressure of the HP compressor during the validation period was 0.6 bar lower than during the calibration period, while that of the LP compressor was 0.2 bar lower. The lower evaporation pressure in the real supermarket led to an increased energy consumption of the compressors. The simulation model did not take into account the lower evaporation pressure, which may be why it underestimated the energy consumption.

Comparison of estimated parameters

Besides the energy consumption, the values of the calibrated parameters also have to be looked at. For the low-temperature cabinets it was found that each customer opens 0.2 doors

Consumer	Energy Simulation in kW h	Energy Measurement in kW h	Deviation in %	Power MAPE in %
Calibration period				
HP compressor	7154	7211	−0.8	6.7
MT cabinets	1720	1710	0.6	5.2
LP compressor	1844	1841	0.1	10.4
LT cabinets	2884	2814	2.5	13.6
Total	13 602	13 576	0.2	7.1
Validation period				
HP compressor	9532	10 086	−5.5	7.8
MT cabinets	1720	1712	0.5	5.0
LP compressor	1876	1908	−1.7	10.9
LT cabinets	2884	2857	1.0	11.8
Total	16 012	16 562	−3.3	7.6

Table 4.6.: Comparison of measurement data and simulations results for each consumer.

($n_{\mathrm{door,per,customer,LT}}$). This value is applied for each horizontal and vertical low-temperature cabinets. Thus, one customer opens approximately 0.4 doors or lids of low-temperature cabinets on average. This value is compared with a second, complementary and independent method. An analysis of sales data shows that typically 0.4 to 0.6 items of frozen food are bought per till receipt. This is very good agreement between door opening values calculated by two independent methods.

It was not possibly to carry out an analysis of sales data for the MT products. The calibrated parameter $n_{\mathrm{door,per,customer,MT}} = 3.6$ means that each customer opens 3.6 doors of medium-temperature cabinets on average. As more dairy products than frozen food are usually sold, this would not seem to be unrealistic. Using detailed data from the receipt, this could also be further analysed for chilled goods.

The calibrated values of the heat transmittance are $k_{\mathrm{LT}} = 0.67\,\mathrm{W\,m^{-2}\,K^{-1}}$ for LT cabinets and $k_{\mathrm{MT}} = 2.02\,\mathrm{W\,m^{-2}\,K^{-1}}$ for MT cabinets. These values describe the overall heat transmittance, including the glass doors and lids. This approach was used because there was no specific information available about the material or geometry of insulation of the cabinets and their doors. These values seem to be plausible: low-temperature cabinets have an better insulation and thus a lower thermal transmittance. Chaomuang (2019) found a value of $0.77\,\mathrm{W\,m^{-2}\,K^{-1}}$ for the overall heat transfer coefficient of the wall of a MT cabinet and $1.02\,\mathrm{W\,m^{-2}\,K^{-1}}$ for a door with double-glazed windows. Thus, the calibrated values are in a similar range to the values analytically estimated by Chaomuang (2019).

Comparison of further values

Besides the energy consumption, additional variables have to be compared to check whether the results are plausible. The following plausibility checks are important to consider when applying the method to other supermarkets.

A second variable for the plausibility check is the suction gas temperature of the high-pressure compressor (Figure 4.3), which is affected by several variables. The suction gas is

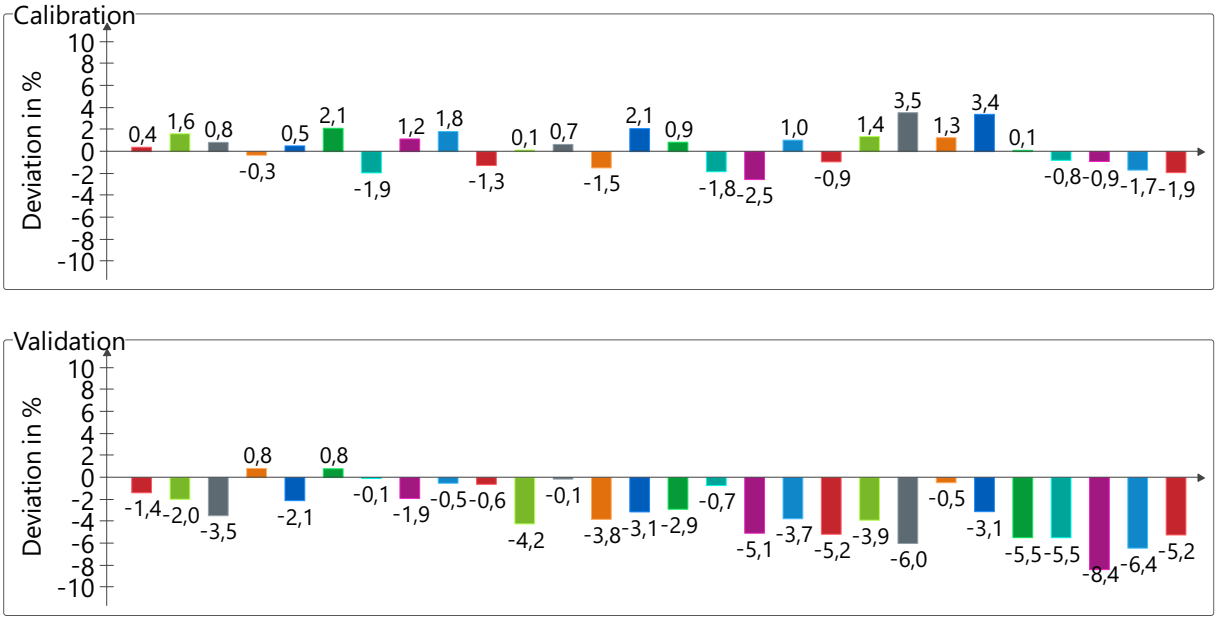

Figure 4.2.: Deviation in percent of simulated and measured daily total energy consumption for calibration and validation periods

a mixture of discharge flow from the LT compressor, flow from the MT evaporators, and flash gas flow from the separator (Figure 2.3)). The suction gas temperature is lower during daytime than during nighttime. During daytime, the ambient temperature is usually higher. This increases outlet temperatures at the gas cooler, which, in turn, leads to higher vapour quality at the separator inlet. This leads to a higher mass flow rate of flash gas which is then throttled in the flash gas bypass valve, added to the suction gas line of the HP compressor and cools it down (Section 2.4.3). The simulated and measured suction gas temperatures are very similar. The mean absolute error (MAE) is 2.2 K. This indicates that the ratio of mass flows from the evaporators and the flash gas are in a realistic order of magnitude. Another variable used for the plausibility check is the discharge temperature of the high pressure compressors. This is affected by the suction and discharge pressure, the suction gas temperature, and by the efficiency of the compressor. The mean absolute error (MAE) between the measured and simulated discharge temperatures is 3.5 K, a good indication that relevant effects of the compressor are modelled. The high-pressure function (Equation 4.3) was also adapted to measurement data. The mean absolute error between the actual high pressure and the simulated high pressure is 1.4 bar, which indicates that the high-pressure function describes the actual high pressure control well.

The next plausibility check is a comparison of cooling loads with data from the literature, specifically of the nominal cooling load per running metre of cabinets. The simulated specific cooling load of the horizontal LT cabinets is 340 $\mathrm{W\,m^{-1}}$. IEA Heat Pump Centre (2017) reported 420 $\mathrm{W\,m^{-1}}$ and Kosar and Dumitrescu (2005) reported 442 $\mathrm{W\,m^{-1}}$ for closed LT island. The test supermarket was opened in in 2017 and the display cabinets are therefore very likely newer and more efficient than those in the literature. Thus, this cooling load is plausible.

Comparison of dimensionless infiltration rate

The approach to modelling display cabinets used in this work include two novelties. Firstly, the interaction between the cabinet and the sales room is described using mass flow rates of

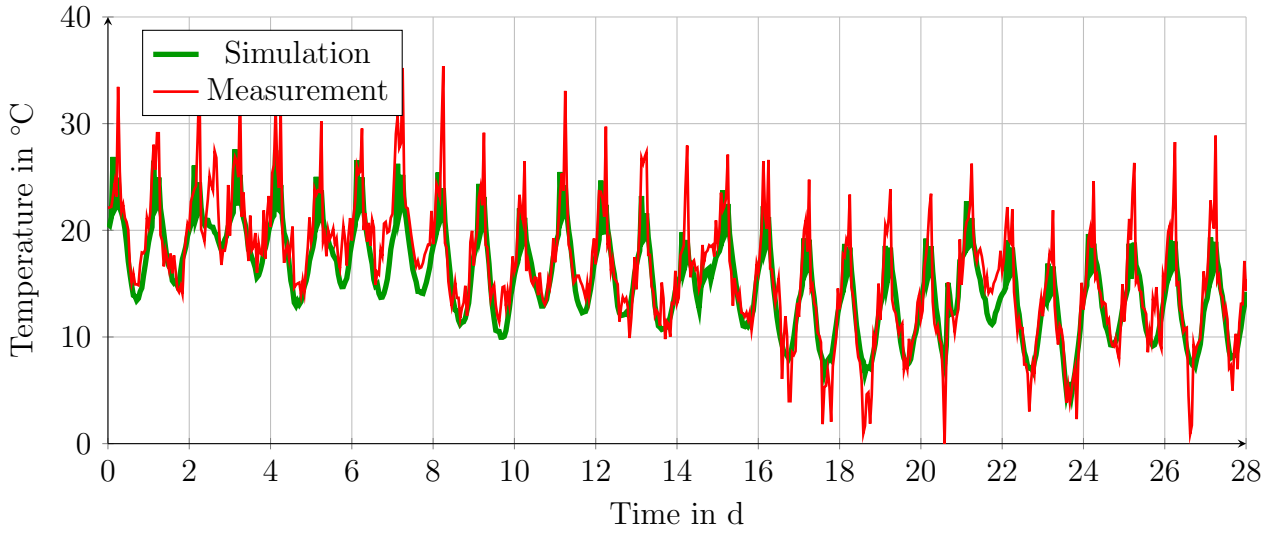

Figure 4.3.: Comparison of measured and simulated suction gas temperatures of HP compressor, validation period

moist air. Secondly, the influence of customers opening cabinet doors is included via the door opening frequency and the number of doors opened per customer (Section 2.4.4).

Therefore, it is expedient to verify the behaviour of this air infiltration separately. Here, the thermal entrainment factor (TEF) for closed cabinet doors is used. It can be interpreted as a dimensionless infiltration rate into the cabinet. For the verification of the air infiltration, the TEF of the simulated MT cabinet is compared to the TEF that is analysed based on monitoring data. In the simulation, the TEF is calculated as the ratio of air flows (Equation 2.67). In the analysis of the monitoring data, the TEF is approximated based on temperature measurements (Equation 2.73). The simulated cabinet does not model frozen evaporators, restocking or other *abnormal operation modes*. Therefore, in the analysis of the monitoring data (Section 3.2), filters have been used to consider only normal operation mode.

The main finding from the data-based analysis of the TEF was that there was an increase of approximately 30 % during an open market compared to a closed supermarket. In the simulation, the TEF is approximately 45 % higher with customers than without customers (Table 4.7). The values from the monitoring system and the simulated values have similar absolute values and similar differences between day and night. It has to be highlighted that the TEF values were determined in two different ways. In the simulation, the TEF was estimated based on the calculated infiltration mass flow rate. For the analysis of the measurement data, it was estimated using different temperature values. This is a relevant indication that the simulations are plausible.

However, there are several issues that have to be taken into consideration when comparing simulation and measurement data. The monitoring data analysis was carried out for vertical MT cabinets using only temperature data. In the simulation, the mass flow rates of *equivalent cabinets* were used. The monitoring data considered solely vertical MT cabinets, while the simulation used an *equivalent MT cabinet*, which included mostly these vertical MT cabinets, but also a few service counters (Table A.1). Thus, the equivalent MT cabinet used in the simulation represents a weighted average of vertical MT cabinets and a few service counters. The TEF describes a ratio of infiltration air flow rate and fan mass flow rate, which are both based on assumptions. Furthermore, the simulation used only typical customer flow data over a period of 2 weeks. The analysis of the monitoring data covered a period of two years, during

	Market closed (night)		Market open (day)		Increase
	Mean	Median	Mean	Median	day to night
Data-based estimation	0.058	0.057	0.074	0.077	$\approx 30\,\%$
Simulation	0.074	0.074	0.107	0.109	$\approx 45\,\%$

Table 4.7.: Comparison of the data based and simulated results of the thermal entrainment factor (TEF) for the vertical MT cabinets in the validation period.

which time the average customer flow rate might vary. Although there are many aspects to take into account regarding the assumptions, limitations and accuracy of the TEF calculation, the comparison of TEF values between simulation and monitoring data encourages the plausibility of the simulations.

4.4. Summary prediction of energy consumption

This section described the predictions of energy consumption by the central refrigeration system and the display cabinets. Since new simulation models are used, several of the required parameters cannot be found in data from manufacturers or in the literature. Therefore, the focus of this chapter was especially laid on the methods for parametrisation. Here, several parameters, such as the thermal transmittance k of the display cabinets or the number of door openings per customer $n_{\mathrm{door,per,customer}}$ were calibrated to measurement data. In the future, it will be possible to estimate these parameters using different methods that were briefly described in this chapter. If these parameters are available in the future, the energy consumption of the display cabinets and the refrigeration system in a supermarket can be predicted using the simulation models developed in this thesis.

It was shown that the consumption of the test supermarket could be predicted very well, with the deviation between predicted and measured total energy consumption at less than 3.5 %. Several additional checks for plausibility and a comparison with literature data indicate that the assumptions and simplifications of the simulation models are justified. Since the methods and choice of parameters are largely based on assumptions for parameters, the plausibility check is very important. The focus on the description of the methods of parametrisation and plausibility check ensure that the models and methods for the prediction of energy consumption can be applied to other supermarkets.

Another result from this chapter is that the interaction between the sales room air and the display cabinets was modelled and quantified in a realistic way. Thus, it can be assumed that the retroactive effect of the display cabinets on the sales room air can also be quantified correctly. This is analysed in the following chapter.

5. Analysis of air exchange between the sales room and the environment and prediction of CO_2 concentration

This chapter describes the investigation of fresh air change rates between sales room air and the environment (control volume *sales room air, ventilation system and occupants* in figure 1.1). Specifically, the effects of customers entering and leaving as well as their duration of stay will be taken into account. In order to assess the fresh air change rates, the CO_2 concentration in the sales room air will be used as an indicator. Firstly, effects that are relevant to the concentration of CO_2 will be analysed. Namely, the concurrent passing of customers through the entrance door and the duration of stay as a function of the number of purchases will be looked at. Secondly, a mathematical model will be developed. This model allows the calculation of CO_2 concentration as a function of the number of receipts and the average number of items per receipt. Finally, the model will be calibrated and validated.

The method proposed in this chapter aims at quantifying the air change rates between the sales room and the environment and bases on the concentration of CO_2 produced by occupants. This CO_2 concentration in supermarkets depends on several opposing effects caused by customers and employees, which are the occupants of a supermarket. On the one hand, they increase the CO_2 concentration by breathing, and on the other hand they reduce it by increasing the air change through the entrance door. Quantifying and combining these effects with CO_2 balance calculations is a novelty.

In this chapter, the following aspects will be described: Firstly, the number of occupants is described via a customer balance. Secondly, the effects of the customer flow on the frequency and duration of door openings will be assessed. Thirdly, a mathematical model describing the CO_2 concentration in the sales room as a function of sales data will be described. This model uses the air infiltration rates into the building as parameters. By calibrating these parameters using measurement data, the fresh air change rates are determined.

5.1. Number of occupants

Customers and employees are the people staying in the sales room and are therefore the occupants. Customers are especially relevant since they have opposing effects on the CO_2 concentration in supermarkets. On the one hand, they breathe and consequently cause an increase of the CO_2 concentration in the sales room air. On the other hand, by entering and leaving the building through doors, they intensify the air exchange between the sales area and the ambient air. Thus, they also cause a reduction of the CO_2 concentration. In the following subsections, these two effects will be investigated and quantified. The fresh air change rate of the sales room air can then be estimated. Two effects related to customers are important for the CO_2 balance in supermarkets:

1. The amount of produced CO_2 depends on the number of people inside the sales rooms
2. The frequency and duration of door openings depend on the number of people entering and leaving

In order to assess these numbers, people are treated as conserved quantities, and a balance equation is set up with the sales room as the control volume. The number of people staying in

the control volume is called n_{people}. Expressing the number of people entering and leaving the control volume as flows ($\dot{n}_{\text{people,entering}}$, $\dot{n}_{\text{people,leaving}}$) leads to the dynamic balance equation of occupants:

$$\frac{\mathrm{d}n_{\text{people}}}{\mathrm{dt}} = \dot{n}_{\text{people,entering}} - \dot{n}_{\text{people,leaving}} \tag{5.1}$$

The number of people staying in the supermarket affects the production of CO_2. The flows of people entering and leaving the market affect the number of door openings that increase the air exchange between the sales room and the environment.

One way of estimating the variables related to people is counting. Counting the number of people who enter and leave the supermarket provide all required information for the balance equation of occupants. The number of people who entered and left the supermarket between a starting point and a certain point of time t are called $n_{\text{people,entered}}$ and $n_{\text{people,left}}$. It is assumed that the supermarket is empty at this starting point:

$$n(t = 0) = 0 \tag{5.2}$$

If these figures are known, the number of people currently staying in the supermarket can be calculated:

$$n_{\text{people}}(t) = n_{\text{people,entered}}(t) - n_{\text{people,left}}(t) \tag{5.3}$$

There are different ways of measuring these variables. Besides the manual counting of people, technical installations such as light barriers or cameras could be used. However, these methods require additional equipment, which is expensive. Another option is to aim at an approximation of these relevant variables based on sales data. This approach will be described in the next section.

5.2. Approximation of customer balance

The total number of people in the supermarket consists of customers n_{customer} and employees n_{empl}. The number of employees is usually known and consequently only the number of customers has to be approximated via the sales data. Sales data are often available in the IT systems of supermarkets. Specifically, the rate of receipts $\dot{n}_{\text{receipt}}$ and the average number of items per receipt n_{item} are available.

In the following paragraphs, the estimation of average values for the customer flow and the number of customers in the sales room will be described. The number of customers entering the supermarket can be approximated using the number of receipts. Often, two or more people go shopping together and share one receipt. This average number of people shopping together is called $n_{\text{person,per,receipt}}$. The customer rate can then be calculated:

$$\dot{n}_{\text{customer,entering}} \approx \dot{n}_{\text{receipt}} \cdot n_{\text{person,per,receipt}} \tag{5.4}$$

The average number of people staying in the sales room can be approximated from the average duration of stay. The average duration of stay is defined as:

$$d_{\text{stay}} = \frac{n_{\text{customer}}}{\dot{n}_{\text{customer,entering}}} \tag{5.5}$$

The average duration of stay can also be expressed as the inverse of the *customer change rate (CCR)*:

$$\mathrm{CCR} = \frac{1}{d_{\text{stay}}} = \frac{\dot{n}_{\text{customer,entering}}}{n_{\text{customer}}} \tag{5.6}$$

The average number of customers in the sales room in the time interval $[t_1, t_2]$ can be approximated using the average duration of stay and the average customer flow for that time interval. The average values are identified by over lined variables:

$$\overline{n}_{\mathrm{customer,t_1,t_2}} = \overline{d}_{\mathrm{stay,t_1,t_2}} \cdot \overline{\dot{n}}_{\mathrm{customer,entering,t_1,t_2}} \tag{5.7}$$

The estimation of the average duration of stay $\overline{d}_{\mathrm{stay,t_1,t_2}}$ based on sales data will be described in the following section.

Duration of stay

The objective is to estimate the duration of stay as a function of the available sales data. There are many different studies about the behaviour of customers in supermarkets (for instance GfK Consumer Panels (2012, 2013a,b) and Sorensen et al. (2017)). However, the objective is to use a simple and yet robust measure to estimate the duration of stay. To this end, the amount of purchased goods is used as an indicator.

The correlation between the amount of purchased goods and the shopping duration is obvious: the more you buy, the more time you need. The amount of purchased goods can be measured using the total number of items or the money spent (Voigt 2018). Here, the number of items per receipt will be used.

Method

Over a period of 1.5 years, data from more than 500 shopping trips made by various test persons was collected. Beside the number of purchased items, several other variables affect the duration of stay. First of all, there are obviously differences between the test persons. Their personal shopping preferences, or their age and physical constitution can affect the shopping duration. The dimensions of a supermarket can also affect the duration of stay. Purchasing the same number of items in a huge supermarket may take longer than in a small one. Another factor that would generally tend to increase the shopping duration is the use of other services and shops located in the sales area. This can be, for instance, a bakery or a return point for reusable plastic bottles.

In order to analyse whether the previous factors do have an impact on the shopping duration, different variables have been collected for each shopping trip. The specific variables which were collected are: 1. name and location of supermarket 2. date 3. time 4. number of persons shopping together 5. duration of stay 6. receipt amount 7. number of items purchased 8. use of bottle return point 9. if a shopping list was used or not 10. use of other services in the sales area (for instance, bakery).

Results and discussion

From the available data, shopping trips to supermarkets and discount stores were filtered. Data from shopping trips to hypermarkets were excluded. Figure 5.1 shows the duration of stay plotted against the number of items purchased. The data comprises 395 shopping trips made by 10 test persons to different supermarkets and discount stores. Additional information about the incidence of each shopping duration can be found in Figure A.5. An overall tendency can be observed: the duration of stay increases with the number of items purchased. Additionally, a huge scattering can be observed. This data includes various test persons and different supermarkets. Additionally, the shopping trips were carried out at different times of the week. Consequently, the occupancy of the supermarkets might have varied. Still, the overall trend is visible. A linear regression has been applied to the data. The linear function has two parameters d_{offset} and d_{var}.

$$d_{\mathrm{stay}} = n_{\mathrm{item}} \cdot d_{\mathrm{var}} + d_{\mathrm{offset}} \tag{5.8}$$

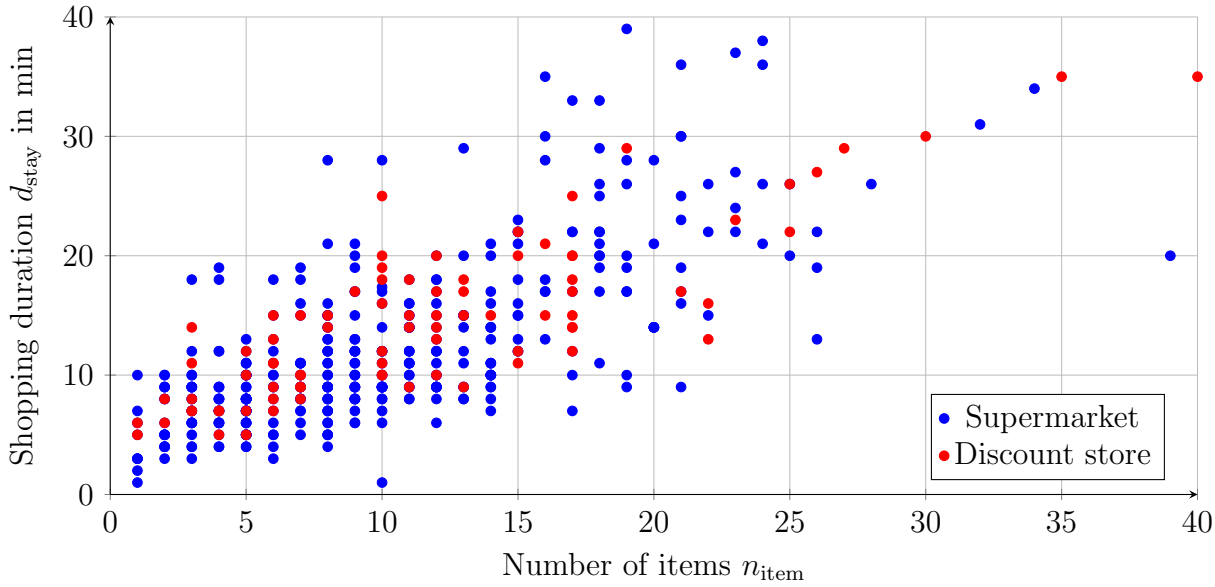

Figure 5.1.: Duration of stay as a function of purchased items for 395 shopping trips by 10 test persons.

The regression for the specific data of supermarkets shown in Figure 5.1 leads to:

$$d_{\text{stay}} = n_{\text{item}} \cdot 48\,\text{s/item} + 254\,\text{s} \tag{5.9}$$

This linear regression can only be a first approximation of the shopping duration. Figure 5.1 shows several shopping trips shorter than 4 min. Effects as the total occupancy of the supermarket affect the waiting time in the queue which is more relevant for short than for long shopping trips. However, although there is data of 395 shopping events, this was not enough to allow a systematic assessment of further influencing factors. For the modelling, some of these occupancy-related effects are considered by introducing a *nominal customer flow* (Section 5.4).

Conclusion

It could be shown that the duration of stay depends on the number of items purchased. But although several other factors exist, their influence on the duration of stay cannot be quantified. More data would be necessary. Nevertheless, the analysed data allows establishing a realistic correlation between the number of items purchased and the duration of stay.

In this section, it has been shown that the balance of people can be approximated using sales data. Specifically the customer rate $\dot{n}_{\text{customer}}$ can be calculated based on the rate of receipt $\dot{n}_{\text{receipt}}$. The average shopping duration can be calculated based on the average number of items per receipt. Here, it has been demonstrated that this approximation is possible.

In order to describe the people balance of a specific supermarket based on the sales data, three parameters have to be assessed/adapted to the specific supermarket:

- average number of people shopping together $n_{\text{person,per,receipt}}$
- regression coefficient d_{var}
- regression coefficient d_{offset}

5.3. Door openings

The entrance area is highly relevant with regard to the air exchange between the sales room and the environment. There is a broad range of entrance areas depending on the type of supermarket. Supermarkets located inside shopping centres often do not have doors to separate them from the main area of the shopping centre. Supermarkets that can be entered directly from outside are usually equipped with doors. Again, there can be different kinds of entrances using doors: There may be separate entrance and exit doors or a single door. Often, a vestibule or other facilities exist, with the aim of reducing the air exchange (Cho et al. 2010, Sawaf et al. 2012, Ye et al. 2017).

The overall aim is the estimation of the air exchange between sales room air and the environment. Although there are many factors influencing this air exchange it is undoubtedly relevant whether the entrance door is open or closed. The effect of air flows induced by the movement of customers or the doors are not especially considered. The most important factor is consequently the total duration of door openings in a certain interval. This duration depends on the number of customers entering and leaving the supermarket, as well as on the duration of a single door opening.

This section investigates the effects of customers on the total duration of door openings. To this end, it looks at a stand-alone supermarket with a single entrance for entering and leaving. The entrance consists of one automatic sliding door.

Effects and outlook

One important aspect of customers entering and leaving is that several customers can cross the door simultaneously (Yuill et al. 2000). *Crossing* here shall be defined as the process of a person crossing the threshold of the door, regardless of the direction. Various people crossing the door simultaneously can reduce the overall door opening frequency compared to individual door crossings.

This section is divided into several parts. Firstly, a simulation approach for the analysis of door openings will be described. Secondly, the door opening frequency as a function of the customer flow will be analysed by contrasting simulation results with field data from a real supermarket. Finally, the total duration of door openings as a function of customer flow is analysed.

5.3.1. Simulation of door openings

Simulations are used to analyse the effect of customers entering and leaving the supermarket on the openings of the door. The objective is to estimate the total duration of door openings and the number of door openings for a given time period with the length D. This time period is typically one hour. The model is based on work by Kohri (2001) who simulated the door opening duration of two double doors with an intermediate vestibule. Here, only a single automatic door is simulated. The model uses random numbers to estimate the moment of entering and leaving of single customers.

The simulation model is based on several simplifying assumptions. All customers enter the supermarket in an arbitrary instant within the time period. Each point in time has the same probability. Each customer's duration of stay is an arbitrary number between the minimum and maximum duration of stay ($d_{\mathrm{stay,min}}$, $d_{\mathrm{stay,max}}$).

The door sliding mechanism is triggered each time a person approaches the door, regardless of whether the person is entering or leaving the supermarket. Triggering the mechanism opens the door. The door is kept open for the minimum door opening time $d_{\mathrm{door,open,min}}$. Afterwards

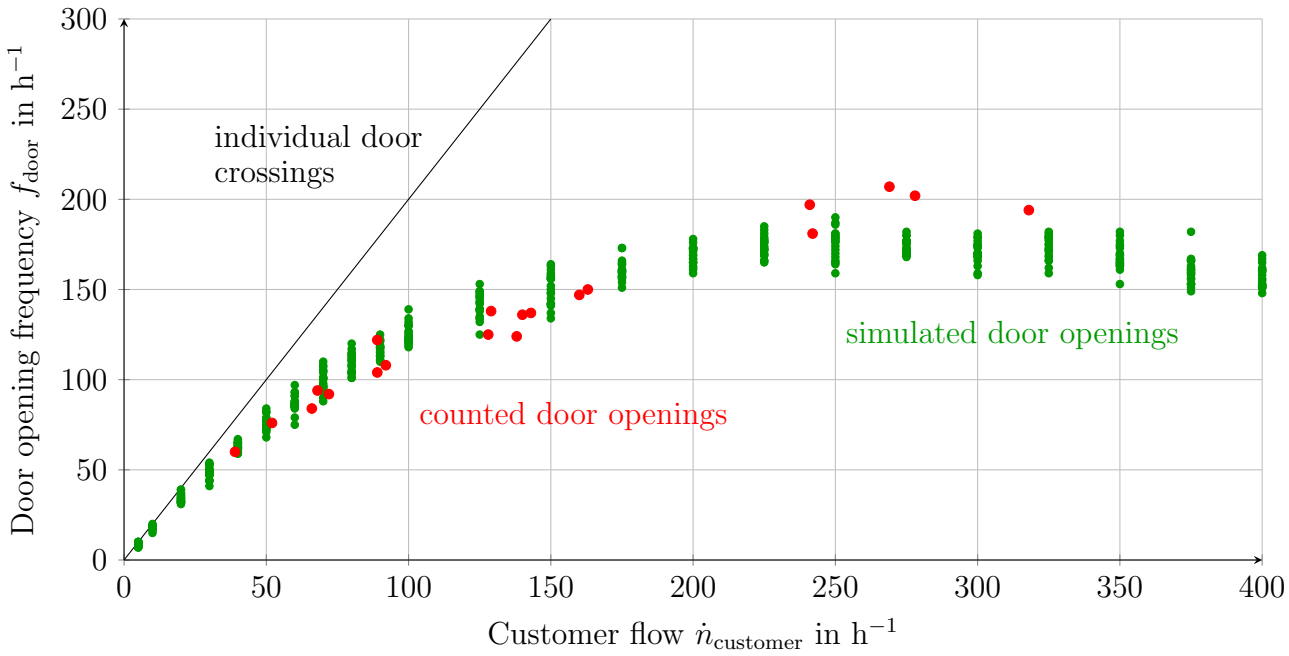

Figure 5.2.: Frequency of door openings as a function of the customer rate. Individual door crossings as well as frequencies based on simulations and counted door openings are shown. Simulated values are based on Monte-Carlo simulation, counted values are based on Voigt (2018)

it closes automatically. If the door is already open when the mechanism is triggered it stays open for a new period of $d_{door,open,min}$

The result of the simulation is the opening status of the entrance door for each instant of the simulated time period. The input values of the simulation are the customer flow per hour $\dot{n}_{customer}$, the minimum and maximum duration of stay $d_{stay,min}$ and $d_{stay,max}$ as well as the minimum door opening time $d_{door,open,min}$.

A time period of length D is looked at and discretised into periods of 1 s length. The simulation repeats the following steps for each customer

1. The moment of entry is estimated based on a random number from the interval [0,D].
2. At this moment of entry, the door sliding mechanism is marked as activated.
3. The shopping duration is estimated based on a random number $d_{rand} \in [d_{stay,min}, d_{stay,max}]$.
4. In the instant of leaving, the door sliding mechanism is marked as activated again.

There are two main results of analysis, which will be discussed in the following two sections:

1. Frequency of door openings: how many times the door was opened in the time period with length D.
2. Total share of door opening time: how long the door stayed open overall in the period of the length D

5.3.2. Frequency of door openings

Firstly, this section investigates the frequency of door openings. The frequency of door openings is the number of door openings in a certain time period and is called $f_{door,open}$. If every customer walked through the door alone, they would cause two door openings: one entering

and one leaving. The corresponding door opening frequency is called $f_{\text{door,indi,crossing}}$ and can be calculated based on the customer rate:

$$f_{\text{door,indi,crossing}} = 2 \cdot \dot{n}_{\text{entering}} \tag{5.10}$$

However, when the customer flow exceeds a certain level, the actual door opening frequency is lower than this frequency of individual door crossings. This is caused by simultaneous door crossings by two or more customers.

Figure 5.2 show the frequency of door openings as a function of the customer flow. It shows the frequency of individual crossings, counted data from the test supermarket and simulated data for the test supermarket.

Voigt (2018) counted the number of door openings and the number of customers entering and leaving during several time periods of 1 h length for the test supermarket. These values are shown as *counted values* in the diagram (Figure 5.2). For a low customer rate ($\dot{n}_{\text{customer}} < 50\,\text{h}^{-1}$), the actual frequency of door openings converges with the door opening frequency for individual crossings. For higher customer rates ($\dot{n}_{\text{customer}} > 250\,\text{h}^{-1}$), the actual frequency is significantly lower than the frequency of individual door openings. This would appear to be plausible: the more people cross the door, the higher the probability that they cross the door at the same time. The minimum door opening time in this supermarket was approximately 7 s. Simulations, as described above, have been carried out using this value $d_{\text{door,open,min}} = 7\,\text{s}$ as a parameter. The shopping duration was assumed to be between 1 min to 16 min. The frequency of shopping durations can be approximated by a log-normal distribution (Sorensen et al. 2017). The distribution of shopping durations based on the analysis of test persons (Section 5.2) is similar to that of a log-normal distribution (Figure A.5). This means that the majority of shopping trips are rather *short*. This does not exclude that single customers need much longer time. The limit of 16 min is an assumption, which however is believed to be realistic for the specific test supermarket. Further investigation using data from a customer balance based on counting could help to refine the simulation and its assumptions.

The results of the simulation are shown as *simulated values* (Figure 5.2). The simulation results are very similar to the field data from Voigt (2018). Thus, it can be concluded that the actual door opening frequency can be expressed as a function of customer flow, shopping duration and minimum door opening time:

$$f_{\text{door,actual}} = f(\dot{n}_{\text{customer}}, d_{\text{stay,min}}, d_{\text{stay,max}}, d_{\text{door,open,min}}) \tag{5.11}$$

5.3.3. Total share of door opening time

As mentioned in the introduction to this section, the main factor that influences the air change rate is the total duration of door openings D_{door} in a certain time interval D. It depends on the frequency of door openings an the duration of each door opening. This total duration of door openings can be estimated using the simulation of door openings described above. In order to eliminate the dependency on the duration of the time interval considered, it is divided by the duration of the time interval:

$$\xi = \frac{D_{\text{door}}}{D} \tag{5.12}$$

Kohri (2001) named this variable *opening time ratio*, here it is called the share of door opening time. It clearly depends on the customer flow and on the duration of door openings. The maximum value is 1, which would mean that the door is open the entire time.

The total share of door opening time was analysed using the previously described simulations. The same parameter ($d_{\text{door,open,min}} = 7\,\text{s}$, $1\,\text{min} < d_{\text{stay}} < 16\,\text{min}$) as before were

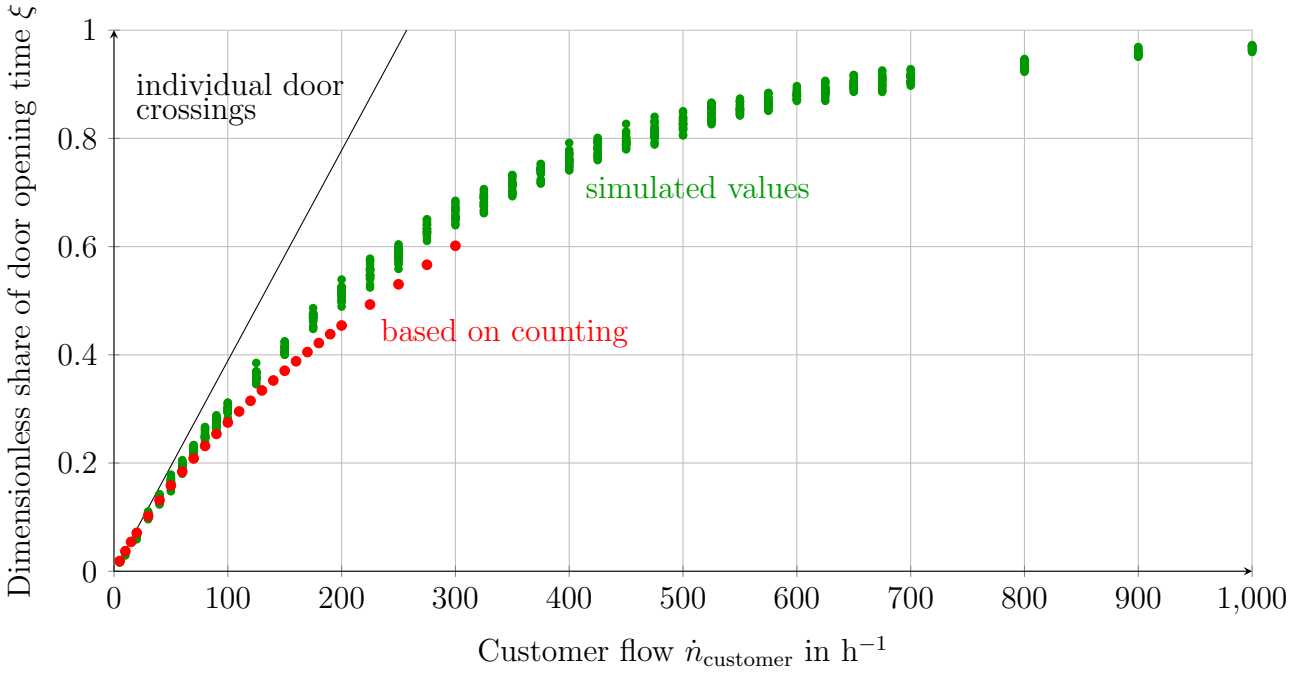

Figure 5.3.: Share of door opening time as a function of the customer flow. Simulated values are based on Monte-Carlo Simulation with $d_{\text{door,open,min}} = 7\,\text{s}$. The counted values are based on data by Voigt (2018)

used. Figure 5.3 shows the dimensionless share of total door opening time as a function of the customer flow. It shows firstly, the simulation results and secondly, a curve based on data from Voigt (2018). Voigt used an accelerometer to estimate the duration of individual door openings and combined it with a manually counted number of customers. Again, the results of the simulation and the data based on measurements are very similar. This is a good indication that the simulations are plausible. The total share of door opening time converges to unity for a high number of customers. This is in line with results shown by Kohri (2001) for two doors with a vestibule in between.

In general, the share of door opening time depends on various factors such as customer flow and the duration of a single door opening:

$$\xi = f(\dot{n}_{\text{customer}}, d_{\text{door}}) \tag{5.13}$$

This result shows that the effect of customers and their door-crossing patterns are very relevant. Additionally, the comparison between measured and simulated door crossings show a good agreement.

Summary

In this section several effects have been explained that affect the duration of door openings and consequently the air exchange between the sales area and the ambient air. A highly relevant effect is the simultaneous crossing of the entrance door by two or more customers. The implications for the number of door openings and the total duration of door openings have been explained. It has been demonstrated that the total duration of door openings can be expressed as a function of the number of customers. The formulas shown in this section have been derived assuming a single door for entering and leaving the market. However, they could also be transferred to supermarkets with separate doors for entering and leaving.

5.4. Modelling of CO_2 concentration

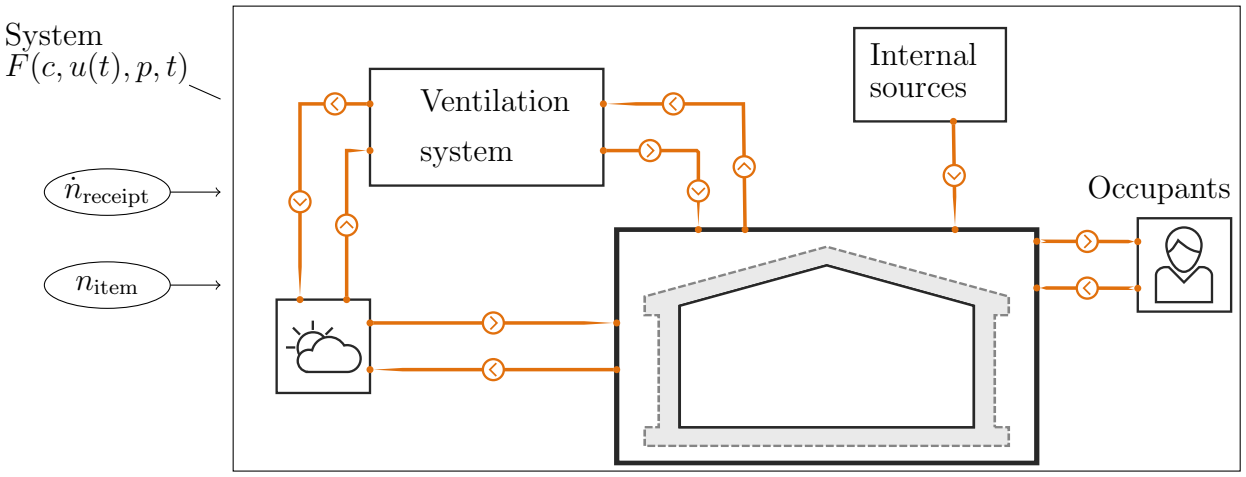

Figure 5.4.: Control volumes and air flows that are relevant for the CO_2 balance as well as boundary of the simulated system and its time dependent input variables

The objective of this chapter is to estimate the air change rates between the sales room and the environment. There are approaches and correlations to estimate the air exchange through doors based on pressure and temperature differences (Yuill et al. 2000). Here, a tracer gas approach is presented that uses the CO_2 produced by customers and employees. The CO_2 concentration in the sales room is affected by several factors. In particular the customers have to be considered, because they both increase and reduce the CO_2 concentration. As previously described, customers have two main effects. Firstly, the production of CO_2 depends on the number of customers staying in the sales area. This number can be approximated based on sales data (Section 5.2). Secondly, the simultaneous crossing of the entrance door depends largely on the customer flow $\dot{n}_{\text{customer}}$ (Section 5.3). In the following, the structure of the model, the parameters and the transport processes are described.

Structure of the model

The model describes the concentration of CO_2 in the sales area as a function of time-dependent input variables $u(t)$, the time t and a set of parameters p:

$$\frac{\mathrm{d}c}{\mathrm{dt}} = F(c, u(t), p, t) \tag{5.14}$$

The time dependent input values $u(t)$ are:

- rate of receipt per hour $\dot{n}_{\text{receipt}} = f(t)$
- number of items per receipt $n_{\text{item}} = f(t)$

The number of items per receipt is time-dependent, because on certain weekdays or times of the day, customers buy more, for instance, on a Saturday morning. In the following the balance equation will be described.

Balance equation CO_2

The dynamic mass balance of CO_2 can be derived from the general mass balance of the sales room air (Equation 2.14). The overall mass balance of sales room air includes the air exchange with display cabinets. Since there are neither sources nor sinks of CO_2 in the display cabinets,

this air exchange can be neglected for the balance equation. There are three mechanisms that have to be included in the dynamic mass balance of CO_2: 1. breathing of occupants in the sales room 2. air exchange with the ambient due to infiltration and ventilation 3. other sources such as fruit respiration. Figure 5.4 is a detail from the scheme for the entire supermarket system (Figure 2.1) showing the relevant interactions for the CO_2 balance.

Here, the concentration is expressed as mole fraction c, because this is the unit used in the measurements. The conversion has been described in Equation 2.9.

$$\begin{aligned} m_{\mathrm{air,sa}} \cdot \frac{\mathrm{dc_{sa}}}{\mathrm{dt}} &= \dot{m}_{\mathrm{air,breathing}} \cdot (c_{\mathrm{breathing}} - c_{\mathrm{sa}}) \\ &+ (\dot{m}_{\mathrm{air,inf}} + \dot{m}_{\mathrm{air,vent}}) \cdot (c_{\mathrm{amb}} - c_{\mathrm{sa}}) \\ &+ \dot{m}_{\mathrm{CO_2,source}} \cdot \frac{M_{\mathrm{air}}}{M_{\mathrm{CO_2}}} \end{aligned} \tag{5.15}$$

This equation includes several assumptions. The air in the control volume is assumed to be perfectly mixed. Consequently, all air flows leaving the control volume have the same concentration as the air in the sales area c_{sa}. The volume of air inside the sales area varies depending on the number of people and amount of goods in the sales area. However, this effect is small and consequently neglected. The effect of density fluctuation caused by variations in temperature or concentrations of CO_2 and humidity is small and the resulting air flow is neglected. This allows the assumption that the mass of air in the control volume is constant.

Respiration

Respiration is the main source of CO_2 in the sales area of a supermarket. Although the amount of CO_2 produced during breathing depends on a variety of factors such as physical condition and activity (Deutsches Institut für Normung 2005), it is assumed that all occupants in the sales area have the same respiration rate $\dot{m}_{\mathrm{breathing,per,person}}$ (Table 2.1). The total airflow rate of respiration can then be calculated using the total number of people n_{people} staying in the sales area:

$$\dot{m}_{\mathrm{air,breathing}} = n_{\mathrm{people}} \cdot \dot{m}_{\mathrm{breathing,per,person}} \tag{5.16}$$

The people in the supermarket are employees and customers

$$n_{\mathrm{people}} = n_{\mathrm{empl}} + n_{\mathrm{customer}} \tag{5.17}$$

The number of employees for a specific supermarket is known (Table 5.1). The number of customer can be approximated from the average duration of stay and the customer flow (Equation 5.5):

$$n_{\mathrm{customer}} = d_{\mathrm{stay}} \cdot \dot{n}_{\mathrm{customer,entering}} \tag{5.18}$$

The customer flow can be approximated from the number of receipts and the average number of persons per receipt (Equation 5.4):

$$\dot{n}_{\mathrm{customer,entering}} \approx \dot{n}_{\mathrm{receipt}} \cdot n_{\mathrm{person,per,receipt}} \tag{5.19}$$

The overall mass flow rate of breathing is:

$$\dot{m}_{\mathrm{air,breathing}} = (n_{\mathrm{empl}} + d_{\mathrm{stay}} \cdot \dot{n}_{\mathrm{receipt}} \cdot n_{\mathrm{person,per,receipt}}) \cdot \dot{m}_{\mathrm{breathing,per,person}} \tag{5.20}$$

The duration of stay was approximated using the number of items purchased per receipt (Equation 5.8). Here, the calculation of the average duration of stay d_{stay} is extended to consider the overall occupancy of the supermarket. The more people go shopping, the longer

a customer needs, because, for instance, the waiting time in the queue is longer. This is considered by a nominal customer flow $n_{\text{customer,nom}}$ as an additional parameter:

$$d_{\text{stay}} = \frac{\dot{n}_{\text{customer,entering}}}{\dot{n}_{\text{customer,nom}}} \cdot (n_{\text{item}} \cdot d_{\text{var}} + d_{\text{offset}}) \tag{5.21}$$

The total mass flow rate of breathing can be calculated using Equations 5.20 and 5.21, the time-dependent input variables $\dot{n}_{\text{receipt}}$ and n_{item}, as well as several other parameters.

Infiltration

The objective of this chapter is the quantification of the air exchange between the supermarket and the environment. Effects on the air exchange such as wind or the speed of customers crossing the entrance door are not specifically modelled. Thus, only the forced air exchange performed by the ventilation system and the air exchange that also occurs when the ventilation system is not in operation are relevant.

The air exchange induced by the ventilation system can be calculated based on the nominal air change rate and the information about the operation status. The nominal air exchange is known from the technical data sheet and forms part of the parameters for a specific supermarket. The operation status of the ventilation system $i_{\text{vent,active}}$ indicates whether it is active or not and is one of the time-dependent input values during calibration. Thus, the air flow rate induced by the ventilation system is:

$$\dot{m}_{\text{air,vent}} = \dot{m}_{\text{air,vent,nom}} \cdot i_{\text{vent,active}} \tag{5.22}$$

The air exchange between the sales room and the environment via the entrance door of a supermarket is a transport process across the system boundaries of the supermarket. As previously described (Section 2.1), the calculation of the flow variable can be a function of the potential difference or calculated without using information about the potential variables. The potential variables for the air exchange are the temperature and the pressure. The calculation of the air infiltration through doors based on pressure differences is well established (Cho et al. 2010). Titze (2017) calculated the volume of air exchange as a function of the temperature difference and geometric parameters of the door. Martin (2017) compared different analytical approaches to estimate the air infiltration through different kinds of open doors. The calculated values differ considerably, depending on the formula and the assumptions made. The calculation of the air exchange based on potential differences requires additional parameters, such as door geometry or pressure drop coefficients. The air pressure inside a supermarket is not modelled and many geometric parameters of the door are not available.

Therefore, this work follows the approach of calculating the air flow without using the potential variables. The air exchange that occurs when the ventilation system is not in operation is assumed to depend only on whether the door is open or closed. The overall air infiltration rate are called $\dot{m}_{\text{inf,door,open}}$ for an open door and $\dot{m}_{\text{inf,door,closed}}$ for a closed door.

$$\dot{m}_{\text{air,inf}} = \begin{cases} \dot{m}_{\text{air,inf,door,open}} & \text{if door is open} \\ \dot{m}_{\text{air,inf,door,closed}} & \text{if door is closed} \end{cases} \tag{5.23}$$

The average air infiltration rate for a period when the door is partly open can be calculated as:

$$\dot{m}_{\text{air,inf}} = \xi_{\text{door,open}} \cdot \dot{m}_{\text{air,inf,door,open}} + (1 - \xi_{\text{door,open}}) \cdot \dot{m}_{\text{air,inf,door,closed}} \tag{5.24}$$

The total share door of the opening time $\xi_{\text{door,open}}$ has been described previously (Section 5.3.3). The equations mentioned earlier describe the air exchange between the sales area

and the ambient air. The overall air exchange between the sales area and the ambient air is described as a function of the number of customers. To this end, the parameters $\dot{m}_{\text{air,inf,door,open}}$ and $\dot{m}_{\text{air,inf,door,closed}}$ have to be calibrated.

Other sources

People staying in the sales area are the main source of CO_2, but they are not the only source. Respiration of fruits, leakage from R-744 refrigeration systems or plants in the shop can also affect the CO_2 concentration. Except for fruit respiration, other factors that could affect the level of CO_2 can hardly be quantified. Leakage of CO_2 from the refrigeration system should not normally occur and is therefore neglected. In supermarkets, there are usually only a few plants, which is why their influence on the CO_2 concentration is also neglected. The influence of fruit respiration is considered, as proposed by Titze (2017). An average emission rate of CO_2 per mass of fruit $\dot{e}_{\text{CO}_2,\text{fruit}}$ is combined with an average mass m_{fruit} of fruit stored in the sales area:

$$\dot{m}_{\text{CO}_2,\text{source}} = \dot{e}_{\text{CO}_2,\text{fruit}} \cdot m_{\text{fruit}} \tag{5.25}$$

Summary

The equations derived in this section form a system of equations. As described above, this model allows the calculation how CO_2 concentration in a supermarket changes over time. This models requires knowledge of some supermarket specific parameters as well as time-dependent input data.

5.5. Prediction of CO_2 concentration in the sales room

So far, a model has been described that allows the calculation of the CO_2 concentration in the sales room of a supermarket as a function of time-dependent sales data $u(t)$ and a limited number of parameters (Table 5.1). This model (Equation 5.15) specifically takes into account the effects of customers and was implemented using Modelica. The air infiltration rates through open and closed doors ($\dot{m}_{\text{inf,door,open}}$, $\dot{m}_{\text{inf,door,close}}$) are currently unknown parameters that need to be calibrated.

In this section, measurement data from the test supermarket will be used and the process of parameter estimation, calibration and validation will be presented. In summer, the separate entrance door to the bakery (Figure A.1) was usually left open, while in winter, it was opened only when a customer walked through. This additional door opening has a large effect on the air exchange in summer. Therefore, the calibration and validation process will be carried out separately for summer and winter.

This section starts by categorising and describing the required parameters (Table 5.1) of the simulation model. It then describes the method and results of the calibration processes. Finally, the simulation model will be validated and the results will be discussed.

5.5.1. Parameter estimation

In this section the parameters are presented. The parameters used for the validation can be divided into three categories.

- General parameters independent of a specific supermarket
- Parameters that need to be adapted for each specific supermarket
- Parameters for a specific supermarket that need to be calibrated

Here, the parameter estimation will be exemplified using data from the test supermarket. Table 5.1 gives an overview of the parameters.

Parameter	Value		Description	Determination
General parameters				
c_{amb}	410	ppm	CO_2 concentration of ambient air	Literature
$c_{CO_2,breathing}$	40 000	ppm	CO_2 concentration of breath	
$\dot{m}_{breathing,per,person}$	0.7	$kg\,h^{-1}$	Mass flow rate of breath	
$\dot{e}_{CO_2,fruit}$	31.5	$mg\,kg^{-1}\,h$	CO_2 production of fruit	
Specific parameters of the test supermarket				
$n_{person,per,receipt}$	1.3		Number of persons per receipt	Customer balance
$\dot{n}_{customer,nom}$	100	$customer^{-1}$	Nominal customer flow	
d_{offset}	254	s	Function parameter	
d_{var}	48	s $article^{-1}$	Function parameter	
$\xi_{door,open,actual}$	Equation 5.26		Actual door opening duration	Simulation
n_{empl}	6	employees	Number of employees	Observation
m_{fruit}	600	kg	Mass of fruit in the sales room	
$m_{air,sa}$	9600	kg	Mass of air in the sales room	Planning data
$\dot{m}_{vent}$	5700	$kg\,h^{-1}$	Mass flow rate ventilations system	
Specific parameters that are calibrated				
$\dot{m}_{inf,door,closed}$	796	$kg\,h^{-1}$	Infiltration, closed door (winter)	Calibration
$\dot{m}_{inf,door,closed}$	631	$kg\,h^{-1}$	Infiltration, closed door (summer)	Calibration
$\dot{m}_{inf,door,open}$	6703	$kg\,h^{-1}$	Infiltration, open door (winter)	Calibration
$\dot{m}_{inf,door,open}$	18 318	$kg\,h^{-1}$	Infiltration, open door (summer)	Calibration

Table 5.1.: Parameters for the CO_2 balance model

The CO_2 concentration of ambient air c_{amb} is assumed to be 410 ppm, which is in line with recent developments (Umweltbundesamt 2019). The values of mass flow rate of breathing and CO_2 concentration of breathing are based on work by Voigt (2018). The specific emission rate of CO_2 per hour and kg of fruit caused by fruit respiration is assumed to be $\dot{e}_{CO_2,fruit} = 31.5\,mg\,kg^{-1}\,h^{-1}$. This is the same value as used by Titze (2017) and based on Bier et al. (1952). These general parameters can be used for different supermarkets.

Some of the parameters need to be adapted for each specific supermarket. The air volume of the sales area is assumed to be $8100\,m^3$ and estimated based on the planning data. This corresponds to a mass of approximately $m_{sa} = 9600\,kg$ at 20 °C. Based on planning data of the test supermarket, the air mass flow rate of the ventilation system is assumed to be $\dot{m}_{vent} = 5700\,kg\,h^{-1}$.

The parameters used to calculate the average duration of stay (d_{min},$d_{per,item}$) are estimated via an analysis of shopping events by the test persons (Section 5.2). The shopping events have not been measured in the specific test supermarket, but in supermarkets of a similar type and size. Nevertheless, the method is applicable to any supermarket. The mass of fruits in the market is an educated guess based on the counting of several fruit showcases in the test supermarket and extrapolation.

The test supermarket has a vestibule with two automatic doors (Figure A.1). Kohri (2001) described the computation of the door opening time of such a door configuration. The computation of this door configuration requires several additional parameters, such as the difference in start time between door openings or the customers' average duration of stay inside the

vestibule. These values were not available or difficult to measure. Therefore, in a first approach, the door opening behaviour of the two automatic doors was approximated based on a single automatic door.

The door opening behaviour of the single, automatic door is described by the total share of door opening time $\xi_{\text{door,open}}$ (Equations 5.12,5.13) as a function of the customer flow. It was estimated via simulations (Section 5.3.1) of a single, automatic door. The minimum door opening time $d_{\text{door,min}} = 7\,\text{s}$ and duration of stay $d_{\text{stay}} \in [1\,\text{min}, 16\,\text{min}]$ are parameters of the simulation that are adapted to the specific test supermarket (see Section 5.3). The results of this Mont-Carlo simulation describe the share of door openings as a function of customer flow $\dot{n}_{\text{customer}}$. These results may resemble the following equation which was estimated using an regression analysis (Figure 5.3).

$$\xi_{\text{door,open,actual}} = (0.0019 \cdot \dot{n}^3_{\text{customer}} - 4.1514 \cdot \dot{n}^2_{\text{customer}} + 3287 \cdot \dot{n}_{\text{customer}}) \cdot 10^{-6} \tag{5.26}$$

It is valid for customer flows ranging from 0 customers/h to 800 customers/h.

Besides theses specific parameters that can be estimated based on planning and sales data or simulations, some parameters need to be calibrated. Specifically, the parameter describing the air infiltration from the ambient into the sales room ($\dot{m}_{\text{air,inf,door,open}}$ and $\dot{m}_{\text{air,inf,door,closed}}$) (Section 5.4) are calibrated.

5.5.2. Calibration

The air infiltration for open and closed doors are unknown and have to be calibrated using the previously described model and measurement data. The air infiltration rates for summer and winter are different, because in summer the door of the bakery was usually kept open. Therefore, the infiltration rates were estimated separately for summer and winter. These periods were chosen based on the availability of the sales data needed as input values.

As in the previous chapter, the calibration is done by solving a dynamic parameter estimation problem. The objective of the calibration is the estimation of $\dot{m}_{\text{air,inf,door,open}}$ and $\dot{m}_{\text{air,inf,door,closed}}$, which describe the air exchange between the sales room and the ambient air. Again, two different periods are used for calibration and validation. In order to calibrate the air infiltration rates, a dynamic parameter estimation problem is solved. One parameter is varied in order to minimise a target variable. This target variable is the integration of squared errors *sqe* between measured and simulated CO_2 concentration.

$$sqe = \int_{t_0}^{t_1} (c_{\text{CO}_2,\text{meas}} - c_{\text{CO}_2,\text{sim}})^2 dt \tag{5.27}$$

The model (Equation 5.14) of the air in the sales area was simulated for a certain period and SciPy library (*SciPy* 2019) was used to find the parameter values of the infiltration rates that minimise the integrated squared error *sqe* (Equation 5.27).

Calibration step	Fitting target	Calibration variable	Condition
1	c_{CO_2}	$\dot{m}_{\text{air,inf,door,closed}}$	Supermarket closed
2	c_{CO_2}	$\dot{m}_{\text{air,inf,door,open}}$	Supermarket open

Table 5.2.: Calibration steps air infiltration building

The calibration was carried out in a specific order (Table 5.2). In a first step, the air infiltration of the closed door $\dot{m}_{\text{air,inf,door,closed}}$ was estimated. For this purpose, the squared

	Winter		Summer	
Period	$MAPE_{0ppm}$	MAE	$MAPE_{0ppm}$	MAE
Calibration	4.3 %	25 ppm	4.9 %	26 ppm
Validation	3.4 %	20 ppm	4.7 %	26 ppm

Table 5.3.: Calibrated parameters and results

error was only integrated for periods when the supermarket was closed, such as at nighttime or on Sundays. In a second step, the air infiltration of the open door $\dot{m}_{air,inf,door,open}$ was estimated. Here, the squared errors were only integrated for periods when the entrance door was opened by visiting customers, i.e. during the opening hours of the supermarket.

This calibration and validation process was carried out both for summer and winter. The specific periods were chosen based on the availability of measurement and sales data for the test supermarket. The periods for validation and calibration of summer lasted one week each (Figures 5.6,A.7). In summer, the entrance door of the bakery stayed open. This affected the air exchange between the sales area and the ambient air. The CO_2 concentration was lower than in winter. The ventilation system was never activated during this time.

For winter, two periods of four days' length each were used for calibration and validation. The calibration period ended the day before Christmas, when there is typically a high occupancy Fidorra (2019b). This led to the activation of the ventilation system the day before Christmas. During the calibration period (Figure A.6), the operation status of the ventilation system $i_{vent,active} = f(t)$ was an additional input. During the validation period, the ventilation system was not in operation.

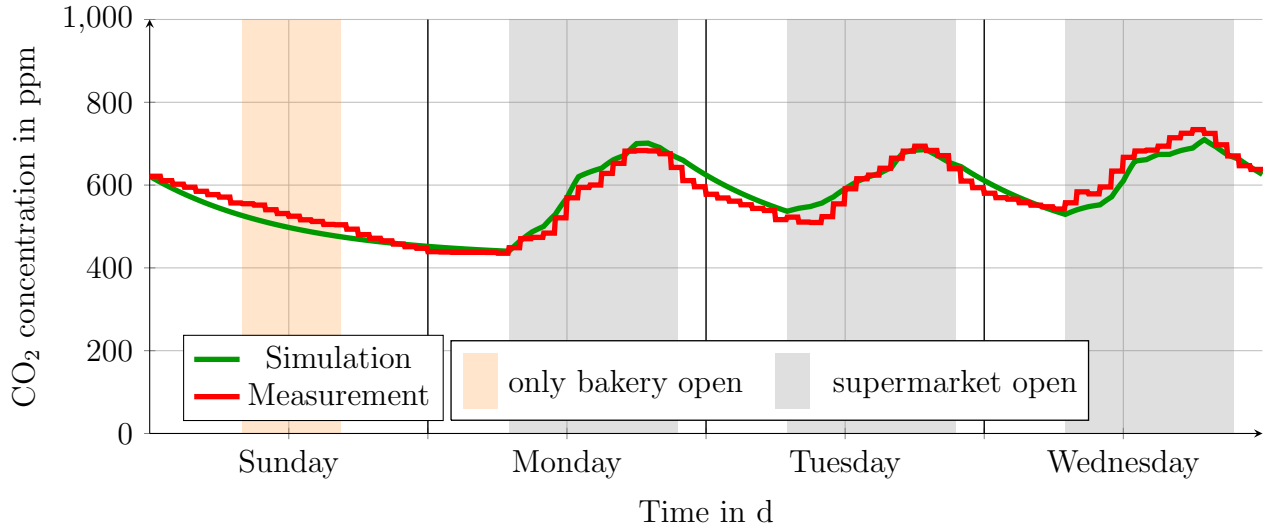

Figure 5.5.: Comparison of measured and simulated CO_2 concentration, validation, winter period,MAE = 20 ppm, $MAPE_{0ppm}$ = 3.4 %

5.5.3. Validation and discussion

The previously described dynamic parameter estimation was solved for both calibrating periods separately. The calibrated values of the infiltration rates $\dot{m}_{air,inf,door,closed}$ and $\dot{m}_{air,inf,door,open}$ for the summer and winter period are shown in Table 5.1. The air infiltration rates for the

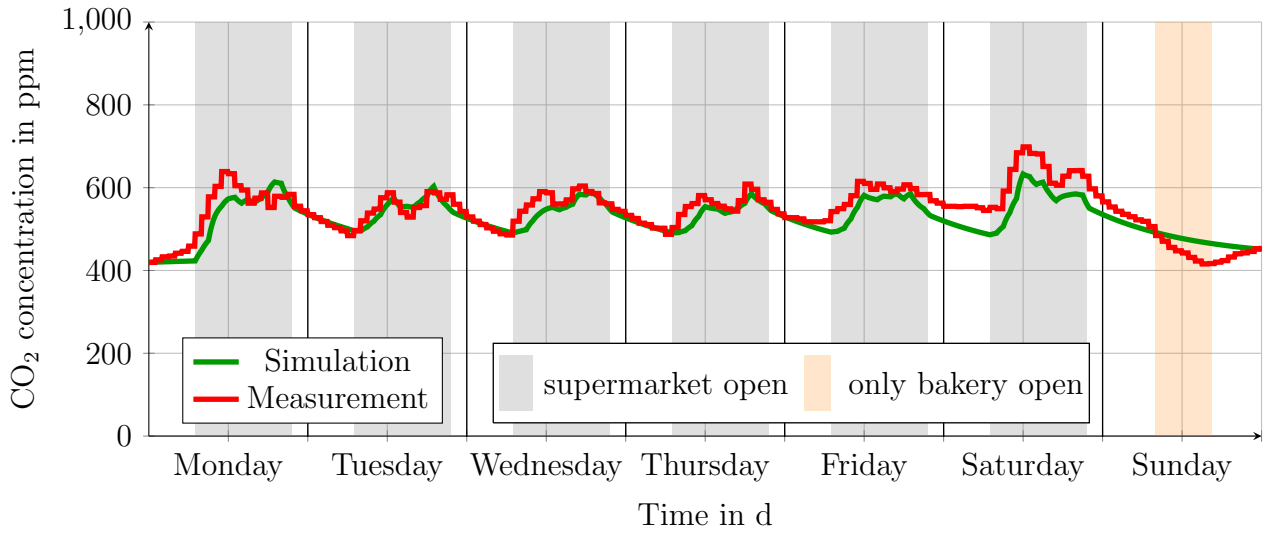

Figure 5.6.: Comparison of measured and simulated CO_2 concentration, validation, summer period, MAE = 26 ppm, $MAPE_{0ppm}$ = 4.7 %

closed door were 631 kg h^{-1} in summer and 796 kg h^{-1} in winter. This means air change rates of approximately 0.07 h^{-1} to 0.08 h^{-1} for closed doors. The air infiltration rates for the open door were 18 318 kg h^{-1} in summer and 6703 kg h^{-1} in winter. The air change rates for the open door were 1.9 h^{-1} in summer and 0.7 h^{-1} in winter. The large difference between the two figures are discussed later.

These air change rates can be compared to the literature. Titze (2017) found values for natural air exchange of 0.18 h^{-1} in a modern supermarket in Norway. This refers to the air change rate in the closed supermarket without customers. This value for the closed supermarket is in a similar order of magnitude as the values found in this work (0.08 h^{-1}). Jareemit et al. (2014) found average air change rates of 1 h^{-1} through automatic entrance doors in supermarkets. For the test supermarket, the air change rates through the open entrance doors were 1.9 h^{-1} in summer and 0.7 h^{-1} in winter. Again, these are is in a similar order of magnitude.

Besides the comparison with values from the literature, indicators are given to assess the quality of the predicted CO_2 concentrations. Firstly, the *mean absolute percentage error* (MAPE) (Equation 3.7) of the estimated and measured concentration of CO_2 in the sales area is given. Here, 0 ppm is used as the reference value for the concentration, in order to compare these values to those shown by Titze (2017). This is indicated by the subscript *0ppm*. Secondly, the *mean absolute error* (MAE) (Equation 4.6) is given. Both indicators serve to assess the quality of the parameter estimation.

During the calibration process, the concentration of CO_2 could be described very well: the $MAPE_{0ppm}$ was below 4.9 % and the MAE value below 26 ppm (Table 5.3). This value is below the static accuracy of the sensors of +/-30 ppm.

The model was simulated again for the validation periods. This time, the previously calibrated parameters were set as fixed parameters and the only input values to the model were the rate of receipt $\dot{n}_{receipt} = f(t)$ and number of items per receipt $n_{item} = f(t)$. The objective was to assess to what extend the CO_2 concentration could be predicted by the model. The results are shown in Figures 5.5 and 5.6.

The quality of the model is assessed based on the mean absolute percentage error (MAPE) and the mean average error (MAE). These results are shown in Table 5.3. In total, the model predicts the CO_2 concentration very well ($MAPE_{0ppm} < 4.7$ %, MAE < 26 ppm). Both in

summer and winter, the infiltration rates are lower for the closed door than for the open door. Additionally, the infiltration rates for the closed door in summer and winter are in the same order of magnitude. However, the fresh air infiltration rate in winter is slightly higher than in summer. In winter the ambient temperature is lower than in summer and thus the difference between sales room air density and ambient air density is higher than in summer. The difference in density is a main driving force of air infiltration. In future research, sensitivity analyses could be carried out to assess the effect of those parameters based on assumptions on those parameters that are calibrated.

Although the main entrance door of the supermarket consists of two automatic sliding doors and a vestibule, a simplified simulation of one single automatic sliding door was used for the estimation of the total share of door opening time ξ (Section 5.3.1). However, the prediction quality of the presented model is very good and the simplification used in the approximation of ξ does not seem to affect the overall result. Other effects such as the bakery door seem to have a great impact on the model accuracy. This can be observed when comparing the infiltration rates for the open door $\dot{m}_{\mathrm{air,inf,door,open}}$ in summer and winter. This infiltration rate is relevant for periods when the supermarket is open and customers enter and leave it via the main entrance. As previously mentioned, the door of the bakery is a second way of entering and leaving the sales room (Figure A.1). At moderate or high ambient temperatures (approximately 15 °C), this bakery door is often kept open the entire day, significantly increasing the air exchange between the sales room and the environment. The parameter for the infiltration rate in the model describes the overall infiltration rate including all openings of the building envelope. In the summer period, the parameter $\dot{m}_{\mathrm{inf,door,open}}$ not only describes the air infiltration through the main entrance door, but the combined infiltration through the main door and the bakery door. The high value of the calibrated parameter is consequently well in line with the observation of the open bakery door.

The modelling objective is to describe the air exchange between the sales room area and the environment. The concentration of CO_2 in the sales room air is used as an indicator for air exchange. The model considers some effects, such as variable shopping duration and joint door crossings that are new compared to previous work, for instance by Titze (2017). The consideration of these additional effects is reflected in the accuracy. Titze (2017) achieved a $\mathrm{MAPE}_{0\mathrm{ppm}}$ between predicted and measured concentration of CO_2 of 11 % and a mean absolute error (MAE) of 66.71 ppm.The model presented in this work achieved a $\mathrm{MAPE}_{0\mathrm{ppm}} < 4.9\,\%$ and $\mathrm{MAE} < 26\,\mathrm{ppm}$. The main reasons for the higher accuracy are the inclusion of additional effects, such as joint door crossings and variable duration of stay.

Summary

In this chapter the fresh air change rates between the ambient air and the sales room air were investigated. These are very relevant in terms of cooling and heating load as well as the cooling demand of the display cabinets and the ventilation demand. The aim was the description and quantification of effects on the air exchange.

The chapter described methods and models for the estimation of the customer balance, the simulation of door opening frequencies and durations, as well as the CO_2 concentration in the sales room of a supermarket. These methods and models can be used for two purposes: firstly, they allow an estimation of the air change rates of a supermarket building based on measurement data of the CO_2 concentration and sales data, namely the rate of receipt $\dot{n}_{\mathrm{receipt}}$ and the number of items per receipt n_{item}. Secondly, once the air change rates are calibrated, the model allows the prediction of the CO_2 concentration in a supermarket. These applications were successfully exemplified using data from the test supermarket. The results of the analysis

described in this chapter are used for the prediction of the humidity ratio of water in the sales room air (Chapter 6).

The methods and models described in this chapter can be applied to different supermarkets and consequently help supermarket operators and planners to compare the air change rates of supermarket buildings and configurations, and to design and optimise ventilation systems and operation strategies (Voigt 2018).

6. Prediction of the humidity in the sales room air

This chapter looks at the humidity balance of the sales room air with the objective of predicting the humidity. Since all interactions in the supermarket affect the water balance, the *entire supermarket* (Figure 1.1,6.1) has to be taken into consideration. Humidity sources play an important role and are specifically analysed in this chapter. Measurement data from the test supermarket are used to exemplify the method of quantifying the humidity sources. A simulation model of the entire supermarket is set up using the parameters and models used in previous chapters (Table 6.1). The entire supermarket is simulated using the temperature and humidity of the ambient air and sales data as input values. A good prediction of the humidity in the sales room air indicates that all interactions in the supermarket related to air exchange are modelled and quantified in a plausible way.

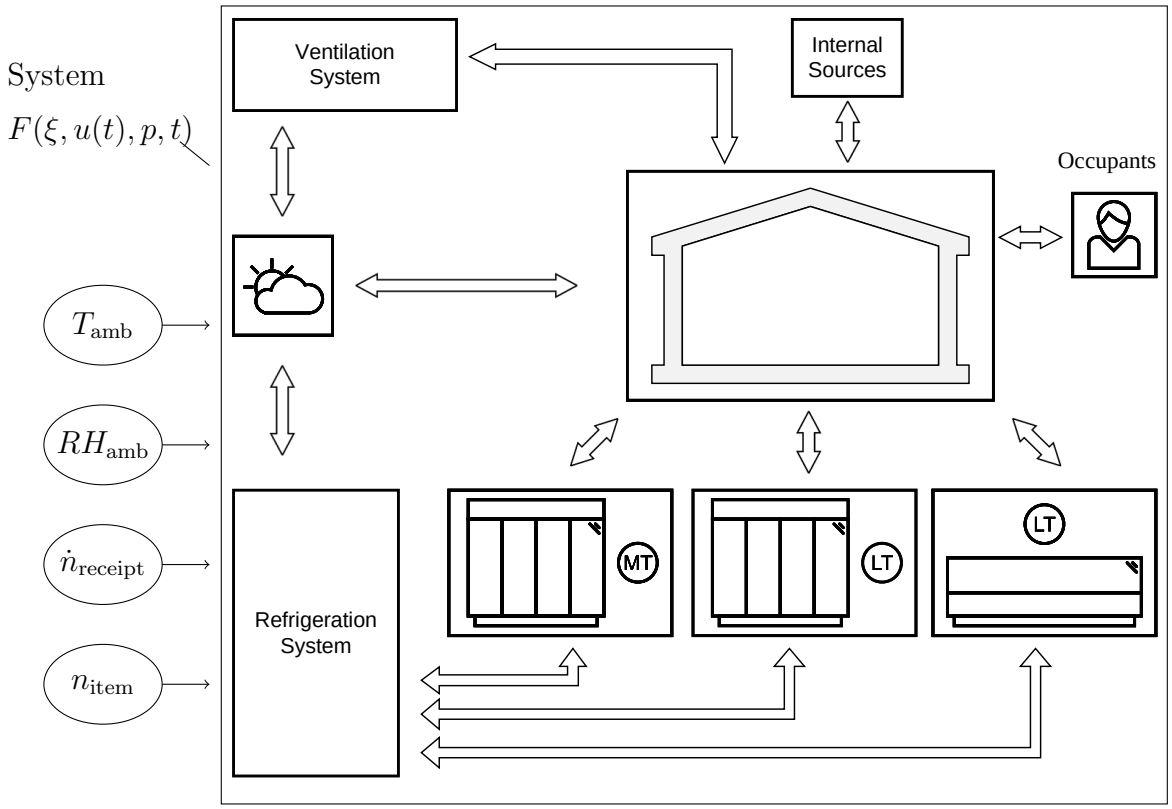

Figure 6.1.: Control volumes and interactions that are relevant for the prediction of the humidity of the sales room air as well as boundary of the simulated system and its time dependent input variables

The calculation of the humidity ratio and estimation of humidity sources in this section includes several novel aspects. As described in the state of the art, a mass balance of water in the sales room of an supermarket has been described previously by Arias (2005) and Marciniak (2016). However, the air exchange between the cabinets and the sales room was either considered as constant mass flows or as a fixed parameter. Howell et al. (1997) and Bahman et al. (2012) considered the influence of humidity in terms of a latent energy balance. In this thesis, variable mass flows depending on the customer rate are considered (Section 2.4.4), which is

a novel approach. In previous publications, the mass flow rate of air exchange between the sales room air and the environment were only linearly dependent on the number of customers. Here, this air exchange is calculated using the relations described in the previous chapter (5), which are highly non-linear. The calculation of the water concentration in the sales room air considering variable and customer flow-dependent air change rates are a new contribution to science.

6.1. System description

The objective of the model is to describe and predict the dynamic behaviour of the water concentration ξ in the supermarket sales room air. The simulation model, which includes all supermarket systems (Figure 6.1) can be described as a system of equations.

$$\frac{\mathrm{d}\xi}{\mathrm{dt}} = F(\xi, u(t), p, t) \tag{6.1}$$

The time-dependent input values $u(t)$ are:

- ambient temperature T_{amb}
- relative humidity of ambient air RH_{amb}
- rate of receipt per hour $\dot{n}_{\mathrm{receipt}}$
- number of items per receipt n_{item}

The models and parametrisation of many of the subsystems have been described in previous chapters. An overview of the subsystems and references to the model description and their parameters are given in Table 6.1. In the following, the balance equation for water in the sales room air is shown to illustrate the interactions that affect the humidity in the air. This equation can be derived from the overall mass balance of the sales room air model (Equation 2.14). Here, only the component of water vapour is considered (Section 2.2):

$$\begin{aligned} m_{\mathrm{air,sa}} \cdot \frac{\mathrm{d}\xi_{\mathrm{sa}}}{\mathrm{dt}} = {} & (\dot{m}_{\mathrm{air,inf}} + \dot{m}_{\mathrm{air,vent}}) \cdot (\xi_{\mathrm{amb}} - \xi_{\mathrm{sa}}) \\ & + \dot{m}_{\mathrm{air,MT,cab}} \cdot (\xi_{\mathrm{MT,cab}} - \xi_{\mathrm{sa}}) \\ & + \dot{m}_{\mathrm{air,LT,cab,horiz}} \cdot (\xi_{\mathrm{LT,cab,horiz}} - \xi_{\mathrm{sa}}) \\ & + \dot{m}_{\mathrm{air,LT,cab,vert}} \cdot (\xi_{\mathrm{LT,cab,vert}} - \xi_{\mathrm{sa}}) \\ & + \dot{m}_{\mathrm{air,ac}} \cdot (\xi_{\mathrm{ac}} - \xi_{\mathrm{sa}}) \\ & + \dot{m}_{\mathrm{air,breathing,people}} \cdot (\xi_{\mathrm{breathing}} - \xi_{\mathrm{sa}}) \\ & + \dot{m}_{\mathrm{water,source}} \end{aligned} \tag{6.2}$$

Although there are self-contained display cabinet in the test supermarket, they do not need to be considered in this humidity balance. The water that condenses in the heat exchanger inside the cabinet is evaporated using waste heat from the integrated refrigeration cycle, and released back to the sales room. An overview of the relevant interactions, the corresponding simulation models, and the parametrisation can be found in Table 6.1. All mass flows of moist air that are exchanged with the sales room air, as well as their concentrations, are calculated in the corresponding models.

The estimation of several of the variables involved in this equation has been described in previous chapters. The air infiltration $\dot{m}_{\mathrm{air,inf}}$ through the building envelope and entrance door has been described in Chapter 5. It has been shown that this air infiltration rate depends on the customer flow through the supermarket. The air exchange caused by the ventilation

Interaction with	Variables	Model description	Parameter description
Environment	$\dot{m}_{\mathrm{air,inf}}$,$\dot{m}_{\mathrm{air,vent}}$	Section 5.4	Table 5.1
MT cabinet	$\dot{m}_{\mathrm{air,MT,cab}}$, $\xi_{\mathrm{MT,cab}}$	Section 2.4.4	Table 4.5
LT horizontal cabinet	$\dot{m}_{\mathrm{air,LT,cab,horiz}}$, $\xi_{\mathrm{LT,cab,horiz}}$	Section 2.4.4	Table 4.2
LT vertical cabinet	$\dot{m}_{\mathrm{air,LT,cab,vert}}$, $\xi_{\mathrm{LT,cab,vert}}$	Section 2.4.4	Table 4.2
Occupants	$\dot{m}_{\mathrm{air,breathing,people}}$, ξ_{breath}	Section 5.4	Table 2.1
Air Conditioning	$\dot{m}_{\mathrm{air,ac}}$, ξ_{ac}	This chapter	Table 6.3
Sources	$\dot{m}_{\mathrm{water,source}}$	This chapter	Table 6.3

Table 6.1.: Parameter overview humidity balance

system $\dot{m}_{\mathrm{air,vent}}$ is only relevant if the ventilation system is switched on (Equation 5.22). The air exchange between the various display cabinets and the sales room air has been described in Chapter 3. Here, again, the approach of *equivalent cabinets* is used. Thus, similar display cabinets are merged into one control volume that has the same interaction with the sales room air as the individual cabinets together. The mass flow rates $\dot{m}_{\mathrm{air,MT,cab}}$, $\dot{m}_{\mathrm{air,LT,cab,horiz}}$ and $\dot{m}_{\mathrm{air,LT,cab,vert}}$ depend on the door opening frequency of each cabinet. The estimation of these mass flow rates has been described in Section 4.2. The mass flow rate of breathing depends on the number of people currently staying in the sales room. The humidity evaporating from customers' wet clothes on a rainy day are not considered here. The number of occupants was estimated based on sales data and a balance of occupants (Section 5.1). The specific equations for estimating the mass flow rates of breathing $\dot{m}_{\mathrm{air,breathing,people}}$ are described during the modelling of the CO_2 balance equation (Section 5.4). There are two more effects influencing the water balance that have not been described yet: 1. Dehumidification from the air conditioning system 2. Additional humidity sources in the sales room, such as plants. The estimation of these effects is described in the following subsections.

Dehumidification from the air conditioning system

The air conditioning system can dehumidify the air. In the test supermarket, air conditioning is achieved using air recirculation through a heat exchanger located below the ceiling of the sales room. The condensate mass flow of dehumidification can be expressed as:

$$\dot{m}_{\mathrm{cond,ac}} = \dot{m}_{\mathrm{ac}} \cdot (\xi_{\mathrm{sa}} - \xi_{\mathrm{ac}}) \tag{6.3}$$

However, it only does so if the cooling temperature is below the dew point of the sales room air. Thus, the return air from the air conditioning system has the following concentration of water:

$$\xi_{\mathrm{ac}} = min(\xi_{\mathrm{sa}}, f(T_{\mathrm{ac}})) \tag{6.4}$$

Additional humidity sources in the sales room

Besides customers, there are also other sources of humidity in the sales room of a supermarket, such as plants, fruit, cleaning machines or the bakery oven. However, not all of these sources emit humidity evenly during the day. The bakery oven is usually not working while the supermarket is closed and the cleaning machines are generally in operation before or after opening hours. Plants and fruit, however, are stored in the sales room day and night and emit humidity independent from the opening hours. In order to identify relevant effects associated with humidity sources, measurement data were analysed. Typical patterns of humidity in the sales room air can be observed as previously shown in Fidorra (2019b). An overall tendency found was, that during opening hours, humidity in the supermarket is higher than during

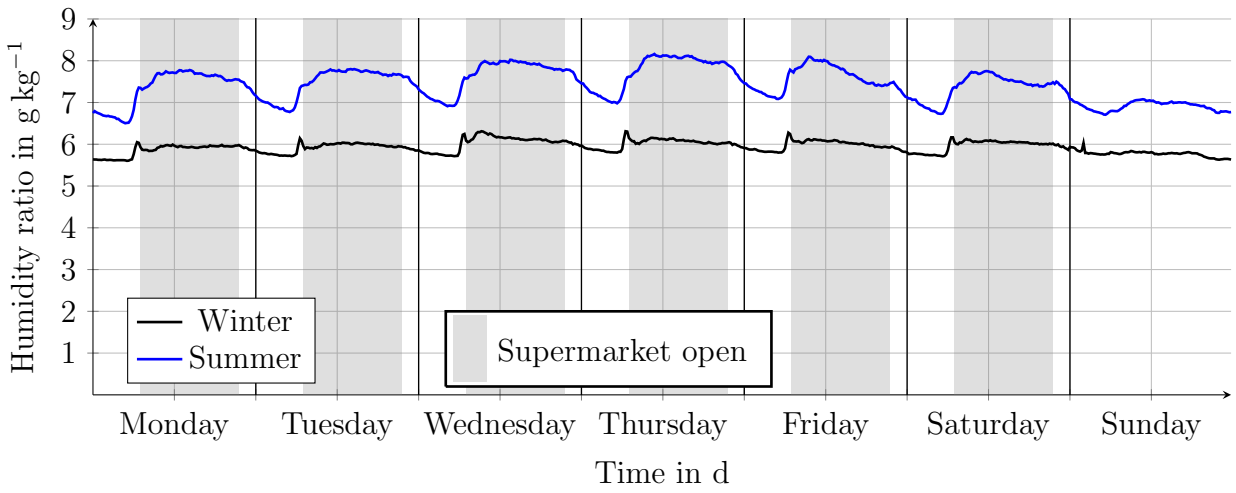

Figure 6.2.: Humidity ratio of the sales area over the course of a week: average values of measurement data from 26 weeks in summer and winter.

closing hours. Additionally, the average humidity is higher in summer than in winter. The typical pattern of the humidity ratio over the course of a week is shown in Figure 6.2. These typical patterns are calculated as the average of the measured humidity ratio over 26 weeks in summer and winter. Here, a steep increase in humidity can be observed in the early morning around 6:00h. This effect is noticeable both in summer and in winter. The specific sources that cause the increase in the early morning cannot be identified based on the measurement data. However, it can be assumed that the main source is the bakery oven, since the bakery starts work at around 5:00h, with the cleaning machine possibly also contributing. In order to account for the different effects of the humidity sources, a day is divided into two periods.

1. Store closed (only plants and fruits are relevant: $\dot{m}_{\text{water,source,night}}$)
2. Store open (bakery begins work: $\dot{m}_{\text{water,source,day}}$).

In terms of water sources, however, the opening periods starts earlier than the opening hours for the customers. It is assumed that the bakery starts at 5:30h. The mass flow rate of water sources can be calculated as:

$$\dot{m}_{\text{water,source}} = \begin{cases} \dot{m}_{\text{water,source,night}} & \text{store closed: 21:30-5:30} \\ \dot{m}_{\text{water,source,day}} & \text{store open: 5:30-21:30} \end{cases} \tag{6.5}$$

The two parameters $\dot{m}_{\text{water,source,night}}$ and $\dot{m}_{\text{water,source,day}}$ are difficult to estimate and will be calibrated to measurement data.

6.2. Parametrisation

Many of the parameters are known from the estimations described in earlier chapters. The previously described models of the cabinets, refrigeration system and the sales room air are combined into one model (Table 6.1). The only remaining parameters for the description of the humidity in the sales room air are those related to the humidity sources (Equation 6.5), such as the bakery oven or plants. Since these parameters are difficult to estimate analytically, they are, again, calibrated. The calibration is carried out separately for the two sub-periods *closed market* and *open market* (Table 6.2). The integrated squared error *sqe* is minimised by variation of the corresponding parameter.

Calibration step	Fitting target	Calibration variable	Condition
1	ξ_{meas}	$\dot{m}_{\text{water,source,night}}$	Supermarket closed (21:30h-05:30h)
2	ξ_{meas}	$\dot{m}_{\text{water,source,day}}$	Supermarket open (05:30h-21:30h)

Table 6.2.: Calibration steps humidity sources

Again, two periods were used for calibration and validation. The ambient temperature T_{amb} and humidity of the ambient air RH_{amb} were always available from the monitoring system (Tables A.14,A.15). A period of 14 days′ length was used for calibration. A second period of 14 days′ was used for validation. These periods were chosen based on the availability of monitoring data. The humidity of the ambient air was only available for certain periods, which not coincide with those periods used for the prediction of the energy consumption or the CO_2 concentration. The actual sales data were not available, and generic profiles for the input values (rate of receipts $\dot{n}_{\text{receipts}}$ and n_{item}) were therefore used (Tables A.16,A.17). The heating system was assumed to keep the sales room temperature always at the desired setpoint temperature $T_{\text{sa,setpoint}}$ (Table 6.3). Both periods were in winter and the air conditioning system was never in operation.

6.3. Results and discussion

Table 6.3 shows the calibrated parameters of the humidity sources in the sales area. The mass flow rate of water emitted by the humidity sources was $1.7\,\text{kg}\,\text{h}^{-1}$ during nighttime ($\dot{m}_{\text{water,source,night}}$) and $3.1\,\text{kg}\,\text{h}^{-1}$ during daytime ($\dot{m}_{\text{water,source,daytime}}$). These values can be checked for plausibility by comparing the nightly humidity emissions with literature data of humidity losses of fruit. In the sales room of the test supermarket, approximately 600 kg of fruit are stored (Table 5.1). Assuming that the only nightly humidity sources are fruit, the specific humidity emission rate of fruit $\dot{e}_{\text{water,fruit}}$ can be calculated as:

$$\dot{e}_{\text{water,fruit}} = \frac{\dot{m}_{\text{water,source,night}}}{m_{\text{fruit}}} \approx 2.8\,\text{g}\,\text{kg}^{-1}\,\text{h} \tag{6.6}$$

Geyer et al. (2010) give an overview of the specific humidity emission rate during storage. The specific values vary considerably: up to $11\,\text{g}\,\text{kg}^{-1}\,\text{h}$ for carrots, but only $0.11\,\text{g}\,\text{kg}^{-1}\,\text{h}$ for apples The specific assortment of fruits in the test supermarket is unknown, but a value of $\dot{e}_{\text{water,fruit}} = 2.8\,\text{g}\,\text{kg}^{-1}\,\text{h}$ seems to be realistic. During the opening hours of the supermarket, the humidity sources are significantly larger, which is plausible because the bakery oven also emits water vapour. In future research, sensitivity analyses could be carried out to assess the effect of those parameters based on assumptions on those parameters that are calibrated.

For the presentation of the results, not the mass fraction of water ξ, but the humidity ratio x is used, since it is common and the values are more intuitive (Section 2.2). Figures 6.3 and 6.4 show the results of the calibration and validation periods. They show the measured and simulated humidity ratios of the sales room air as well as the humidity ratio of the ambient air. The simulated and measured humidity ratios are in very good agreement (Table 6.4). During the calibration period, the mean absolute percentage error (MAPE) of the humidity ratio is 3.6 % and the mean absolute error (MAE) is $0.2\,\text{g}\,\text{kg}^{-1}$. In the validation period, a MAPE of 5.4 % and a MAE of $0.3\,\text{g}\,\text{kg}^{-1}$ was achieved. It can be observed that the humidity of the sales room air increases when the humidity of the ambient air increases, which has been previously described by Arias (2005).

Parameter	Value		Description	Determination
Humidity sources				
$\dot{m}_{\text{water,source,night}}$	1.7	$\text{kg}\,\text{h}^{-1}$	Water mass flow during nighttime	Calibration
$\dot{m}_{\text{water,source,day}}$	3.1	$\text{kg}\,\text{h}^{-1}$	Water mass flow during daytime	
Air conditioning system				
$\dot{m}_{\text{ac}}$	4900.0	$\text{kg}\,\text{h}^{-1}$	Mass flow rate of air via AC system	Planning data
T_{ac}	14.0	°C	Air temperature of AC systems	
Heating system				
$T_{\text{sa,setpoint}}$	19.0	°C	Setpoint temperature sales room	Planning data

Table 6.3.: Parameters of humidity sources and air conditioning and heating system

Discussion of inaccuracies

Although the simulation results are in very good agreement with the humidity ratio in the sales room, there are several reasons for inaccuracies that have to be mentioned and discussed here. Firstly, the most important error source is the possible deviation in the amount of humidity emitted by the fruits and the bakery oven between the calibration and the validation periods. Secondly, although effects, such as rain and wet clothes of the customers were not taken into consideration, they could affect the humidity balance. Thirdly, the prediction of the humidity sources is based on the interaction of three different kinds of display cabinets, the shopping duration of the customers and the air exchange between the sales room and the environment (Figure 6.1). The calculation of the air exchange with each of these other thermal systems contains errors. The CO_2 concentration in the sales room air was used as an indicator for correctly predicting the air exchange between the sales room and the environment as well as the shopping behaviour of the customers. For the calibration and validation periods used in this chapter, the actual sales data were not available and typical sales data were used instead. Here, the prediction of the CO_2 concentration has a mean absolute error of 36 ppm to 41 ppm (Table 6.4), which is higher than for the prediction of the air change rates (Chapter 5) but still reasonably accurate. In summary, the humidity balance is the result of combining various interactions between different supermarket systems. The inaccuracies of the different parameter estimations are combined and thus lead to a higher inaccuracy of the humidity balance. However, it could be shown that the physical parameters of the interactions could be estimated with reasonable accuracy. The good prediction of the humidity ratio of the sales room air and the previous validations of the individual interactions indicate that the physical model of the entire supermarket is a good representation of the actual physical interactions.

Conclusion

This section presented the humidity balance of the sales room air. The simulation models in this chapter include the entire supermarket because all thermal systems affect the humidity balance. The humidity sources inside the sales room play an important role and are therefore added to the simulation model. Since these sources are difficult to quantify, calibration is again used to estimate these parameters. The simulation models were calibrated and validated using different time periods. In the validation period, the humidity ratio of the sales room air could be predicted with a mean absolute error of $0.3\,\text{g}\,\text{kg}^{-1}$ (MAPE = 5.4 %). This reasonably accurate prediction and the previous validations of the individual interactions indicate that the physical model of the entire supermarket is a good representation of the actual physical interactions taking place between the thermal systems in a supermarket.

	CO_2 concentration		Humidity ratio x	
Period	$MAPE_{0ppm}$	MAE	MAPE	MAE
Calibration	6.6 %	41 ppm	3.6 %	0.2 g kg^{-1}
Validation	6.2 %	36 ppm	5.4 %	0.3 g kg^{-1}

Table 6.4.: Deviation of measured and simulated concentration of CO_2 and water

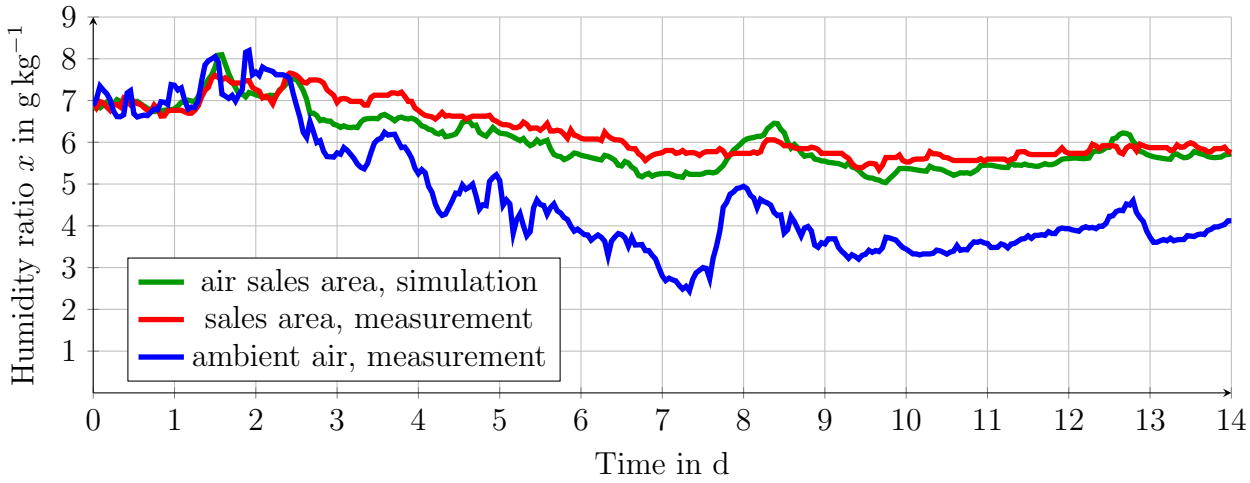

Figure 6.3.: Comparison of measured and simulated humidity ratio in the sales room and the measured ambient humidity ratio for the calibration period.

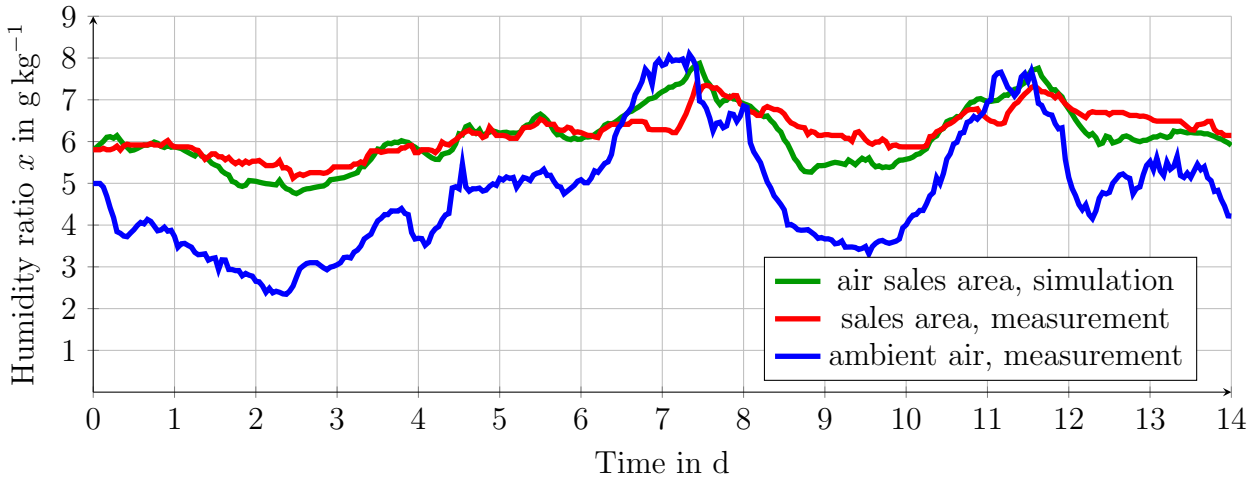

Figure 6.4.: Comparison of measured and simulated humidity ratio in the sales room and the measured ambient humidity ratio for the validation period.

7. Quantification of interactions and benchmarking

This thesis deals with the physical modelling of thermal systems in supermarkets and the interactions between them. The objective of this chapter is to exemplify some of the possible applications of the physical models of supermarkets developed in this thesis (see also Fidorra et al. (2014a)). In this work, the focus lays on two relevant interactions in supermarkets: 1. The air exchange between the display cabinets and the sales room 2. The air exchange between the sales room and the environment. These interactions are qualitatively well known. Some effects arising from them have been quantified in previous studies, such as the dependency of the cooling load of display cabinets on the temperature and humidity of the sales room air. Other effects, such as the dehumidification of the sales room air caused by the air exchange with display cabinets, have rarely been quantified. The physical models developed and validated in this thesis allow the quantification of several values that can hardly be measured in reality. This is exemplified in this chapter. Since the models and methods developed in this thesis are new, so are the results in this chapter.

7.1. Part load operation of refrigerated display cabinets

Display cabinets are often tested in a laboratory, but these experiments are time-consuming and expensive. Here, a closed display cabinet is tested virtually, with the objective of quantifying the impact of the boundary conditions on the cooling load and the amount of condensate. The amount of condensate is of interest because it affects the defrost operation and demonstrates the dehumidification effect of the sales room air. The boundary conditions are the temperature and humidity of the sales room air as well as the door opening frequency.

The physical model of the display cabinet and its required parameters has been described in Chapter 2.4.4. Here, a *typical* MT display cabinet shall be analysed. This means that the parameters do not describe one specific cabinet of a specific manufacturer, but a generic vertical MT cabinet. Several parameters can be estimated based on typical technical data sheets or name plates (Table 7.1). Other parameters are assumed to be the same as in the validated model of the vertical display cabinets in the test supermarket, such as the specific infiltration rates $\underline{\dot{m}}_{\mathrm{door,closed}}$ and $\underline{\dot{m}}_{\mathrm{door,open}}$ or the thermal transmittance k. The fan mass flow rate $\dot{m}_{\mathrm{air,fan}}$ has been scaled down using the number of doors of the cabinet. Table 7.1 gives an overview of the parameters and how they are determined.

The objective is to calculate the cooling load $\dot{Q}_{\mathrm{cab}}$ (Equation 2.60) and the mass flow rate of condensate $\dot{m}_{\mathrm{cond}}$ (Equation 2.56) for the display cabinet as a function of the temperature T_{sa} of the sales room air, humidity of the sales room air RH_{sa}, and the door opening frequency f_{door}:

$$\dot{Q}_{\mathrm{cab}} = f(T_{\mathrm{sa}}, RH_{\mathrm{sa}}, f_{\mathrm{door}}) \tag{7.1}$$

and

$$\dot{m}_{\mathrm{cond}} = f(T_{\mathrm{sa}}, RH_{\mathrm{sa}}, f_{\mathrm{door}}) \tag{7.2}$$

Table 7.2 shows the cooling load $\dot{Q}_{\mathrm{cabinet}}$ and condensate mass flow $\dot{m}_{\mathrm{cond}}$ for different boundary conditions. Both, the cooling load and condensate mass flow, increase with the temperature and humidity of the sales room as well as with the door opening frequency, which is plausible. The cooling load, for instance, increases by 50 % at 25 °C and 60 % relative humidity

Parameter	Value		Description	Determination
w	3.75	m	Width	
n_{door}	6		Number of doors	
A	29.0	m^2	Total surface area of the cabinet	
T_{setpoint}	6.0	°C	Temperature setpoint	Technical data
$P_{\text{el,int,day}}$	240.0	W	Electrical power daytime	sheet
$P_{\text{el,int,night}}$	50.0	W	Electrical power nighttime	
$\Delta T_{\text{sh,evap,setpoint}}$	9.0	K	Evaporator superheat	
$\dot{m}_{\text{air,fan}}$	280.0	g s^{-1}	Fan mass flow rate	
$d_{\text{door,open}}$	10.0	s	Average duration of door opening	
$\underline{\dot{m}}_{\text{door,closed}}$	3.5	g s^{-1}	Infiltration rate, door closed	Table 4.5
$\underline{\dot{m}}_{\text{door,open}}$	150.0	g s^{-1}	Infiltration rate, door open	
k	2.02	$\text{W m}^{-2}\,\text{K}^{-1}$	Average thermal transmittance	

Table 7.1.: Parameters of a typical vertical MT cabinet. Here, only single points of operation, without defrost, are looked at.

compared to 20 °C and 50 %. Another way to check the plausibility of the cooling load is the comparison with the literature. The cooling load is often given per metre width of a cabinet. IEA Heat Pump Centre (2017) reported a specific cooling load of $650\,\text{W m}^{-1}$ for vertical closed cabinets. Here, the specific cooling load $\dot{Q}_{\text{cab}}$ per width w is approximately $665\,\text{W m}^{-1}$ at 25 °C and 60 % relative humidity, which corresponds to a typical climate class 3 (Deutsches Institut für Normung 2012).

Door openings undoubtedly have an effect on the cooling load. Lindberg et al. (2010a) reported an increase of 16 % of the cooling load for a door opening frequency of $30\,\text{h}^{-1}$ compared to a frequency of $10\,\text{h}^{-1}$. The same variation of the door opening frequency in the simulations led to an increase of the cooling load in the range 11 % to 14 % (Table 7.2). Again, these results are very similar to those in the literature.

This simulation of a generic display cabinet and the results can help with supermarket planning (Fidorra et al. 2013, Fidorra 2014, 2016a). Specifically, the results can help in dimensioning the refrigeration system. Vallée (2015) showed that the actual temperature and humidity in the sales room air seldom reach the design point and that display cabinets usually operate in part load conditions. The simulation model of the display cabinet allows a prediction of the cooling load as a function of the actual conditions in the sales room (Equation 7.1). This prediction can consequently help to dimension and plan the refrigeration system. Since, however, the parameters of some specific display cabinets may be different, depending on the specific type or manufacturer, it is necessary to estimate the parameters of specific types of display cabinets to facilitate planning of supermarkets.

Summary quantification display cabinets

Here, a typical vertical MT cabinet has been simulated for different boundary conditions. Namely, the cooling load and the condensate mass flow were estimated as a function of the temperature and humidity of the sales room air and the door opening frequency. The results were compared with data from the literature and found to be plausible. The parameters of the display cabinet model were estimated in experiments and calibration using measurement data from a supermarket. Additionally, the results show that a large amount of water condensates in the display cabinet and is withdrawn from the sales room air. This highlights the need to

f_{door} in h^{-1}	T_{sa} in °C	RH_{sa} in %	$\dot{Q}_{\text{cab}}$ in kW	$\dot{m}_{\text{cond}}$ in $\text{g}\,\text{h}^{-1}$
0	20	50	1.62	200
0	25	60	2.50	549
10	20	50	1.72	236
10	25	60	2.70	646
30	20	50	1.91	304
30	25	60	3.09	834

Table 7.2.: Results of virtual tests with the physical display cabinet models

consider the humidity balance for the calculation and simulation of entire supermarkets.

7.2. Benchmarking entire supermarkets

In the previous section, display cabinets were analysed in a virtual laboratory, in order to quantify certain interactions. Although there are laboratories resembling the sales room of a supermarket on a small scale, it is barely possible to analyse an entire supermarket controlling all ambient and operating conditions. The objective of the following analysis is to quantify certain interactions and their energetic impact on supermarkets for three different scenarios (winter, spring, summer), and two shopping trips, one short and one long, which differ regarding the number of cabinet doors opened. Using the validated simulation model of the test supermarket, two aspects are analysed. The air exchange and its impact on the energy and water balance of the sales room air is quantified firstly. Then, the impact of the short and the long shopping trips on the cooling demand of the display cabinets Q_{cab} and the electrical energy demand of the refrigeration system E_{el} is assessed.

Here, the entire supermarket (Figure 6.1) is looked at. An overview of the parameters can be found in Table 6.1. The input values are the temperature T_{amb} and humidity RH_{amb} of the ambient air as well as the customer flow $\dot{n}_{\text{customer}}$. Additional parameters, such as temperature T_{sa} and humidity RH_{sa} of the sales room air are shown in Table 7.3.

Three scenarios are looked at (Table 7.3). An early Monday morning in winter is characterised by a low ambient temperature and a small number of customers visiting the store. A Saturday morning in spring is characterised by mild temperatures and a large number of customers. A weekday in summer during lunchtime is characterised by high ambient temperatures and an intermediate occupancy with customers.

Here, the impact of the *additional* air exchange caused by one customer on the water and energy balance of the sales room air is analysed. The reference case is the operational supermarket including the customer flow indicated for each scenario. To interpret the additional energy consumption caused by one additional customer, the term of *marginal costs* can be used, which is widely known and used in economics (for instance Roth (2016)). The *marginal energetic costs* shown here can be interpreted as the difference in effort, in terms of the energy that is necessary to *produce one additional unit*, which here is the shopping trip by one customer.

To analyse the interaction between the sales room and the environment, several variables are looked at. Firstly, the mass of air m_{air} that is additionally exchanged. Since the sales room air and the ambient air have different temperatures and humidities, this exchange of air imply transport of thermal energy Q and gaseous water m_{water}. Here, the transported thermal energy refers only to the sensible heat. A positive sign means that thermal energy or water

	Winter		Spring		Summer	
Scenario description	Monday morning		Saturday morning		Weekday lunchtime	
Input values for each scenario						
Temperature ambient air T_{amb}	−3	°C	15	°C	30	°C
Relative Humidity ambient air RH_{amb}	70	%	45	%	40	%
Customer flow $\dot{n}_{\mathrm{customer}}$	10	h^{-1}	150	h^{-1}	50	h^{-1}
Small shopping trip	2 MT, 0 LT cabinet doors opened					
Large shopping trip	8 MT, 6 LT cabinet doors opened					
Parameters						
Temperature Sales Room Air T_{sa}	19	°C	20	°C	23	°C
Relative Humidity Sales Room Air RH_{sa}	40	%	20	%	40	%
Impact on the interaction between the sales room and the environment						
Mass of air infiltrated m_{air}	18.9	kg	12.8	kg	17	kg
Sensible heat infiltrated Q	−420	kJ	−65	kJ	121	kJ
Water infiltrated m_{water}	−65	g	−11	g	62	g
Energetic impact of one small shopping trip						
Cooling load MT cabinets $Q_{\mathrm{cab,MT}}$	42	kJ	52	kJ	65	kJ
Cooling load LT cabinets $Q_{\mathrm{cab,LT}}$	0	kJ	0	kJ	0	0 kJ
Mass of condensate in cabinets m_{cond}	2	g	5	g	7	g
Electrical energy consumption E_{el}	5	kJ	12	kJ	26	kJ
Energetic impact of one large shopping trip						
Cooling load MT cabinets $Q_{\mathrm{cab,MT}}$	167	kJ	209	kJ	259	kJ
Cooling load LT cabinets $Q_{\mathrm{cab,LT}}$	282	kJ	30	kJ	325	kJ
Mass of condensate in cabinets m_{cond}	36	g	55	g	64	g
Electrical energy consumption E_{el}	120	kJ	191	kJ	318	kJ

Table 7.3.: Energetic impact of short and long shopping trips of an individual customer for different scenarios. Heat recovery of the refrigeration system is not considered.

are added to the sales room air.

The simulations show that, in winter and spring, the air exchange between the sales room and the environment cause a net loss of thermal energy and humidity. This is caused by the lower temperature and lower absolute humidity of the ambient air. In summer, the air exchange imply a net gain of both thermal energy and humidity. This leads to an increased cooling demand and increase in humidity.

Customers have an impact not only on the exchange of air between the sales room and the environment, but also on the display cabinets and the refrigeration system. Opening the doors and lids of display cabinets also intensifies the air exchange between the display cabinets and the sales room air. Because of the low absolute humidity inside the display cabinets, the air exchange between them and the sales room lead to a dehumidification of the sales room air.

Here, two kinds of generic customers are distinguished. Firstly, a customer who only buys a

small snack and opens two doors of MT cabinets (*small shopping trip*). Secondly, a customer who buys a larger number of items. It is assumed that this customer opens eight doors of MT cabinets, three doors of vertical and three lids of horizontal LT cabinets (*large shopping trip*). This customer behaviour is not representative, but used to exemplify the variation between different shopping trips.

The objective is to analyse the impact of both types of shopping trips on the cooling demand at MT ($Q_{\mathrm{cab,MT}}$) and LT levels ($Q_{\mathrm{cab,LT}}$), the total amount of water condensed in the display cabinets m_{cond}, as well as the energy consumption of the compressors of the central refrigeration system E_{el} (integrated compressor power, Equation 2.25). Here, the cooling load includes the latent heat of condensing water in the evaporator, which needs to be withdrawn from the refrigeration system. Again, the *additional* values caused by the specific shopping trip are looked at. The results are shown in Table 7.3 and exemplify several effects taking place in supermarkets. The additional cooling load for the refrigeration system that is caused by one customer depends on the number of cabinet doors that are opened. The small shopping trip results in a cooling demand that is approximately four times lower than for a large shopping trip. The cooling load also depends on the climate conditions in the sales room, as shown in the previous section. In spring, the cooling demand of the MT cabinet per customer is approximately 25 % higher than in winter, and in summer it is even 50 % higher. A third effect is the efficiency of the refrigeration system that is reduced at high ambient temperatures. Since heat recovery is not considered, the central refrigeration system has a very high efficiency in winter. This leads to a significantly lower energy consumption of the compressors in winter.

In terms of water balance, there is an interesting observation to be made: in summer, the amount of water brought into the sales room is higher than the amount of water condensed in the cabinets during a small shopping trip. Thus, customer behaviour increases the humidity in the sales room air.

Summary benchmarking entire supermarkets

Physical modelling allows the quantification of variables and effects that could hardly be measured in real markets or experiments. Here, two examples were shown. Firstly, the impact one single customer has on the energy and humidity balance of the sales room air by entering and leaving the supermarket was shown. The net gain or loss of thermal energy naturally depends on the conditions of the ambient air. Secondly, the impact on the cooling load, mass of condensate and energy consumption of the central refrigeration system was compared for two generic shopping trips, a small and a large trip which differs regarding the number of opened display cabinet doors. These values of the additional impact of one customer on the operation of an entire supermarket cannot be measured in a real system. Firstly, it would be necessary to run two tests with identical boundary and operation conditions, the only difference being the one additional customer. Secondly, the increase in energy consumption would be smaller than the measurement accuracy.

Overall, it was demonstrated and quantified how the energy consumption of the refrigeration system as well as the cooling and heating demand depend largely on the boundary conditions and the operating status, i.e. the temperature and humidity setpoints of the sales room. These numerous dependencies of the energy consumption severely complicate the energy benchmarking of supermarkets. In future, the additional impact of one single customer, which can be interpreted as marginal energetic costs, could be the basis for the energetic benchmarking of supermarkets. Several representative scenarios of supermarket operation could be defined. For each scenario, the *marginal energetic costs* could be calculated and then be used to realistically compare different supermarkets.

8. Summary

The usage of natural refrigerants, the integration of systems, standardisation of equipment and the integration of supermarkets into smart (thermal) grids constitute trends in the area of supermarket systems. This implies that thermal systems in supermarkets are becoming more and more complex and integrated, for instance with the integration of air conditioning and refrigeration systems.

To achieve high energy efficiencies, the correct dimensioning of thermal systems is crucial. This requires the correct prediction of the energy consumption and the quantification of interactions between the thermal systems in a supermarket.

The main goal of this thesis was to describe the interactions between thermal systems in supermarkets by means of physical models and to quantify their energetic impact. To achieve this overall goal, three subgoals were defined.

The first subgoal was the breakdown of supermarkets into control volumes and the definition of physical interactions between them. In this work, *physical modelling* was used. In this work it refers to the usage of *first principle models* and *physical connections* between objects. Interfaces and model equations describing the sales room air, the refrigeration system and display cabinets were presented. The modelling of the refrigeration systems used well-established equations. However, the display cabinet model implied several new approaches. For instance, the air exchange between the display cabinet and the sales room was modelled via flows of moist air. With this approach, it was possible to account for the retroactive effect that the display cabinets have on the sales room, especially the dehumidification of the sales room air. Modelling this effect using both, the energy balance and the mass balances of water, is new.

The second subgoal refers to the analysis of the air exchange between refrigerated display cabinets and the sales area, which is one of the most important interactions in a supermarket. The focus was on the quantification of the air exchange and the determination of the influence of door openings on the air exchange. In laboratory tests, an adapted tracer gas method using CO_2 was used to determine the air change rates between the display cabinets and the sales room for three typical supermarket cabinets: 1. a vertical medium-temperature cabinet 2. a vertical low-temperature cabinet 3. a horizontal low-temperature cabinet. The specific air infiltration rates per closed and open door were estimated and used as parameters in the newly developed display cabinet model.

Typical air infiltration rates through the gaps of one closed door are in the range of $0\,\mathrm{g\,s^{-1}}$ to $5\,\mathrm{g\,s^{-1}}$, while for one open door, the specific infiltration rate can go up to $190\,\mathrm{g\,s^{-1}}$.

In the laboratory, the impact of door openings was quantified in tracer gas experiments using the absolute air infiltration rate per door. Additionally, a second way of quantifying the impact of door openings on the air infiltration used dimensionless numbers and was based on temperature measurements. The so-called *thermal entrainment factor* (TEF) can be interpreted as a dimensionless infiltration rate and can be approximated using solely temperature data for a display cabinet and the sales room. Data from the operational test supermarket were used to analyse the variation of the TEF values between opening hours and at nighttime for one specific type of display cabinet. It could be shown that the average dimensionless infiltration rate during opening hours was approximately 30 % higher than at nighttime.

The ability to predict the energy consumption was exemplified using measurement data from the test supermarket. The control volumes looked at comprised the display cabinets and the refrigeration system. The input values were the ambient temperature, the temperature and humidity of the sales room, as well as the customer flow. The simulation model of the

display cabinet developed in this thesis are new, which is why the required parameters are not available in the literature or in technical data sheets from the manufacturers. Therefore, the parametrisation was carried out on several bases: experimental data, planning data of the supermarket, and calibration to monitoring data. The methodology of parametrisation was extensively described, since this makes it possible to apply this simulation method to other supermarkets. The simulation model was separately calibrated and validated using periods of four weeks length each. During the validation period, the overall energy consumption of the refrigeration system and the display cabinets was predicted with a deviation of $-3.3\,\%$. The mean absolute percentage error (MAPE) of total power consumption was $7.6\,\%$. Besides the energy consumption, several other variables were looked at and the simulation results could be verified. This demonstrated prediction of the energy consumption including the customer flow as an input variable is a novelty.

The analysis of the effects of incoming and outgoing customers on fresh air change rates was the third subgoal of this thesis. This air exchange is highly relevant because it affects the thermal loads of the heating and air conditioning system as well as the need for ventilation. In order to estimate the air change rates, a model of the CO_2 concentration in the sales room air was developed, which uses the air change rates of the closed and opened entrance door as parameters. Compared to previous models of CO_2 concentration in supermarkets, several new effects were considered, for instance: the effect of joint door crossings on the total share of door opening time, or the shopping duration as a function of the number of purchased items.

The entire simulation model allows prediction of the CO_2 concentration based on the number of customers per hour and the average number of purchased items. The model was calibrated using measurement data and again validated. The results showed that the air change rate of the building, with closed entrance doors, was smaller than $0.1\,\mathrm{h}^{-1}$, which is a very low value. In winter, the air change rate of the building with open doors was $0.7\,\mathrm{h}^{-1}$. The accuracy of the prediction (mean absolute error (MAE) = 26 ppm) lay within the limits of the measurement accuracy. Compared to previous research in this field, it is a significant improvement in accuracy and means that the several newly considered effects are relevant.

The main goal of the thesis was the description of interactions between thermal systems and the quantification of their energetic impact. The humidity in the sales room air is affected by the interaction of all thermal systems. Being able to predict the sales room humidity therefore indicates that the physical model of the entire supermarket is a good representation of the actual physical interactions taking place between the thermal systems in a supermarket. Furthermore, humidity is very relevant, because the condensation of water vapour inside the display cabinets is responsible for a huge share of the cooling load and consequently affects the electrical energy consumption of the refrigeration system. All the mathematical models developed in this work (refrigeration system, display cabinets, customer balance equation, air exchange with the environment) were combined into one model of the entire supermarket and describe the humidity of the sales room air. This made it possible to calculate the humidity inside the sales room as a function of the temperature and humidity of the ambient air conditions as well as the sales data, namely the number of receipts per hour and the average number of items per receipt. Humidity sources in the sales room, such as plants, cleaning machines or a bakery oven, are very important. Here, their humidity emission were not measured directly, but calibrated to measurement data. Again, the model was calibrated and validated using two different time periods. During the validation period, the humidity ratio of the sales room air was predicted very well (MAPE = $5.4\,\%$, MAE = $0.3\,\mathrm{g\,kg}^{-1}$). The very accurate prediction of the of the sales room air humidity therefore indicates that the interactions between the thermal systems in the supermarket were modelled and quantified

correctly. This conclusion is supported by the previous validation of the individual interactions.

Finally, the validated simulations models were used to exemplify the quantification of several interactions. Firstly, a typical vertical MT cabinet was virtually tested to describe its part load operation. The cooling load was calculated for different temperatures and humidities of the sales room air as well as for different door opening frequencies. The results illustrate the huge impact that these boundary conditions have on the cooling load. The cooling load increases by 50 % at 25 °C and 60 % relative humidity compared to 20 °C and 50 %. Increasing the door opening frequency from $10\,h^{-1}$ to $30\,h^{-1}$ increases the cooling load by approximately 11 % to 14 %. If those physical parameters of display cabinets were available for different types of display cabinets, this could facilitate the planning of supermarkets and the dimensioning of refrigeration systems. Secondly, the entire supermarket was looked at and the energetic impact of a single shopping trip was evaluated for three different scenarios (winter, spring and summer). It could be shown that the energetic impact of a single customer depends largely on the ambient conditions as well as the operation conditions of the supermarket. The impact of one customer on the cooling demand, condensate in the display cabinets and the electrical energy consumption of the refrigeration system was assessed. These values depend largely on the number of opened display cabinets as well as ambient temperature and humidity.

This thesis and the results obtained do not analyse or optimise one specific supermarket, but focus on the description of methods, which supports the transferability to other supermarkets. The simulation models were built according to object-oriented principles; the described simulation approaches are tool-independent and can be used both with causal and acausal modelling. Consequently, they can be adapted to other topologies of supermarkets or refrigeration systems. The models and methods for the prediction of energy consumption, of the CO_2 concentration, and of the sales room air humidity were successfully demonstrated and validated. The description of each of these predictions addresses specifically the methods of parametrisation, which helps to apply the methods to other supermarkets. The overall interrelatedness and the interactions between the thermal systems in a supermarket are well known from a qualitative perspective. Here, several of these interactions were quantified for the first time: for instance as the specific air infiltration rate per door opening of display cabinets, the additional air exchange caused by one customer entering the sales room, or the specific dehumidification effect of display cabinets on the sales room air. The models and methods for estimating parameters or predicting energy consumption and concentration variables of the sales room air can be used for several applications. As shown in the work by Voigt (2018), the prediction of CO_2 concentration can help to dimension the ventilation system in a more realistic way. Besides planning and dimensioning, validated simulation models can be used in a virtual test bed for benchmarking supermarkets.

Outlook

There are several issues that could be addressed in further research. The simulations models and approaches described in this thesis could be combined with a component catalogue to form a tool for the planning and energy-benchmarking of supermarkets. The concept of such a tool has been described by the author in several previous publications, referred to there as *The SuperSmart Tool*. Using the models and approaches of this thesis for supermarket planning or energy-benchmarking requires further work.

Firstly, the accuracy of the results could be improved by extending the data base. 1. Additional experiments could be carried out to quantify the air exchange between the display cabinets and the sales room air. Besides tracer gas experiments, CFD simulations or experiments measuring the mass of condensate could also be applied. 2. Additional data using more

shopping trips and test persons should be collected. This would allow refining the approximation of the shopping duration and could take into account the overall occupancy of the supermarket as an additional cause variable. 3. The data-based estimation of the dimensionless air infiltration into display cabinets could be extended using further data. In particular, a larger number of display cabinets in different supermarkets should be analysed, using - if possible - a higher temporal resolution of temperature data.

Secondly, the simulation models could be improved. The simulation models used in this work showed very good results. However, at several instances in the modelling processes, simple models were chosen, where more complex models could have been applied: 1. The pressure losses in the R-744 refrigeration system were neglected. The model could be extended considering these losses. 2. The display cabinet model used one overall, average transmittance for the entire cabinet envelope. The model could be extended and the geometry and material properties of the back panel, walls, doors etc. considered separately. 3. The simulations of the joint door crossings and the door opening frequency were carried out for one single, automated entrance door. The simulation could be extended to model other typical supermarket entrance areas: two automated doors with an intermediate vestibule or separate doors for entering and leaving the store. 4. The air exchange via the entrance door did not consider the differences in pressure or temperature between the sales room and the environment. The model could be extended considering these potential differences. The decision for the simpler models proved to be very successful in this thesis. When applying more complex models, more parameters and assumptions would be needed. The additional effort should always be weighed up again the possible gain in accuracy.

Thirdly, parameters of further types of display cabinets, refrigeration systems and supermarkets should be collected. In this thesis, one test supermarket was looked at and many of the parameters were estimated specifically for this store. However, these parameters, such as the number of people shopping together, the duration of stay in the sales room, or the number of door openings per customer, could be different in other stores. Additionally, there are many different types of display cabinets and refrigeration systems. In future work, the methods described in this thesis could be applied to analyse other supermarkets and technical equipment to generate a catalogue with parametrised models.

A. Annex

A.1. Test supermarket

The test supermarket used throughout this thesis is a typical, modern supermarket in Germany. It has a stand-alone building with a sales area of 1000 m^2. The main entrance door of the supermarket has a vestibule with two automated sliding doors and an air curtain on the inside. In the entrance area, there is a bakery with a separate entrance door (see a schematic floor plan in Figure A.1). On Sundays, the bakery is opened and accessible only via the bakery door. The access to the supermarket sales floor is closed. The refrigeration system consists of a R-744 booster system with a flash gas bypass and an internal heat exchanger. Several medium and low temperature display cabinets are connected to this central refrigeration system (section A.1). The ventilation system is used for heating and cooling. The heating demand is primarily covered by heat recovery from the booster system. Heat pumps are used for space cooling and for additional heating. The usual opening hours are 7:00 to 21:30h. A broad range of data (temperature, humidity, pressure, power consumption) from the refrigeration system, cabinets and sales area are available.

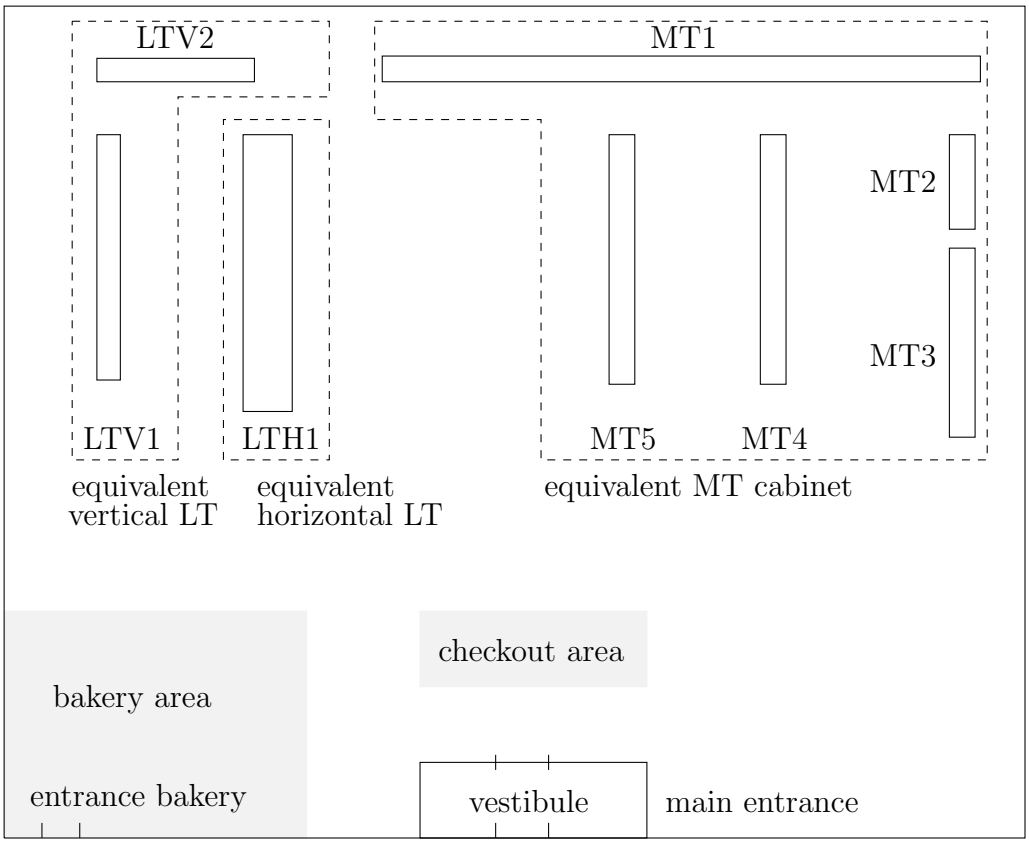

Figure A.1.: Schematic floor plan. It shows the display cabinet line ups that are aggregated into the equivalent display cabinets. The checkout and bakery area are shown for orientation. For clarity purpose, further information is omitted.

Equivalent display cabinets

Typically, there is a huge number of similar display cabinets in a supermarket. If the behaviour of *individual cabinets* is not of specific interest, several cabinets of the same type can be

combined to a so-called *equivalent cabinet* model. An *equivalent cabinet* is defined as a control volume that comprises of several identical or similar display cabinets. The equivalent cabinet provides the same interaction between sales area and refrigeration system as the multiple number of individual display cabinets. An equivalent cabinet is described by the same model using different parameter values for the overall surface A and the number of doors n. Table A.1 gives an overview of the display cabinet lines-up in the test supermarket and the parameters of the corresponding equivalent display cabinets.

Cabinet	length in m	width in m	height in m	n_{doors}	Surface A in m^2	cabinet type
MT cabinets						
MT1	21.25	1.05	2.20	34	142.7	dairy
MT2	3.75	1.05	2.20	06	29.0	meat
MT3	7.50	1.05	0.90	12	31.1	service counter
MT4	10.00	1.05	2.20	16	69.6	dairy
MT5	10.00	1.05	2.20	16	69.6	dairy
equivalent MT cabinet				84	342.0	
vertical LT cabinets						
LTV1	9.40	1.0	2.20	12	64.6	
LTV2	6.25	1.0	2.20	8	44.4	
equivalent vertical LT cabinet				20	109.0	
horizontal LT cabinets						
LTH1	10.89	1.95	0.90	34	65.6	
equivalent horizontal LT cabinet				34	65.6	

Table A.1.: Geometric data of display cabinet line ups on the floor plan and data of equivalent display cabinets

A.2. High pressure function R-744 Booster System

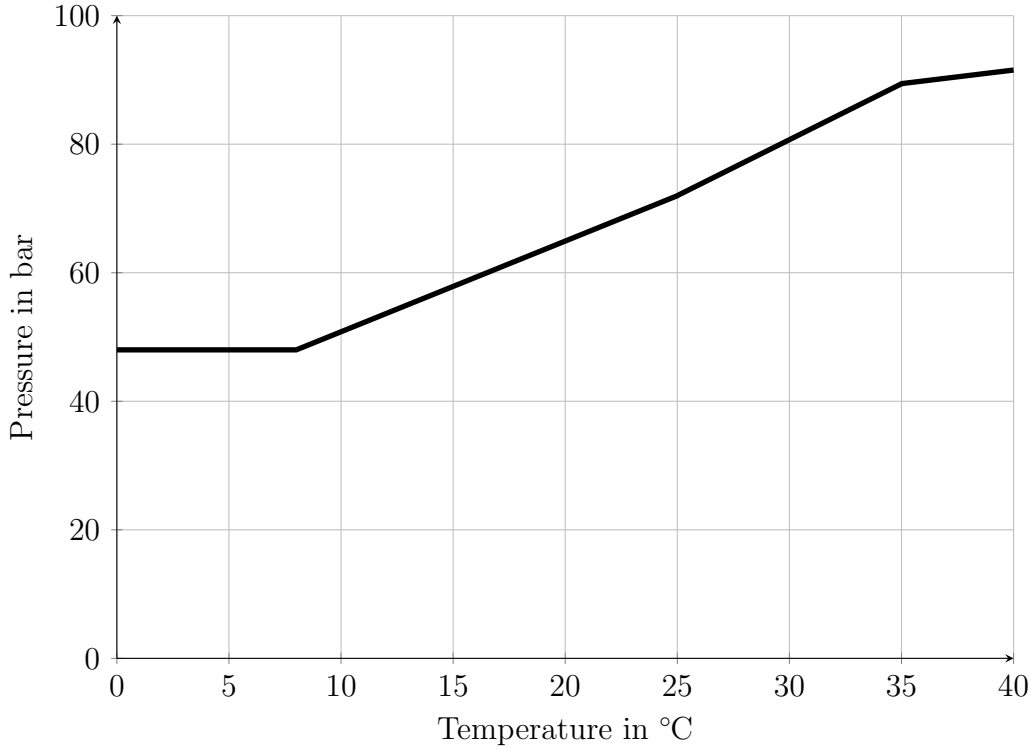

Figure A.2.: High pressure function of the R-744 booster systems in the test supermarket

A.3. Power consumption LT cabinet

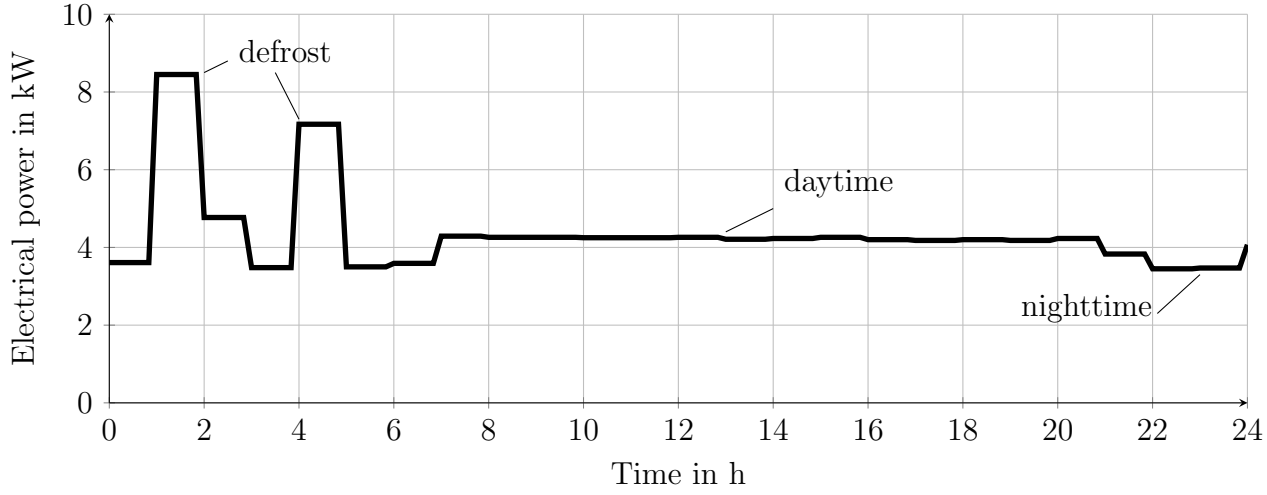

Figure A.3.: Typical profile of internal power $P_{\mathrm{el,cab,LT}}$ of all LT cabinets in the test supermarket in the course of a day. Values for daytime, nighttime and defrost periods are indicated.

A.4. Power consumption MT cabinet

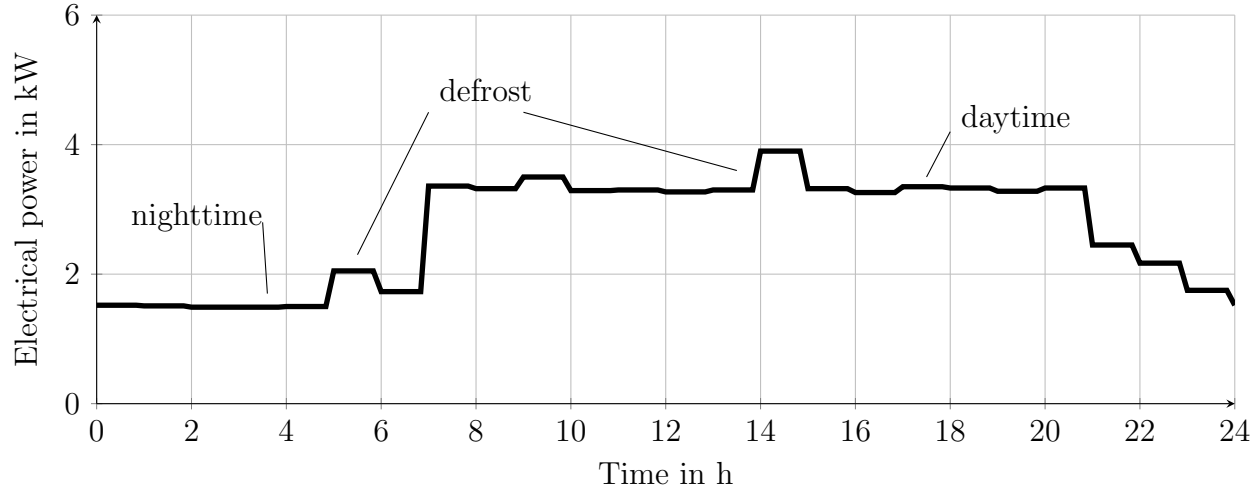

Figure A.4.: Typical profile of internal power $P_{\mathrm{el,cab,MT}}$ of all MT cabinets in the test supermarket in the course of a day. Values for daytime, nighttime and defrost periods are indicated. Defrost power belongs to a single meat cabinet with electrical defrost.

A.5. Shopping duration

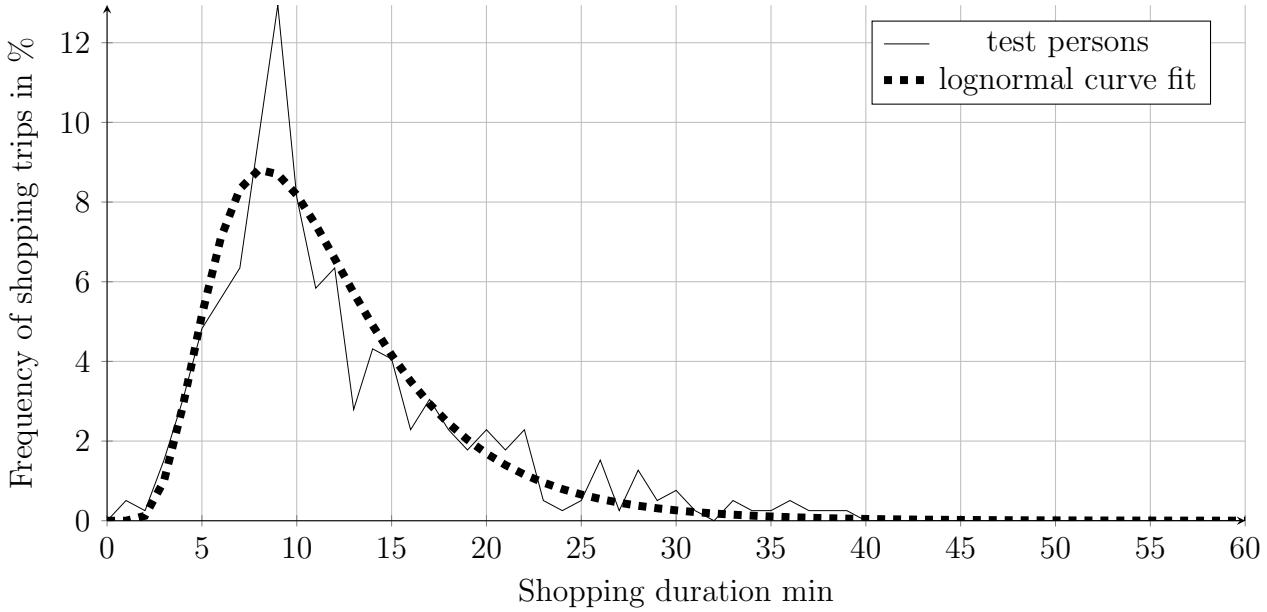

Figure A.5.: The frequency of shopping duration based on 395 shopping trips collected by 10 test persons (Section 5.1) and the fit of a lognormal function is shown.

A.6. Prediction CO_2 concentration, calibration winter

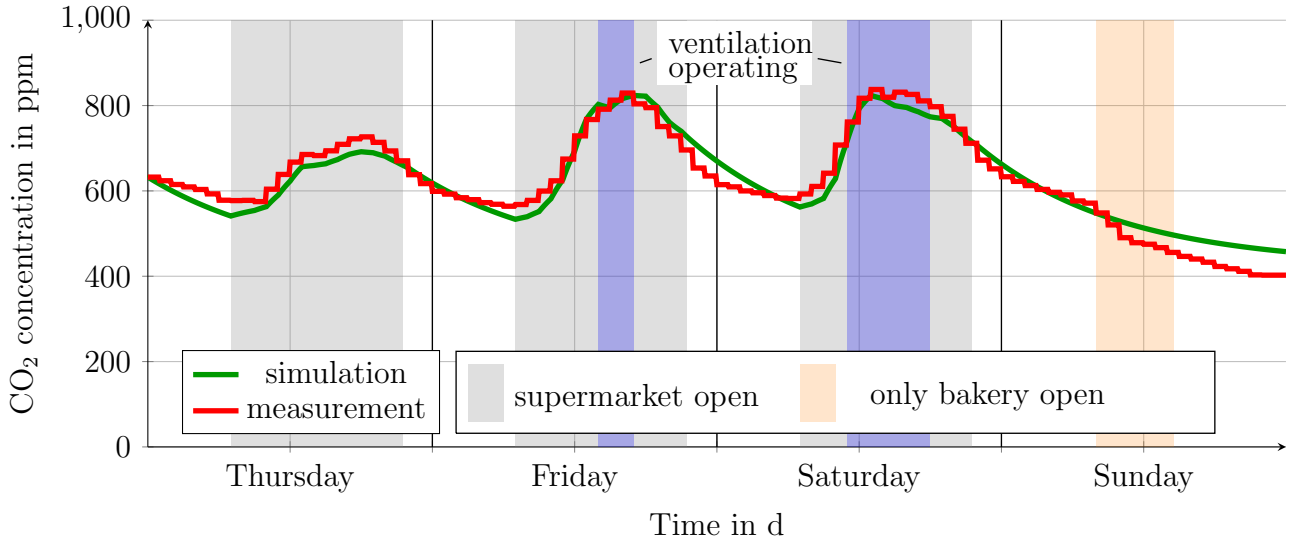

Figure A.6.: Comparison of measured and simulated CO_2 concentration, calibration, winter period, MAE = 25 ppm, $MAPE_{0ppm}$ = 4.3 %

A.7. Prediction CO_2 concentration, calibration winter

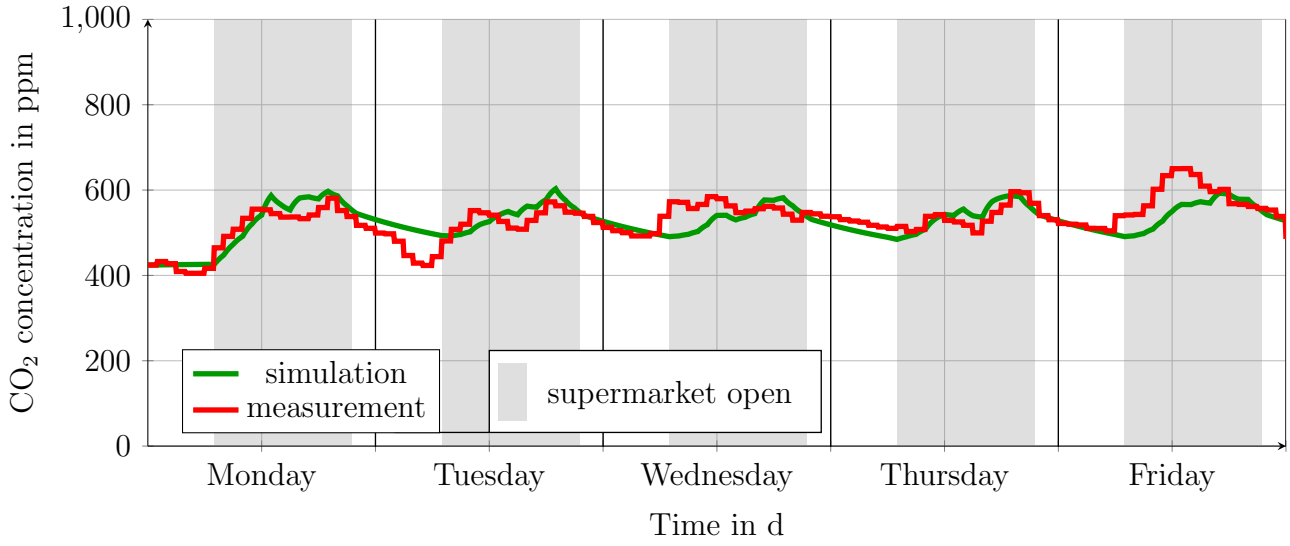

Figure A.7.: Comparison of measured and simulated CO_2 concentration, calibration, summer period, MAE = 26 ppm, $MAPE_{0ppm}$ = 4.9 %

A.8. Ambient temperature

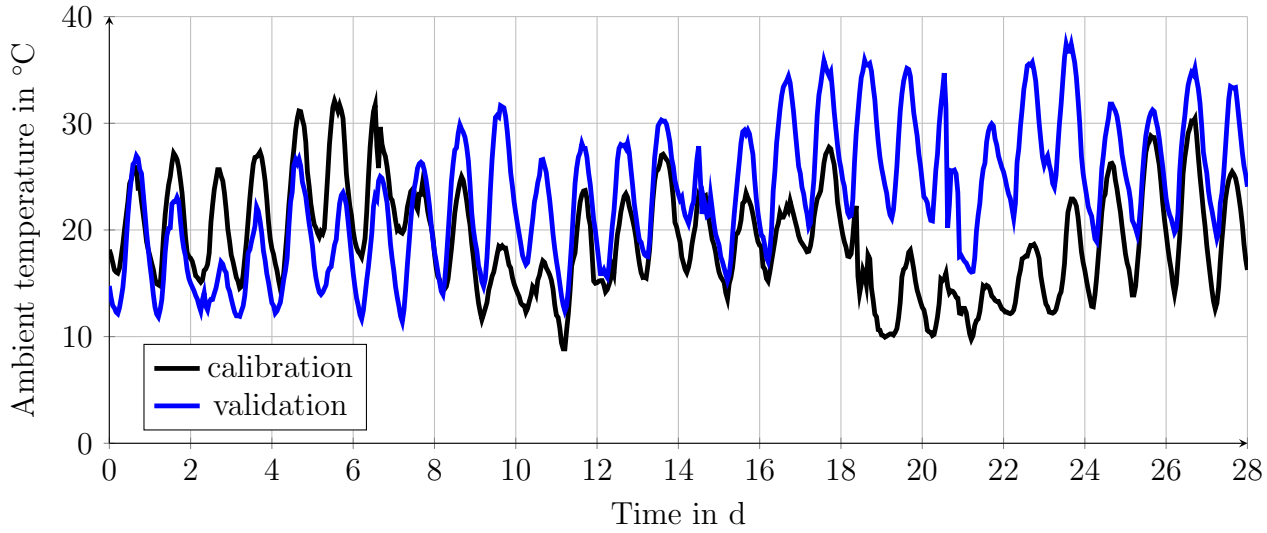

Figure A.8.: Input values of the ambient temperature T_{amb} for predicting the energy consumption of refrigeration system and display cabinets (Chapter 4)

A.9. Sales room temperature

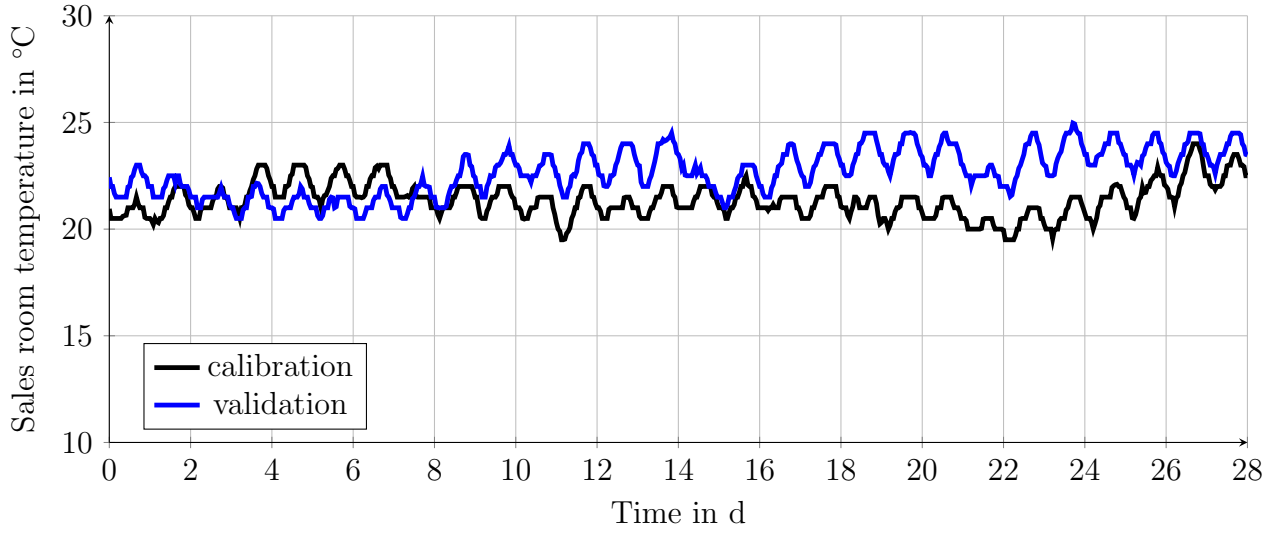

Figure A.9.: Input values of the sales room temperature T_{sa} for predicting the energy consumption of refrigeration system and display cabinets (Chapter 4)

A.10. Sales room relative humidity

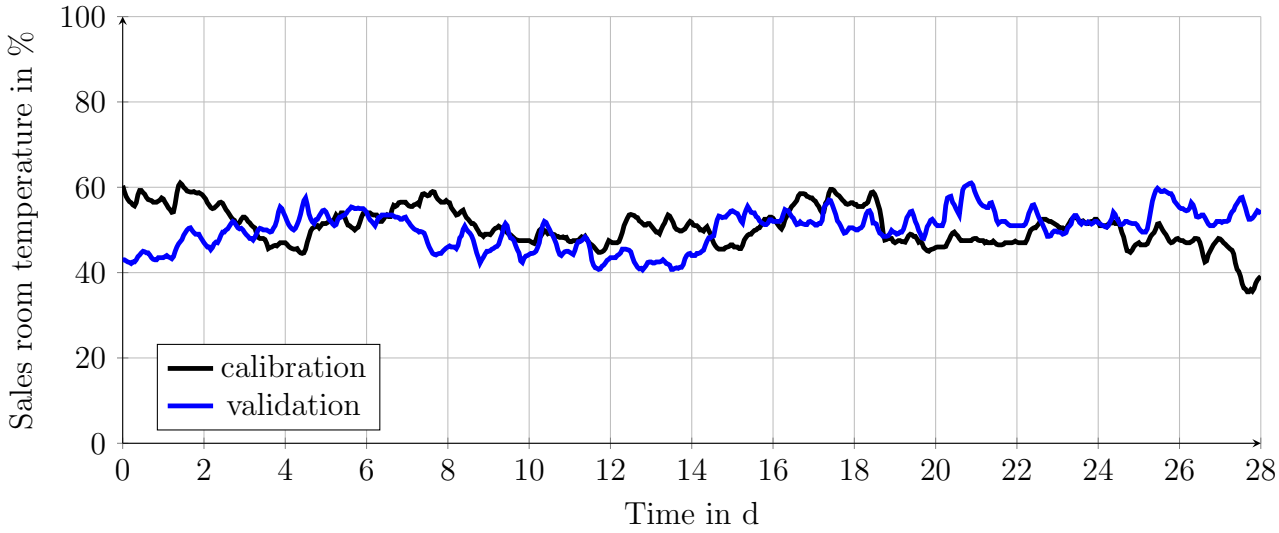

Figure A.10.: Input values of the sales room relative humidity RH_{sa} for predicting the energy consumption of refrigeration system and display cabinets (Chapter 4)

A.11. Customer flow profile

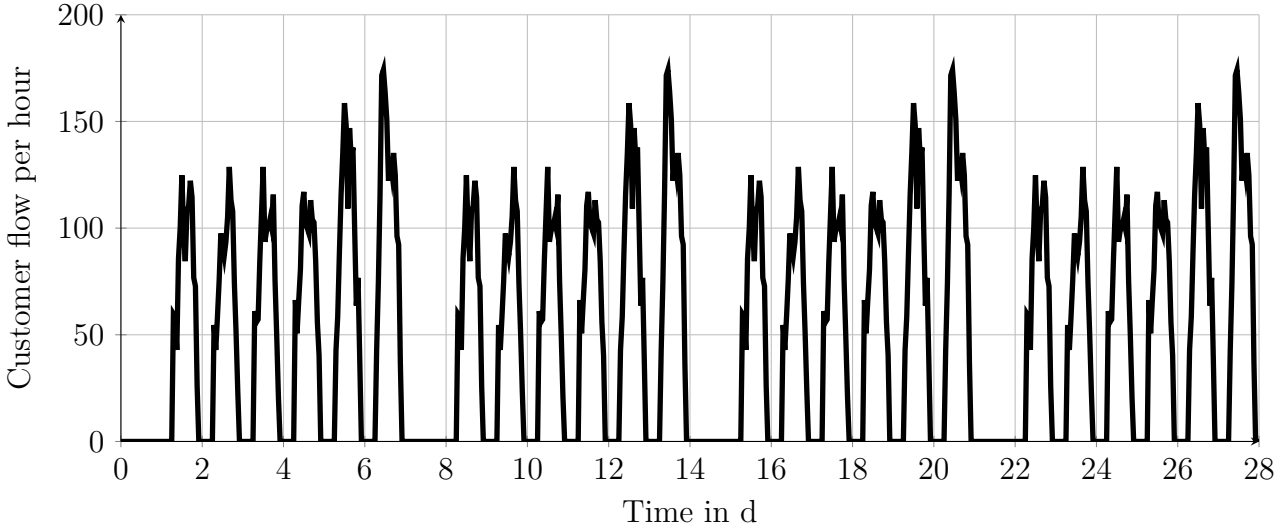

Figure A.11.: Generic profile of the customer flow $\dot{n}_{\mathrm{customer}}$ as input for predicting the energy consumption of refrigeration system and display cabinets (Chapter 4)

A.12. Total power consumption, calibration

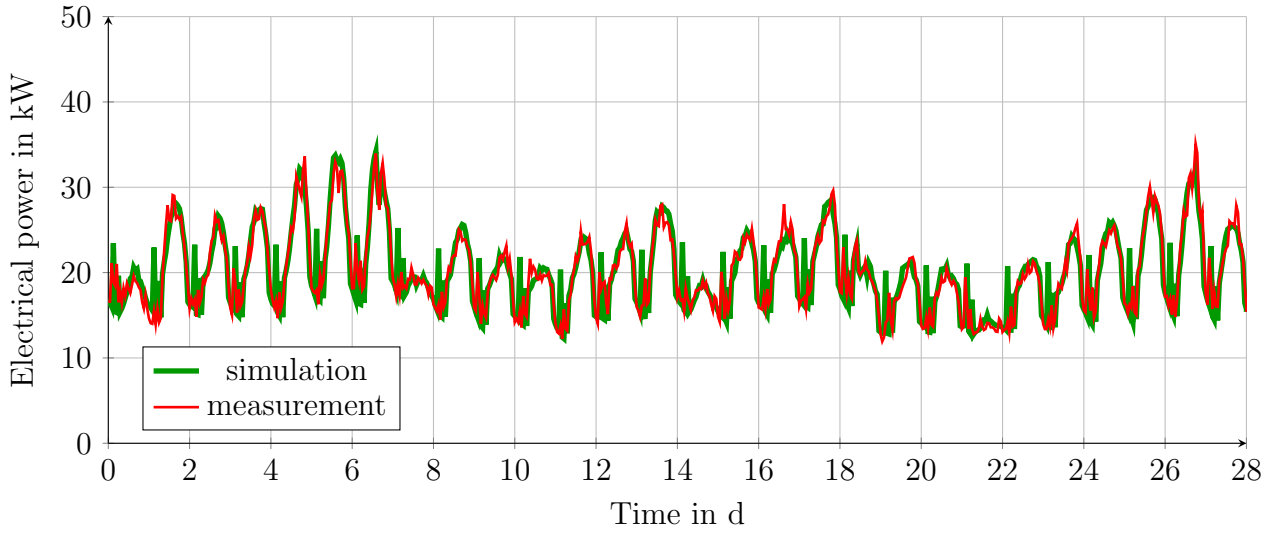

Figure A.12.: Total electrical power consumption P_{el} of the refrigeration system and display cabinets; calibration period (MAPE = 7.1 %) (Chapter 4)

A.13. Total Power consumption, validation

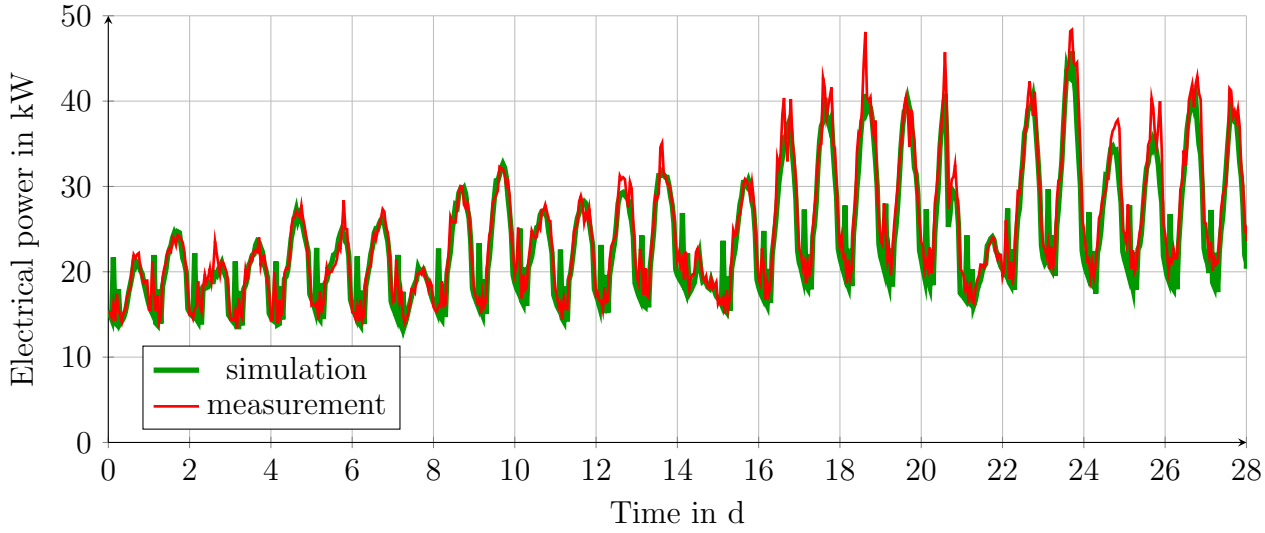

Figure A.13.: Total electrical power consumption P_{el} of the refrigeration system and display cabinets; validation period (MAPE = 7.6 %) (Chapter 4)

A.14. Ambient temperature

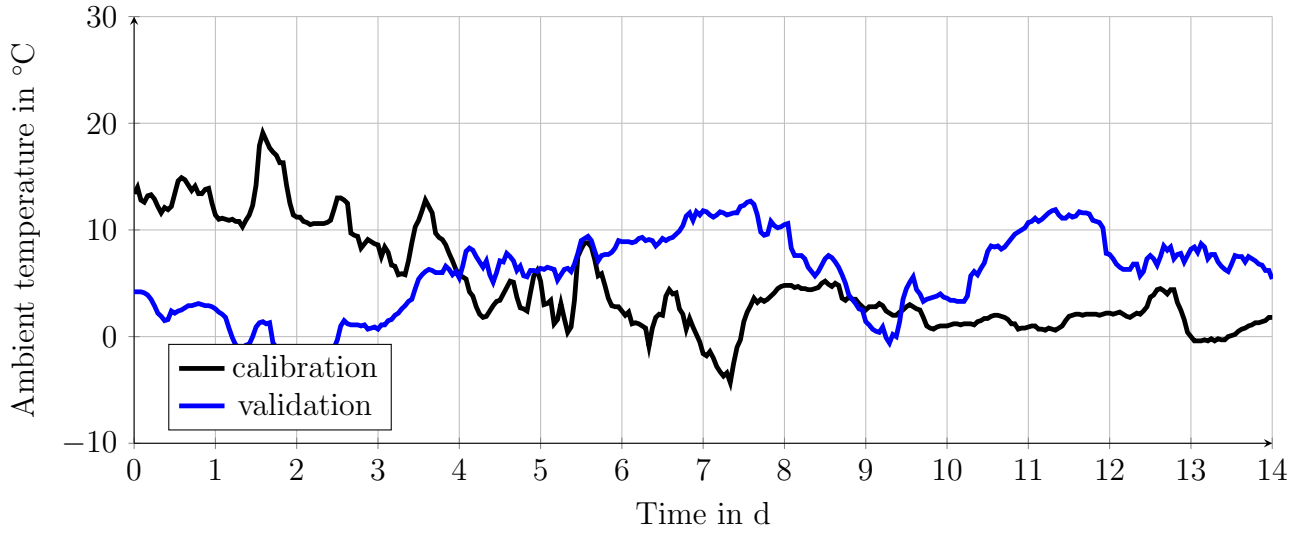

Figure A.14.: Input values of the ambient temperature T_{amb} for predicting the humidity in the sales room air (Chapter 6)

A.15. Ambient relative humidity

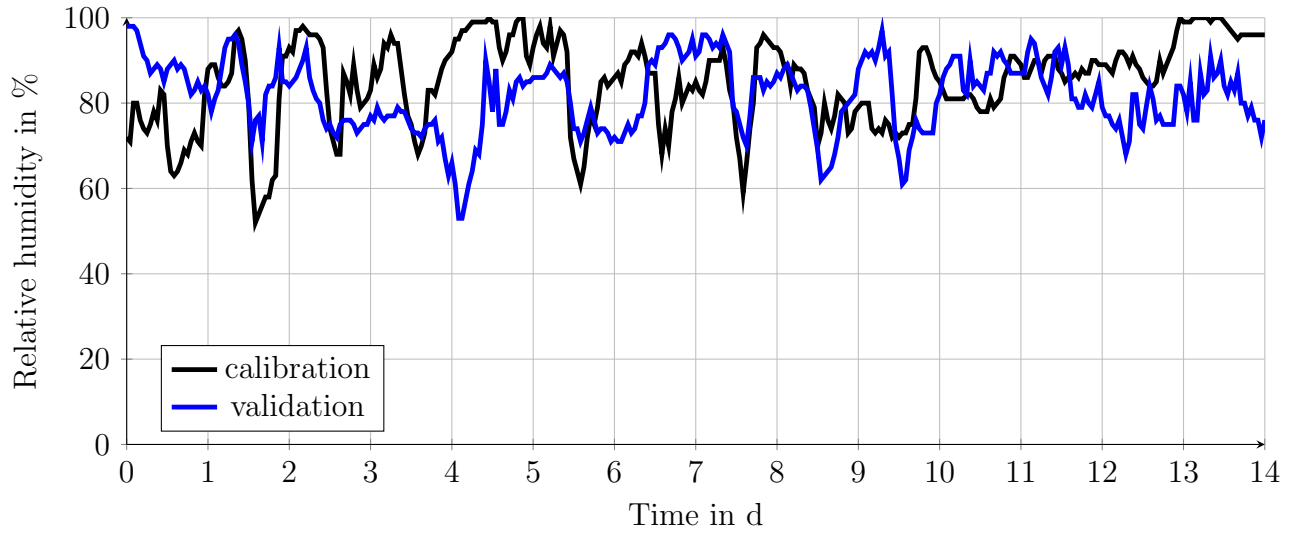

Figure A.15.: Input values of the ambient relative humidity RH_{amb} for predicting the humidity in the sales room air (Chapter 6)

A.16. Flow of receipt

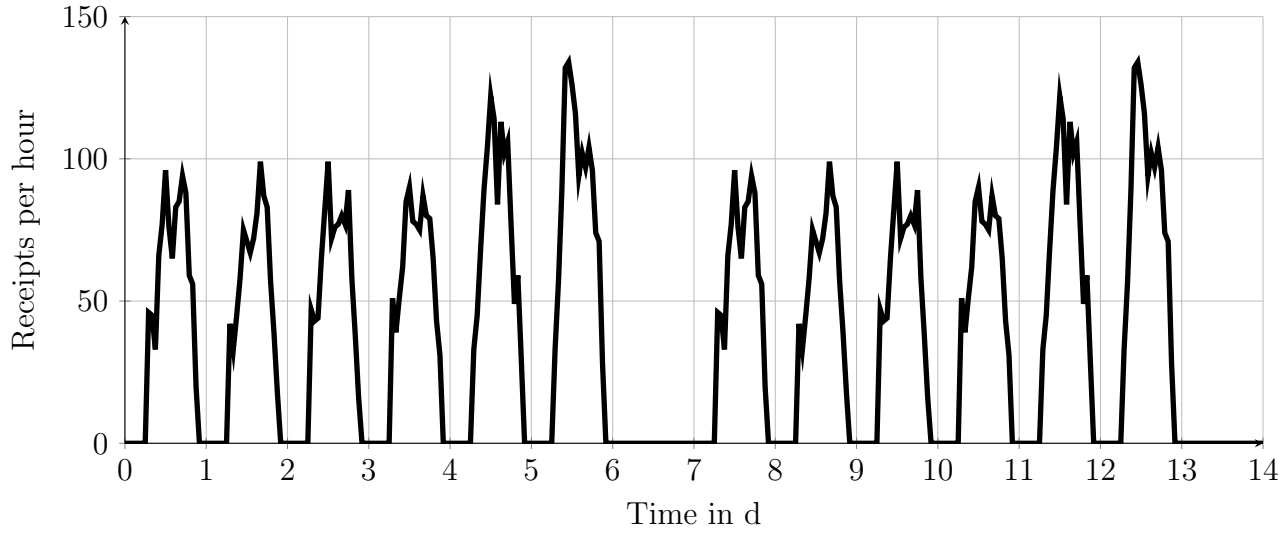

Figure A.16.: Generic profile of the rate of receipts per hour $\dot{n}_{\text{receipt}}$ as input for predicting the humidity in the sales room air (Chapter 6)

A.17. Number of items per receipt

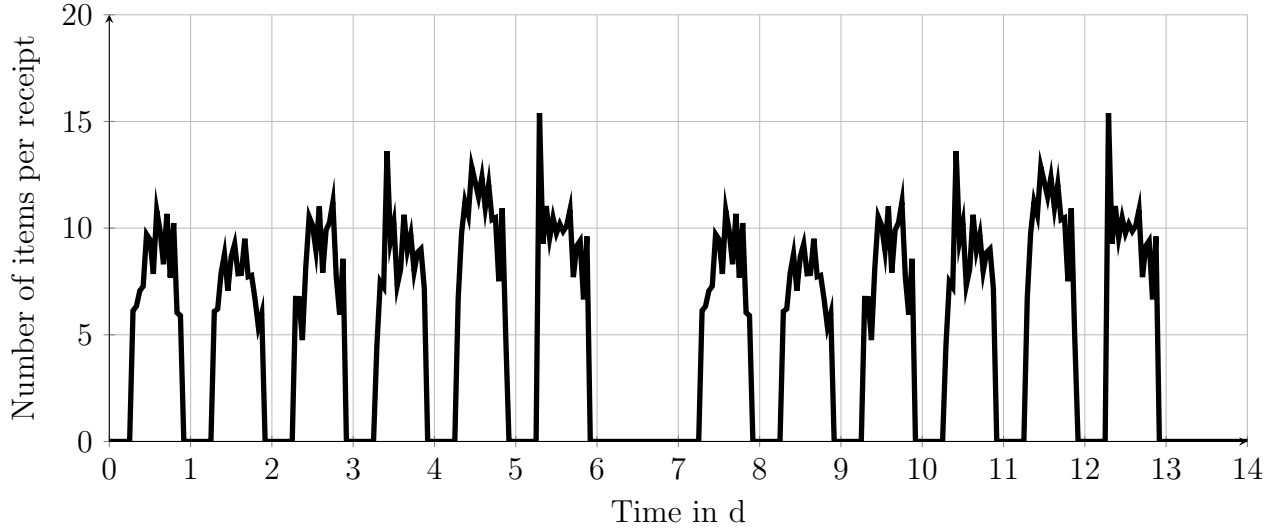

Figure A.17.: Generic profile of the number of items per receipt n_{item} as input for predicting the humidity in the sales room air (Chapter 6)

B. Nomenclature

Acronym

ACR	Air change rate
CCR	Customer change rate
CFD	Computational Fluid Dynamics
CTES	Cold Thermal Energy Storages
FGB	Flash Gas Bypass
FMI	Functional Mockup Interface
FMU	Functional Mockup Unit
HP	High Pressure
HVAC	Heating Ventilation Air Conditioning
IHX	Internal Heat Exchanger
LP	Low Pressure
LT	Low Temperature
MAE	Mean Absolute Error
MAPE	Mean Absolute Percentage Error
MT	Medium Temperature
NIR	Non-dimensional Infiltration Rate
ppm	parts per million
RH	Relative Humidity
TEF	Thermal Entrainment Factor

General Symbols

A	Area in m^2
c	Concentration in ppm
c	Specific heat capacity in $\mathrm{J\,kg^{-1}\,K^{-1}}$
d	Duration of a single event in s
$\overline{d}$	Average duration of a single event in s
D	Duration of a time interval in s
E	Energy in J
$\dot{e}$	Specific emission per mass of substance in $\mathrm{kg\,s^{-1}\,kg^{-1}}$
f	Frequency in $\mathrm{h^{-1}}$
h	Specific enthalpy in $\mathrm{J\,kg^{-1}}$
k	Thermal transmittance in $\mathrm{W\,m^{-2}\,K^{-1}}$
m	Mass in kg
$\dot{m}$	Mas flow in $\mathrm{kg\,s^{-1}}$
$\underline{\dot{m}}$	Specific mass flow rate per cabinet door in $\mathrm{kg\,s^{-1}}$
M	Molar mass in $\mathrm{kg\,mol^{-1}}$
n	Amount of substance in mol
n	Number of countable objects
$\overline{n}$	Average number of countable objects
$\dot{n}$	Flow of countable objects in $1\,\mathrm{h^{-1}}$
$\overline{\dot{n}}$	Average flow of countable objects in $1\,\mathrm{h^{-1}}$
p	Pressure in Pa
p	Parameter
Q	Heat in J
$\dot{Q}$	Heat flow in W
sqe	square error
t	Time in s
T	Temperature in K
$u(t)$	Time dependent input values
V	Volume in m^3
w	Width of a display cabinet in m
$\dot{V}$	Volume flow in $\mathrm{m^3\,s^{-1}}$
x	Humidity Ratio in $\mathrm{kg\,kg^{-1}}$

Greek Symbols

π	Pressure ratio −
τ	Time constant in s
ξ	Share of Door opening time
ξ	Mass concentration in $\mathrm{kg\,kg^{-1}}$
$\vec{\xi}$	Mass concentration vector of air in $\mathrm{kg\,kg^{-1}}$

Subscripts

0ppm	0 parts per million, reference
ac	Air conditioning
active	Active
air	Air as a mixture of gases
amb	Ambient
breathing	Breathing
cab	Cabinet
closed	Closed
comp	Compressor
cond	Condensate
CO_2	Carbon Dioxide
CR	Cold room
cs	Chilled space
customer	Customer
day	Day
defrost	Defrost
door	Door
dryair	Dry air
effis	Effective isentropic
el	Electric
empl	Employee
end	End
entered	Entered
entering	Entering
evap	Evaporation
exp	Experiment
fan	Fan
fruit	Fruit
gas	Gas
gc	Gas cooler
horiz	Horizontal
HP	High pressure
ice	Ice
IHX	Internal heat exchanger
in	Incoming or inflowing
indi	Individual
inf	Infiltration
int	Internal
is	Isentropic
item	Item
leaving	Leaving
left	Left
light	Light
line	Line
liquid	Liquid
LP	Low pressure
LT	Low temperature
max	Maximum
meas	Measurement
min	Minimum
MT	Medium temperature
night	Night
nom	Nominal
offset	Offset
open	Open
out	Outgoing or outflowing
people	People
person	Person
rand	Random
receipt	Receipt
ref	Refrigerant
return	Return air
sa	Sales area
sat	Saturated
sep	Separator
setpoint	Setpoint
sh	Superheat
sim	Simulation
solidif	Solidification
source	Source
start	Start
stay	Stay
suct	Suction
supply	Supply air
var	Variable
vent	Ventilation
vert	Vertical
wall	Wall
water	Water

C. List of Figures

D. List of Tables

E. Bibliography

[1] C. F. Afonso and M. D. Castro: "Air Infiltration: a Key Issue on Household Refrigerators". In: *The 7th International Conference on Sustainable Energy Technologies (SET 2008)* (Seoul, Korea). 2008.

[2] M. Amin; D. Dabiri, and H. K. Navaz: "Tracer gas technique. A new approach for steady state infiltration rate measurement of open refrigerated display cases". In: *Journal of Food Engineering* 92 (2 2009), pp. 172–181. DOI: 10.1016/j.jfoodeng.2008.10.039.

[3] J. Arias: "Energy Usage in Supermarkets - Modelling and Field Measurements". Dissertation. Stockholm: Royal Institut of Technology, 2005.

[4] M. Axell and P. Fahlén: *Vertical Display Cabinet*. report. SP The Swedish National Testing and Research Institute, 2018. 14 pp.

[5] H. D. Baehr and S. Kabelac: *Thermodynamik. Grundlagen und technische Anwendungen*. 15. Auflage. Berlin, Heidelberg: Springer Vieweg, 2012. ISBN: 978-3-642-24160-4.

[6] G. Bagarella; R. Lazzarin, and M. Noro: "Annual energy analysis of a water-loop self-contained refrigeration plant and comparison with multiplex systems in supermarkets". In: *International Journal of Refrigeration* 45 (2014), pp. 55–63. DOI: 10.1016/j.ijrefrig.2014.05.024.

[7] A. Bahman; L. Rosario, and M. M. Rahman: "Analysis of energy savings in a supermarket refrigeration/HVAC system". In: *Applied Energy* 98 (2012), pp. 11–21. DOI: 10.1016/j.apenergy.2012.02.043.

[8] E. Bellos and C. Tzivanidis: "A comparative study of CO_2 refrigeration systems". In: *Energy Conversion and Management: X* 1 (2019), p. 100002. DOI: 10.1016/j.ecmx.2018.100002.

[9] R. Ben-abdallah; D. Leducq; H. M. Hoang; O. Pateau; B. Ballot-Miguet; A. Delahaye, and L. Fournaison: "Modeling and experimental investigation for load temperature prediction at transient conditions of open refrigerated display cabinet using Modelica environment". In: *International Journal of Refrigeration* 94 (2018), pp. 102–110. DOI: 10.1016/j.ijrefrig.2018.02.017.

[10] J. Bender: "Algorithmisch orientiere Berechnung des thermischen Haushalts von Fahrzeugkabinen". Diploma Thesis. Marburg: Philipps-Universität Marburg, 1997.

[11] M. Bier; W. Diemair; H. Kühlwein; F. F. Nord; K. Paech; G. Steiner, and J. E. Wolf: *Biochemische Grundlagen der Lebensmittelfrischhaltung*. Berlin and Heidelberg: Springer, 1952. ISBN: 978-3-642-94595-3. DOI: 10.1007/978-3-642-94595-3.

[12] T. Blockwitz et al.: "Functional Mockup Interface 2.0. The Standard for Tool independent Exchange of Simulation Models". In: 9th International MODELICA Conference, Munich, Germany. Linköping Electronic Conference Proceedings. Linköping University Electronic Press, 2012, pp. 173–184. DOI: 10.3384/ecp12076173.

[13] L. Cecchinato; M. Corradi, and S. Minetto: "Energy performance of supermarket refrigeration and air conditioning integrated systems". In: *Applied Thermal Engineering* 30 (14-15 2010), pp. 1946–1958. DOI: 10.1016/j.applthermaleng.2010.04.019.

[14] L. Cecchinato; M. Corradi, and S. Minetto: "A critical approach to the determination of optimal heat rejection pressure in transcritical systems". In: *Applied Thermal Engineering* 30 (13 2010), pp. 1812–1823. DOI: 10.1016/j.applthermaleng.2010.04.015.

[15] F. E. Cellier: *Continuous System Modeling*. New York, NY: Springer, 1991. ISBN: 978-1-4757-3924-4. DOI: 10.1007/978-1-4757-3922-0.

[16] F. E. Cellier and E. Kofman: *Continuous System Simulation*. Boston, MA: Springer Science+Business Media Inc, 2006. ISBN: 978-0-387-30260-7. DOI: 10.1007/0-387-30260-3.

[17] N. Chaomuang: "Experimental characterization and modeling of airflow and heat transfer in a closed refrigerated display cabinet". Dissertation. Paris: Institut agronomique, vétérnaire et forestier de France, 2019.

[18] N. Chaomuang; D. Flick; A. Denis, and O. Laguerre: "Experimental analysis of heat transfer and airflow in a closed refrigerated display cabinet". In: *Journal of Food Engineering* 244 (2019), pp. 101–114. DOI: 10.1016/j.jfoodeng.2018.09.009.

[19] N. Chaomuang; D. Flick; A. Denis, and O. Laguerre: "Influence of operating conditions on the temperature performance of a closed refrigerated display cabinet". In: *International Journal of Refrigeration* 103 (2019), pp. 32–41. DOI: 10.1016/j.ijrefrig.2019.03.031.

[20] N. Chaomuang; O. Laguerre, and D. Flick: "Dynamic heat transfer modeling of a closed refrigerated display cabinet". In: *Applied Thermal Engineering* 161 (2019), p. 114138. DOI: 10.1016/j.applthermaleng.2019.114138.

[21] N. Chaomuang; O. Laguerre, and D. Flick: "A simplified heat transfer model of a closed refrigerated display cabinet". In: *Thermal Science and Engineering Progress* (2020), p. 100494. DOI: 10.1016/j.tsep.2020.100494.

[22] M. Chasserot: "Natural Refrigeration Trends in Commercial refrigeration". Presentation. In: *ATMOsphere Network EuroShop* (Duesseldorf). Shecco. 2020.

[23] B. Chini: "Forschungsergebnisse zum Energiemanagement im Einzelhandel". Presentation. In: *Supermarkt Symposium* (Darmstadt). ZVKKW. 2019.

[24] H. Cho; K. Gowri, and B. Liu: *Energy Saving Impact of ASHRAE 90.1 Vestibule Requirements. Modeling of Air Infiltration through Door Openings*. report. Pacific Northwest National Laboratory, 2010. 48 pp. DOI: 10.2172/1017117.

[25] G. Cortella: "CFD-aided retail cabinets design". In: *Computers and Electronics in Agriculture* 34 (1-3 2002), pp. 43–66. DOI: 10.1016/S0168-1699(01)00179-X.

[26] G. Cortella and F. Polonara: "Retail display equipment". In: *Managing Frozen Foods - A volume in Woodhead Publishing Series in Food Science, Technology and Nutrition // Managing frozen foods*. Ed. by C. J. Kennedy and C. Kennedy. Woodhead Publishing in food science and technology. Boca Raton, Fla and Cambridge, England: CRC Press, 2000, pp. 233–262. ISBN: 9781855734128. DOI: 10.1533/9781855736528.233.

[27] F. R. d'Ambrosio Alfano; M. Dell'Isola; G. Ficco; B. I. Palella; G. Riccio, and A. Frattolillo: "Thermal comfort in Supermarket's refrigerated areas. An integrated survey in central Italy". In: *Building and Environment* 166 (2019), p. 106410. DOI: 10.1016/j.buildenv.2019.106410.

[28] Deutsches Institut für Normung, ed.: *Ergonomie der thermischen Umgebung - Bestimmung des körpereigenen Energieumsatzes (ISO 8996:2004)*. DIN EN ISO. 2005.

[29] Deutsches Institut für Normung, ed.: *Verkaufskühlmöbel - Teil 2: Klassifizierung, Anforderungen und Prüfbedingungen (ISO 23953-2:2005)*. DIN EN ISO. 2012.

[30] B. Dong; M. Gorbounov; S. Yuan; T. Wu; A. Srivastav; T. Bailey, and Z. O'Neill: "Integrated energy performance modeling for a retail store building". In: *Building Simulation* 6 (3 2013), pp. 283–295. DOI: 10.1007/s12273-013-0109-8.

[31] European Union: *Regulation (EU) No 517/2014 of the European Parliament and of the Council of 16 April 2014 on fluorinated greenhouse gases and repealing Regulation (EC) No 842/2006Text with EEA relevance*. 2014.

[32] J. A. Evans: *Are doors on fridges the best environmental solution for the retail sector? Background paper to IOR Debate*. Tech. rep. 2014. 11 pp.

[33] J. A. Evans and A. M. Foster: *Sustainable Retail Refrigeration*. Hoboken: John Wiley & Sons Incorporated, 2016. ISBN: 978-1-118-92740-3.

[34] J. A. Evans; S. Scarcelli, and M. Swain: "Temperature and energy performance of refrigerated retail display and commercial catering cabinets under test conditions". In: *International Journal of Refrigeration* 30 (3 2007), pp. 398–408. DOI: 10.1016/j.ijrefrig.2006.10.006.

[35] R. T. Faramarzi; Coburn B., and A. Sarhadian R.: "Performance and Energy Impact of Installing Glass Doors on an Open Vertical Deli/Dairy Display Case". In: *Winter Meeting* (Atlatic City, NJ). Ed. by American Society of Heating, Refrigeration and Air-Conditioning Engineers. 2002, pp. 673–679.

[36] R. T. Faramarzi; Sarhadian R., and Sweetser R.: "Assessment of Indoor Relative Humidity Variations on the Energy Use and Thermal Performance of Supermarkets' Refrigerated Display Cases". In: *Proceedings from ACEEE Summer Studies on Energy Efficiency in Buildings*. American Council for an Energy-Efficient Economy. 2000.

[54] M. Franceschi; M. Orlandi; F. Scuderi, and Camporese R.: "PREDICTION OF THE HEAT EXTRACTION RATE OF A VERTICAL OPEN DISPLAY CABINET IN A SUPERMARKET". In: *The 23rd IIR International Congress of Refrigeration* (Prague). 2011.

[55] R. Franke; F. Casella; M. Otter; M. Sielemann; H. Elmqvist; S. E. Mattson, and H. Olsson: "Stream Connectors – An Extension of Modelica for Device-Oriented Modeling of Convective Transport Phenomena". In: The 7 International Modelica Conference, Como, Italy. Linköping Electronic Conference Proceedings. Linköping University Electronic Press, 2009, pp. 108–121. DOI: 10.3384/ecp09430078.

[56] B. Fricke and B. R. Becker: *Comparison of vertical Display Cases: Energy And Productivity Impacts of Glass Doors Versus Open vertical Display Cases. ASHRAE Research Project 1402*. final report. American Society of Heating, Refrigeration and Air-Conditioning Engineers, 2009. 113 pp.

[57] B. Fricke and B. R. Becker: "Energy Use of Doored and Open Vertical Refrigerated Display Cases". In: *13th International Refrigeration and Air Conditioning Conference at Purdue*. 2010.

[58] B. Fricke; T. Kuruganti; J. Nutaro; D. Fugate, and J. Sanyal: "Utilizing Thermal Mass in Refrigerated Display Cases to Reduce Peak Demand". In: *16th International Refrigeration and Air Conditioning Conference at Purdue*. 2016.

[59] B. Fricke and V. Sharma: *Demand Defrost Strategies in Supermarket Refrigeration Systems*. Oak Ridge National Laboratory. 2011.

[60] T. Funder-Kristensen; L. Larsen, and J. E. Thorsen: "Integration of the hidden refrigeration capacity as heat pump in smart energy systems". In: *12th IEA Heat Pump Conference* (Rotterdam). Ed. by IEA. 2017.

[61] P. D. Gaspar; Carrilho Concalves L.C., and Pitaarma R.A: "Experimental Analysis of the Thermal Entrainment Three Dimensional Effects in Re-Circulated Air Curtains". In: *Roomvent 2007. 10th International Conference on Air Distribution in Rooms*. Ed. by O. Seppänen and J. Säteri. Roomvent 2007 and International Conference on Air Distribution in Rooms. Helsinki: FINVAC, 2007. ISBN: 9789529989812.

[62] P. D. Gaspar; L. C. Carrilho Gonçalves, and R. A. Pitarma: "THREE-DIMENSIONAL CFD MODELLING AND ANALYSIS OF THE THERMAL ENTRAINMENT IN OPEN REFRIGERATED DISPLAY CABINETS". In: *ASME Summer Heat Transfer Conference* (Jacksonville, Florida). ASME. 2008.

[63] P. D. Gaspar; L. C. Carrilho Gonçalves, and R. A. Pitarma: "Experimental analysis of the thermal entrainment factor of air curtains in vertical open display cabinets for different ambient air conditions". In: *Applied Thermal Engineering* 31 (5 2011), pp. 961–969. DOI: 10.1016/j.applthermaleng.2010.11.020.

[64] P. D. Gaspar; L. C. Carrilho Gonçalves, and R. A. Pitarma: "CFD Parametric Studies for Global Performance Improvement of Open Refrigerated Display Cabinets". In: *Modelling and Simulation in Engineering* 2012 (1 2012), pp. 1–15. DOI: 10.1155/2012/867820.

[65] Y. Ge and S. Tassou: "Performance evaluation and optimal design of supermarket refrigeration systems with supermarket model "SuperSim", Part I: Model description and validation". In: *International Journal of Refrigeration* 34 (2 2011), pp. 527–539. DOI: 10.1016/j.ijrefrig.2010.11.010.

[66] Y. Ge and S. Tassou: "Performance evaluation and optimal design of supermarket refrigeration systems with supermarket model "SuperSim". Part II: Model applications". In: *International Journal of Refrigeration* 34 (2 2011), pp. 540–549. DOI: 10.1016/j.ijrefrig.2010.11.004.

[67] H. Getu and P. Bansal: "Modeling and performance analyses of evaporators in frozen-food supermarket display cabinets at low temperatures". In: *International Journal of Refrigeration* 30 (7 2007), pp. 1227–1243. DOI: 10.1016/j.ijrefrig.2007.02.003. (Visited on 05/29/2013).

[68] M. Geyer; W. Herppich; B. Herold; O. Schlüter, and M. Linke: *Obst und Gemüse nach der Ernte. Frische, Qualität, Sicherheit*. ger. report. Version 2., veränd. Neuaufl. Geyer, Martin (VerfasserIn) Herppich, Werner (VerfasserIn) Herold, Bernd (VerfasserIn) Schlüter, Oliver (VerfasserIn) Linke, Manfred (VerfasserIn). Bonn: AID-Infodienst, 2010. 59 pp.

[69] GfK Consumer Panels: "Einkaufen in Zeiten knapper Zeit". In: *GFK consumer index* (08 2012).

[70] GfK Consumer Panels: "Der 'tägliche Einkauf' - ein Fall fürs Wochenende". In: *GFK consumer index* (05 2013).

[71] GfK Consumer Panels: "Zwischen Acht und Acht - Einkaufen im Tagesverlauf". In: *GFK consumer index* (08 2013).

[77] P. Gullo; A. Hafner, and G. Cortella: "Multi-ejector R744 booster refrigerating plant and air conditioning system integration – A theoretical evaluation of energy benefits for supermarket applications". In: *International Journal of Refrigeration* 75 (2017), pp. 164–176. DOI: 10.1016/j.ijrefrig.2016.12.009.

[78] P. Gullo; A. Hafner, and K. Banasiak: "Transcritical R744 refrigeration systems for supermarket applications. Current status and future perspectives". In: *International Journal of Refrigeration* 93 (2018), pp. 269–310. DOI: 10.1016/j.ijrefrig.2018.07.001.

[79] P. Gullo; K. M. Tsamos; A. Hafner; K. Banasiak; Y. T. Ge, and S. A. Tassou: "Crossing CO_2 equator with the aid of multi-ejector concept. A comprehensive energy and environmental comparative study". In: *Energy* 164 (2018), pp. 236–263. DOI: 10.1016/j.energy.2018.08.205.

[80] A. Hafner; S. Foersterling, and K. Banasiak: "Multi-ejector concept for R-744 supermarket refrigeration". In: *International Journal of Refrigeration* 43 (2014), pp. 1–13.

[81] G. G. Heidinger; Nascimento S.M., and Gaspar P.D.: "IMPACT OF ENVIRONMENTAL CONDITIONS ON THE PERFORMANCE OF OPEN MULTIDECK DISPLAY CASE EVAPORATORS". In: *2nd IIR International Conference on Sustainability and the Cold Chain* (Paris). 2013.

[82] G. G. Heidinger; S. M. Nascimento; P. D. Gaspar, and P. D. Silva: "EXPERIMENTAL STUDY OF THE INFLUENCE OF CONSUMERS MOVEMENT PARALLEL TO THE FRONTAL OPENING OF MULTIDECK DISPLAY CASE ON THE EVAPORATOR'S THERMAL PERFORMANCE". In: *The 24th IIR International Congress of Refrigeration* (Yokohama, Japan). 2015.

[83] R. H. Howell: "Calculation of Humidty effects on energy requirements of refrigerated display cases". In: *ASHRAE Transactions* 99 (1993), pp. 679–693.

[84] R. H. Howell; L. Rosario, and A. Bula: "EFFECTS OF INDOOR RELATIVE HUMIDITY ON REFRIGERATED". In: *CLIMA 2000* (Brussels). 1997. URL: http://www.inive.org/members_area/medias/pdf/Inive/clima2000/1997/p275.pdf.

[85] R. H. Howell; L. Rosario; D. Riiska, and M. Bondoc: "POTENTIAL SAVINGS IN DISPLAY CASE ENERGY WITH REDUCED SUPERMARKET RELATIVE HUMIDITY". In: *The 20th IIR International Congress of Refrigeration* (Sydney). 1999.

[86] IEA Heat Pump Centre: *IEA Heat Pump Program Annex 31. ADVANCED MODELING AND TOOLS FOR ANALYSIS OF ENERGY USE IN SUPERMARKET SYSTEMS*. Final Report. Tech. rep. International Energy Agency, 2011. 106 pp.

[87] IEA Heat Pump Centre: *Performance indicators for energy efficient supermarket building. Report No. HPT-AN44-1*. Final Report. IEA Heat Pump Centre, 2017. 126 pp.

[88] D. Jareemit; S. Shu, and J. Srebric: "A Field Investigation of Air Infiltration Rates through Automatic Entrance Doors in Retail Buildings". In: *International Journal of Building, Urban, Interior and Landscape Technology* 2014 (2014), pp. 51–59. DOI: 10.14456/built.2014.9.

[89] J.-N. Jäschke: "Strukturelle Analyse und abstrakte Modellierung eines Supermarktes als thermisches System". Master Thesis. Braunschweig: TU Braunschweig, 2015.

[91] M. Karampour and S. Sawalha: *effsys - Supermarket refrigeration and heat recovery using CO_2 as refrigerant. A comprehensive evaluation based on field measurements and modelling*. 2014. URL: http://kth.diva-portal.org/smash/get/diva2:849667/FULLTEXT01.pdf (visited on 07/17/2020).

[92] M. Karampour and S. Sawalha: "THEORETICAL ANALYSIS OF CO_2 TRANSCRITICAL SYSTEM WITH PARALLEL COMPRESSION FOR HEAT RECOVERY AND AIR CONDITIONING IN SUPERMARKETS". In: *The 24th IIR International Congress of Refrigeration* (Yokohama, Japan). 2015.

[93] M. Karampour; S. Sawalha, and J. Arias: *Eco-friendly supermarkets - an overview*. public report. SuperSmart Project, 2016. 54 pp.

[94] KI Kälte Luft Klimatechnik: "Innovatives Kälte-Wärme-Verbund-System im Discount-Filialnetz. Aldi Nord und Viessmann stelen gemeinsames Energieprojekt vor". In: *KI Kälte Luft Klimatechnik* 2017 (04 2017), pp. 14–16.

[96] K. Kohri: "A SIMULATION ANALYSIS OF THE OPENING AREA OF ENTRANCE DOORS AND WINTER AIRFLOW INTO THE ENTRANCE HALL OF A HIGH-RISE OFFICE BUILDING". In: *7th International IBPSA Conference* (Rio de Janeiro). International Building Performance Simulation Association. 2001.

[97] M. Kolokotroni; S. A. Tassou, and B. L. Gowreesunker: "Energy aspects and ventilation of food retail buildings". In: *Advances in Building Energy Research* 9 (1 2014), pp. 1–19. DOI: 10.1080/17512549.2014.897252.

[98] D. Kosar and O. Dumitrescu: "Humidity Effects on Supermarket Refrigerated Case Energy Performance: A Database Review". In: *ASHRAE Transactions* 111 (2005), pp. 1051–1060.

[99] D. Laussmann and D. Helm: "Air Change Measurements Using Tracer Gas". In: *Chemistry, Emission Control, Radioactive Pollution and Indoor Air Quality*. Ed. by N. A. Mazzeo. INTECH Open Access Publisher, 2011. ISBN: 978-953-307-316-3.

[100] S. Liao; T. Zhao, and A. Jakobsen: "A correlation of optimal heat rejection pressures in transcritical carbon dioxide cycles". In: *Applied Thermal Engineering* 20 (9 2000), pp. 831–841. DOI: 10.1016/S1359-4311(99)00070-8.

[101] U. M. Lindberg; M. Axell, and P. Fahlén: "Vertical Display cabinets with Doors - Influence of the door-opening frequency on storage temperature and cooling demand". In: *IIR/Eurotherm sustainable refrigeration and heat pump technology conference* (Stockholm, Sweden). 2010.

[102] U. M. Lindberg; M. Axell, and P. Fahlén: "Vertical Display cabinets without and with doors - a comparison of measurements in a laboratory and in a supermarket". In: *1st IIR International Conference on Sustainability and the Cold Chain* (Cambridge, United Kingdom). 2010.

[103] X. Lu; T. Lu, and M. Viljane: "Estimation of Space Air Change Rates and CO_2 Generation Rates for Mechanically-Ventilated Buildings". In: *Advances in Computer Science and Engineering*. Ed. by M. Schmidt. InTech, 2011. ISBN: 978-953-307-173-2. DOI: 10.5772/16062.

[105] T. Månsson: "Energy in Supermarktes. An overview on the energy flows and refrigeration controls". Licentiate thesis. Göteborg: Chalmers University of Technology, 2016.

[106] T. Månsson and Y. Ostermeyer: "Potential of Supermarket Refrigeration Systems for Grid Balancing by Demand Response". In: *Proceedings of the 8th International Conference on Smart Cities and Green ICT Systems* (Heraklion, Crete, Greece). 2019.

[107] T. Månsson; A. Rukundo; M. Almgren; P. Tsigas; C. Marx, and Y. Ostermeyer: "Analysis of door openings of refrigerated display cabinets in an operational supermarket". In: *Journal of Building Engineering* (2019), p. 100899. DOI: 10.1016/j.jobe.2019.100899.

[108] K. Marciniak: "Simulation of transient heat and mass flows in a supermarket". Master Thesis. Göteborg: Chalmers University of Technology, 2016.

[109] J. Martin: "Untersuchung von Maßnahmen zur Steigerung der Energieeffizienz in Supermärkten". Bachelor Thesis. Braunschweig: TU Braunschweig, 2017.

[111] A. Müller: "Energielieferung aus dem Supermarkt". In: *Energie & Management* (14 2019), p. 17.

[112] Z. Mylona; M. Kolokotroni, and S. A. Tassou: "A study of improving energy efficiency of small supermarkets by modelling interactions between building hvac, refrigeration and display product". In: *5th IIR International Conference on Sustainability and the Cold Chain* (Bejing). 2018.

[113] M. Ndoye; S. Mousset; J. Carlier, and G. Arroyo: "EXPERIMENTAL STUDY OF THE COLD AISLE PHENOMENON IN SUPERMARKET DISPLAY CABINETS". In: *The 23rd IIR International Congress of Refrigeration* (Prague). 2011.

[114] M. Nöding: "Energieoptimierte Regelung von CO_2-Kompressionskältekreisläufen". Dissertation. Braunschweig: TU Braunschweig, 2019.

[116] M. Orlandi; F. M. Visconti, and S. Zampini: "CFD ASSISTED DESIGN OF CLOSED DISPLAY CABINETS". In: *2nd IIR International Conference on Sustainability and the Cold Chain* (Paris). 2013.

[117] M. Orphelin; D. Marchio, and S. D'Alanzo: "Are there optimum temperature and humidity set points for supermarkets?" In: *Winter Meeting*. Winter Meeting (Chicago, IL). Ed. by American Society of Heating, Refrigeration and Air-Conditioning Engineers. 1999, pp. 497–507.

[118] Á. Á. Pardiñas: *SuperSmart-Rack. Energy-efficient and environmentally friendly integrated CO_2 vapour compression units for supermarktes.* project information. Sintef. 1 p. URL: https://www.sintef.no/globalassets/project/highefflab/supersmartrack_v2_final.pdf (visited on 09/07/2019).

[119] L. Patryarcha and H. Dreisbach: "Temperaturverteilung in Verkaufskühlmöbel". In: *DKV Jahrestagung* (Hannover). 2013.

[120] R. Pedersen; C. Sloth; R. Wisniewski, and T. Green: "Supermarket defrost cycles as flexible reserve". In: *2015 IEEE Conference on Control Applications (CCA)*. 2015 IEEE Conference on Control Applications (CCA) (Sydney, Australia). IEEE, 2015, pp. 744–749. ISBN: 978-1-4799-7787-1. DOI: 10.1109/CCA.2015.7320706.

[121] G. Perrino: "Plusenergiefiliale Migros Zuzwil". Presentation. In: *Supermarkt Symposium* (Darmstadt). ZVKKW. 2018.

[122] S. Poppi: "Development of Commercial Refrigeration Systems". Master Thesis. Trondheim: Norwegian University of Science and Technology, 2010.

[123] Projektträger Jülich: *Verbundvorhaben: flexess - Entwicklung von Strategien und Lösungen zur Ausschöpfung zukünftiger Flexibilitätspotentiale vollelektrischer Haushalte, Gewerbe, Industrien und Elektromobilität. Teilvorhaben: Zukünftige Topologien und Betriebsstrategien thermischer Systeme mit Anbindung an einen Flexibilitätsmarkt*. 2020. URL: https://www.enargus.de/pub/bscw.cgi/?op=enargus.eps2&q=%2201189747/1%22&v=10&id=1249724 (visited on 05/23/2020).

[124] G. Purper: *Die Betriebsformen des Einzelhandels aus Konsumentenperspektive*. Deutscher Universitäts-Verlag, 2005. ISBN: 978-3-8350-0322-4.

[125] G. Quaas: *Modellvergleich.pdf*. URL: http://www.georg-quaas.de/modellvergleich.pdf (visited on 09/17/2019).

[126] N. Réhault: *ALDI 2010 – Hocheffizienter Supermarkt mit geothermiegestütztem Kälteverbund*. 2013.

[127] D. Rettich; T. Köberle, and M. Becker: "Systematische Analyse und Bewertung von Energiekonzepten bei Supermärkten und Discountern". In: *DKV Jahrestagung* (Hannover). 2013.

[128] J.-M. Rhiemeier; J. Harnisch; C. Ters; M. Kauffeld, and A. Leisewitz: *Vergleichende Bewertung der Klimarelevanz von Kälteanlagen und -geräten für den Supermarkt*. Forschungsbericht 206 44 300 12. Dessau-Roßlau: Umweltbundesamt, 2008. 493 pp.

[129] C. C. Richter: "Proposal of New Object-Oriented Equation-Based Model Libraries for Thermodynamic Systems". Dissertation. Braunschweig: TU Braunschweig, 2008.

[130] A. F. Ronzoni; G. Heinzle; A. Furlan; M. C. Nazário, and D. Hense: "A Theoretical and Experimental Analysis of a Self-contained R-290 Refrigeration Unit Applied to a Glass Door Reach-in Supermarket Display Case". In: *17th International Refrigeration and Air Conditioning Conference at Purdue*. 2018.

[131] S. J. Roth: *VWL für Einsteiger*. 5., überarbeitete Auflage. Konstanz and München: UVK Verlagsgesellschaft mbH and UVK/Lucius, 2016. ISBN: 978-3-8252-4657-0.

[132] C.-A. Roulet and F. Foradini: "Simple and Cheap Air Change Rate Measurement Using CO_2 Concentration Decays". In: *International Journal of Ventilation* 1 (1 2002), pp. 39–44. DOI: 10.1080/14733315.2002.11683620.

[133] A. A. Al-Sahhaf: "INVESTIGATION OF THE ENTRAINMENT AND INFILTRATION RATES OF AIR CURTAINS IN OPEN LOW-FRONT REFRIGERATED DISPLAY CABINETS". Dissertation. London: Brunel University, 2011.

[134] S. Sawaf; H. Awbi; J. Barlow; J. Broadbent, and B. Gregson: "Review of Factors Affecting Uncontrolled Ventilation in Food Supermarkets". In: *TSBE EngD Conference* (Reading, England). TSBE Centre, University of Reading. 2011.

[135] S. Sawaf; J. F. Barlow; E. Essah; J. Broadbent, and B. Gregson: "Wind lobby analysis. Effects of uncontrolled ventilation in food supermarkets". In: *7th International Cold Climate HVAC Conference* (2012), pp. 396–403.

[136] C. Schulze: "A Contribution To Numerically Efficient Modelling Of Thermodynamic Systems". Dissertation. Braunschweig: TU Braunschweig, 2013.

[137] *SciPy*. URL: https://www.scipy.org/ (visited on 09/17/2019).

[138] A. Sevault; K. Banasiak; J. Bakken, and A. Hafner: "A novel PCM accumulator for refrigerated display cabinet: design and CFD simulations". In: *12t^h IIR Conference on Phase-Change Materials and Slurries for Refrigeration and Air Conditioning (PCM 2018)*. 2018.

[139] M. H. Sherman and R. Chan: *Building Airtightness. Research and Practice*. Report No. LBNL-53356. Lawrence Berkely National Laboratory, 2004.

[140] K. Skacanova: *Guide to natural refrigerants training in Europe 2017*. report. 2017. 132 pp.

[141] K. Z. Skačanová and A. Gkizelis: *Technical report on energy efficiency in HFC-free supermarket refrigeration. Climate For the project Global Corporate and Policy Measures to Incentivise Highly Efficient HFC-Free Cooling*. Tech. rep. 2018. 74 pp.

[142] K. Z. Skačanová; A. Gkizelis; D. Belluomini; M. Battesti, and T. Willson: *IMPACT OF STANDARDS ON HYDROCARBON REFRIGERANTS IN EUROPE. Market research report*. Market research report. lifefront Project, 2018. 92 pp.

[143] H. Sorensen; S. Bogomolova; K. Anderson; G. Trinh; A. Sharp; R. Kennedy; B. Page, and M. Wright: "Fundamental patterns of in-store shopper behavior". In: *Journal of Retailing and Consumer Services* 37 (2017), pp. 182–194. DOI: 10.1016/j.jretconser.2017.02.003. URL: http://www.sciencedirect.com/science/article/pii/S0969698916303186.

[144] T. Stovall and v. Baxter: *Modeling Supermarket Refrigeration with EnergyPlus*. Tech. rep. Heat Pump Centre, 2010. 5 pp.

[145] J. Sun; K. M. Tsamos, and S. A. Tassou: "CFD comparisons of open-type refrigerated display cabinets with/without air guiding strips". In: *Energy Procedia* 123 (2017), pp. 54–61. DOI: 10.1016/j.egypro.2017.07.284.

[146] SuperSmart Project: *Proposal for the Development of the EU Ecoloabel Criteria for Food Retail Stores. Technical Report*. Tech. rep. 2019. 216 pp.

[147] W. Tegethoff: "Eine objektorientierte Simulationsplattform für Kälte-, Klima- und Wärmepumpensysteme". Dissertation. Braunschweig: TU Braunschweig, 1999.

[150] M. Titze: "Energetic analysis and optimisation strategies of a modern northern European supermarket". Dissertation. Braunschweig: TU Braunschweig, 2017.

[151] TRNSYS: *TRNSYS Transient System Simulation Tool – Homepage*. URL: http://www.trnsys.com/ (visited on 04/27/2020).

[152] E. Tschegg; W. Heindl, and A. Sigmund: *Grundzüge der Bauphysik. Akustik, Wärmelehre, Feuchtigkeit*. Vienna: Springer Vienna, 1984. ISBN: 978-3-7091-8771-5. DOI: 10.1007/978-3-7091-8771-5.

[153] U.S. Department of Energy: *Engineering Reference. EnergyPlusTM Version 8.9.0 Documentation*. Tech. rep. 2018. 1716 pp.

[154] Umweltbundesamt: "Gesundheitliche Bewertung von Kohlendioxid in der Innenraumluft. Mitteilungen der Ad-hoc-Arbeitsgruppe Innenraumrichtwerte der Innenraumlufthygiene-Kommission des Umweltbundesamtes und der Obersten Landesgesundheitsbehörden". ger. In: *Bundesgesundheitsblatt, Gesundheitsforschung, Gesundheitsschutz* 51 (11 2008), pp. 1358–1369. DOI: 10.1007/s00103-008-0707-2. eprint: 19043767.

[155] Umweltbundesamt: *Atmosphärische Treibhausgas-Konzentrationen*. Ed. by Umweltbundesamt. 2019. URL: https://www.umweltbundesamt.de/daten/klima/atmosphaerische-treibhausgas-konzentrationen (visited on 10/21/2019).

[156] P. Vale Pereira; A. Sgrott; L. F. Back; D. T. Kohara, and C. Melo: "A Methodology for Measuring the Air Infiltration Rates into Refrigerated Compartments". In: *16th International Refrigeration and Air Conditioning Conference at Purdue*. 2016.

[157] C. Vallée: "ENERGY SAVING POTENTIAL AT PARTIAL LOAD FOR VERTICAL GLASS DOOR REFRIGERATED DISPLAY CABINETS". In: *The 24th IIR International Congress of Refrigeration* (Yokohama, Japan). 2015.

[158] F. M. Visconti; D. Mazzola, and M. Orlandi: "CFD analysis of interaction between low temperature display cabinet layout and HVAC". In: *3rd IIR International Conference on Sustainability and the Cold Chain* (London). 2014.

[159] M. Voigt: "Untersuchung von Lüftungsanlagen im Supermarkt". Bachelor Thesis. Braunschweig: TU Braunschweig, 2018.

[160] B. Weigand; J. Köhler, and J. v. Wolfersdorf: *Thermodynamik kompakt*. Berlin and Heidelberg: Springer-Verlag, 2010. ISBN: 978-3-642-13112-7.

[161] F. Wenig; P. Klanatsky; C. Heschl; C. Mateis, and N. Dejan: "Exponential pattern recognition for deriving air change rates from CO_2 data". In: *2017 IEEE 26th International Symposium on Industrial Electronics (ISIE)* (Edinburgh, United Kingdom). 2017, pp. 1507–1512. ISBN: 978-1-5090-1412-5. DOI: 10.1109/ISIE.2017.8001469.

[162] E. Wiedenmann and J. Schönenberger: "Zusammenspiel einer CO_2-Kälteanlage mit Eisspeicher und Photovoltaik". In: *DKV Jahrestagung* (Aachen). 2018.

[163] H. Ye; J. Yu; B. Wang; Y. Liu; H. Guo, and L. Tian: "Study on the influence of air curtain barrier efficiency on infiltration air volume and temperature distribution in large space in winter". In: *Procedia Engineering* 205 (2017), pp. 2509–2516. DOI: 10.1016/j.proeng.2017.09.982.

[164] C. Younes; C. A. Shdid, and G. Bitsuamlak: "Air infiltration through building envelopes. A review". In: *Journal of Building Physics* 35 (3 2012), pp. 267–302. DOI: 10.1177/1744259111423085.

[165] K.-z. Yu; G.-l. Ding, and T.-j. Chen: "A correlation model of thermal entrainment factor for air curtain in a vertical open display cabinet". In: *Applied Thermal Engineering* 29 (14-15 2009), pp. 2904–2913. DOI: 10.1016/j.applthermaleng.2009.02.016.

[166] G. K. Yuill; R. Upham, and C. Hui: "Air leakage through automatic doors". In: *ASHRAE Transactions* 106 (2000), pp. 145–160.

[167] M. Zaatari; E. Nirlo; D. Jareemit; N. Crain; J. Srebric, and J. Siegel: "Ventilation and indoor air quality in retail stores. A critical review (RP-1596)". In: *HVAC&R Research* 20 (2 2014), pp. 276–294. DOI: 10.1080/10789669.2013.869126.

[168] B. Zühlsdorf; A. R. Christiansen; F. M. Holm; T. Funder-Kristensen, and B. Elmegaard: "Analysis of possibilities to utilize excess heat of supermarkets as heat source for district heating". In: *Energy Procedia* 149 (2018), pp. 276–285. DOI: 10.1016/j.egypro.2018.08.192.

F. List of publications

[37] N. Fidorra: ""SuperSmart"-Werkzeug für die Energieverbrauchsberechnung von Supermärkten". Presentation. In: *Supermarkt Symposium* (Darmstadt). ZVKKW. 2014.

[38] N. Fidorra: "Untersuchung der Betriebsstrategie von CO2 Supermarkt-Kälteanlagen unter Berücksichtigung von schwankenden Energiepreisen". Presentation. In: *Supermarkt Symposium* (Darmstadt). ZVKKW. 2015.

[39] N. Fidorra: *Computational tools for supermarket planning*. public report. SuperSmart Project, 2016. 40 pp.

[40] N. Fidorra: "DAS EUROPÄISCHE SUPERSMART PROJEKT: ENTWICKLUNG EINES EU ECOLABELS UND ABBAUT NICHT-TECHNISCHER HÜRDEN FÜR ENERGIEEFFIZENTE SUPERMÄRKTE". Presentation. In: *Supermarkt Symposium* (Darmstadt). ZVKKW. 2016.

[41] N. Fidorra: "Energetische Betrachtung unterschiedlicher Wasserkreislaufsysteme für die Anwendung im Supermarkt". Presentation. In: *Supermarkt Symposium* (Darmstadt). ZVKKW. 2018.

[42] N. Fidorra: "Energetischer Vergleich von R744-Verbundkälteanlagen und R290- Wasserkreislaufsystemen für Supermärkte. Vorstellung einer Fallstudie und Diskussion". Presentation. In: *Arbeitskreis Kältetechnik* (Bad Pyrmont). EHI Retail Institute. 2019.

[43] N. Fidorra: "Theorie und Praxis im Supermarkt. Wechselwirkung von Verkaufsraumluft, Kundenverhalten und Kältelasten in realen Anlagen". Presentation. In: *Supermarkt Symposium* (Darmstadt). ZVKKW. 2019.

[44] N. Fidorra; A. Hafner; N. Lemke, and J. Köhler: "SuperSmart-Energiebenchmarktool für Supermärkte". In: *DKV Jahrestagung* (Hannover). 2013.

[45] N. Fidorra; A. Hafner; S. Minetto, and J. Köhler: "APPLICATIONS OF THE SUPERSMART ENERGY-BENCHMARK TOOL FOR SUPERMARKETS". In: *11^{th} IIR Gustav Lorentzen Conference on Natural Refrigerants* (Hangzhou, China). 2014.

[46] N. Fidorra; A. Hafner; S. Minetto, and J. Köhler: "SIMULATION MODELS IN THE SUPERSMART SUPERMAREKT ENERG-BENCHMARKT TOOL". In: *3^{rd} IIR International Conference on Sustainability and the Cold Chain* (London). 2014.

[47] N. Fidorra; A. Hafner; S. Minetto, and J. Köhler: "LOW TEMPERATURE HEAT STORAGES IN CO2 SUPERMARKET REFRIGERATION SYSTEMS". In: *The 24^{th} IIR International Congress of Refrigeration* (Yokohama, Japan). 2015.

[48] N. Fidorra; A. Hafner; P. Nekså, and J. Köhler: "ENERGY COST ANALYSIS OF HEAT RECOVERY IN CO2 SUPERMARKET REFRIGERATION SYSTEMS". In: *Ammonia and CO2 Refrigeration Technologies* (Ohrid, Macedonia). Ed. by IIR/IIF. 2015.

[49] N. Fidorra; J. Kistner; W. Tegethoff, and J. Köhler: "Energetische Bewertung von Wasserkreislauf-Systemen für Supermärkte". In: *DKV Jahrestagung* (Bremen). 2017.

[50] N. Fidorra and J. Köhler: "Energetische Untersuchung integrierter Supermarktkonzepte". In: *DKV Jahrestagung* (Kassel). 2016.

[51] N. Fidorra; S. Minetto; A. Hafner; K. Banasiak, and J. Köhler: "Analysis of Cold Thermal Energy Storage Concepts in CO_2 Refrigeration Systems". In: *12th IIR Gustav Lorentzen Natural Working Fluids Conference* (Edingburgh). 2016.

[52] N. Fidorra and A. Schulte: "VEOTOP - Verfahren zur optimalen Synthese und Topologieoptimierung komplexer thermischer Systeme". Presentation. In: *Research Insights* (Braunschweig, 2018). Ed. by TU Braunschweig, Stadt der Zukunft. 2018.

[53] N. Fidorra; W. Tegethoff, and J. Köhler: "Energetic Assessment of Water Loop Systems for Supermarket Refrigeration". Presentation. In: *ATMOsphere Europe* (Berlin). Shecco. 2017.

[72] A. Gibelhaus; N. Fidorra; F. Lanzerath; U. Bau; L. Schnabel; J. Köhler, and A. Bardow: "Hybrid refrigeration with CO2 vapor compression cycle and adsorption chiller: Anefficient combination of natural working fluids". In: *International Sorption Heat Pump Conference* (Tokyo). 2017.

[73] A. Gibelhaus; N. Fidorra; F. Lanzerath; L. Schnabel; J. Köhler, and A. Bardow: "Effiziente Kältebereitstellung durch Kopplung von Adsorptions- und CO_2 Kompressionskalteanlage". In: *KI Kälte, Luft, Klimatechnik* 12 (2016), pp. 46–50.

[74] A. Gibelhaus; N. Fidorra; F. Lanzerath; L. Schnabel; J. Köhler, and A. Bardow: "Effiziente Kältebereitstellung durch Kopplung von Adsorptions- und CO_2 Kompressionskälteanlage". In: *DKV Jahrestagung* (Kassel). 2016.

[75] A. Gibelhaus; N. Fidorra; F. Lanzerath; U. Bau; J. Köhler, and A. Bardow: "Hybrid refrigeration by CO_2 vapour compression cycle and water-based adsorption chiller. An efficient combination of natural working fluids". In: *International Journal of Refrigeration* 103 (2019), pp. 204–214. DOI: 10.1016/j.ijrefrig.2019.03.036.

[76] R. Graf; N. Fidorra; A. Schröder; J. L. Corrales Ciganda; F. Ziegler, and J. Köhler: "Untersuchung der Kopplung von Absorptionskältemaschinen und CO_2 Dampfkompressionsanlagen zur effizienten Kältebereitstellung". In: *DKV Jahrestagung* (Dresden). 2015.

[90] J.-N. Jäschke; N. Fidorra; C. Schulze, and J. Köhler: "ABSTRACT DESCRIPTION OF SUPERMARKET SYSTEMS AND SIMULATION USING THE FUNCTIONAL MOCK-UP INTERFACE". In: *12th IIR Gustav Lorentzen Natural Working Fluids Conference* (Edingburgh). 2016.

[95] J. Kistner; Tegethoff W.; N. Fidorra, and J. Köhler: "Approach for Synthesis and Optimization of Complex Thermal Systems for Supermarkets". In: *Simulation Notes Europe SNE* 29 (2 2019), pp. 93–100.

[104] R. Manescu; A. Hafner; N. Fidorra; S. Foersterling, and J. Köhler: "A NEW APPROACH FOR COLD THERMAL ENERGY STORAGES IN SUPERMARKET REFRIGERATION". In: *Ammonia and CO_2 Refrigeration Technologies*. Ammonia and CO2 Refrigeration Technologies (Ohrid, Macedonia). Ed. by IIR/IIF. IIR/IIF. 2017.

[110] S. Minetto; A. Hafner; A. Rossetti, and N. Fidorra: *"SuperSMART: expertise hub for a market uptake of energy-efficient supermarkets by awareness raising, knowledge transfer and pre-preparation of an EU Ecolabel" The New EU project that helps to make supermarkets more efficient and environmentally friendly.* Tech. rep. 2017. 5 pp.

[115] M. Nöding; N. Fidorra; M. Gräber, and J. Köhler: "ECOS 2016: Operation Strategy for Heat Recovery of Transcritical CO2 Refrigeration Systems with Heat Storages". In: *29th International Conference on Efficiency, Cost, Optimisation, Simulation and Environmentl Impact of Energy Systems* (Portoroz). 2016.

[148] W. Tegethoff; J.-N. Jäschke; C. Schulze, and N. Fidorra: "Verschaltung von Functional-Mockup-Units (FMUs) mit physikalischen Konnektoren am Beispiel der thermischen Simulation eines Supermarktes". In: *ASIM-Treffen STS/GMMS*. Ed. by D. Tikhomirov; H.-T. Mammen, and T. Pawletta. ARGESIM Verlag Wien, 2016. ISBN: 978-3-901608-48-3.

[149] W. Tegethoff; J.-N. Jäschke; J. Schulze, and N. Fidorra: "Verschaltung von FMUs mit physikalischen Konnektoren am Beispiel eines Supermarktes". Presentation. In: *ASIM-Treffen STS/GMMS*. Ed. by D. Tikhomirov; H.-T. Mammen, and T. Pawletta. ARGESIM Verlag Wien, 2016. ISBN: 978-3-901608-48-3.